INVESTIGATING THE STRUCTURAL DOMAINS REQUIRED FOR ACTIVATION OF THE HUMAN DISCOIDIN DOMAIN RECEPTORS, DDR1 AND DDR2

Nafeesa Alibhai Noordeen

A thesis submitted for the degree of
Doctor of Philosophy
In the
University of London

University College London
Department of Medicine, Rayne Institute
5 University St., London, WC1E 6JJ

ProQuest LLC
789 East Eisenhower Parkway
P.O. Box 1346
Ann Arbor, MI 48106-1346

Abstract

The human discoidin domain receptors (DDRs), DDR1 and DDR2, are a unique subfamily of receptor tyrosine kinase as they bind to and are activated by the extracellular matrix protein collagen. The DDRs are expressed widely and play an important role in cell-matrix interaction, cell adhesion, motility and proliferation. Several different collagen types activate the DDRs, and both DDRs bind only native, triple-helical collagen and not denatured collagen. The DDRs need to be dimerised in order to bind collagen, as shown by studies using soluble extracellular domain (ECD) constructs of DDR1 and DDR2. However, the oligomerisation state of the full-length receptors on the cell surface has not been investigated. In this study, chemical cross-linking analysis and co-immunoprecipitation of FLAG- and MYC-tagged receptors show that full-length DDRs, expressed on the cell surface, exist as preformed oligomers in the absence of ligand. The DDR domains involved in dimerisation were investigated. Both DDR1 and DDR2 are composed of an N-terminal discoidin domain followed by a region of no known sequence homology that is predicted to be folded, named domain X in this study. A transmembrane (TM) domain ensues, followed by a juxtamembrane domain and a C-terminal catalytic tyrosine kinase domain (KD). DDR1 contains an additional region rich in proline and glycine situated between the domain X and the TM domain. Chemical cross-linking analysis and co-immunoprecipitation studies of DDR1 and DDR2 deletion mutants indicate that more than one receptor domain is involved in receptor dimerisation, as the deletion of any one of the above mentioned receptor domains was not sufficient to abolish oligomerisation. Furthermore, the role of the TM domain in DDR dimerisation was investigated. DDR mutants containing mutations to disrupt two potential TM dimerisation motifs, a leucine zipper and a GxxxG motif, were studied. Neither motif was required for DDR dimerisation in the absence of ligand. However, the leucine zipper, but not the GxxxG motif, was found to be required for DDR activation in the presence of collagen I, indicating that upon collagen binding, the DDR TM domains self-assemble, and this interaction occurs via the leucine zipper motif.

Acknowledgements

First and foremost, I would like to thank my supervisors, Prof. Michael Horton and Dr. Birgit Leitinger for their guidance, support and dedication. I would like to especially thank Birgit for her advice and assistance throughout the project and for her help with editing and revising this thesis. I would like to thank the Wellcome Trust for their generous funding.

I am very grateful to my lab colleagues - Moyu Watari, Macarena Blanco, Jaco De Groot, Tania Maffuci, Steve Nesbitt, Brian Nicoles and Gudrun Stenbeck for their advice and assistance.

I wish to extend a big thank you to all my friends for their understanding and support.

Finally and hugely, I would like to thank my mother, father and my brothers for their love and encouragement at all times.

Abbreviations

Ab	Antibody
ATP	Adenosine Triphosphate
dATP	Deoxyadenosine Triphosphate
BALF	Bronchoalveolar Lavage Fluid
BSA	Bovine Serum Albumin
BS^3	Bis(sulfosuccinimidyl)suberate
BRET	Bioluminescence Resonance Energy Transfer
CAT	Chloroamphenicol Acetyltransferase
cDNA	Complementary Deoxyribonucleic Acid
CFP	Cyan Fluorescent Protein
CYTO	Cytosolic Domain
CRD	Cysteine Rich Domain
CRP	Collagen-related peptide
CTLD	C-type lectin-like domains
dCTP	Deoxycytidine Triphosphate
DDR	Discoidin Domain Receptor
DS	Discoidin Domain
DMEM	Dulbecco's Modified Eagle's Medium
DNA	Deoxyribose Nucleic Acid
DMSO	Dimethyl sulphoxide
ECD	Extracellular Domain
ECM	Extracellular Matrix
ECL	Enhanced Chemiluminescence
EDTA	Ethylenediamine Tetra-acetic Acid
EGF	Epidermal Growth Factor
EGFR	Epidermal Growth Factor Receptor
Endo H	Endoglycosidase H
Epo	Erythropoetin
ERK	Extracellular Signal-Regulated Kinase

FCS	Foetal Calf Serum
FGF	Fibroblast Growth Factor
FGFR	Fibroblast Growth Factor Receptor
FLIM	Fluorescence Lifetime Imaging
FN	Fibronectin
FRET	Fluorescence Resonance Energy Transfer
GFP	Green Fluorescent Protein
GH	Growth Hormone
GPVI	Glycoprotein VI
GPA	Glycophorin A
GPI	Gycosyl-Phosphatidylinositol
dGTP	Deoxyguanosine Triphosphate
HEK	Human Embryonic Kidney
HGF	Hepatocyte Growth Factor
HRP	Horseradish Peroxidase
Ig	Immunoglobulin
Kb	Kilobase
KD	Kinase Domain
kDa	Kilodalton
LAM	Lymphangioleiomyomatosis
LB	Luria Bertani
mAb	Monoclonal Antibody
MAPK	Mitogen Activated Protein Kinase
MCP	M13 major coat protein
MDCK	Manine-Darby Canine Kidney
MMP	Matrix Metalloprotease
MW	Molecular Weight
NF-κB	Nuclear Factor-κB
N-linked	Asparagine-linked
NP40	Nonidet P-40
OD	Optical Density

O-linked	Serine/threonine-linked
PAGE	Polyacrylamide Gel Electrophoresis
PBS	Phosphate Buffered Saline
PCR	Polymerase Chain Reaction
PDGF	Platelet Derived Growth Factor
P/G	Proline and Glycine
PKC	Protein Kinase C
PM	Plasma Membrane
PMA	Phorbol 12-Myristate 13-Acetate
PMSF	Phenylmethylsulfonyl Fluoride
PNGase F	Peptide-N-Glycosidase F
P/S	Penicillin and Streptomycin
rpm	Revolutions per minute
RT	Room Temperature
RTK	Receptor Tyrosine Kinase
SDS	Sodium Dodecyl Sulfate
SUMO	Small Ubiquitin-like Modifier
TAB1	TGF-β-activated protein kinase 1-binding protein 1
TAE	Tris Acetate EDTA
TGF-β	Transforming Growth Factor β
TNF	Tumour Necrosis Factor
TRAF6	TNF receptor-associated factor 6
Tris	Tris(hydroxymethyl)aminoethane
TM	Transmembrane
dTTP	Deoxythymidine Triphosphate
uPA	Urokinase-type Plasminogen Activator
uPAR	Urokinase-type Plasminogen Activator Receptor
WT	Wild Type
YFP	Yellow Fluorescent Protein

Contents

Figures

Tables

Chapter 1

General Introduction

1.1. Receptor Tyrosine Kinases

Receptor Tyrosine Kinases (RTKs) play an important role in the control of cell growth, differentiation, metabolism and cell migration (reviewed in Hunter, 2000; Schlessinger, 2000). RTKs exist as membrane-spanning cell surface receptors; they function as mediators to relay signals from the extracellular environment to the inside of the cell. So far more than 16 structural subfamilies of these receptors have been identified (reviewed in Heldin, 1996). Structurally, RTKs are characterized by an extracellular ligand binding domain, a single transmembrane (TM) region, and a cytoplasmic region which contains a conserved catalytic protein tyrosine kinase domain (KD) (reviewed in Hubbard *et al.*, 1998). The structures of seven subfamilies, which are present in mammals, are depicted in Figure 1.1. The extracellular domains (ECDs) of these receptors are composed of diverse protein modules, including fibronectin-like and immunoglobulin-like domains, leucine-rich and cysteine-rich domains (Heldin, 1995). These receptors are activated by extracellular signal proteins, ligands, which include a wide variety of growth factors and hormones. Usually these are soluble proteins found in blood or other body fluids, for example, the platelet-derived growth factor, PDGF, and epidermal growth factor, EGF (Carpenter and Cohen, 1990; Yu *et al.*, 2003), or, as has been recently discovered, membrane bound ligands. For example, the fibroblast growth factor, FGF, needs the membrane bound heparin sulphate proteoglycan receptor in order to activate its receptor (Yayon *et al.*, 1991). For all RTKs, the binding of ligand to the extracellular ligand binding domain activates the intracellular tyrosine KD. Once activated, the KD catalyzes transfer of the γ-phosphate group from ATP to selected tyrosine side-chains on the receptor and on intracellular signalling proteins which bind to the phosphorylated receptors (reviewed in Hunter, 1998).

Receptor dimerisation is thought to be an important step in the activation process leading to tyrosine kinase autophosphorylation. In addition, it has been suggested that receptor oligomerisation allows for generation of signal diversity,

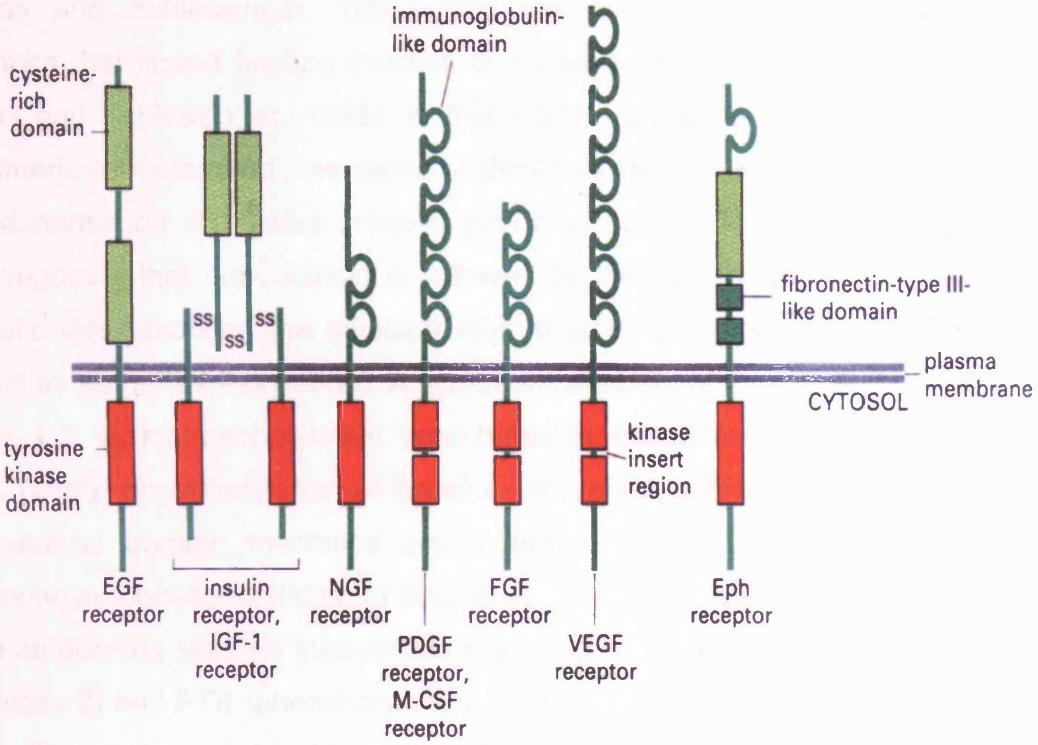

Figure 1.1: Seven subfamilies of RTKs. All RTKs contain an extracellular ligand binding domain, TM domain and a cytosolic conserved catalytic KD. The extracellular domain characterises the individual subfamilies and determines ligand specificity. (Figure taken from Alberts *et al.*, 2001, Molecular Biology of the Cell, 4th ed., page 872)

as each monomer within a dimer can recruit a different set of signalling proteins (Lemon and Schlessinger, 1994). The classical model of RTK activation describes that ligand binding induces dimerisation and activation of receptors (Weiss and Schlessinger, 1998). In this model, ligand binding to the ECD of monomeric receptors induces receptor dimerisation. The mechanism by which RTK dimerisation stimulates catalytic activity is not fully understood. Available data suggests that dimerisation is followed by the re-arrangement of receptor cytosolic tails, enabling the adjacent KDs to cross phosphorylate one another (known as autophosphorylation). A schematic diagram of this model is shown in Figure 1.2. Autophosphorylation contributes to the activation process in two ways. Firstly, phosphorylation of tyrosines within the activation loop (A-loop) of the catalytic domain maintains and increases the catalytic kinase activity. Secondly, autophosphorylation of additional tyrosines in the non-catalytic region serve as docking sites for intracellular signalling molecules containing SH2 (Src Homology 2) and PTB (phosphotyrosine binding) domains (reviewed in Pawson, 1995). The binding of signalling molecules to phosphorylated tyrosines leads to the assembly of an intracellular signalling complex and signal transduction. The classical model of RTK activation proposes that dimerisation stabilizes the conformation of the A-loop is an 'open conformation' allowing ATP and substrate binding, thus enabling transphosphorylation of the A-loop and stabilizing the catalytic domain in an active conformation. An alternative mechanism is that receptor dimerisation increases the local concentration of the KD leading to more efficient transphosphorylation of the A-loop (Weiss and Schlessinger, 1998).

Recently, a different model for receptor activation has been described. Certain cytokine receptors, such as the erythropoetin (Epo) receptor (Constantinescu *et al.*, 2001;) and growth hormone (GH) receptor (Brown *et al.*, 2005), and the RTK epidermal growth factor receptor (EGFR) (Moriki *et al.*, 2001), are able to dimerise in the absence of ligand and are activated by a ligand-induced conformational change. In this model, receptors exist as inactive,

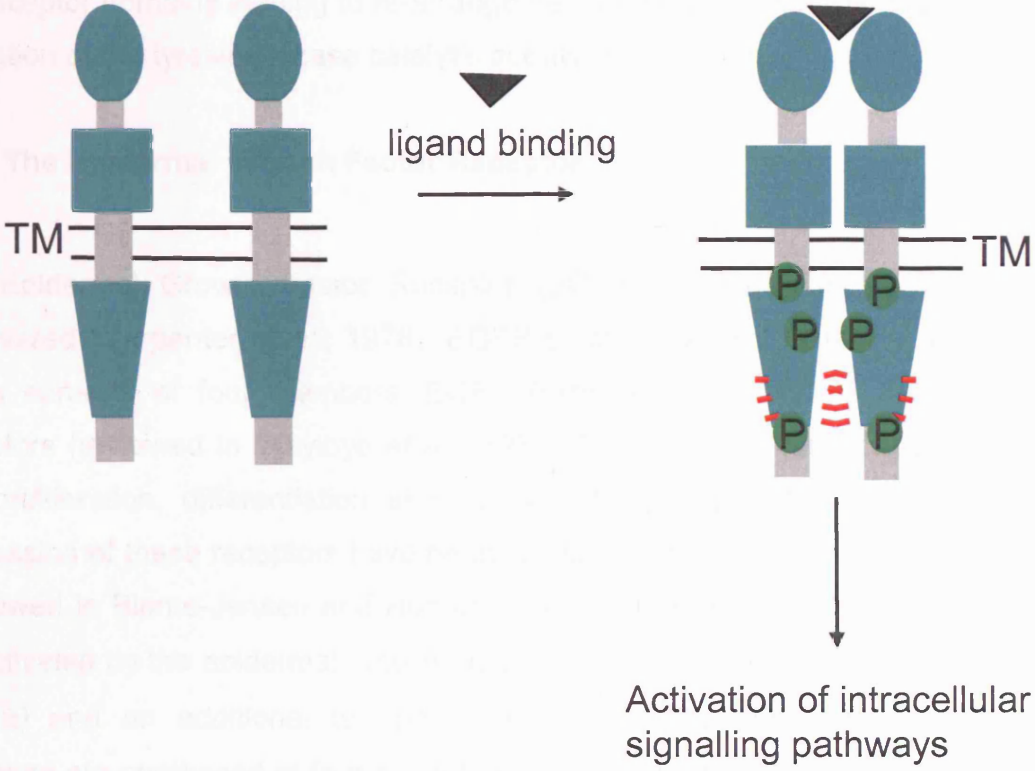

Figure 1.2: The classical model of RTK activation. Receptors exist as monomers on the cell surface. Ligand binding to the extracellular domain induces receptor dimerisation and re-arrangement of the receptor cytosolic region leading to activation of the catalytic tyrosine kinase and receptor autophosphorylation.

preformed dimers on the cell surface. Ligand binding causes a re-orientation of the receptor domains leading to re-arrangement of the cytosolic tails followed by activation of the tyrosine kinase catalytic activity (Figure 1.3).

1.1.1 The Epidermal Growth Factor Receptor

The Epidermal Growth Factor Receptor (EGFR) was the first RTK to be discovered (Carpenter *et al.*, 1978). EGFR belongs to the Erb family of RTKs which consists of four members, EGFR (ErbB1), ErbB2, ErbB3 and ErbB4 receptors (reviewed in Olayioye *et al.*, 2000). Together they function to control cell proliferation, differentiation and survival. Activating mutations and over-expression of these receptors have been shown to result in a variety of cancers (reviewed in Blume-Jensen and Hunter, 2001). These receptors were found to be activated by the epidermal growth factor (EGF), transforming growth factor α (TGFα) and an additional ten potential ligands. The large ECD of these receptors are composed of four subdomains, denoted as I, II, III, and IV (Figure 1.4). Domains I and III form the ligand binding domain of EGFR while other parts of the ECD are involved in receptor dimerisation (Schlessinger, 2002). The prevailing model for the mechanism of activation of EGFR is thought to be that ligand binding induces receptor dimerisation (Schlessinger, 2000). This concept is supported by a number of biochemical, biophysical and crytallographic studies. Biophysical studies have demonstrated that two EGF molecules bind to two EGFR molecules simultaneously forming a 2:2 EGF-EGFR complex formed from stable 1:1 EGF-EGFR complexes (Lemmon *et al.*, 1997). Crystallographic studies of ligand:receptor complexes have given insight into the details of how ligand binding induces EGFR dimerisation (Garrett *et al.*, 2002; Ogiso *et al.*, 2002). The crystal structures are consistent with a 'receptor mediated' mechanism of receptor dimerisation (Lemmon *et al.*, 1997). The binding of EGF to EGFR induces a conformational change which exposes a site in the ECD. This site consists of a specific loop which projects from domain II, called the

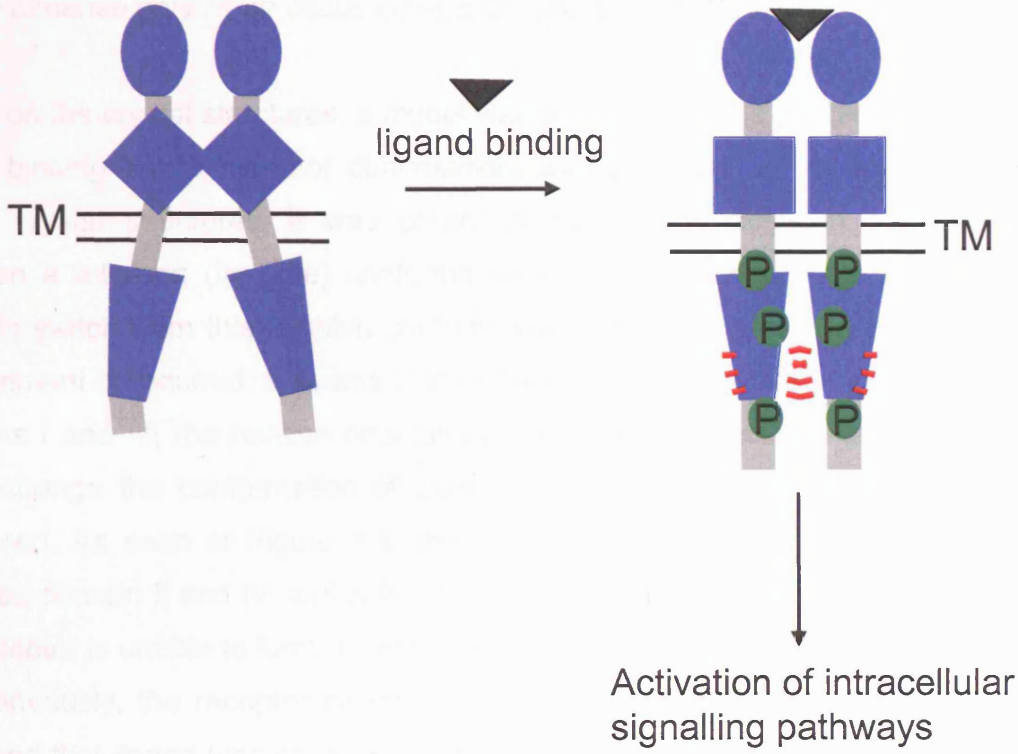

Figure 1.3: An alternative model of RTK activation. Receptors exist as inactive, preformed dimers on the cell surface in the absence of ligand. Ligand binding leads to re-orientation of receptor domains. This conformational change is transmitted into the cytosolic region, resulting in the activation of the catalytic tyrosine kinase and receptor autophosphorylation.

'dimerisation loop'. This finding suggests that two EGFR monomers would be able to dimerise only when occupied by EGF (Burgess *et al.*, 2003).

Based on the crystal structures, a model was proposed for the process by which ligand binding drives receptor dimerisation. By comparing active and inactive EGFR crystal structures, it was proposed that EGFR exists in equilibrium between a tethered (inactive) conformation and an extended (active) one. In order to switch from this inactive conformation to the active one, a domain re-arrangement is required. It seems that by ligand binding simultaneously to both domains I and III, the relative orientation of the two domains are altered. This could change the conformation of domain II so that its ability to dimerise is enhanced. As seen in Figure 1.4, there is a direct intermolecular interaction between domain II and IV, which buries the dimerisation loop of domain II, thus the receptor is unable to form dimers. For a ligand to bind both domains I and III simultaneously, the receptor needs to adopt the 'extended conformation'. It is proposed that ligand binding actually 'traps' the extended configuration, shifting the equilibrium to the right and thus the majority of receptor molecules will be in the extended state, and will be able to dimerise (Figure 1.4). Thus the crystal structure provides good evidence for ligand-induced dimerisation and activation of EGFR (Burgess *et al.*, 2003).

A contradiction to this classical model has been proposed by several independent groups, who provide evidence for a proportion of EGFR molecules existing as preformed dimers on the cell surface (Gadella and Jovin, 1995; Chu *et al.*, 1997; Sako *et al.*, 2000; Moriki *et al.*, 2001; Martin-Fernandez *et al.*, 2002; Yu *et al.*, 2002). A series of biochemical studies involving chemical cross-linking analysis of cell surface EGFRs, co-immunoprecipitation and sucrose density gradient centrifugation experiments *in vitro,* showed that EGFR has the ability to form dimers in the absence of bound ligand (Chu *et al.*, 1997; Moriki *et al.*, 2001; Yu *et al.*, 2002). Biophysical studies using single molecule tracking of EGFR dimerisation (Gadella and Jovin, 1995) and Fluorescence Resonance Energy

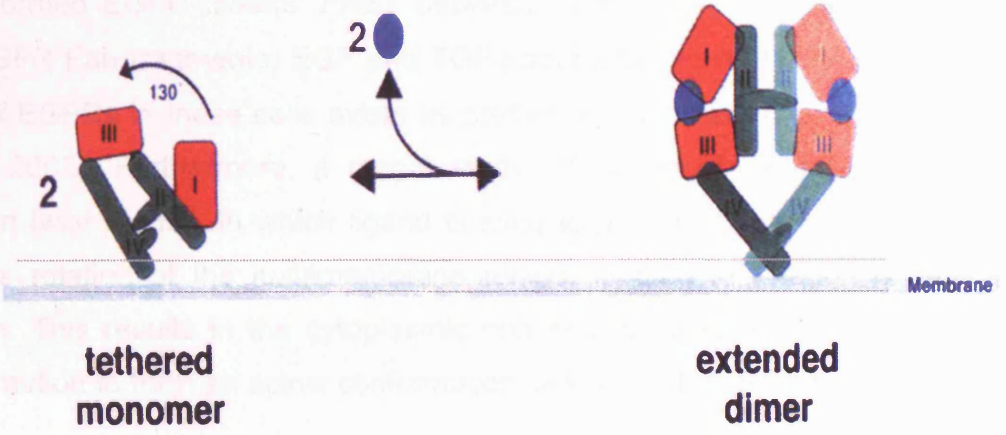

Figure 1.4: A model for EGFR activation by ligand-induced dimerisation and conformational change. The inactive receptor is shown on the left as a monomer. Domains II and IV interact thus burying the dimerisation arm of domain II and the receptor is unable to dimerise (tethered conformation). Upon EGF binding, a conformational change occurs resulting in an extended conformation of the two receptors allowing receptor dimerisation as shown on the right. (Figure taken from Burgess *et al.*, 2003).

Transfer (FRET) analysis (Sako *et al.*, 2000) in live cells, indicate the presence of preformed EGFR dimers. FRET between fluorescently labelled monoclonal anti-EGFR Fab fragments, EGF and TGFα bound to live A431 cells, show that 14% of EGFRs in these cells exists as preformed oligomers (Martin-Fernandez *et al.*, 2002). Furthermore, a recent study (Moriki *et al.*, 2001) proposed a 'rotation twist model', in which ligand binding to predimerised, inactive EGFRs induces rotation of the juxtamembrane region, leading to rotation of the TM domain. This results in the cytoplasmic domains dissociating from an inactive conformation to form an active conformation, leading to the activation of the KD.

1.2. The Extracellular Matrix

The extracellular matrix (ECM) is the extracellular space surrounding cells in tissues. The matrix is composed of a variety of proteins and polysaccharides that are secreted by the cells within the matrix and assembled by these cells into an organized meshwork.

There are two main types of ECM molecules: first, polysaccharide chains of glycosaminoglycans and proteoglycans and second, fibrous proteins such as collagen, elastin, fibronectin and laminin. The proteoglycan molecules form a hydrated gel-like base in which the fibrous proteins are embedded. The gel resists compressive forces on the matrix and allows rapid diffusion of nutrients, metabolites and hormones between blood and cells. The collagen fibres strengthen and help organize the matrix and rubber-like elastin fibres give it resilience. Most of the matrix proteins help cell attachment. Thus the ECM functions as a scaffold for cells, provides a substrate for cell anchorage, guides cell migration and contributes to the mechanical strength of the tissues (reviewed in Katz *et al.*, 2000). Figure 1.5 shows a schematic diagram of connective tissue underlying an epithelium, containing a variety of matrix molecules which are secreted mainly by fibroblasts within the tissue. In addition

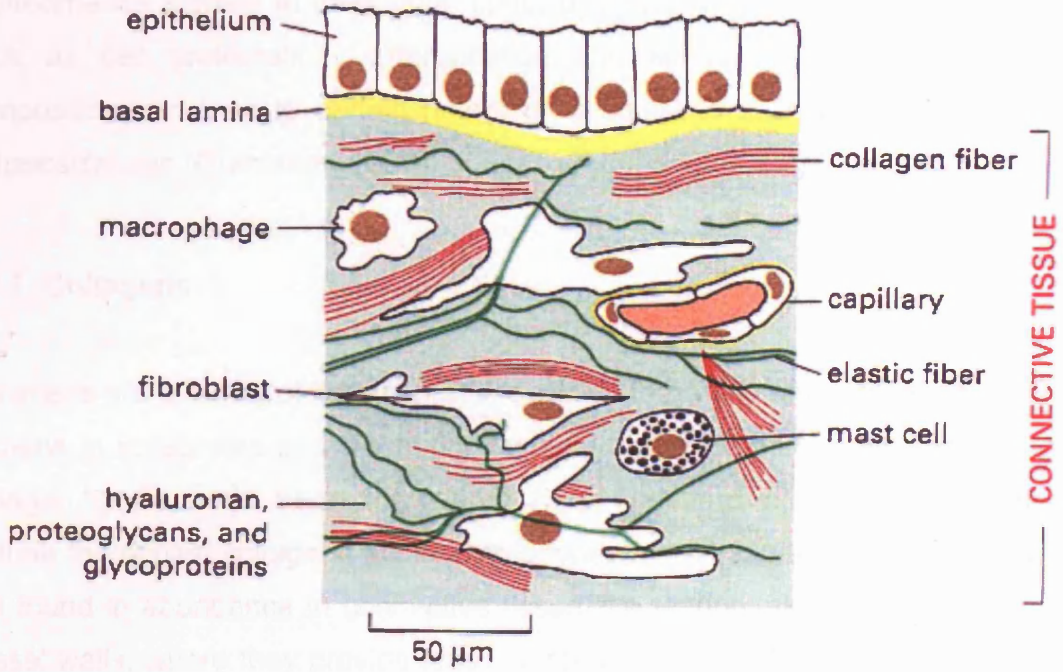

Figure 1.5: Connective tissue underlying an epithelium. Fibroblasts in the connective tissue secrete the extracellular matrix consisting of collagen fibres, elastic fibres and proteoglycans. (Figure taken from Alberts *et al.*, 2001, Molecular Biology of the Cell, 4th ed., page 972).

to these scaffolding functions, the ECM is also responsible for transmitting environmental signals to cells, thus controlling fundamental cellular processes such as cell proliferation, differentiation and survival. Altering the matrix composition can lead to certain pathological diseases such as restinosis and artherosclerosis (Gumbiner, 1996).

1.2.1. Collagens

Collagens are a family of fibrous proteins known to be one of the most abundant proteins in vetebrates and the major proteins of the ECM. Around 27 different collagen types have been discovered (Boot-Handford *et al.*, 2003). These include the fibrillar collagens (for example types I, II, III, V, XI and XXVII), which are found in abundance in connective tissue like tendon, skin, bone and blood vessel walls, where they provide tensile strength (reviewed in van der Rest and Garrone, 1991). Collagen types IX, XII, XIV, XVI and XIX are fibril-associated collagens as they decorate the surface of collagen fibrils and link the fibrils to one another and to other ECM components. Type IV, VIII and X are non-fibrillar, network-forming collagens. Type IV collagens, found in basal laminae, form a meshwork, while type VII collagens form dimers which assemble into anchoring fibrils. There are also collagens that form beaded filaments (type VI), and collagens with a TM domain (types XIII and XVII) (reviewed in Prockop and Kivirikko, 1995).

Mutations in collagen genes cause a variety of human diseases (reviewed in Myllyharju and Kivirikko, 2001). For example, mutations in type I collagen genes cause bone defects such as osteogenesis imperfecta and osteoporosis. Mutations in the gene for type II collagen can produce cartilage disorders such as chondrodysplasias and certain forms of osteoarthritis. The renal disease called Alport syndrome results from mutations in type IV collagen. Epidermolysis bullosa, a disease characterised by severe blistering and scarring of the skin, is thought to be caused by mutations in type VII collagen, which form anchoring

fibrils for basement membranes. Transgenic mice with mutated collagen genes have proved useful for defining the functions of various collagens and studying collagen-related diseases (reviewed in Myllyharju and Kivirikko, 2001).

Structurally all collagens are long, stiff triple-helices made up of three polypeptides chains (α-chains) which are wound around each other to form a triple-helix (reviewed in Brodsky and Ramshaw, 1997). An α-chain consists of Gly-X-Y triple repeats, in which X and Y are often proline and hydroxyproline, respectively. Collagens are synthesised as precursor pro-α-chains, which contain short amino acid sequences at the N- and C-terminal ends called pro-peptides. In the ER lumen, selected prolines and lysines get hydroxylated to form hydroxyproline and hydroxylysine, at the same time some hydroxylysines are glycosylated. Each pro-α-chain gets H-bonded to two other α-chains to form a triple-stranded, helical molecule called pro-collagen. The soluble pro-collagen molecules are secreted and further processed by cleavage of the N- and C-terminal pro-peptides by specific proteinases. The monomers self-assemble spontaneously to form large collagen fibrils (10-300 nm in diameter). Formation of covalent cross-links between lysine residues of collagen molecules greatly enhances the strength of the collagen fibrils. Collagen fibrils then aggregate to form larger collagen fibres of several micrometers in diameter (reviewed in Prockop and Kivirikko, 2001).

The three α-chains are non-identical in type I collagen, unlike those of type II and type III. A type I molecule consists of two identical α1- and one α2-chain. Each α-chain has, at both ends, a short sequence of residues in which glycine no longer occupies every third position. These ends, called 'telopeptides', adopt less regular conformations. The presence of glycine at every third position enables close packing of the α-chains. The abundance of the imino acids, proline and hydroxyproline, allows for hydrogen bonding between the three α-chains and stabilizes helix-helix interactions, thus enabling the formation of a

right-handed super-helix. Clusters of charged residues, which are important for triple-helix self-association and ligand binding, are interrupted with imino-rich regions. Molecular modelling of collagen containing adjacent charged residues Glu and Arg, suggest that the side-chains of these charged residues can be involved in the formation of intra-chain and intra-helix ion pairs (Katz and David, 1990; Katz and David, 1992). Details on the molecular structure of collagen have been discovered by X-ray crystallography of different collagen peptides (Bella *et al.*, 1994; Kramer *et al.*, 1998; Kramer *et al.*, 1999).

Fibrillar collagens are the most abundant matrix component (Kucharz, 1992). The triple-helical domain of fibrillar collagens are around 300 nm long, and each of the three collagen α-chains consists of approximately 1000 amino acids. The structure of a triple-helical collagen monomer and a schematic representation of the assembly of monomers to form a collagen fibril are shown in Figure 1.6 (a). Electron microscopy images of collagen fibers reveal a regular, transverse banding of the long fibrils (shown in Figure 1.6, b). This banding is pattern results when adjacent, parallel triple-helical monomers are staggered axially by 67 nm (or 244 amino acids), thus forming a 67 nm wide repeat structure known as the 'D period' (Kadler *et al.*, 1996).

1.3. Collagen Receptors

In addition to providing mechanical strength for the ECM and structural support in tissues, collagens act as an adhesive substrate for cell attachment and migration. They also mediate signalling events by binding to cell surface receptors such as integrins. Apart from the α1β1, α2β1, α10β1, α11β1 and αVβ3 integrins, other collagen receptors identified are the proteoglycans (Clemetson *et al.*, 1999) and syndecans (San Antonio *et al.*, 1994), the discoidin domain receptors DDR1 and DDR2 (Shrivastava *et al.*, 1997; Vogel *et al.*, 1997), glycoprotein VI (Clemetson *et al.*, 1999) and Endo 180 (East *et al.*, 2003).

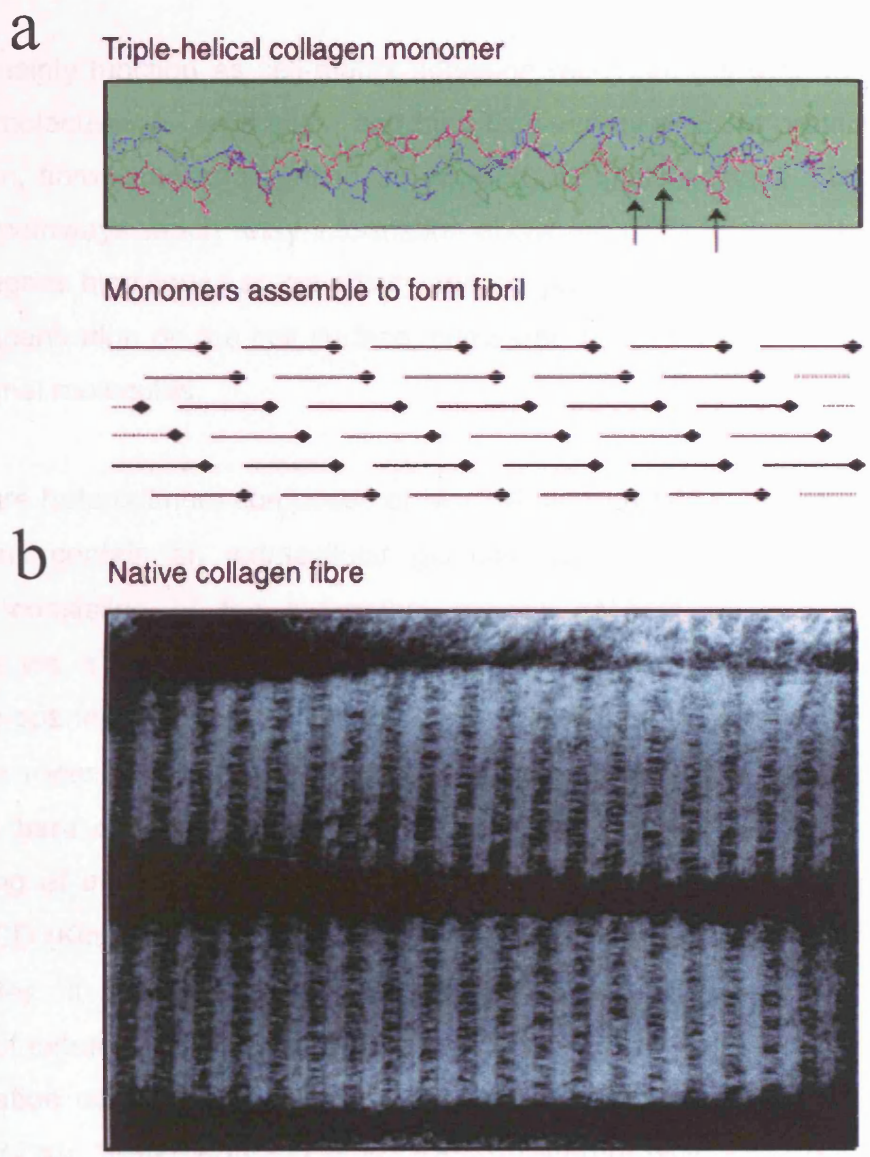

Figure 1.6: Collagen structure and assembly. (a, upper panel) Triple-helical structure of a collagen monomer. The proline and hydroxyproline rings are oriented away from the axis of the helix (black arrows), and glycine occupies the axial core of the triple-helix. (a, lower panel) Schematic representation of the self-assembly of collagen monomers, in a quarter staggered array, to form the collagen fibril. (b) Transmission electron micrograph of large collagen fibres which are formed by collagen fibrils. (Figure taken from Siljander and Farndale, 2002).

1.3.1. Integrins

Integrins mainly function as cell-matrix adhesion receptors (as well as cell-cell adhesion molecules in blood cells) and bind to a variety of ECM proteins such as collagen, fibronectin and laminin. In addition, integrins activate intracellular signalling pathways which relay information about the ECM to the cell (Hynes, 1992). Integrins bind ligand at low affinity and are present at ten to hundred fold higher concentration on the cell surface, compared to cell surface receptors for soluble signal molecules.

Integrins are heterodimers composed of two TM glycoprotein subunits, α and β. All integrins contain an extracellular globular head approximately 70 Å in diameter, consisting of the N-terminal regions of both α- and β-chains, connected via a long rigid stalk (approximately 100 Å long) to a pair of membrane-spanning helices and short C-terminal cytoplasmic tails (Erb *et al.*, 1997). The recently determined crystal structure of the ECD of integrin αvβ3, revealed a 'bent' conformation of the ECD, in the absence of ligand (Xiong *et al.*, 2001; Xiong *et al.*, 2002). Integrin activation leads to the straightening of the integrin ECD (Kim *et al.*, 2003). Both α- and β-subunits contain divalent cation binding sites. It has been shown that ligand binding is dependent on the presence of extracellular divalent cations, calcium or magnesium and the type of divalent cation can influence the affinity and the specificity of ligand binding (Tuckwell *et al.*, 1995; Dickeson *et al.*, 1997). Different types of integrins bind different ligands and multiple integrins can recognise a single type of ECM protein. In mammals, 24 distinct integrins can be formed by a combination of 8 types of α-subunits and 18 types of β-subunits and further diversity is introduced by alternative splicing of mRNA (Humphries, 2000).

By binding to matrix proteins outside the cell and the cytoskeleton inside the cell, integrins link the cells to the ECM. This cell-matrix interaction allows the cells to grip the matrix. Interaction with the actin cytoskeleton occurs via other

intracellular proteins such as talin, α-actinin, filamin and vinculin (Zamir and Geiger, 2001). Upon ligand binding, the cytoplasmic tail of the α-subunit interacts with these proteins which link to actin filaments. This leads to clustering of the integrins and formation of focal adhesions. If the cytoplasmic tail of the α-subunit is deleted, ligand binding still occurs but cell adhesion is greatly reduced, and clustering at focal adhesions does not occur. This indicates that integrins must link to the cytoskeleton in order to bind cells to the matrix. This cytoskeleton-integrin attachment may help cluster the integrins, thus resulting in a stronger bond or alternatively, lock the integrin in a conformation which allows it to bind its ligand more tightly (Calderwood *et al.*, 2000). Integrins also function as signal transducers, activating intracellular signalling pathways by recruiting cytoplasmic tyrosine kinases and adaptor proteins to focal adhesions (Schwartz, 2001). Integrins and conventional signalling receptors often co-operate to promote cell growth, survival and differentiation. Signalling via integrins relies on focal adhesion kinase (FAK), a cytoplasmic, tyrosine phosphorylated kinase found abundantly in focal adhesions. Upon integrin clustering FAK is recruited to focal adhesions by intracellular anchor proteins which bind to integrin α-subunit (talin) or β-subunit (paxillin). Here cross phosphorylation of FAK occurs which enables docking of Src kinases onto phosphorylated tyrosines, leading to additional tyrosine phosphorylation of FAK and recruitment of a variety of intracellular signalling proteins (Parsons *et al.*, 2000).

Integrins and other cell surface receptors such as G-protein coupled receptors (GPCRs) or RTKs act in concert, synergistically activating a multitude of signalling pathways which enable cell proliferation, differentiation, cell shape and migration. Integrin signalling and signalling via growth factor receptors can interact and re-enforce one another (Assoian and Schwartz, 2001). For example, signalling via integrins and growth factor receptors act together to sustain activation of the Ras-Mitogen Activated Protein Kinase (MAPK) pathway long enough to induce cell proliferation. Integrins activate signalling pathways to promote cell survival: When cells in culture are attached, due to signalling via

integrins, these cells can then respond to growth factors. Signalling via growth factor receptors then enables cell growth and proliferation. Also, signalling pathways activated by conventional receptors increase the expression of integrins or ECM molecules, while signalling by integrins can increase the expression of growth factor receptors or ligands (Giancotti and Ruoslahti, 1999; Miranti and Brugge, 2002).

Signals generated inside the cell can either enhance or inhibit the ability of integrins to bind ligand, known as 'inside out signalling'. Regulation of integrin activity by the cells is important in leukocytes and platelets where integrins are required to be activated before being able to mediate adhesion (Harris *et al.*, 2000; Plow *et al.*, 2000). The major platelet integrin, αIIbβ3, is usually present in the inactive OFF state on the cell surface. Upon platelet activation the integrins are activated by signals from within the cell, leading to a conformational change in the ECD. The integrins can then bind fibrinogen, von Willebrand factor and fibronectin, thus adhering strongly to the walls of blood vessels. Cross-linking of integrins to fibrinogen molecules bound to the surface of adjacent platelets, induces platelet aggregation. Integrins also intercommunicate with each other, thus activating or inhibiting each other. For example collagen signalling through another platelet integrin, α2β1, triggers the activation of αIIbβ3 on the platelet cell surface (Schwartz and Ginsberg, 2002).

The α1β1 and α2β1 integrins are the major integrin collagen receptors; these integrins as well as two other β1 integrins, α10β1 and α11β1, recognise native, triple-helical collagen (reviewed in Heino, 2000). Another integrin collagen receptor, αvβ3, binds gelatine, the denatured form of collagen I (reviewed in Hemler, 1999). Integrin-collagen interactions are shown to be involved in many important physiological processes including cell adhesion, cell growth and differentiation and pathological states such as thrombosis and tumour metastasis.

The integrin α1β1 is abundant on mesenchymal cells (Gardner *et al.*, 1996), whilst α2β1 is an important collagen receptor on platelets, where it is required for platelet adhesion to collagens present in the vascular subendothelium (Siljander and Farndale, 2002). α1β1 and α2β1 have different binding affinities to collagen (reviewed in Heino, 2000). For example, α1β1 prefers network-forming collagen type IV over collagen type I, whilst α2β1 binds type I collagen more strongly than type IV collagen. In addition, the signalling pathways initiated by these two receptors are distinct. Activation of α1β1 integrin leads to downregulation of collagen I synthesis (Langohlz *et al.*, 1995; Gardner *et al.*, 1999), and increased cell proliferation by stimulating signalling via the adaptor protein Shc and activation of Ras and extracellular-signal regulated kinase (Erk) (Pozzi *et al.*, 1998). In contrast, α2β1 integrin increases type I collagen and matrix metalloproteinase (MMP) synthesis (Langholz *et al.*, 1995) via p38 kinase signalling (Ravanti *et al.*, 1999).

Early studies carried out to identify the integrin binding sites on collagen, involving the fragmentation of collagen I, resulted in the identification of several integrin α2β1 sites on the collagen molecule (Morton *et al.*, 1994). Subsequently, based on the above findings, overlapping triple-helical collagen peptides were made and studied, resulting in the identification of a 15 residue triple-helical sequence of the collagen I α1(I)-chain (Knight *et al.*, 1998). Experiments carried out by the same group then showed that the α2β1 as well as the α1β1 recognition site lies within just 6 residues, GFOGER, of this 15 residue sequence (Knight *et al.*, 2000). Since the above study, additional recognition motifs within collagen I α1-chain have been found with the motif Gxx'GER, such as GLOGER and GASGER (Xu *et al.*, 2000). Recently, a peptide of collagen III containing the motif GMOGER, was shown to bind with moderate affinity to β1 integrins (Siljander *et al.*, 2004). Following this study, a larger scale investigation sought to locate novel integrin α2β1 binding motifs in collagen III (Raynal *et al.*, 2005). Using a set of synthetic peptides covering the

whole triple-helical domain of collagen III, the investigators found that wild-type integrin α2β1 bound with high affinity to two motifs, GROGER and GLOGEN, and with intermediate affinity to a third motif, GLKGEN.

Nine integrin α-subunits contain a ~200 amino acid insert called the I (or A)-domain (Humphries, 2000). Integrins α1β1, α2 β1, α10β1 and α11β1 interact with collagen via the I-domain of the α-subunit, as shown by studies using recombinant I-domains which exhibit ligand binding properties of intact integrin (Kamata and Takada, 1994; Tuckwell *et al.*, 1995). The α-subunit contains a β-propeller structure into which the I-domain is inserted, between blades two and three. The I-domain contains a divalent cation binding site called MIDAS, for Metal Ion Dependant Adhesion Site (Lee *et al.*, 1995). Mutagenesis studies have shown that the MIDAS motif plus surface side-chains are required for ligand binding (Kern *et al.*, 1994; Kamata *et al.*, 1999). Several studies have reported a conformational change of the integrin I-domain upon ligand binding (Lee *et al.*, 1995; Qu and Leahy, 1995).

More detailed evidence comes from the crystal structure of the I-domain of α2 with bound triple-helical collagen peptide GFOGER (Emsley *et al.*, 2000). The crystal structure shows that three loops on the upper surface of the I-domain that co-ordinate the metal ion are also involved in binding to the collagen, with the collagen glutamate residue in turn completing the co-ordination of the metal ion (Figure 1.7). Upon comparison with the unliganded I-domain structure (Emsley *et al.*, 1997) a model for allosteric activation of integrins was proposed, where ligand binding to the I-domain induces a conformational change within the I-domain, and this conformational change is propagated to the other parts of the integrin molecule. Recently the crystal structure of the isolated α2β1-binding collagen peptide (IBP) was solved (Emsley *et al.*, 2004), enabling comparison of the GFOGER hexapeptide containing IBP in bound and unbound state. A direct, water mediated interaction between a Glu and Arg residue between two collagen strands is observed in the unbound sate; this interaction is disrupted in

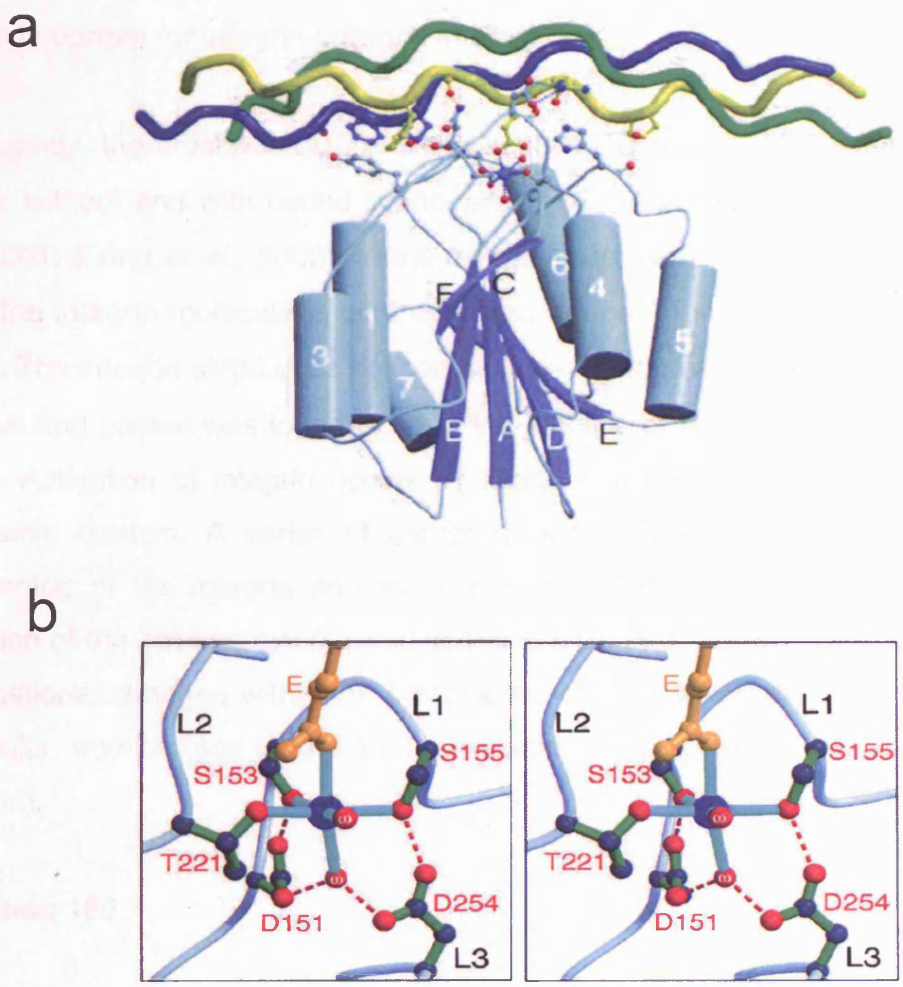

Figure 1.7: Structure of the integrin α2-I-domain:collagen complex. (a) Stereo diagram of the α2-I-domain in complex with the collagen peptide. The I-domain helices are shown as cylinders, *β*-strands as arrows. The three strands of the collagen triple-helix are shown in green (leading strand), yellow (middle strand) and blue (trailing strand). The residues of the motif GFOGER, of both the green and yellow strands, make contacts with the I-domain. The blue strand does not make any contacts with the I-domain. (b) Stereo diagram of the MIDAS motif of integrin α2-I-domain. The glutamate residue (E) from the collagen middle strand co-ordinates the metal ion (blue ball). Residues from the three loops (L1, L2, and L3; gray ribbons) of the α2-I-domain co-ordinate the metal ion either directly or through water molecules (*ω*). (Both figures taken from Emsley *et al.*, 2000).

the bound state. In addition, the region GFOGER is shown to be flexible, which could be important for integrin-collagen interaction.

Subsequently, the crystal structure of the entire ECD of the αVβ3 integrin was obtained without and with bound ligand, an Arg-Gly-Asp (RGD) peptide (Xiong *et al.*, 2001; Xiong *et al.*, 2002). In the crystal structure of αVβ3 with no ligand bound, the integrin molecule is bent over and the bent form is supposed to be inactive. The integrin αVβ3 does not contain a α-I-domain and the location of the ligand binding pocket was found to be at the junction of the β-propeller and β-I-domain. Activation of integrin occurs by ligand binding or by changes in the cytoplasmic domain. A series of conformational changes then leads to the straightening of the integrin and the separation of the legs, followed by the separation of the TM and cytoplasmic domains (Kim *et al.*, 2003). This results in conformational changes within the cytoplasmic domain which allows binding of intracellular proteins (see Figure 1.8 for the schematic representation of integrin activation).

1.3.2. Endo 180

Endo 180, a member of the mannose receptor family, is a collagen binding cell surface receptor expressed in a restricted range of cell types which include fibroblasts, macrophages and certain endothelial cells (Isacke *et al.*, 1990; Sheikh *et al.*, 2000; Schnack Nielson *et al.*, 2002). Importantly, Endo 180 expression is upregulated in tumour endothelium and breast cancer cells (St Croix *et al.*, 2000; Schnack Nielson *et al.*, 2002). The ECD of this receptor is characterized by an N-terminal cysteine rich domain (CRD) followed by a fibronectin type II (FNII) domain and 8 C-type lectin-like domains (CTLDs). The cytoplasmic tail is short, and contains a dihydrophobic endocytosis motif and PKC phosphorylation sites (East *et al.*, 2002). Transglutaminase cross-linking studies revealed that Endo 180 forms a tri-molecular complex with urokinase-type plasminogen activator (uPA) and its GPI-anchored membrane receptor

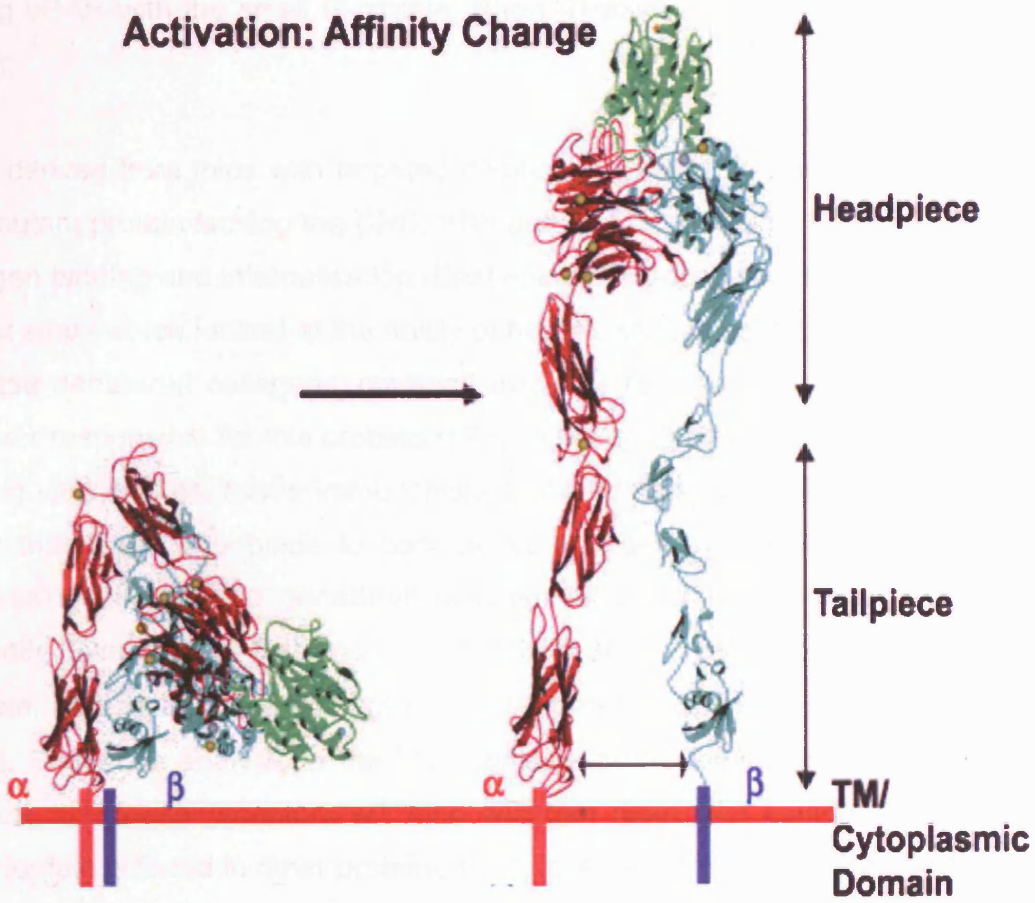

Figure 1.8: Schematic representation of integrin activation. In the bent conformation extensive interactions are present between the integrin headpiece and tailpiece. In addition, the juxtamembrane C-terminal segments of the α- and β-subunit ECDs are in proximity to one another. In the extended conformation (right), there is no interaction between the α- and β-subunits in the tailpiece. (Figure modified from Kim *et al.*, 2003).

(uPAR). Endo 180 acts as a TM adaptor protein for uPAR during chemotaxis by linking uPAR with the small G-protein, Rho GTPase activation (Behrendt *et al.*, 2000).

Cells derived from mice with targeted deletion in Endo 180 gene, which results in a mutant protein lacking the CRD, FNII and CTLD1 domains, have a defect in collagen binding and internalisation (East *et al.*, 2003, Engelholm *et al.*, 2003). A recent study which looked at the ability of hepatic stellate cells to internalise and degrade denatured collagens, provided evidence for Endo 180 being the main receptor responsible for this process (Mousavi *et al.*, 2005). Further proof comes from *in vitro* studies, tissue immunohistochemistry and cell-based assays which show that Endo 180 binds to both native collagens (types V, I, II, IV with decreasing affinity) and denatured collagen or gelatin (Wienke *et al.*, 2003). Recently it was shown that Endo 180 bind to a defined region of collagen type I α-chain, namely the C-terminal glycine repeat and C-prodomain (Thomas *et al.*, 2005). Sequence analysis of the FNII domains of the mannose receptor family predicts that these receptors will bind collagen (East and Isaake, 2002). The FNII domain is found in other proteins such as fibronectin and MMP2 and MMP9 gelatinases, and enables binding of these proteins to denatured collagen or gelatin (Steffenson *et al.*, 1999; Pickford *et al.*, 2001). The Endo 180 FNII domain shows sequence conservation with these other FNII domains, thus the Endo 180 FNII domain is responsible for mediating collagen binding. Binding to collagen by Endo 180 most probably involves CTLD1 domain in addition to the FNII domain. However Endo 180 contains only one FNII domain, whereas the other gelatin/collagen binding receptors contain multiple FNII domains. For example in MMP2 all three tandem FNII domains are needed to mediate high affinity collagen binding (Banyai *et al.*, 1994). The three-dimensional structure of the N-terminal region of Endo 180 was obtained by single particle electron microscopy and revealed that the CRD contacts the second CTLD, bringing the FNII domain spatially close to the CTLD1 domain (Rivera-Calzada *et al.*, 2003) thus indicating that these two domains likely interact to stabilize and enhance

collagen binding. Also, clustering of Endo 180 in clathrin-coated pits might enhance collagen binding (Rivera-Calzada *et al.*, 2003). Further studies would need to be carried out in order to prove that CTLD1 is also involved in collagen interaction and to gain insight into the FNII-mediated collagen binding.

Endo 180 constitutively recycles between the plasma membrane and the endosomal compartments (East *et al.*, 2002). This enables internalisation of native and denatured collagens via clathrin-coated vesicles that are delivered to lysosomes for degradation, as shown by experiments using cell culture systems where expression of Endo 180 results in rapid uptake of gelatin by the cells (Wienke *et al.*, 2003). Thus Endo 180 could have a role in extracellular matrix remodelling, which occurs during tissue development and homeostasis, by facilitating the uptake and degradation of collagens.

It has been shown that native collagen type IV is a principle ligand of Endo 180 in murine kidney as collagen type IV and soluble Endo 180 protein show co-localisation in these cells (Kjoller *et al.*, 2004). In normal breast tissue, Endo 180 is expressed by myoepithelial cells and intra/interlobular fibroblasts that align with collagen fibrils, whilst in breast tumour Endo 180 is expressed by cells within the remodelled collagen matrix as seen by immunohistochemistry. Thus, Endo 180 could play a role in remodelling of the ECM during tumour growth and progression (Howard *et al.*, 2004). Endo 180 was identified as a key mediator of collagen turnover in mammary carcinogenesis, as genetic ablation of this receptor disrupted collagen turnover that is required for tumour progression (Curino *et al.*, 2005).

1.3.3. Glycoprotein VI

Glycoprotein VI (GPVI) is an important signalling receptor for collagen that is expressed only on platelets (Miura *et al.*, 2000). Studies using collagen and collagen related peptide (CRP), which mimics triple-helical collagen, showed

that collagen acts as a ligand for this receptor. Upon collagen binding and activation of GPVI, tyrosine phosphorylation of a number of intracellular proteins occurs, leading to platelet activation (Nieswandt and Watson, 2003). It has been shown that GPVI binds only to fibrous collagens and not soluble collagens (Moroi *et al.*, 1996).

The structure of this receptor was identified by cDNA cloning and revealed that GPVI belongs to the immunoglobulin superfamily as the extracellular region of this receptor contains two immunoglobulin C2-like domains (Clemetson *et al.*, 1999). It is thought that GPVI forms a complex with the Fc receptor (FcR) γ-chain, a TM protein containing an immunoreceptor tyrosine activation motif (ITAM) (Gibbins *et al.*, 1996). By site-directed mutagenesis studies, it was shown that this interaction occurs via an arginine residue in the GPVI TM domain which makes a salt bridge with an aspartic acid residue of FcR γ-chain (Tsuji *et al.*, 1997). Activation of platelets by collagen induces tyrosine phosphorylation of FcR γ-chain ITAM motif, followed by assembly of various signalling molecules, leading to downstream signalling from GPVI (Poole *et al.*, 1997; Tsuji *et al.*, 1997; Nieswandt *et al.*, 2000). Associated Src-family tyrosine kinases, such as Fyn and Lyn have been suggested to be required for phosphorylation of FcRγ, upon collagen binding to GPVI (Ezumi *et al.*, 1998; Briddon *et al.*, 1999)

It has been suggested that GPVI is present as preformed dimers on the platelet surface (Miura *et al.*, 2002; Farndale *et al.*, 2003). Using soluble ECDs of the receptor (a monomeric and a dimeric Fc-tagged form) Miura *et al.* showed that the dimeric Fc-tagged form binds fibrous collagen with high affinity, whilst the monomeric form does not. However, further studies would be needed to provide conclusive evidence for the existence of GPVI dimers on the cell surface. It has been shown, using a triple-helical CRP composed of ten repeated G-P-O triplets, that GPVI recognizes the sequence G-P-O (O denotes hydroxyproline) within collagen (Kehrel *et al.*, 1998). The hydroxyproline of the G-P-O sequence

is thought to be required for GPVI-collagen binding (Perret *et al.*, 2003). A recent study using site-directed mutagenesis and blocking phage antibody, identifies the collagen binding region on GPVI to be at the apex of the junction between the two Ig-like domains (Smethurst *et al.*, 2004).

1.4. Discoidin Domain Receptors

The Discoidin Domain Receptors (DDRs) are a novel subfamily of RTKs. Two members of this family exist, DDR1 {previously known as DDR (Johnson *et al.*, 1993), trkE (Di Marco *et al.*, 1993), NEP (Zerlin *et al.*, 1993), RTK6 (Laval *et al.*, 1994, Cak (Perez *et al.*, 1994), Ptk-3 (Sanchez *et al.*, 1994), MCK10 (Alves *et al.*, 1995), EDDR1 (Shelling *et al.*, 1995), and NTRK4 (Valent *et al.*, 1996)} and DDR2 {also known as TKT (Karn *et al.*, 1993), Tyro 10 (Lai and Lemke, 1994) CCK-2 (Alves *et al.*, 1995)}. The DDRs were named as such due to the presence of a motif in the ECD, which is homologous to the *Dictyostelium discoideum* protein, discoidin 1 (Vogel *et al.*, 1997).

Most RTKs bind soluble protein present in blood or other body fluids. DDR1 and DDR2 are an unusual class of RTKs, as they bind collagen in the ECM (Shrivastava *et al.*, 1997; Vogel *et al.*, 1997). Several different collagens act as physiological ligands that activate DDR1 and DDR2. Both are activated by fibrillar collagens I, II, III and V (and VIII in the case of DDR1), whereas only DDR1 responds to non-fibrillar collagen type IV (Shrivastava *et al.*, 1997; Vogel, 1999; Hou *et al.*, 2001). Both DDR1 and DDR2 only bind native, triple-helical collagen and not collagen which has been heat denatured, nor do they bind to gelatine (Vogel *et al.*, 1997). Furthermore, collagen treated with collagenase, which disrupts Gly-X-Y repeats, does not activate the DDRs, whereas treatment of collagen with pepsin, which digests only at the N- and C-terminal non-helical regions, has no effect on DDR activation. It has been suggested that carbohydrates bound to the collagen may be involved in DDR-collagen recognition and activation as periodate treatment of collagen, which results in

partial deglycosylation of collagens, prevented full activation of DDR2 (Vogel *et al.*, 1997). It has been demonstrated by using recombinant DDR ECDs that DDR binding to collagens is direct, occurs with high affinity and does not require a co-receptor or accessory proteins (Leitinger, 2003). The kinetics of DDR activation by collagen is very slow, differing from the kinetics of growth factor activation of most RTKs. For example EGF and PDGF stimulate receptor activation within seconds, whereas DDR tyrosine phosphorylation is detected only after 30-60 minutes of collagen stimulation and the phosphorylation is sustained for up to 18 hours (Shrivastava *et al.*, 1997; Vogel *et al.*, 1997). The reason for such slow kinetics is unclear, however in a study which sought to look at the effect of adhesion on DDR1 activation, it was found that cells in suspension were able to activate DDR1 rapidly, when compared with adherent cells (L'hote *et al*, 2002). The authors proposed that in adherent cells, there may be a phosphatase which inhibits DDR1. Another possibility is that DDR1 may be involved in cell adhesion itself or bound to an inhibitory matrix protein and therefore not easily accessible to collagen in adherent cells. Further research is needed to prove these hypotheses and find the mechanism for slow phosphorylation kinetics of the DDRs.

1.4.1. DDR Structure

Both DDR1 and DDR2 contain an N-terminal ECD which contains a discoidin homology domain (DS) domain of about 150 amino acids. This domain is homologous to the discoidin 1 protein of *Dictyostelium discoideum*, which functions as a sugar-binding lectin (Springer *et al.*, 1984). Mammalian examples of DS domain containing proteins are secreted proteins such as the blood coagulation factors V and VIII (reviewed in Baumgartner *et al.*, 1998); and membrane-bound proteins such as neurexins, neuropillins (Lee *et al.*, 2003) trkA receptor; and the matrix-binding proteins Del-1 and aortic carboxypeptidase-like protein (reviewed in Baumgartner *et al.*, 1998; Vogel, 1999).

In the DDRs, the DS domain is followed by a region of about 220 amino acids with no known sequence homology, which most likely folds into a domain (named domain X in this report), as suggested by findings with ECD constructs of varying lengths (E.Hohenester - personal communications). It was found that a construct containing the DS domain on its own is a monomer, while further constructs extending the DS domain by a stepwise addition of 20 amino acids did not express until a construct consisting of the DS domain and the following 170 amino acids (up to Asp 354), showed expression and dimerisation. It is most likely, therefore, that the region after the DS domain folds into a domain and is not unstructured. In DDR1, a largely hydrophilic region rich in proline and glycine (P/G) residues follows the domain X. The TM domain region ensues, consisting of a single α helix of 23 amino acids. The amino acid sequence of the TM domain is greatly similar between DDR1 and DDR2. The TM domain is followed by a cytoplasmic juxtamembrane region, which is unusually long in both DDRs compared with other RTKs (176 and 147 amino acids in DDR1 and DDR2, respectively) and a C-terminal catalytic tyrosine KD, which is highly conserved among all RTKs studied so far and 45% homologous to the KD of NGF receptor, TrkA (Foehr *et al.*, 2000). In addition, the G-X-G-X-X-G 'signature' sequence, found in N-terminal region of most other RTK KDs, is displaced by 12 residues in the DDRs relative to other RTKs (Foehr *et al.*, 2000). Figure 1.9 shows a schematic diagram of DDR1 and DDR2 domain organisation.

DDR1 consists of three active isoforms a, b and c, as a result of alternative splicing in the cytoplasmic region (Alves *et al.*, 2001). Compared to DDR1a, DDR1b has an insertion of 37 amino acids in the juxtamembrane region encoded by exon 11. DDR1c contains six additional amino acids inserted at the start of the KD. In addition, two kinase deficient DDR1 isoforms, DDR1d and DDR1e were identified (Alves *et al.*, 2001). DDR1d protein lacks the KD domain altogether, while DDR1e has a deletion of exons 10a, 11, and 12 plus an altered

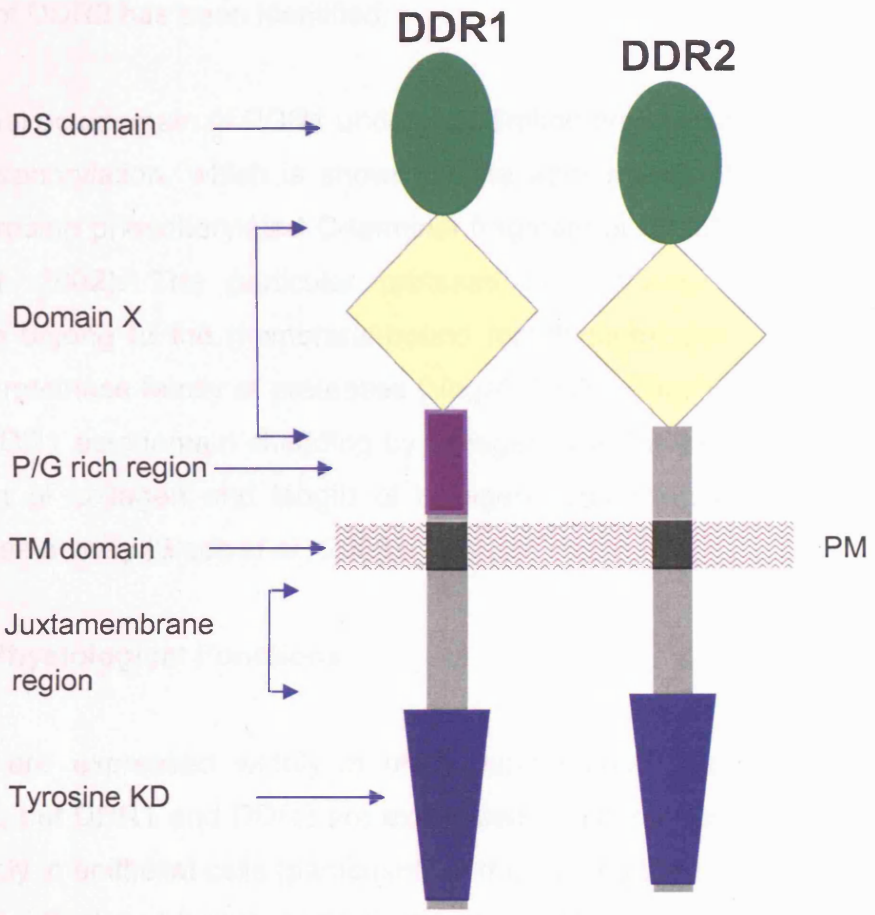

Figure 1.9: Schematic diagram of DDR1 and DDR2 domain architecture. Both DDR1 and DDR2 contain an N-terminal discoidin (DS) domain, followed by a region with no known homology or domain X, a transmembrane (TM) domain, a cytosolic juxtamembrane region and a C-terminal tyrosine KD. DDR1 contains a proline and glycine (P/G) rich region between the domain X and TM domain which is not present in DDR2.

sequence in the juxtamembrane region, rendering it kinase dead. So far, only one isoform of DDR2 has been identified.

The N-terminal ectodomain of DDR1 undergoes limited proteolysis (~10%) upon tyrosine phosphorylation, which is shown by the appearance of a membrane anchored, tyrosine phosphorylated C-terminal fragment of 62 kDa (Alves *et al.*, 1995; Vogel, 2002). The particular protease or sheddase involved was suggested to belong to the membrane-bound metalloproteinase or disintegrin and metalloproteinase family of proteases (Vogel, 2002). Recently, Slack *et al.*, found that DDR1 ectodomain shedding by collagen type I is dependent on the concentration of collagen and length of collagen stimulation as well as Src tyrosine kinase activity (Slack *et al.*, 2006).

1.4.2. DDR Physiological Functions

Both DDRs are expressed widely in most human adult tissue and during development, but DDR1 and DDR2 are expressed in different cell types. DDR1 is found mainly in epithelial cells (particularly in the skin epithelium, kidney, lung, gastrointestinal tract and brain), corneal and dermal fibroblasts, and leukocytes (Alves *et al.*, 1995; Chin *et al.*, 2001; Kamohara *et al.*, 2001; Mohan *et al.*, 2001; Sakamoto *et al.*, 2001). DDR2 is expressed in mesenchymal cells such as skeletal muscle, heart, blood vessels and connective tissues (Vogel, 1999). In addition, DDR1 mRNA is upregulated in several human malignant tumours originating in the breast (Barker *et al.*, 1995; Perez *et al.*, 1996), ovaries (Laval *et al.*, 1994), eosophagous (Nemoto *et al.*, 1997), pediatric brain (Weiner *et al.*, 1996; Weiner *et al.*, 2000). It has been found that DDR2 protein is present in stromal cells surrounding highly invasive, DDR1 positive tumours (Alves *et al.*, 1995).

The physiological functions of the DDRs are being discovered, but it is now clear that these receptors play an important role in cell adhesion, cell migration and

motility, cell differentiation, proliferation, and matrix remodelling. Female DDR1 knockout mice (DDR1-/-) were viable, but significantly smaller than control mice (Vogel *et al.*, 2002). Figure 1.10 (a) shows X-rays of 10-week-old DDR1 heterozygous (DDR1+/-) and DDR1-/- mice. Importantly, DDR1-/- contained severe mammary gland development defects and impaired blastocyst implantation. DDR1-/- mice were unable to lactate due to aberrant mammary gland ductal morphogenesis (Vogel *et al.*, 2001). Most significantly, mice lacking the primary mammary collagen receptor, $\alpha 2\beta 1$ integrins, showed decreased branching morphogenesis but no lactational defect (Chen *et al.*, 2002) – therefore a more severe mammary gland defect is seen in DDR1-/- mice when compared with integrin $\alpha 2\beta 1$-/- mice. Insight into the role of DDR1 in mammary gland function and lactogenesis (Faraci-Orf *et al.*, 2006), showed that DDR1 signalling is essential to maintain Stat5 activation, a downstream signal transducer of the prolactin pathway, the signalling pathway which is required for the transcription of milk proteins. DDR2 deficient mice (DDR2-/-) exhibit dwarfism and shortening of long bones, due to reduced chondrocyte proliferation (Labrador *et al.*, 2001). Figure 1.10 (b) compares images of Alizarin red-stained tibia and humerus bones from DDR2-/- and WT DDR2 mice.

The DDRs are associated with a variety of human diseases. Both DDRs are linked with different types of cancers (Laval *et al.*, 1994; Barker *et al.*, 1995 Nemoto *et al.*, 1997; Perez *et al.*, 1996; Weiner *et al.*, 1996; Weiner *et al.*, 2000; Heinzelmann-Schwarz *et al.*, 2004; Dejmek *et al.*, 2005; Ram *et al.*, 2005; Wall *et al.*, 2005). The DDRs are suggested to play a role in artherosclerosis (Ferri *et al.*, 2004) and osteoarthritis (Xu *et al.*, 2004). The DDRs are implicated in fibrotic diseases of the liver (Olaso *et al.*, 2001; Olaso *et al.*, 2002) and lung (Matsuyama *et al.*, 2005; Matsuyama *et al.*, 2006a; Matsuyama *et al.*, 2006b). The roles played by the DDRs in these diseases will be described in more detail.

Recently, DDR1a was shown to be involved in glioblastoma multiforme, a malignant astrocytic glioma (Ram *et al.*, 2005). Both DDR1a and DDR1b protein

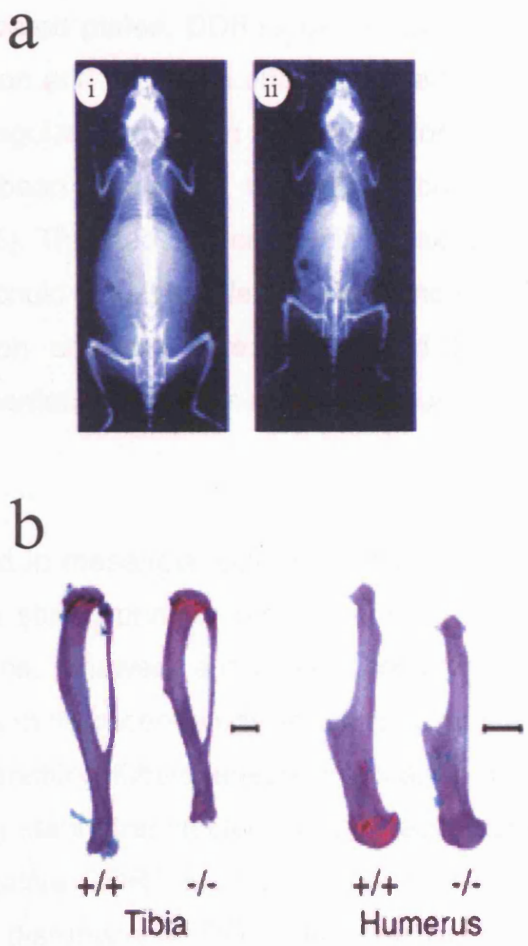

Figure 1.10: DDR1 and DDR2 null mice. (a) X-rays of 10-week-old heterozygous DDR1+/- (i) and DDR1-/- (ii) female mice. (Image taken from Vogel *et al.*, 2001). DDR1 null mice are viable, although on average, had a 35% lower body weight than heterozygous mice. (b) Alizarin red-stained bones from DDR2 wild-type (+/+) and homozygous mutant (-/-) mice. DDR2-/- mice show shortening of long bones compared with DDR2 wild-type mice. Scale bar=2 mm. (Image taken from Labrador *et al.*, 2001).

was found to be over-expressed in glioma tissue, and resulted in increased adherence to collagen I coated plates. DDR1a over-expression in glioma cells displayed enhanced invasion and migration and stimulated activation of MMP2, implicating that DDR1a regulates invasion and adhesion of glioma cells by activating MMP2. It has been suggested that DDR2 could regulate tumour formation (Wall *et al.*, 2005). The study which sought to explore the mechanism by which fibrillar collagen could inhibit proliferation of tumour cells, independent of cytoskeletal organization and cell spreading, found that DDR2 induced signalling was a central mediator of fibrillar collagen induced tumour cell cycle arrest (Wall *et al.*, 2005).

DDR1 has been implicated in mesangial cell proliferation and adhesion (Curat and Vogel, 2002). In this study, primary mesangial cells, obtained from the kidney from DDR1-/- mice, showed enhanced proliferation and adhesion compared with WT cells. A more recent study sought to examine the function of DDR1 in HGF-induced branching tubulogenesis in collagen gel culture system (Wang *et al.*, 2005). Using stably transfected MDCK cells over-expressing WT DDR1 or a dominant negative DDR1 mutant, it was shown that either over-expressing WT DDR1 or disruption of DDR1 function by dominant negative DDR1 was inhibitory for branching tubulogenesis. Further experiments by these investigators suggested that DDR1 regulates branching tubulogenesis by modulating cell survival, proliferation and migration. DDR1 has also been shown to be required for arterial wound repair as primary vascular smooth muscle cells isolated from DDR1-/- mice showed decreased proliferation, collagen attachment, and migration *in vitro* (Hou *et al.*, 2001; Hou *et al.*, 2002). In addition, DDR1 signalling is essential for cerebellar granule differentiation (Bhatt *et al.*, 2000).

DDR1 upregulation has been detected in human leukocytes (such as neutrophils, monocytes and lymphocytes) *in vitro,* and it was shown that DDR1 was responsible for leukocyte activaton, including adhesion, migration

differentiation and cytokine/chemokine production (Yamashiro *et al.*, 2001; Kamohara *et al.*, 2001). The DDR1a isoform promotes migration of leukocytes in three dimensional (3D) collagen (Kamohara *et al.*, 2001). Using the human monocytic leukaemia cell line, THP-1, overexpressing DDR1a or DDR1b, the investigators showed that the DDR1a isoform specifically enhanced migration in cell culture inserts and 3D collagen lattices, whilst DDR1b had no effect. Collagen activation of DDR1b, but not DDR1a, facilitated the differentiation of THP-1 cells and human monocyte derived primary macrophages (Matsuyama *et al.*, 2003b). Activation of the DDR1b isoform has also been shown to promote differentiation of monocyte derived dendritic cells (Matsuyama *et al.*, 2003a). In this study, the activation of DDR1b isoform in combination with other dendritic cell maturation signals, resulted in the expression of cell surface molecules characteristic of mature dendritic cells. Recently, DDR1b activation was shown to be responsible for the production of cytokines and chemokines by macrophages (Matsuyama *et al.*, 2004). Using cDNA array analysis and Nothern blotting, the investigators showed that in the presence of collagen, a THP-1 cell line over-expressing DDR1b had significant upregulation of cytokine/chemokine mRNA compared with mock transfected cells.

The role of DDR1 in idiopathic pulmonary fibrosis (IPF), a chronic lung disorder,has been recently described (Matsuyam *et al.*, 2005; Matsuyama *et al.*, 2006a; Matsuyama *et al.*, 2006b). DDR1b expression was shown to be higher in bronchoalveolar lavage fluid (BALF) cells from IPF patients, compared with control samples. In addition, DDR1 activation in BALF cells from IPF patients induced chemokine production and MMP-9 expression, implicating DDR1 involvement in the pathogenesis of IPF (Matsuyama *et al.*, 2005). DDR1b was shown to contribute to the survival of lung fibroblast in IPF (Matsuyama *et al.*, 2006a). Using primary fibroblasts obtained from IPF and non-IPF patients, DDR1b expression was examined and found to be significantly higher in fibroblasts from IPF patients. In addition, DDR1 activation in IPF fibroblasts inhibited Fas ligand-induced apoptosis. Furthermore, a role for DDR1 in

attenuating lung inflammation was demonstrated using RNA interference and a bleomycin-induced pulmonary fibrosis mouse model (Matsuyama *et al.*, 2006b). Suppression of DDR1 expression *in vivo* reduced infiltration of inflammatory cells, inflammatory cell counts, certain cytokine concentrations and TGFβ up-regulation in bronchoalveolar lavage fluid as well as reduction of collagen deposition in the lung.

DDR2 is involved in the regulation of cell proliferation of chondrocytes, hepatic stellar cells and fibroblasts (Labrador *et al.*, 2001; Olaso *et al.*, 2001; Olaso *et al.*, 2002). During liver injury, DDR2 expression and signalling is induced in hepatic stellate cells, promoting proliferation and invasion of these cells by inducing the expression of MMP2, a collagenase which degrades the ECM by breaking down mainly collagen type IV (Olaso *et al.*, 2001). In addition, DDR2 plays an important role in wound healing, as revealed by delayed wound healing in DDR2-/- (Olaso *et al.*, 2002). The investigators demonstrated that activation of DDR2 in wound fibroblasts during wound healing induced enhanced expression of MMP2, which in turn results in enhanced migration of these cells. In addition, the activation of DDR2 increases the expression of MMP1 suggesting a role for DDR2 in collagen-matrix recognition and remodelling (Vogel *et al.*, 1997). Increased expression of DDR2 in knee cartilage of mice which developed osteoarthritis as a result of a heterozygous mutation in type XI collagen, correlated with elevated expression of MMP13 (Xu *et al.*, 2004). Further experiments using cultured chondrocytes, suggested that collagen II mediated DDR2 activation was responsible for MMP13 expression, thereby contributing to cartilage damage in osteoarthritis.

Both DDRs are upregulated in smooth muscle cells in lesions of artherosclerosis and lymphangioleiomyomatosis (LAM), obstructive diseases of blood vessels and lung, respectively (Ferri *et al.*, 2004). Furthermore, it was demonstrated that the DDR signalling in cultured human smooth muscle cells down regulates collagen I production and induces collagen degradation though the activation of

MMP1 and MMP2. Both MMP levels were increased in LAM nodules, and taken together with the above data, the investigators suggested that collagen-mediated activation of the DDRs plays a role in smooth muscle cell-mediated collagen remodelling in lesions of artherosclerosis and LAM.

1.4.3. DDR Signalling

Little is known about the signalling pathways activated by the DDRs in response to collagens. The 37 amino acid insertion found in the juxtamembrane of DDR1b, contains the LXNPXY motif, which is required for the binding of the PTB domain of the adaptor protein Shc. It has been shown that tyrosine phosphorylation and activation of DDR1b recruits Shc (Vogel *et al.*, 1997; Foehr *et al.*, 2000; Vogel *et al.*, 2000). Using chimaeric receptors containing the DDR1a juxtamembrane domain, Foehr *et al.* also show that FGF receptor substrate 2 (FRS-2) binds to the juxtamembrane region of DDR1a *in vivo* (Foehr *et al.*, 2000). Activation of DDR2 also results in association with Shc; this interaction is thought to be mediated by Src tyrosine kinase (Ikeda *et al.*, 2002). Recently, Yang *et al.* demonstrated that Src phosphorylates Tyr 740 in the activation loop of DDR2 KD, which in turn stimulates intramolecular autophosphorylation, leading to phosphotyrosine formation in the DDR2 cytosolic domain and formation of Shc signalling complexes at the DDR2 cytosolic domain (Yang *et al.*, 2005).

It has was shown that DDR1b transcription and activation is induced by the p53 tumour suppressor gene in response to DNA damage (Ongusaha *et al.*, 2003). In HEK293T cells transfected with DDR1b, activation of DDR1b induces activation of the classical Ras/raf/MAPK pathway, therefore promoting cell survival. However, the Ras/MAPK pathway was not found to be activated by DDR1 in another study (Vogel *et al.*, 2000). Data from this study suggested that there is no activation of MAPK, ERK1 or ERK2 in the human mammary tumour cell line T47D endogenously expressing DDR1b.

In addition, there is evidence for DDR1 activation of the p38 MAPK signalling pathway in leukocytes (Matsuyama *et al.*, 2003a; Matsuyama *et al.*, 2004).This signalling pathway was thought to be the underlying mechanism for the differentiation of macrophages (Matsuyama *et al.*, 2003a) and up-regulation of chemokine production by these cells (Matsuyama *et al.*, 2004). The investigators tested the involvement of TNF receptor-associated factor 6 (TRAF6), TGF-β-activated protein kinase 1-binding protein 1 (TAB1) as a mechanism to activate p38 MAPK in differentiated THP-1 cells. They found that activation of DDR1b with collagen induced formation of a protein complex consisting of the above three components, followed by autophsophorylation of p38αMAPK; indicating the TRAF6/TAB1β/p38α cascade in DDR1b signalling. Mutational analysis and co-immunoprecipitation of Shc with phosphorylated DDR1b in differentiated THP-1 cells showed that Shc was recruited to activated DDR1b in macrophages. In addition, the activation of DDR1b in macrophages was shown to activate nuclear factor-κB (NF-κB) (Matsuyama *et al.*, 2004). Recruitment of Shc and TRAF6 were shown to be important for signalling leading to activation of NF-κB. Using RNA interference, the NF-κB activator, Act1, was shown to be involved in IκB degradation. A schematic representation of the above described DDR1b signalling pathway in differentiated THP-1 cells is shown in Figure 1.11.

The potential interaction of β1 integrins with DDR1 has been investigated (Vogel *et al.*, 2000). The investigators demonstrated that DDR1 is fully activated in the presence of blocking antibodies to the β1 integrins. In addition, full DDR1 activation was detected in cells lacking β1 integrins; therefore β1 integrins are not essential for DDR1 signalling to occur. There is evidence for the requirement of the Wnt5A signalling protein for DDR1 activation, as investigated in HB2 and MCF-7 mammary carcinoma cell lines (Jonsson and Andersson, 2001; Dejmek *et al.*, 2003). In these cells, the effect of Wnt5A on DDR1 is thought to be mediated by the G-protein signalling pathway and suggested to regulate normal

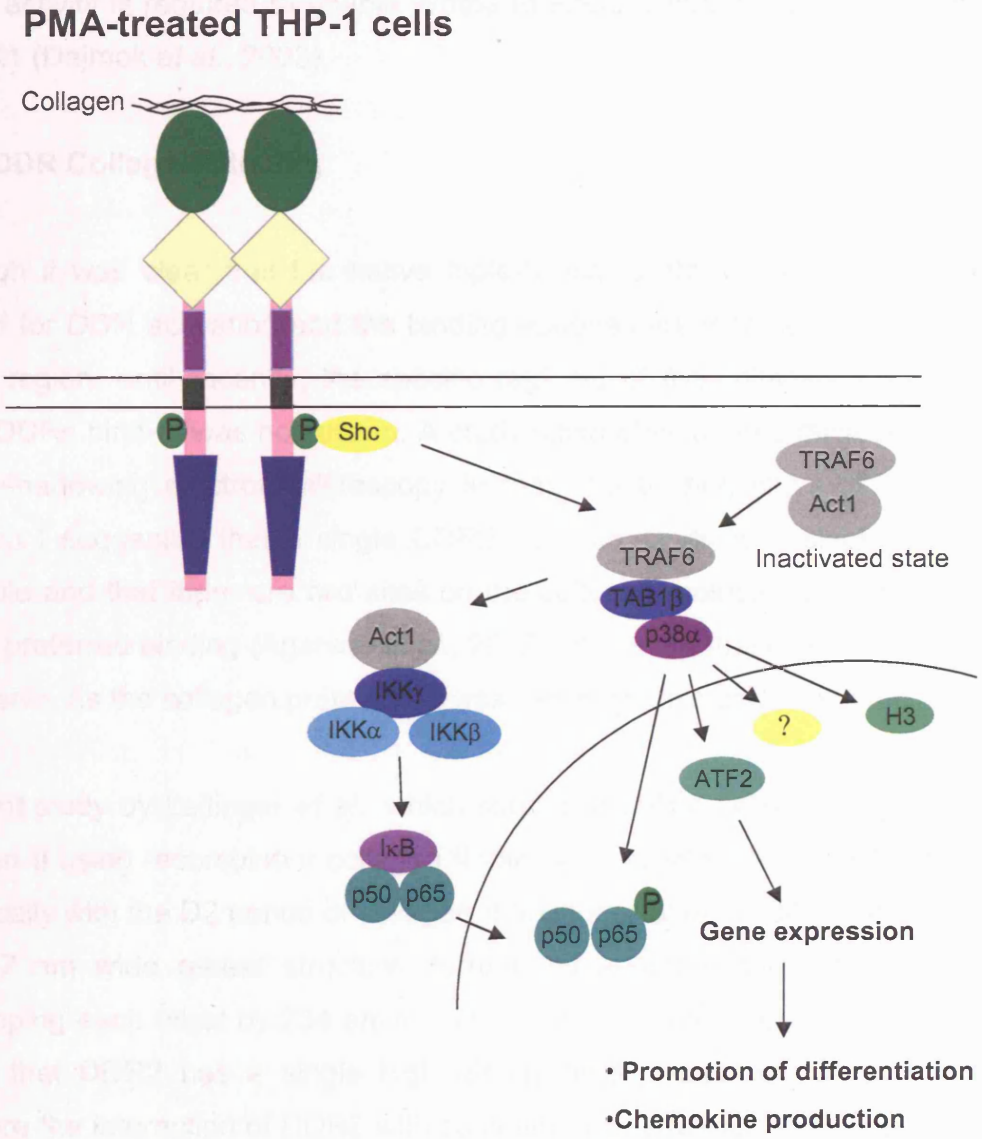

Figure 1.11: DDR1b signalling in differentiated THP-1 cells. Collagen activation of DDR1b induces the recruitment of Shc and transduces signals that lead to the activation of p38 MAPK and NF-κB. TRAF6 is an important signalling molecule involved in DDR1b signalling. (Figure adapted from Yoshimura *et al.*, 2005).

mammary cell adhesion. Additionally, Dejmek *et al.* discovered that Src tyrosine kinase activity is required to enable Wnt5a to effect collagen-induced activation of DDR1 (Dejmek *et al.*, 2003).

1.4.4. DDR Collagen Binding

Although it was clear that the native triple-helical conformation of collagen is needed for DDR activation and the binding epitopes are located in the Gly-X-Y repeat region, until recently, the specific region/s of the collagen molecule to which DDRs bind to was not known. A study using atomic force microscopy and rotary shadowing electron microscopy to map the binding site/s of DDR2 on collagen I suggested that a single DDR2 complex binds to a single collagen molecule and that there are two sites on the collagen molecule to which DDR2 shows preferred binding (Agarwal *et al.*, 2002). However, these results were not conclusive, as the collagen preparation was heterogenous and lacked polarity.

A recent study by Leitinger *et al.*, which sought to define DDR binding sites on collagen II using recombinant collagen II variants, revealed that DDR2 interacts specifically with the D2 period of collagen II (Leitinger *et al.*, 2004). The D period is a 67 nm wide repeat structure, formed by adjacent collagen monomers overlapping each other by 234 amino acids within the collagen fibril. This study shows that DDR2 has a single high affinity binding site on collagen II and therefore the interaction of DDR2 with collagen has sequence specificity. This is in contrast to the integrins, $\alpha 1\beta 1$ and $\alpha 2\beta 1$, which recognise collagen I at multiple recognition sites (Morton *et al.*, 1994; Xu *et al.*, 2000), and the platelet GPVI receptor which is also expected to have multiple binding sites on the collagen triple-helix. As mentioned before, GPVI recognises the sequence G-P-O, which occurs with relatively high frequency within collagen I - approximately 12% of the primary sequence (Kehrel *et al.*, 1998).

It has been shown that the extracellular N-terminal DS domain is required for collagen binding (Curat *et al.*, 2001; Leitinger, 2003). In order to investigate whether the DS domain of DDR2 was sufficient for high affinity binding to collagen I, soluble ECD fragments of DDR deletion mutants were produced and tested for collagen I binding using a solid phase binding assay (Leitinger, 2003). An ECD fragment containing the DDR2 DS domain with the domain X missing, bound to collagen I with high affinity. In addition, when a DDR2 mutant lacking the domain X was expressed on the cell surface and stimulated with collagens, it was observed that autophosphorylation of this mutant occurred in a manner similar to WT DDR2, demonstrating that the collagen binding site on DDR2 is contained within the DS domain.

The DDR DS domain contains four potential surface exposed loops (Leitinger, 2003). Homologous loop regions found in other DS domains, such as the factor V and VIII, are critical for ligand binding (Fuentes-Prior *et al.*, 2002). In a study which looked at DDR-collagen binding sites in more detail, the DDR2 DS domain loops were replaced with loops from a functionally unrelated DS domain (Leitinger, 2003).Three of the four loop chimeras lost the ability to bind collagen I, and were not activated upon stimulation with collagen I. Thus three potential loops of the DS domain of DDR2 are critical for collagen binding and signalling. Subsequently, a very similar study was carried out for DDR1 (Abdulhussein *et al.*, 2004). A three-dimensional model of DDR1 DS domain, based on the related domains of factor V and VIII was created. Individual amino acids were mutated or short sequences were deleted within four neighbouring cell surface exposed loops of the DS domain, in context of full-length DDR1. Collagen binding ELSA using these loop mutants showed that loops 1 and 3 were required for DDR1-collagen recognition.

1.4.5. Mechanism of DDR Activation

Recent studies using soluble ECDs showed that the DDRs need to be dimerised in order to bind ligand (Leitinger, 2003). Chemical cross-linking analysis and gel filtration results of soluble N-terminally His-tagged DDR2 ECD showed His-DDR2 to exist mainly as a dimer while His-DDR1 forms monomers. Thus there is a difference in the DDRs in their ability to dimerise. In contrast to His-DDR2 which bound collagen I with high affinity, His-DDR1 showed no recognition of collagen. DDR1 bound collagen with high affinity only when fused to a dimerising Fc tag, indicating that DDR dimerisation is required for collagen binding. Another study by Agarwal *et al.* reported that a DDR2-Fc fusion protein needed to be clustered or multimerised by antibodies in order to bind collagen I (Agarwal *et al.*, 2002).

DDR1 and DDR2 differ in the contribution of receptor domains needed for activation and dimerisation (Leitinger, 2003). DDR1 and DDR2 deletion mutants were constructed and studied for their ability to be activated by collagen I. DDR1 deletion mutants lacking the domain X, both domain X and the P/G rich region, or the DS domain, did not show autophosphorylation in response to collagen I. In the case of DDR2 deletion mutants, a mutant lacking the DS domain was not activated upon collagen stimulation, although a mutant lacking the domain X was able to respond to collagen as WT DDR2. Thus, DDR1 needs the entire extracellular region whilst DDR2 needs only the DS domain for collagen binding and receptor activation. Therefore, despite the close similarity between DDR1 and DDR2 protein sequence, it appears that the two receptors use different mechanisms for receptor dimerisation and/or conformational change propagation.

HYPOTHESIS

As the DDR ECDs bind collagen only when dimerised, we hypothesise that the DDRs exist as preformed oligomers on the cell surface, in the absence of ligand. In addition, there might be a difference between DDR1 and DDR2 in the contribution of receptor domains needed for dimerisation.

PROJECT AIMS

The overall aim of this project is to investigate the mechanism of activation of DDR1 and DDR2. In order to do so, this study looks at two specific areas of interest:

1) The above described studies using the ECD of DDRs give insight into the oligomerisation state of these receptors; however, the presence of other domains such as the TM, cytoplasmic and juxtamembrane domain can influence the oligomeric state of DDRs on the cell surface. Therefore, the first aim is to investigate the oligomeric state of WT, full-length DDRs on the cell surface in the absence of ligand.

2) The second aim is to investigate the DDR domains required for receptor oligomerisation.

Chapter 2

Materials and Methods

2.1. Materials

2.1.1. Chemicals, reagents and buffers

2.1.1.1. Mammalian cell culture and transfection

Human embryonic kidney 293 cells (HEK293 and HEK293 TSA 201 cells: obtained from the American tissue culture collection, Manassas, VA.
MCF-7 cells: were obtained from Dr. Maffucci (UCL).
Rat-1 cells: were obtained from Dr. Michel Faure (SUGEN Inc., San Francisco, CA).
Dulbecco's modified Eagle's medium/F-12 nutrient mixture, Dulbecco's modified Eagle's medium (without sodium pyruvate), Trypsin-EDTA and Zeocin (100 mg/ml): Invitrogen, Paisley, UK.
100x P/S (1000 U/ml penicillin and 1000 μg/ml streptomycin in PBS) and 100x Glutamine (1000 U/ml): Gibco Life Technologies, Paisley, UK.
FuGENE 6: Roche Diagnostics, Indianapolis, IN.
Di-methyl-sulfonylfluoride (DMSO): Sigma-Aldrich Inc., Dorset, UK.
2x HBS: 290 mM NaCl, 50 mM HEPES buffer, 1.5 mM Na_2HPO_4, pH 7.1.
ddH_20: distilled, autoclaved H_20.

2.1.1.2. Receptor assays, mammalian cell lysis, immunoprecipitation and carbohydrate analysis

*Aprotonin and collagen I (*acid-soluble from rat tail, C-7661): Sigma-Aldrich, Saint Louis, MO.
Bis(sulfosuccinimidyl) suberate (BS^3): Perbio Science,Tattenhall, UK.
Sulfosuccinimidyl-6-(biotin-amido)-6-hexanoate(Sulfo-NHS-LC-Biotin):Pierce, Rockford, Illinois.
Protein A, protein G sepharose beads and streptavidin sepharose beads: Amersham Biosciences, Buckinghamshire, UK.
Protease inhibitor cocktail: Roche Diagnostics, Indianapolis, IN.
Endoglycosidase H (Endo H) and Peptide: N-Glycosidase F (PNGaseF): 500,000 units/ml, New England Biolabs (Hitchin, UK).

Endoglycosidase reaction buffer pack: New England Biolabs, Hitchin, UK – *description of components as follows:*
1x G7 reaction buffer (for PNGase F): 50 mM sodium phosphate, pH 7.5.
1x G5 reaction buffer (for Endo H): 50 mM sodium citrate, pH 5.5.
1x glycoprotein denaturing buffer: 0.5% SDS, 1% *β*-mercaptoethanol.
Neuraminidase (1 unit/ml) and O-glycosidase (0.5 units/ml): Roche Diagnostics, Indianapolis, IN.

2.1.1.4. SDS-PAGE and Western blotting

Pre-stained protein marker (moleculer weight range: 175, 83, 62, 47.5, 32.5, 25, 16.5 and 6.5 kDa) and broad range protein marker (molecular weight range: 212, 158, 116, 97, 66, 56, 43, 35, 27, 20, 14, 6.5, 2.4 kDa): New England Biolabs, Hitchin, UK.
2x SDS sample buffer: 125 mM Tris-HCl (pH 6.8), 4% SDS, 10 % glycerol, 0.1%, bromophenol blue and 1% β-mercaptoethanol for reduced sample buffer.
5x SDS sample buffer: 300 mM Tris-HCl pH 6.8, 10% SDS, 10% glycerol, 0.1% bromophenol blue and 10% β-mercaptoethanol for reduced sample buffer.
30% a*crylamide/0.8% bisacrylamide:* Amresco, Solon, Ohio.
Tetraethylmethylenediamine (TEMED): Fluka BioChemika (Buchs, Switzerland)
Nitrocellulose (NitroBlind, 0.22 micon): Satouris Ltd, Epson, UK.
DE81 DEAE paper: Whatman
SDS running buffer (1X): 25 mM Tris base, 250 mM glycine, 0.1% SDS, pH 8.3.
SDS blotting buffer (1X): 25 mM Tris base, 192 mM glycine, 20% methanol, 0.01% SDS, pH 7.5.
PBS (1x): 1.4 M NaCl, 0.018 M KH_2PO_4, 0.027 M KCl, 0.08 M $Na_2H\ PO_4$

Tween 20, ponceau-S solution (0.1% ponceau-S, 1% acetic acid), SDS (electrophoresis-grade), Triton X-100, β-mercaptoethanol, $CaCl_2$, *NaCl,* Na_2HPO_4, NaH_2PO_4, *methanol, ethanol, isopropanol, acetic acid, ammonium persulphate, Tris base (electrophoresis grade), glycine (electrophoresis grade) and HEPES:* Sigma-Aldrich, Saint Louis, MO.
Enhanced chemi-luminescent (ECL) western blotting detection reagents 1 and 2: Amersham Pharmacia Biotech, Little Chalfont, UK.
Stripping buffer: 62.5 mM Tris, pH 6.8, 2% SDS, 100 mM β-mercaptoethanol.
Antibody stripping solution: Alpha Diagnostic International, San Antonio, TX.

2.1.1.5. Antibodies and sources

Primary Antibodies

Rabbit anti-DDR1 Ig, sc-532 and goat anti-DDR2 Ig, sc-7554 (recognises C-terminal DDR1 and DDR2 epitope, respectively): Santa Cruz Biotechnology,
Rabbit anti-DDR1 Ig, 74A: obtained from Dr. Michel Faure, SUGEN Inc., San Francisco, CA (recognises N-terminal DDR1 epitope).
Mouse anti-MYC tag, clone 9E10 and anti-phophotyrosine, clone 4G10: Upstate Biotechnology, Lake Placid, NY.
Rabbit anti-MYC tag, sc-789: Santa Cruz Biotechnology, Santa Cruz, CA.
Mouse anti-FLAG, M2 and rabbit anti-FLAG polyclonal, F7425: Sigma-Aldrich, Saint Louis, MO.
Goat anti-ERK2, sc1549 and rabbit anti-Rho-GDI, A-20: Santa Cruz Biotechnology, Santa Cruz, CA.

Secondary Antibodies

Goat anti-mouse Ig-HRP: Amersham Biosciences UK, Little Chalfont, UK.
Goat anti-rabbit Ig-HRP: Dako, Ely, UK.
Rabbit anti-goat IgG-HRP: ZYMED Laboratories Inc. San Francisco, CA.

2.1.1.6. PCR, sub-cloning and DNA gel electrophoresis

PCR primers (PAGE purified, 0.05 μg scale): Sigma Genosys or Invitrogen Ltd, Paisley, UK.

Restriction enzymes (BamHI, EcoRI, NotI, NcoI, NarI, XhoI, XbaI) and respective reactions buffers, bovine serum albumin (BSA, 10 mg/ml): Promega, Southampton, UK.

Pfu DNA polymerase (1 unit/ml) and 10x Pfu buffer (10 mM $(NH_4)_2SO_4$, 10 mM KCl, 2 mM $MgSO_4$, 0.1% Triton X-100, 20 mM Tri-HCl, pH 8.8): Stratagene, Amsterdam, The Netherlands.

*Taq DNA polymerase (*5 units/μl) and *10x Taq buffer (1.5 mM $MgCl_2$, 50 mM KCl, 0.1% Triton X-100, 10 mM Tris-HCl, pH 9.0):* Promega, Southampton, UK.

dNTP mix: 10 mM, contains dATP, dTTP, dCTP and dGTP (2.5 mM each), New England Biolabs, Hitchin, UK.

T4 DNA ligase and 5x T4 ligase buffer (10 mM $MgCl_2$, 1 mM ATP, 10 mM dithiothreitol, 25 μg/ml BSA, 50 mM Tris-HCl, pH 7.5): Invitrogen, Paisley, UK.

PCR-grade mineral oil, Ampicillin (1 mg/ml) and Ethidium Bromide: Sigma-Aldrich, Saint Louis, MO.

Plasmid mini-, midi- and maxi-prep kits: QIAGEN, Crawley, UK.

Luria Bertani (LB) and LB-agar: Sigma-Aldrich, Saint Louis, MO.

DH5α competent E.coli: Invitrogen Ltd, Paisley, UK.

DNA ladder, 1 kb (molecular weight markers: 10, 8, 6, 5, 4, 3, 2, 1.5, 1, and 0.5 kb) and DNA ladder, 100 bp (molecular weight markers: 1500, 1000, 900, 800, 700, 600, 500, 400, 300, 100 bp): Promega, Southampton, UK.

Orange DNA loading buffer (6x): 20% ficoll, 0.25% Orange G, 0.1 M EDTA, pH 8.0)

TE Buffer: 10 mM Tris-HCl (pH 7.5), 1 mM EDTA.

Solution I: 30 mM KOAc, 50 mM MnCl, 100 mM KCl, 10 mM $CaCl_2$, 15 % glycerol, pH to 5.8.

Solution II: 10 mM MOPS pH 7.0, 75 mM $CaCl_2$, 10 mM KCl, 15% glycerol.

2.2. Methods

The table below lists the names of plasmid vectors and constructs used:

Plasmid vectors	**Obtained from/made by**
pSP72	Invitrogen
pcDNA3.1/Zeo	Invitrogen
pS-DDR1b	B.Leitinger
pc-DDR1b	B.Leitinger
pc-DDR1-MYC	N.Noordeen
pc-DDR1-FLAG	N.Noordeen
pRK-DDR1a	Dr. Michel Faure (SUGEN Inc., San Francisco, CA)
pRK-DDR1b	Dr. Michel Faure (SUGEN Inc., San Francisco, CA)
pRK-MDN	Dr. Michel Faure (SUGEN Inc., San Francisco, CA)
pc-DS-DDR1	B.Leitinger
pc-DS-DDR1-MYC	N.Noordeen
pc-DS-DDR1-FLAG	N.Noordeen
pc-DS-DDR1-2	B.Leitinger
pc-DS-DDR1-2-MYC	N.Noordeen
pc-DS-DDR1-2-FLAG	N.Noordeen
pc-ΔDS-DDR1	B.Leitinger
pc-ΔDS-DDR1-MYC	N.Noordeen
pc-ΔDS-DDR1-FLAG	N.Noordeen
pc-ΔPG-DDR1	B.Leitinger
pc-ΔPG-DDR1-MYC	N.Noordeen
pc-ΔPG-DDR1-FLAG	N.Noordeen
pc-DDR1-ECTM	B.Leitinger
pc-DDR1-ECTM-MYC	N.Noordeen
pc-DDR1-ECTM-FLAG	N.Noordeen

pc-DDR1-TM1	B.Leitinger
pc-DDR1-TM1-MYC	N.Noordeen
pc-DDR1-TM1-FLAG	N.Noordeen
pc-DDR1-TM2	B.Leitinger
pc-DDR1-TM2-MYC	N.Noordeen
pc-DDR1-TM2-FLAG	N.Noordeen
pc-DDR1-TM3	B.Leitinger
pc-DDR1-TM3-MYC	N.Noordeen
pc-DDR1-TM3-FLAG	N.Noordeen
pc-DSTM1-DDR1-MYC	N.Noordeen
pc-DSTM1-DDR1-FLAG	N.Noordeen
pc-ΔDSTM1-DDR1-MYC	N.Noordeen
pc-ΔDSTM1-DDR1-FLAG	N.Noordeen
pc-DSΔCYTO-DDR1-MYC	N.Noordeen
pc-DSΔCYTO-DDR1-FLAG	N.Noordeen
pc-ΔDSΔCYTO-DDR1-MYC	N.Noordeen
pc-ΔDSΔCYTO-DDR1-FLAG	N.Noordeen
pc-DSTM1ΔCYTO-DDR1-MYC	N.Noordeen
pc-DSTM1ΔCYTO-DDR1-FLAG	N.Noordeen
pc-ΔDSTM1ΔCYTO-DDR1-MYC	N.Noordeen
pc-ΔDSTM1ΔCYTO-DDR1-FLAG	N.Noordeen
pc-DDR1-TA	P.Bhattia
pS-DDR2	N.Noordeen
pBSTyro10	Dr. Michel Faure (SUGEN Inc., San Francisco, CA)
pc-DDR2	B.Leitinger
pc-DDR2-MYC	N.Noordeen
pc-DDR2-FLAG	N.Noordeen
pc-DS-DDR2	B.Leitinger
pc-DS-DDR2-MYC	N.Noordeen
pc-DS-DDR2-FLAG	N.Noordeen
pc-ΔDS-DDR2	B.Leitinger

pc-ΔDS-DDR2-MYC	N.Noordeen
pc-ΔDS-DDR2-FLAG	N.Noordeen
pc-DDR2-ECTM-MYC	N.Noordeen
Pc-DDR2-ECTM-FLAG	N.Noordeen
pc-DDR2-TM1	N.Noordeen
pc-DDR2-TM1-MYC	N.Noordeen
pc-DDR2-TM1-FLAG	N.Noordeen
pc-DDR2-TM2	N.Noordeen
pc-DDR2-TM3	N.Noordeen
pc-DSTM-DDR2-MYC	N.Noordeen
pc-DSTM-DDR2-FLAG	N.Noordeen
pc-ΔDSTM-DDR2-MYC	N.Noordeen
pc-ΔDSTM-DDR2-FLAG	N.Noordeen
pMIRB/mFGFR2c-MYC	K.Yu (Washington University Medical School, St. Louis, MO)

Table 2.1: Plasmid vectors, constructs and sources

2.2.1. Sub-cloning

2.2.1.1. Preparation of competent XL-1 Blue E.coli

XL-1 Blue cells were scraped from a glycerol stock, streaked onto LB-agar plates and incubated at 37°C overnight. A single colony was picked the next day and grown in 100 ml of LB broth at 37°C. The growth of the culture was monitored by measuring the absorbance at 590 nm. After the optical density reached 0.5, the cells were collected by centrifugation at 3500 rpm (GS-6R Centrifuge, Beckman) for 5 minutes at RT and the pellet re-suspended in 20 ml Solution I (30 mM KOAc, 50 mM $MnCl_2$, 100 mM KCl, 10 mM $CaCl_2$, 15 % glycerol, pH to 5.8) and placed on ice for 30 minutes. The cells were spun again at 3500 rpm for 5 minutes (GS-6R Centrifuge, Beckman), 4°C and resuspended in 2 ml Solution II (10 mM MOPS pH 7.0, 75 mM $CaCl_2$, 10 mM KCl, 15% glycerol) and stored at 4°C overnight. The next day the cells were aliquoted and frozen at -80°C.

2.2.1.2. Extraction and purification of plasmid DNA

DNA mini-, midi- or maxi-preps were carried out in order to obtain purified plasmid DNA from bacterial cultures. Ampicillin resistant colonies were grown in 4 ml (mini-preps) or 50 ml (midi-preps) or 100 ml (maxi-preps) of LB broth containing ampicillin (80 μg/ml), overnight at 37°C with shaking. The next day the culture was spun [1 minute at 13 000 rpm for mini-preps (Heraeus Biofuge); 10 minutes at 3500 rpm for midi- and maxi-preps (GS-6R Centrifuge, Beckman) to pellet the cells. The extractions were carried out using the QIAGEN Plasmid Mini (or Midi) Prep Kit (QIAGEN) according to the manufacturer's protocol.

2.2.1.3. Determination of DNA concentration

DNA purified from mini- and maxi-preps was quantified by UV absorbance at 260 nm using 1 cm quartz cuvettes and a DU 530 Life Science UV/Vis™

spectrophotometer (Beckman). The concentration was calculated using formula 1.

Formula 1:
DNA concentration = OD_{260} x 50 x dilution factor

Alternatively, DNA concentrations were estimated by agarose gel electrophoresis by comparison to a DNA ladder (1 kb or 100 bp) of known concentration.

2.2.1.4. Restriction digestion analysis

Restriction digestion analysis was carried out on 1 μg of purified midi- or maxi-prep DNA to verify the concentration and assess the presence of the DNA of interest. For DNA obtained from mini-preps, 3 μl of DNA was analysed by restriction digestion to assess the presence of the DNA of interest. The digested samples were run on a 1, 1.5 or 2% agarose gel depending on the size of the DNA to be assessed.

2.2.1.5. Agarose gel preparation and electrophoresis

Agarose was added to 1x TAE buffer to give a final concentration of 1-2% (e.g. 1% agarose: 1.0 g agarose powder in 100 ml 1x TAE). The mixture was dissolved by heating in a microwave for 2-3 minutes, with intermittent stirring. Ethidium bromide was added to the dissolved agarose to a final concentration of 0.5 μg/ml, under a fume-hood and stirred until mixed. Gels were cast in cleaned agarose gel-trays containing well combs and allowed to set for 15-30 minutes in a fume-hood. Samples were loaded in 1x orange DNA loading buffer. DNA marker (1 μg of 1 kb or 100 bp DNA ladder) was also loaded. The gels were run in electrophoresis tanks (BioRad, Hertfordshire), containing 1x TAE buffer, at a constant voltage of 60-90 V for 30-40 minutes. Gels were visualised and photographed using an UV transluminator (UVP, Cambridge).

2.2.1.6. Purification of DNA from agarose gels

The appropriate DNA band was excised from the agarose gel using clean scalpels, under low intensity UV light. The gel slice was placed in an Eppendorf tube, weighed and purified using the QIAquick Gel Extraction Kit (QIAGEN) according to the manufacturer's instructions.

2.2.1.7. Bacterial cell transformation

XL-1 Blue competent *E.coli* (90 μl) or DH5α competent *E.coli* (50 μl, Invitrogen) were incubated with DNA (10 μl of ligation mix) for 30 minutes on ice. The XL-1 Blue cells were heat shocked at 42°C for 2 minutes, and the DH5α were heat shocked at 37°C for 20 seconds, and the tubes were placed on ice. The mixture (50 μl) was plated onto LB-agar plates containing 80 μg/ml ampicillin. The plates were incubated at 37°C overnight.

2.2.1.8. Ligations

For each ligation, 1 μl of T4 DNA Ligase (1 unit/μl, Promega or Invitrogen) and 2 μl of 10x Ligase buffer (Promega) or 4 μl of 5x Ligase buffer (Invitrogen) were mixed along with 50 ng of vector and insert DNA, the amount of which was calculated using formula 2 and the insert:vector ratio (a 3:1 insert:vector molar ratio was used for each ligation). Control reactions containing vector DNA without insert were also prepared. Ligations were performed in a total volume of 20 μl, for 1 hour at RT. The DNA was then transformed into XL-1 Blue or DH5α competent cells, plated on LB-ampicillin plates and incubated overnight at 37°C.

Formula 2:

$$\text{Insert (ng)} = \frac{\text{vector (ng) x size of insert (kb)}}{\text{vector size (kb)}} \times \text{(insert:vector molar ratio)}$$

2.2.2. Polymerase chain reaction (PCR)

PCR reactions used 1 unit of Pfu (Invitrogen) or Vent (NEB) DNA polymerase. The reaction mixtures contained: 1x Pfu or Vent reaction buffer (Invitrogen or NEB, respectively), 250 μM dNTPs (Promega), 1 ng/μl template DNA, 2.5 ng/μl each forward and reverse primer (Sigma Genosys or Invitrogen), made up to a total volume of 100 μl with ddH20. PCR reactions were carried out in a DNA Thermal Cycler™ (Perkin-Elmer) - which required overlay of reactions with 30 μl of PCR–grade mineral oil (Sigma) or alternatively GeneAmp PCR System 9700 (PE Applied Biosystems). PCR reactions were carried out using the programme shown below:

Initial denaturation: 94°C, 5 minutes
Denaturation: 94°C, 45 seconds
Annealing: (temperature varies by primer pair used), 45 seconds } 25 cycles
Extension: 72°C, 1 minute
Final extension: 72°C, 10 minutes
Soak: 4°C

PCR products (10 μl aliquot) were visualised by electrophoresis on 1.5% or 2% agarose gels stained with ethidium bromide (see section 2.2.1.5). DNA product sizes were measured against a 100 bp DNA ladder (Promega). PCR products were purified either by agarose gel electrophoresis and purification of DNA from gel (section 2.2.1.6) or without running on a gel (using the QIAquick PCR purification kit).

2.2.2.1. Colony PCR

Colonies obtained after ligation were screened either by restriction enzyme digestion of mini-prep DNA or by PCR. PCR was performed in order to screen a large number of colonies. Forward and reverse primers which flank the insertion site were used, to detect whether ligation has occurred. A master mix containing 2.5 ng/μl primers, 1.5 mM $MgCl_2$ (Promega), 250 μM dNTP mix (Promega), 1x Taq polymerase buffer and 1 unit Taq polymerase

(Promega) was made in ddH_20. Individual colonies were picked and dipped into separate reaction tubes containing 25 μl of the PCR mix. The PCR reaction was carried out as follows:

Denaturation: 94°C, 45 seconds
Annealing: 50°C, 30 seconds
Extension: 72°C, 45 seconds
} 25 cycles
Soak: 4°C

The products were separated on a 2% agarose gel. Colonies which were positive for the correct insert were re-picked and plasmid DNA isolated by mini-prep.

2.2.2.2. DNA sequencing

Sequencing of PCR amplified DNA was carried out by the Wolfson Institute of Biomedical Research (University College London). 1000-500 ng of DNA in 6 μl of ddH20 was sent with 2 pmols/μl of primer. Sequencing was also carried out by the Advanced Biotechnology Centre (Imperial College, London). Each sequencing reaction contained 1 μg of template DNA and 12.8 pmols primer in 12 μl ddH_20. Sequences were checked against published sequences of DDR1 and DDR2, obtained from www.ncbi.nlm.nih.gov. Sequence alignment was carried out using Clustalw (www.ebi.ac.uk/clutalw) and re-checked with Chromas (version 1.45).

2.2.3. C-terminally MYC- and FLAG-tagged DDR constructs

C-terminally MYC- and FLAG-tagged DDR1 and DDR2 constructs were made using Overlap Extension PCR (Horton *et al.*, 1993). Using this method, two cDNA fragments can be amplified using specific primers such that the 3' end of fragment A overlaps with the 5' end of fragment B. The overlaps serve as primers for extension by DNA polymerase to produce a single PCR product with the desired insertion, deletion or mutation. Figure 2.1 outlines

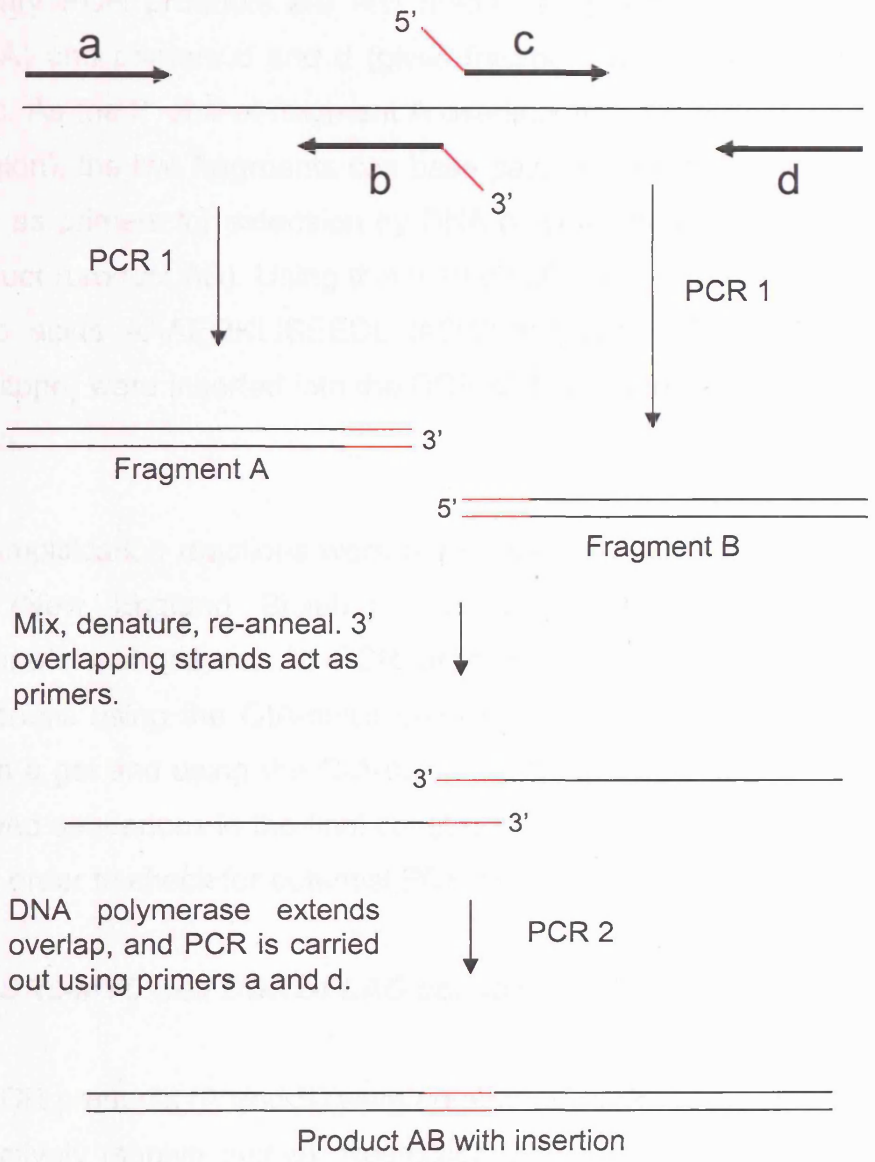

Figure 2.1: Schematic representation of Overlap Extension PCR.

how a DNA sequence with a desired insertion can be made by this method. Two primary PCR products are first made using primers a and b (gives fragment A) and primers c and d (gives fragment B). Primers b and c are mutagenic. As the 3' end of fragment A overlaps with the 5' end of fragment B (red region), the two fragments can base pair, and the overlapping 3' ends can serve as primers for extension by DNA polymerase to give a secondary PCR product (product AB). Using this method cDNA sequences encoding for the amino acids AAAEQKLISEEDL (MYC epitope) and AAADYKDDDDK (FLAG epitope) were inserted into the DDR cDNA sequences, just before the stop codon.

All PCR amplification reactions were performed with either Pfu (Strategene) or Vent (New England Biolabs) DNA polymerase according to the manufacturer's instructions. All PCR products were purified either by gel electrophoresis using the QIA-quick Gel extraction kit (QIAGEN) or without running on a gel and using the QIA-quick PCR purification kit (QIAGEN). All PCR derived sequences in the final construct were sequenced using relevant primers in order to check for potential PCR mutations.

2.2.3.1. DDR2-MYC and DDR2-FLAG constructs

Primary PCR products (A and B) were created using the primer pairs a-b and c-d respectively (shown below). Restriction enzyme sites introduced are in bold and the sequence of primes are depicted 5' to 3':

DDR2-MYC, DDR2-FLAG
primer a: CTCAAGGACCCAAACATCATCCA

DDR2-MYC
primer b:
NotI
CTCTGAGATGAGCTTCTGTTCT**GCGGCCGC**CTCGTCGCCTTGTTGAAGGAGCA

DDR2-MYC
primer c: CAGAACAGAAGCTCATCTCAGAGGAGGATCTGTGATGCTGTCAGTGCCTGG

DDR2-MYC, DDR2-FLAG
primer d: CGTTAGAACGCGGCTACAATTAATACA

DDR2-FLAG
NotI
primer b: CGTCATCGTCCTTATAGTCT**GCGGCCGC**CTCGTCGCCTTGTTGAAGGAGCA

DDR2-FLAG
primer c: CGCAGACTATAAGGACGATGACGATAAGTGATGCTGTCAGTGCCTGG

The pS-DDR2 vector (pSP72 vector containing DDR2 cDNA insert) was used as the template. PCR programme: 95°C for 5 minutes, 95°C for 45 seconds, 56°C (T_m) for 45 seconds, 72°C for 1 minute and (DNA Thermo Cycler 480, Perkin-Elmer). Both fragments were purified by gel electrophoresis (using QIA-quick Gel Extraction kit). A second PCR reaction was set up to fuse the two primary products using the primer pair a-d. PCR programme used: 95°C for 5 minutes, 95°C for 45 seconds, 56°C (T_m) for 45 seconds, 72°C for 1 minute 30 seconds.

The amplified fused PCR product AB was digested with restriction enzymes *BclI* and *XhoI* and ligated into the vector pS-DDR2 cut with *BclI* and *XhoI*. For expression in eukaryotic cells, the full-length C-terminally tagged DDR2-FLAG or DDR2-MYC cDNAs were cloned into pcDNA3.1/Zeo vector by cutting with *EcoRI-XhoI*.

The DDR2 MYC- and FLAG-tagged constructs were designed with a *NotI* site just before the epitope tag and stop codon in order that the 'vector' containing epitope tag from these two constructs can be used to create DDR1 and DDR mutant MYC- and FLAG-tagged constructs.

2.2.3.2. DDR1-MYC and DDR1-FLAG constructs

A three-piece ligation of A, B and C DNA fragments was carried out to give the constructs pc-DDR1-MYC and pc-DDR1-FLAG. The production of these constructs are described below and represented schematically in Figure 2.2.

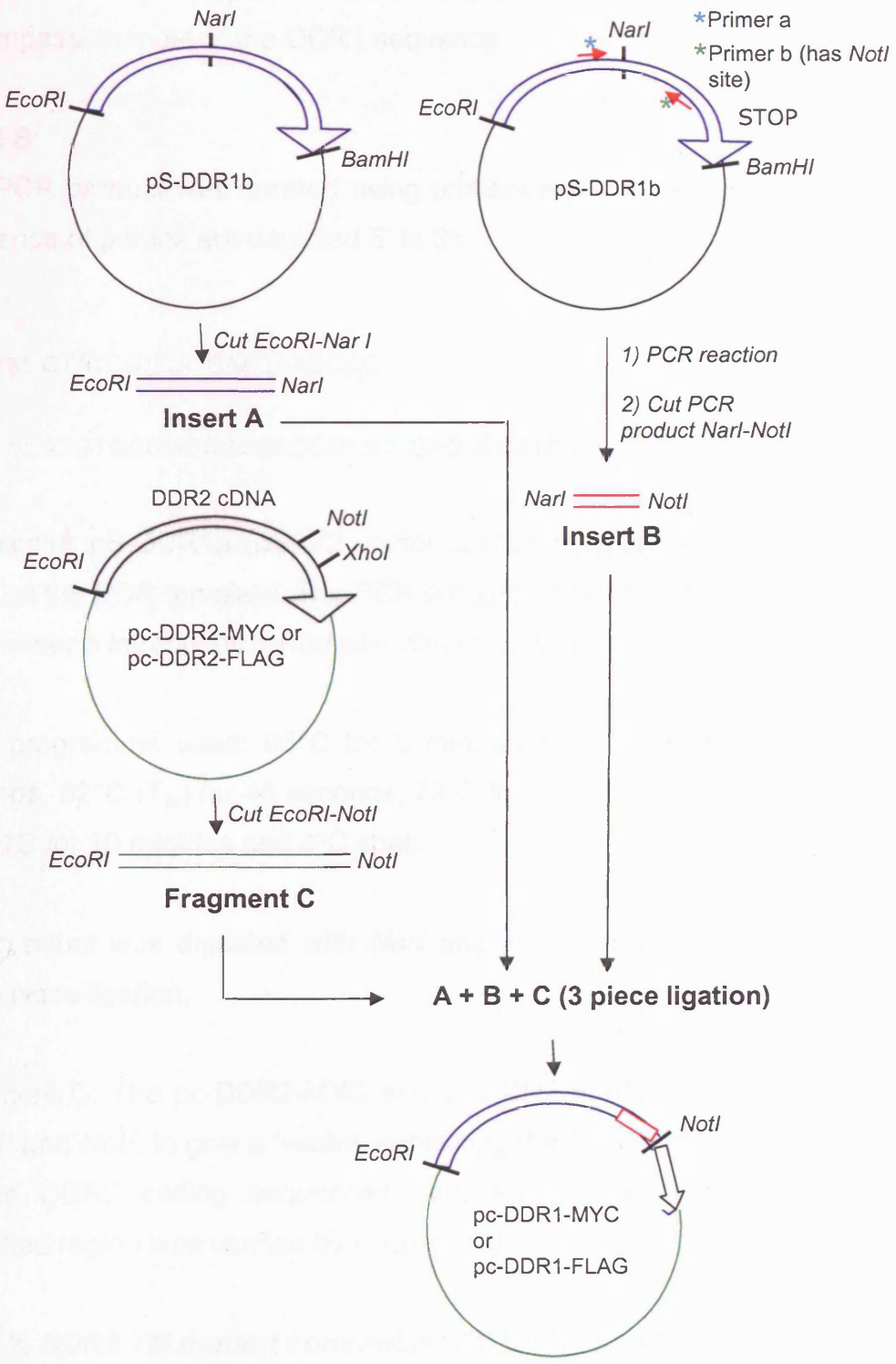

Figure 2.2: Schematic representation of the production of DDR1-MYC and DDR1-FLAG constructs.

Insert A:
pS-DDR1a vector was cut with *EcoRI* and *NarI* to give a fragment encompassing most of the DDR1 sequence.

Insert B:
The PCR product was created using primers a and b as shown below. The sequence of primes are depicted 5' to 3':

primer a: CTATCCTCATCAACAACCGC

NotI
primer b: ATGT**GCGGCCGC**CACCGTGTTGAGTGCATCCTCT

The vector pS-DDR1a (pSP72 vector containing DDR1b cDNA insert) was used as the PCR template. The PCR product ends just before the stop codon (the primer b introduces a *NotI* site, shown in bold).

PCR programme used: 95°C for 5 minutes for 1 cycle then 95°C for 45 seconds, 52°C (T_m) for 45 seconds, 72°C for 1 minute for 25 cycles followed by 72°C for 10 minutes and 4°C soak.

The product was digested with *NarI* and *NotI* in order to be used for the three-piece ligation.

Fragment C: The pc-DDR2-MYC and pc-DDR2-FLAG vectors were cut with *EcoRI* and *NotI*, to give a 'vector' containing the MYC and FLAG tags with all of the DDR2 coding sequences removed. The sequence of the PCR amplified region was verified by sequencing.

2.2.3.3. DDR2 TM mutant constructs, TM1, TM2 and TM3

These mutants were made by the overlap extension PCR method described in section 2.2.3. For each construct, the primary PCR products A and B, using the primer pairs a-b and c-d respectively are shown below. Primers are depicted 5' to 3' and the mutagenic sequences are in red bold:

DDR2 TM1, TM2, TM3
primer a: GTTTCTGCAGATTGACTTGCAC

DDR2 TM1
primer b: TGATGGC**CGGGCC**GATAAAGATGATGGCCACCAA

DDR2 TM1
primer c: CTTTATC**GGCCCG**GCCATCATTGTCATCATC

DDR2 TM2, TM2, TM3
primer d: GAACTCCTCCACAGCCACAT

DDR2 TM2
primer b: GATGAC**AGGGCC**GGCCAGGAGGATAAAGATGA

DDR2 TM2
primer c: CTGGCC**GGCCCT**GTCATCATCCTCTGGAGGCA

DDR2 TM3
primer b: GATGAT**GAC**CACCAAGCAGCCAATCAGGAT

DDR2 TM3
primer c: GCTGCTTGGTG**GTC**ATCATCTTTATCCTCCTGGC

DDR2 TM1 primers b and c contain the mutagenic sequence which codes for a glycine and proline residue instead of two leucine residues present in WT DDR2. For DDR2 TM2 primers b and c contain the mutagenic sequence which codes for a glycine and proline residue instead of two isoleucine residues present in WT DDR2. For DDR2 TM3, primers b and c contain a mutated codon which encodes for a valine instead of an alanine residue present in WT DDR2.

The pS-DDR2 vector was used as the template for the synthesis of the primary PCR products for all three mutant constructs. For DDR2 TM1, the PCR programme was as follows: 95°C for 5 minutes for 1 cycle then 95°C for 45 seconds, 52°C (T_m) for 45 seconds, 72°C for 1 minute for 25 cycles followed by 72°C for 10 minutes and 4°C soak. For DDR2 TM2 and TM3 the

PCR programme was as above except the primer annealing temperature (T_m) was changed to 53°C.

PCR products were purified by gel electrophoresis using QIA-quick Gel Extraction kit. A second PCR reaction was set up to fuse the two primary products using the primer pair a-d. PCR programme used: 95°C for 5 minutes, 95°C for 45 seconds, 50°C (T_m) for 45 seconds, 72°C for 1 minute 30 seconds and 4°C soak.

The amplified fused PCR product was purified using the Qia-quick PCR purification kit, follwed by digestion with restriction enzymes *NarI* and *NcoI*. The product was ligated into the vector pS-DDR2 cut with *NarI* and *NcoI*. These constructs were sequenced using relevant primers in order to verify the presence of the site-directed mutation and check for potential PCR mutations. For expression in eukaryotic cells, the full-length DDR2 TM1, TM2 and TM3 cDNAs were cut with *EcoRI* and *XhoI* and cloned into pcDNA3.1/Zeo vector cut with *EcoRI* and *XhoI*.

2.2.3.4. DDR2 cytosolic domain deletion construct, DDR2 ECTM

To delete the entire cytosolic region of DDR2, a PCR reaction was carried out using the primers shown below. Restriction enzyme sites introduced are in bold and primers are depicted 5' to 3':

EcoRI
primer a: CG**GAATTC**ACAGAGAATGCTCTGCACCCGTT

NotI
primer b: ATGT**GCGGCCGC**TTTCTGCCAGAACTGCCTCCAGAG

The forward primer a, contains an *EcoRI* site, which is for sub-cloning of the PCR product. The reverse primer d anneals to the DDR2 sequence coding for part of the TM domain and cytosolic juxtamembrane region and has a *NotI* site just before the stop codon. This produces a final PCR product which encodes for only six amino acids after the DDR2 TM domain.

A PCR reaction was carried out using pSDDR2 as a template and the above two primers. The PCR programme was as follows: 95°C for 5 minutes for 1 cycle then 95°C for 45 seconds, 59°C (T_m) for 45 seconds, 72°C for 1 minute and 30 seconds for 25 cycles followed by 72°C for 10 minutes and 4°C soak.

PCR products were digested with restriction enzymes *EcoRI* and *NotI*. The products were ligated into the vector pc-DDR2-MYC or pc-DDR2-FLAG cut with *EcoRI* and *NotI* to give pc-DDR2-ECTM-MYC and pc-DDR2-ECTM-FLAG.

2.2.3.5. DDR2 double deletion mutant constructs, DS2TM and ΔDS2TM

To obtain a DDR2 construct which has either the DS domain deleted, or the domain X, in addition to deletion of the entire cytosolic region, a PCR reaction was carried out using the constructs pc-DS-DDR2 and pc-ΔDS-DDR2 as templates and primer pair described in section 2.2.3.4. Restriction enzyme sites introduced are in bold and primer sequences are depicted 5' to 3'. The PCR programme is was carried out as described in section 2.2.3.4. PCR products were digested with restriction enzymes *EcoRI* and *NotI*. The products were ligated into the vector pc-DDR2-MYC or pc-DDR2-FLAG cut with *EcoRI* and *NotI* to give pc-DS-DDR2-MYC, pc-ΔDS-DDR2-MYC, pc-DS-DDR2-FLAG and pc-ΔDS-DDR2-FLAG.

2.2.3.6. DDR1 double mutant constructs, DS1TM1 and ΔDS1TM1

To obtain a DDR1 construct which has either the DS domain or domain X and P/G rich region deleted in addition to the TM1 mutation in the TM domain, overlap extension PCR was carried out. Primary PCR products A and B, were created using the primer pairs a-b and c-d, respectively, as shown below. Primers are depicted 5' to 3' and the mutagenic sequences, corresponding to the DDR1 TM1 mutation, are in shown in red bold:

DS1TM1
primer a: ATGGTTGCCCGACTGGTT

primer b: ATGAG**CGGCCC**GAGCAGGATGATGGCCAC
primer c: ATCCTGCTC**GGGCCG**CTCATCATTGCCCT
primer d: GCATAATGGGGGACGCTGT

The pc-DS-DDR1-2 vector was used as the template for the synthesis of the primary PCR products. The PCR programme was as follows: 95°C for 5 minutes for 1 cycle then 95°C for 45 seconds, 52°C (T_m) for 45 seconds, 72°C for 1 minute for 25 cycles followed by 72°C for 10 minutes and 4°C soak. A second PCR reaction was set up to fuse the two primary products using the primer pair a-d. PCR programme used: 95°C for 5 minutes, 95°C for 45 seconds, 55°C (T_m) for 45 seconds, 72°C for 1 minute 30 seconds and 4°C soak.

The amplified fused PCR product was digested with restriction enzymes *SacI* and *NarI*. The product was ligated into the vector pS-DDR1b (pSP72 vector with WT DDR1b cDNA inserted) cut with *SacI* and *NarI*. In order to express the gene in eukaryotic cells and introduce C-terminal MYC- and FLAG-tags, the cDNA was cut with *EcoRI* and *NarI* and cloned into pc-DDR1-MYC and pc-DDR1-FLAG vector cut with *EcoRI* and *NarI*, to give pc-DS1TM1-MYC and pc-DS1TM1-FLAG.

To obtain the double mutant ΔDS1TM1, a three-piece ligation was carried out with the components obtained as follows:

Fragment A: pc-DDR1-TM1 construct cut with *NcoI* and *NotI*.

Fragment B: pc-DDR2-MYC or pc-DDR2-FLAG cut with *EcoRI* and *NotI*.

Fragment C: pc-ΔDS-DDR1 cut with *EcoRI* and *NcoI*.

The three fragments A, B and C were ligated in a single reaction to give pc-ΔDS1TM1-MYC and pc-ΔDS1TM1-FLAG.

2.2.3.7. DDR1 double deletion mutants, DS1ΔCYTO, ΔDS1ΔCYTO, and triple mutants, DS1TM1ΔCYTO and ΔDS1TM1ΔCYTO

DDR1 double deletion mutant constructs which have either the DS domain or the domain X and the P/G rich region deleted, in addition to the deletion of the entire cytosolic region, were made. DDR1 triple mutants were made, both of which contain the TM1 mutation in the TM domain in addition to the deletion of the cytosolic region, with either the DS domain or the domain X plus the P/G rich region deleted. PCR reactions were carried out using the constructs pc-DS-DDR1 and pc-ΔDS-DDR1 as templates for the double deletion mutants and pc-DS1TM1-DDR1 and pc-ΔDS1TM1-DDR1 as templates for the triple mutants, respectively.

The primer pair used for these constructs is shown below. Restriction enzyme sites introduced are in bold and primer sequences are depicted 5'-3':

EcoRI
primer a: CG**GAATTC**AGAGATGCTGCCCCCACCCCCT

NotI
primer b: ATGT**GCGGCCGC**CCTGCGCCAGTGCAGCCGCCAG

The PCR programme was as follows: 95°C for 5 minutes for 1 cycle then 95°C for 45 seconds, 54°C (T_m) for 45 seconds, 72°C for 1 minute and 30 seconds for 25 cycles followed by 72°C for 10 minutes and 4°C soak.

PCR products were digested with restriction enzymes *EcoRI* and *NotI*. The products were ligated into the vector pc-DDR1-MYC or pc-DDR1-FLAG cut with *EcoRI* and *NotI* to give the epitope-tagged double deletion mutants and triple mutants as follows:

Double deletion mutants: pc-DS1ΔCYTO-DDR1-MYC, pc-ΔDS1ΔCYTO-DDR2-MYC, pc-DS1ΔCYTO-DDR1-FLAG and pc-ΔDS1ΔCYTO-DDR1-FLAG

Triple mutants: pc-DS1TM1ΔCYTO-DDR1-MYC, pc-ΔDS1TM1ΔCYTO-DDR1-MYC, pc-DS1TM1ΔCYTO-DDR1-FLAG and pc-ΔDS1TM1ΔCYTO-DDR1-FLAG.

2.2.3.8. MYC- and FLAG-tagged DDR1 TM mutants, TM1, TM2 and TM3

pc-DDR1-TM1, pc-DDR1-TM2 and pc-DDR1-TM3 were digested with *EcoRI* and *NarI,* and the resulting cDNA fragments were sub-cloned into pc-DDR1-MYC and pc-DDR1-FLAG cut with *EcoRI* and *NarI*. This produces pc-DDR1-TM1-MYC, pc-DDR1-TM1-FLAG and the corresponding TM2 and TM3 constructs. The resulting clones were sequenced in order to verify the presence of the specific TM mutations.

2.2.3.9. MYC- and FLAG-tagged DDR1 deletion constructs, DS1-1, DS1-2, ΔDS1, ΔPG and ECTM1

pc-DS-DDR1, pc-DS-DDR1-2, pc-ΔDS-DDR1 and pc-ΔPG-DDR1 were digested with *EcoRI* and *NarI* and sub-cloned into pc-DDR1-MYC and pc-DDR1-FLAG digested with *EcoRI* and *NarI*, to give corresponding MYC- and FLAG-tagged constructs.

2.2.3.10. MYC- and FLAG-tagged DDR2 TM1 constructs

pS-DDR2-TM1 was digested with *NarI* and *NcoI* and sub-cloned into pS-DDR2-MYC and pS-DDR2-FLAG cut with *NarI* and *NcoI*, to give pS-DDR2-TM1-MYC and pS-DDR2-TM1-FLAG. The latter constructs were digested with *EcoRI* and *NotI* and sub-cloned into pc-DDR2-MYC and pc-DDR2-FLAG to obtain pc-DDR2-TM1-MYC and pc-DDR2-TM1-FLAG. The final constructs were sequenced in order to verify the presence of the TM mutation.

2.2.3.11. MYC- and FLAG-tagged DDR2 deletion constructs, DS2 and ΔDS2

The constructs, pc-DS-DDR2 and pc-ΔDS-DDR2 were digested with *EcoRI* and *NcoI* and sub-cloned into pS-DDR2-MYC and pS-DDR2-FLAG vectors cut with *NarI* and *NcoI*, to give pS-DS-DDR2-MYC, pS-ΔDS-DDR2-MYC and corresponding FLAG tagged constructs. These constructs were digested with *EcoRI* and *XhoI* and sub-cloned into pc-DDR2-MYC and pc-DDR2-FLAG vectors digested with *EcoRI* and *XhoI*.

2.2.4. Mammalian cell culture and protein methods

2.2.4.1. Mammalian cell lines and culture medium

Human embryonic kidney 293 cells (HEK293), HEK293 TSA 201 cells, Rat-1 cells, HEK293 TSA DDR1 and HEK293 TSA DDR2 cells were cultured in Dulbecco's modified Eagle medium, Invitrogen) containing 10% foetal bovine serum. 100 μg/ml zeocin (for the latter two cell lines) in order to maintain episomal expression of the DDR genes. 100 μg/ml puromycin was added to the culture medium to selectively maintain the Rat-1 cell line. MCF-7 cells were cultured in Dulbecco's modified Eagle medium (without sodium pyruvate, Invitrogen) containing 10% foetal bovine serum.

2.2.4.2. Trypsinisation and passaging of cells

All cell lines were cultured in T25 or T75 tissue culture flasks (Nunc) at 37°C in a 5% CO_2 incubator. Cell lines were sub-cultured every third day. Culture medium was aspirated and the adherent cells growing in tissue culture flask were washed in PBS. Trypsin/EDTA (Gibco) at RT was added to the cells (0.5 ml per T25) for 1 minute at RT. The cells were dislodged by tapping of the flask after which a suitable volume of medium containing 10% FCS was added to inactivate the trypsin. The cells were then split into a tissue culture

flask for maintenance or culture plate in order to perform an experiment, and incubated at 37°C, 5% $C0_2$.

2.2.4.3. Freezing and storage of cells

Cells grown to sub-confluency in T75 flasks were trypsinised, washed into 15 ml complete medium (RT) and centrifuged at 1000 rpm for 5 minutes (GS-6R Centrifuge, Beckman). The pellet was re-suspended in 2 ml complete medium containg 10% DMSO. Aliquots (0.5 ml) were put into Nunc vials and placed at -80°C overnight. The cells were then transferred to liquid nitrogen for storage.

2.2.4.4. Thawing of cells

Cells frozen in liquid nitrogen were thawed in a 37°C water bath and immediately added to 10 ml of culture medium in order to dilute out the DMSO. The cells were spun down at 1000 rpm for 5 minutes (GS-6R Centrifuge, Beckman) and re-suspended in 5 ml medium containing FCS, transferred to a T25 and incubated at 37°C, 5% CO_2.

2.2.4.5. Cell transfection

Calcium phosphate precipitation method: Cells were grown to ~50% confluency in tissue culture plates and the medium was changed 2-3 hours prior to transfection. For 12 well tissue culture plates, 2.5 μg of DNA/ well was used; for 6 well plates 5 μg of DNA /well was used. DNA/$CaCl_2$ mixture was prepared by adding $CaCl_2$ to a final concentration of 0.25 M to DNA-H_2O mixture and vortexing briefly (volume of the DNA/CaCl2 mixture = volume of 2X HBS). The DNA/$CaCl_2$ was added slowly, drop-wise, to 100 μl 2X HBS solution (50 mM HEPES pH 7.1, 280 mM NaCl, 1.5 M Na_2HPO_4) per 12 well or 200 μl per 6 well, while gently vortexing the tube containing HBS. The mix was incubated at RT for 30 minutes, vortexed, and added drop-wise to the

wells. The cells were incubated at 37°C, 5% CO_2. 18 hours later the culture medium was changed to fresh complete medium.

FuGENE 6 method: Cells were grown to ~50% confluency. The medium was changed to complete medium just before transfecting. FuGENE (3 μl) was added to 97 μl of serum free medium and incubated at RT for 5 minutes. DNA (1 μg) was added to a second tube. The diluted FuGENE was added drop-wise to the DNA and incubated at RT for 15 minutes. The mixture was added to the cells drop-wise and incubated at 37°C, 5% CO_2.

2.2.4.6. DDR2-positive stable cell line

A DDR2 expressing HEK293 stable cell line was created using the HEK293 TSA cells, which contain the SV40 large T antigen, which enables episomal replication of transfected vectors. HEK293 TSA 201 cells were grown to 50% in a T25 flask and transfected with 1 μg DNA vector containing the DDR2 gene (pcDDR2) using the FuGENE method of transfection. 24 hours later, the medium was aspirated and replaced with complete medium containing 100 μg/ml zeocin, in order to select for DDR2 positive cells. The medium was changed every third day to eliminate dead cells and debris; after about two weeks colonies of zeocin resistant cells were visible and these cells were propagated in the presence of zeocin.

2.2.4.7. Activation of sodium orthovanadate

Activated sodium orthovanadate is required for maximal inhibition of protein tyrosine phosphatases. A 200 mM solution of sodium orthovanadate (Sigma) was prepared and adjusted to pH 10.0. The yellow solution obtained was boiled for approximately 10 minutes, until colourless, and cooled to RT. The temperature was re-adjusted to pH 10.0. The solution was re-boiled and cooled to RT; this step was repeated until the solution remained colourless and the pH stabilized at 10.0. The activated sodium orthovanadate was stored at -20°C

2.2.4.8. Preparation of whole cell lysate

The culture medium was removed and cells were washed x1 in cold PBS. A suitable volume of ice cold NP40 lysis buffer (1% NP40, 150 mM NaCl, 50 mM Tris, pH 7.4, 1 mM EDTA) containing proteinase inhibitors [1 mM phenylmethylsulfonyl fluoride (PMSF) and 50 μg/ml aprotonin], was added to the cells and plates were placed on ice on a shaker for 20 minutes. The cells were then scraped off into Eppendorf tubes and lysed on ice for 1 hour; then spun at 13 000 rpm for 10 minutes (Heraeus Biofuge) to recover the detergent soluble fraction. Cell lysates were stored frozen at -20°C or directly processed for SDS-PAGE.

2.2.4.9. SDS-PAGE

Mini-gels were prepared using the mini-protean 3 gel cast with 0.75 mm spacers (BioRad, Hertfordshire). 7.5% SDS-PAGE resolving gels were made as follows: 7.5% acrylamide/0.2% bisacrylamide, 375 mM Tris-HCl pH 8.8, 0.1% SDS, 0.04% APS and 0.2% TEMED. 5% or 10% gels were made by varying the percentage of acrylamide/bisacrylamide accordingly. 4% stacking gels were used through out and contained 4% acrylamide/0.1% bisacrylamide, 125 mM Tris-HCl pH 6.8, 0.1% SDS, 0.2% TEMED and 0.04% APS. Protein loading buffer was added to the lysates or immunoprecipitates and the samples were boiled at 100°C for 3 minutes. 15 μl of each sample was loaded on a 7.5%, 5% or 10% gel, along with pre-stained MW markers (6 μl, NEB). Broad range markers (10 μl, NEB), was additionally loaded when a more accurate estimation of protein MW was required. The proteins were separated using a Mini Protean 3 Cell tank (BioRad), containing SDS running buffer. The gels were run at a constant voltage of 50-100 V initially until the samples entered the resolving gel, after which the voltage was increased to 120-150 V.

2.2.4.10. Western blotting

After SDS-PAGE, proteins were blotted onto nitrocellulose membrane using a wet transfer Mini-Trans blot apparatus (BioRad). Blotting was carried out at 4°C for 1 hour at 200 mA constant current in SDS blotting buffer. Following transfer, the nitrocellulose membrane was stained with Ponceau-S solution (0.1% Ponceau-S, 1% acetic acid) and de-stained with H_2O, in order to visualise the blotted proteins. The membrane was incubated in blocking solution (3% Marvel milk powder, in PBS) for 1 hour at RT on a rotating platform or overnight at 4°C. The membrane was briefly washed in PBS and incubated with the primary Ab (diluted in PBST to the required concentration), either for 2 hours at RT or 4°C overnight, on a roller-shaker. The blots were washed x3 in PBST (1X PBS containing 0.05% Tween 20), for 10 minutes each and incubated with the relevant secondary Ab (diluted in PBST to the required concentration) for 1 hour at RT, on a roller-shaker. The blots were washed x5, for 5 minutes per wash, and incubated with enhanced chemiluminescence (ECL) detection reagents as specified by the manufacturer (Amersham). The blots were exposed to film (KODAK BIOMAX LIGHT) and developed using a Compact X4 film developer (Xograph imaging systems).

2.2.4.11. Chemical cross-linking

Cross-linking was carried out for 30 minutes at RT or 30 minutes at 37°C or 1 hour at 4°C using the homobifunctional cross-linking reagent bis(sulfosuccinimidyl) suberate (BS^3). Different concentrations of BS^3 in a final volume of 500 µl PBS were added to confluent cells in 12 well tissue culture plates. The reaction was quenched by addition of 20 mM Tris pH 7.4 and incubating at RT for 15 minutes followed by cell lysis.

2.2.4.12. Molecular weight analysis

Molecular weight (MW) analysis of proteins was carried out in order to estimate the MWs of DDR oligomers obtained in cross-linking experiments.

As 5% gels give a better resolution of large proteins than the 7.5% gels usually used to separate the DDR proteins, 5% gels were run for MW analysis of large protein complexes.

Broad range protein markers (NEB) containing MW range *212, 158, 116, 97, 66, 56, 43, 35, 27, 20, 14, 6.5, 2.4 kDa,* were used to obtain a standard curve from which the MWs of the DDR complexes could be obtained. The distance migrated was measured for each marker band from a fixed line on the blot and a graph plotted of distance migrated (mm) versus Log MW (kDa). The distances migrated of the DDR complexes were measured from the same fixed line on the blot and the corresponding MWs were obtained from the standard curve.

2.2.4.13. Collagen activation assay

HEK293 cells in 12 well tissue culture plates were transfected by calcium phosphate precipitation with the relevant DDR expression vectors and 24 hours later, the cells were incubated in serum free medium for 16 hours. Cells were then stimulated with 10 μg/ml collagen I or 1 mM sodium orthovanadate for 90 minutes at 37°C. After washing with PBS cells were lysed in 1% NP40, 150 mM NaCl, 50 mM Tris, pH 7.4, 1 mM EDTA, 1 mM PMSF, 50 μg/ml aprotonin, 1 mM sodium orthovanadate, 5 mM NaF.

The detergent soluble fraction was recovered by centrifugation and aliquots were analysed by SDS-PAGE on 7.5% polyacrylamide gels followed by blotting onto nitrocellulose membranes at 200 mA for 1 hour. The blots were blocked overnight in 3% milk-PBS and probed with mouse anti-phosphotyrosine mAbs (1:666) for 2 hours. After washing x3 with PBST, the blots were incubated with goat anti-mouse HRP (1:10 000) secondary Ab for 1 hour followed by washing x5 with PBST. The signals were detected by ECL (Amersham).

To re-probe the blots, the membrane was stripped in 62.5 mM Tris, pH 6.8, 2% SDS, 100 mM β-mercaptoethanol at 55°C for 30 minutes or in Antibody stripping solution (Alpha Diagnostic International) for 10 minutes. The blots were re-probed with rabbit anti-DDR1 (1:200) or goat anti-DDR2 (1:200) Abs followed by goat anti-rabbit Ig-HRP (1:4000) or rabbit anti-goat IgG-HRP (1:20,000), respectively.

2.2.4.14. Co-immunoprecipitation

HEK293 cells at ~50% confluency were transfected by calcium phosphate precipitation. Cells were co-transfected with plasmid vectors containing MYC- and FLAG-tagged WT or mutant DDR1 and DDR2 cDNA. Single transfectants, with either one of the plasmids alone, were also carried out as controls.

48 hours later, cells were lysed in NP40 lysis buffer and centrifuged for 10 minutes at 13,000 rpm (Heraeus Biofuge) to recover the detergent soluble fraction. Anti-MYC or anti-FLAG antibody were added to aliquots of lysate at 2 μg Ab (rabbit anti-MYC) or 3 μg Ab (mouse anti-FLAG M2 mAb, mouse anti-MYC mAb) per 500 μl lysate and incubated on a rotating wheel at 4°C over night. 16 hours later 20 μl (40 μl 1:1 mix of beads to PBS buffer) of protein A beads (for samples containing rabbit anti-MYC Ab) or protein G beads (for samples containing mouse anti-FLAG mAb, mouse anti-MYC mAb) were added and incubated for 1.5 hours on a rotating wheel at 4°C.

The samples were spun for 1 minute at 13,000 rpm (Heraeus Biofuge) to precipitate the beads, and the supernatants were aspirated followed by washing each sample four times with 1 ml NP40 lysis buffer. After the final wash and spin, all of the supernatant was removed followed by addition of 18 μl of 2x reducing sample buffer. The samples were boiled for 5 minutes to release bound antibody and antigen from the beads.

Samples were run on SDS-PAGE and blotted and then blocked as described above. The blots were probed with primary Abs; rabbit anti-MYC (1:200) or mouse anti-FLAG M2 mAbs (1:200) for 2 hours. After washing x3 with PBS containing 0.05% Tween 20 (PBST) the blots were incubated with goat anti-rabbit HRP (1:4000) or goat anti-mouse HRP (1:8000) secondary Ab, for 1 hour, followed by washing x5 with PBST. The signals were detected by enhanced chemiluminescence (Amersham Biosciences UK).

2.2.4.15. Cell surface biotinylation

HEK293 cells at ~50% confluency were transiently transfected with plasmid constructs containing WT or mutant DDR1 or DDR2 cDNA and 48 hours later the cells were washed once with ice cold PBS and incubated with Sulfo-NHS-LC-Biotin in PBS for 30 minutes on ice. The reaction was quenched by washing twice with 100 mM glycine in cold PBS. The cells were lysed in NP40 lysis buffer as described previously. Streptavidin sepharose beads were washed x3 in PBS and a 1:1 mixture of beads:PBS was prepared. 500 μl of cell lysates was incubated for 2 hours with 30 μl streptavidin sepharose beads in PBS, to pull down biotinylated cell surface receptors. The mixture was centrifuged for 1 minute at 4°C to pellet the beads. Streptavidin sepharose beads in PBS (30 μl) was added to the recovered supernatant and the mixture incubated for 2 hours at 4°C, in order to remove any remaining biotinylated cell surface receptors. The mixture was centrifuged for 1 minute at 4°C to pellet the beads. The beads from the first and second pull down were pooled and washed x4 in NP40 lysis buffer then boiled in 18 μl of 2x reduced SB for 5 minutes to release bound protein. The supernatant from the second pull down was recovered and incubated with anti-DDR Ab, to immunoprecipitate the intracellular DDR receptor pool. To analyze the total DDR protein in the sample, 500 μl of starting lysate was incubated with anti-DDR Ab. Immunoprecipitations were carried out as described in 2.2.4.14. All samples were run reduced on 7.5% SDS-PAGE and analysed by Western blot.

2.2.4.16. Enzymatic deglycosylation

HEK293 cells at 50% confluency were transfected with cDNA of WT or mutant DDR construct, and 48 hours later the cells were lysed and the lysates immunoprecipitated with anti-DDR Ab. Immunoprecipitations were carried out as described in 2.2.4.14. The beads were washed x2 in NP40 lysis buffer and x2 in 50 mM sodium phosphate buffer, pH 7.0, to remove ions which may inhibit enzyme activity.

The precipitated material was denatured in 1x glycoprotein denaturing buffer (0.5 % SDS and 1% β-mercaptoethanol) and 15-20 μl of immunoprecipitated sample was incubated with various endo- and exo-glycosidases as follows:

Endo H: Denatured immunoprecipitates were incubated with 1x Endo H reaction buffer and 5 units Endo H. Incubated 3 hours at 37°C.

PNGase F: Denatured immunoprecipitates were incubated with 1x PNGase reaction buffer, 1% NP40 and 5 units PNGase F. Incubated 3 hours or 20 hours at 37°C.

Neuraminidase: Denatured immunoprecipitates were incubated with 1 mU of enzyme. Incubated 3 hours at 37°C.

Neuraminidase and O-glycosidase double digest: Denatured immunoprecipitates were incubated with 1 mU of Neuraminidase for 1 hour at 37°C, then 1 mU of O-glycosidase was added for the final 2 hours.

Neuraminidase, Olgycosidase and PNGase F triple digest: Denatured immunoprecipitates were incubated with 1 mU of neuraminidase and 5 units of PNGase F, 1x PNGase reaction buffer and 1% NP40 for 1 hour at 37°C, then O-glycosidase was added for the final 2 hours.

Control sample with no enzyme. Denatured immunoprecipitates were incubated for 3 hours at 37°C.

All sample volumes were made equal by addition of 50 mM sodium phosphate buffer, pH 7.0. Sample buffer was added (5x) and samples were boiled and separated by SDS-PAGE until the gel front was run off. Samples were run on 7.5% gels until the 62 kDa marker was run off the gel bottom. This was done in order to detect shifts in protein MW, that are produced by deglycosylation. The gels were analysed by Western blotting as described in 2.2.4.10.

Chapter 3

Investigating the oligomerisation state of the DDRs in the absence of ligand

3.1. Introduction

The DDRs are activated upon collagen stimulation, which leads to autophosphorylation of conserved cytosolic tyrosine residues and further activation of the KD. The phosphorylated tyrosines can be detected by SDS-PAGE and Western blotting with an anti-phosphotyrosine mAb. As seen in Figure 3.1 (upper panel), both DDR1 (DDR1b isoform) and DDR2 are phosphorylated in response to collagen I in HEK293 cells. The corresponding DDR1 and DDR2 proteins are shown in the lower panel. In the case of DDR1, two MW forms are present, whereas for DDR2 three MW forms can be seen. We wanted to know which DDR protein forms were on the cell surface and which protein forms were intracellularly localised. In addition, we reasoned that the lower forms were different biosynthetic intermediates and therefore we investigated post-translational modifications which could account for the differences between the various DDR forms. To this end, we performed cell surface biotinylation and enzymatic deglycosylation experiments.

So far, DDR oligomerisation has been studied *in vitro* using soluble ECD constructs (Leitinger, 2003). In this study, it was shown that a His-tagged ECD construct of DDR2, His-DDR2, existed as a non-covalent dimer in solution, whilst His-tagged ECD of DDR1, His-DDR1, was a monomer. His-DDR2 recognised collagen, but the ECD of DDR1 recognised collagen only as a dimeric DDR1-Fc construct, not as the monomeric His-DDR1, proving that the DDRs need to be dimerised in order to bind collagen. In addition to the ECD, full-length DDRs contain a TM domain, juxtamembrane domain and a KD. We wanted to know if the DDRs formed dimers in the context of the full-length receptor and therefore we performed chemical cross-linking analysis of full-length DDRs on the cell surface. Co-immunoprecipitation studies were carried out to verify the cross-linking results and to demonstrate a physical association between DDR monomers *in vivo*.

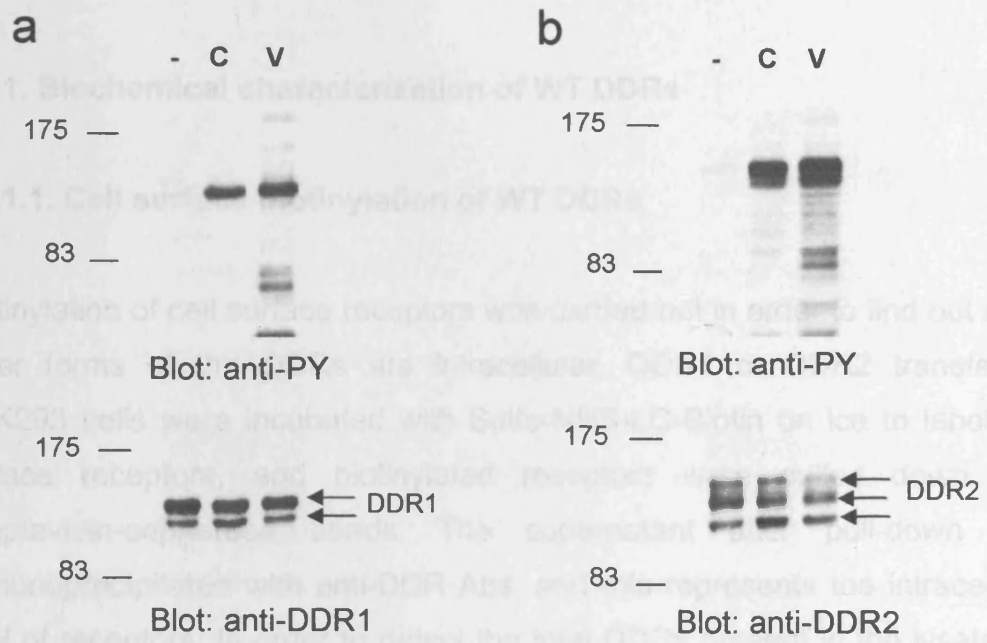

Figure 3.1: Collagen I-induced autophosphorylation of WT DDR1 and DDR2 in HEK293 cells. DDR1 (a) or DDR2 (b) were transiently expressed in HEK293 cells. After stimulation with 10 μg/ml collagen I (C) or 1 mM sodium orthovanandate (V), cell lysates were analysed by SDS-PAGE and Western blotting. The blots were probed with anti-phosphotyrosine mAb 4G10 to visualize phosphorylated receptors (a and b, upper panels). The blots were stripped and re-probed with anti-DDR1 Ab or anti-DDR2 Ab to detect total DDR protein levels (a and b, lower panels). The position and sizes (in kDa) of MW markers are indicated.

3.2. Results

3.2.1. Biochemical characterisation of WT DDRs

3.2.1.1. Cell surface biotinylation of WT DDRs

Biotinylation of cell surface receptors was carried out in order to find out if the lower forms of the DDRs are intracellular. DDR1 or DDR2 transfected HEK293 cells were incubated with Sulfo-NHS-LC-Biotin on ice to label cell surface receptors, and biotinylated receptors were pulled down with streptavidin-sepharose beads. The supernatant after pull-down was immunoprecipitated with anti-DDR Abs, and this represents the intracellular pool of receptors. In order to detect the total DDRs present in the lysate, an equivalent lysate volume was immunoprecipitated with anti DDR Ab. In addition, the above experiment was carried out in the presence of collagen I, in order to detect a potential downregulation of the DDRs which might occur upon collagen stimulation. Receptor down regulation has been shown to occur for other cell surface receptors upon ligand stimulation. For example, EGFR has been shown to intracellularly re-localise via clathrin-coated vesicle-mediated endocytosis mechanism upon stimulation with EGF (Haigler *et al.*, 1979; Wiley *et al.*, 1991). DDR transfected HEK293 cells were incubated with 10 μg/ml collagen I for 90 minutes followed by cell surface biotinylation and processing as described above.

As shown in Figure 3.2 (a) the lower form of DDR1 is present only in the intracellular pool (lane I) whereas the upper form is present both in the cell surface as well as in the intracellular pool. For DDR2, only the two upper forms are present in the cell surface pool, and all three forms present in the intracellular pool (Figure 3.2, b). A control experiment was carried out where an intracellular protein, ERK2, was subjected to the same procedure, showing no intracellular protein in the cell surface pool (c). Taken together, these results suggest that the upper forms of the DDRs are present on the cell surface as well as in intracellular compartments. In the presence of

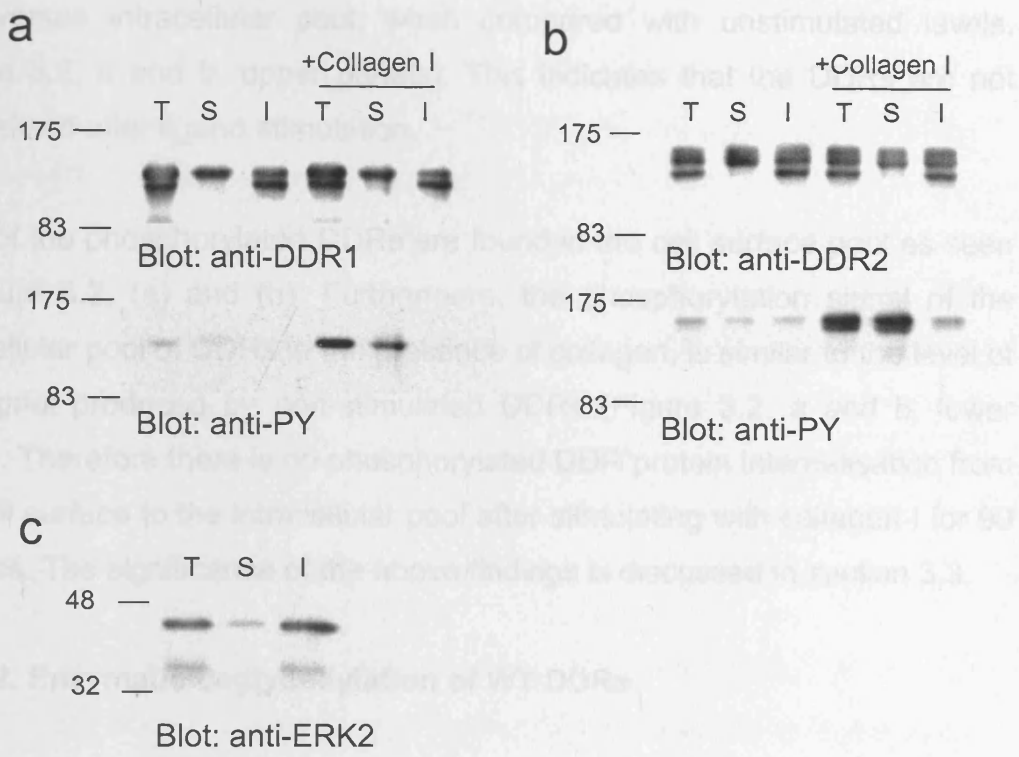

Figure 3.2: Cell surface biotinylation of WT DDR1 and DDR2. HEK293 cells transiently expressing DDR1 (a) or DDR2 (b) were incubated with 10 μg/ml collagen I or left untreated. After washing twice with cold PBS the cells were incubated with 3.5 mM Sulfo-NHS-LC-Biotin in PBS for 30 minutes on ice. The reaction was quenched by the addition of 100 mM glycine. The cell lysates were incubated with streptavidin sepharose beads and the bound and free protein was separated by centrifugation to a pellet (containing cell surface receptors) and supernatant (containing intracellular receptors) fraction. The supernatant was immunoprecipitated with anti-DDR1 Ab (a) or anti-DDR2 Ab (b). An equivalent lysate volume was incubated with anti-DDR1 Ab to analyze the total DDR protein in the sample. All samples were analysed by SDS-PAGE and Western blot. Blots (a) and (b) were first probed with anti-phosphotyrosine mAb, 4G10 (a and b, lower panels), then stripped and re-probed with anti-DDR1 or anti-DDR2 Ab (a and b, upper panels). A control experiment was carried out for the intracellular protein ERK2 (c). T-total protein present in 0.5 ml lysate, S-cell surface receptors, I-intracellular receptors. The position and sizes (in kDa) of MW markers are indicated.

collagen, there is no change in the levels of DDR protein in the cell surface pool versus intracellular pool, when compared with unstimulated levels. (Figure 3.2, a and b, upper panels). This indicates that the DDRs are not internalised after ligand stimulation.

Most of the phosphorylated DDRs are found in the cell surface pool as seen in Figure 3.2, (a) and (b). Furthermore, the phosphorylation signal of the intracellular pool of DDRs in the presence of collagen, is similar to the level of the signal produced by non-stimulated DDRs (Figure 3.2, a and b, lower panel). Therefore there is no phosphorylated DDR protein internalisation from the cell surface to the intracellular pool after stimulating with collagen I for 90 minutes. The significance of the above findings is discussed in section 3.3.

3.2.1.2. Enzymatic deglycosylation of WT DDRs

Both DDRs are predicted to contain asparagine-linked (N-linked) glycosylation sites on the ECD. The DDRs contain four NXS/T motifs (the consensus motif for N-linked glycosylation, where X is not specified) - two of these motifs are within domain X and two are in the N-terminal juxtamembrane region (shown schematically in Figure 3.3). It is therefore likely that the differences in MW of the DDR forms are due to N-linked glycosylation. To confirm this hypothesis, we carried out enzymatic digestion with PNGase F, an endoglycosidase which cleaves all N-linked complex, hybrid or high mannose oligosaccharides which are accessible on the protein. To investigate whether the intracellular form was a biosynthetic precursor, digestion with Endo H was carried out. Endo H is an endoglycosidase which cleaves only high mannose oligosaccharides, which are present only on proteins which are in-between the ER and cis-Golgi biosynthetic pathway.

Digestion analysis was carried out on immunoprecipitated WT DDR1. For WT DDR2 however, we had technical difficulties in carrying out immunoprecipitations using an anti-DDR2 Ab. We instead expressed a C-terminal MYC-tagged DDR2 construct (this construct is described in section

3.2.3) and carried out immunoprecipitation of DDR2-MYC protein with an anti-MYC Ab. Immunoprecipitates of WT DDR1 and DDR2-MYC were denatured and incubated with Endo H or PNGase F for 3 hours at 37°C or left untreated. The digests were run on SDS-PAGE and analysed by Western blot. As seen in Figure 3.3 (a), lane 1, only the lower form of DDR1 is Endo H sensitive, whilst the upper form is Endo H resistant, indicating that the lower form carries high mannose oligosaccharides and is a biosynthetic form. If the difference between the two forms was only due to N-linked glycosylation one would expect a single MW species after digestion with PNGase F. However, in the presence of PNGase F, DDR1 is still present as two forms (lane 3), with the lower form corresponding in MW to the deglycosylated high mannose species (approximately 100 kDa; lane 1 versus lane 3).

A similar enzymatic digestion analysis was carried out for DDR2, as shown in Figure 3.3 (b). As DDR2 consists of three MW species, the analysis is less straight-forward. As seen in lane 1, only the lower band is Endo H sensitive and therefore a biosynthetic form of DDR2. With PNGase F, however, three different MW species are present (lane 3). Even upon digesting for 20 hours with excess enzyme, there is no further reduction in the complexity of the observed pattern of bands (lane 4).

To further investigate the reason for heterogeneity, we tested for the presence of serine- or threonine-linked (O-linked) glycans. Unlike for N-glycosylation, there is no consensus motif for O-glycosylation and this type of glycosylation is therefore difficult to predict. We used NetOGlyc 3.1 software (Julenius et al., 2005), which identifies O-glycosylation motifs. This predicts a putative threonine O-glycosylation site in the DDR ECD, in the extracellular juxtamembrane region near the TM domain which is conserved between DDR1 and DDR2 (Thr 361 and Thr 358, in DDR1 and DDR2, respectively; see Figure 3.4, c). Deglycosylation using O-glycosidase, which cleaves serine or threonine-linked, unsubstituted Gal-β(1-3)-GalNAc-α- (O-linked core) was carried out. O-glycosidase cannot cleave the O-linked core structure if the O-linked core is modified, usually with mono, di or trisialylation.

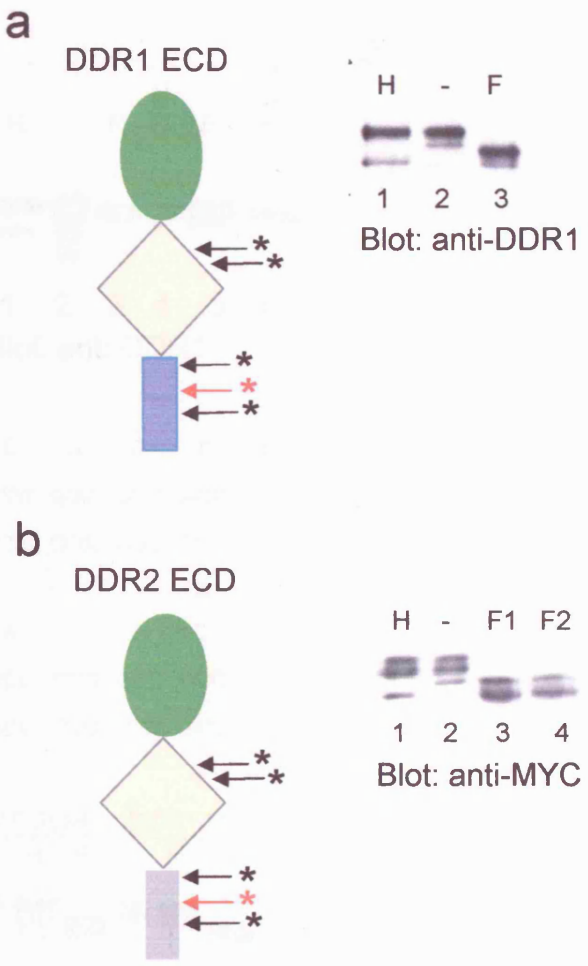

Figure 3.3: Enzymatic deglycosylation of WT DDR1 and DDR2-MYC. (a) and (b), Schematic diagram showing putative N-linked (black arrows) and O-linked (red arrows) glycosylation sites on DDR1 and DDR2 ECDs. Lysates of HEK293 cells transiently expressing DDR1 (a) or DDR2-MYC (b) were immunoprecipitated with anti-DDR1 Ab (a) or anti-MYC Ab (b). The precipitated material was denatured and incubated with either Endo H (H), PNGase F (F and F1), no enzyme (-), and for 3 hours at 37°C. In addition, DDR2-MYC immunoprecipitate was incubated with PNGase F for 20 hours at 37°C (F2). The samples were separated by SDS-PAGE, blotted onto nitrocellulose and probed with anti-DDR1 or anti-MYC Ab.

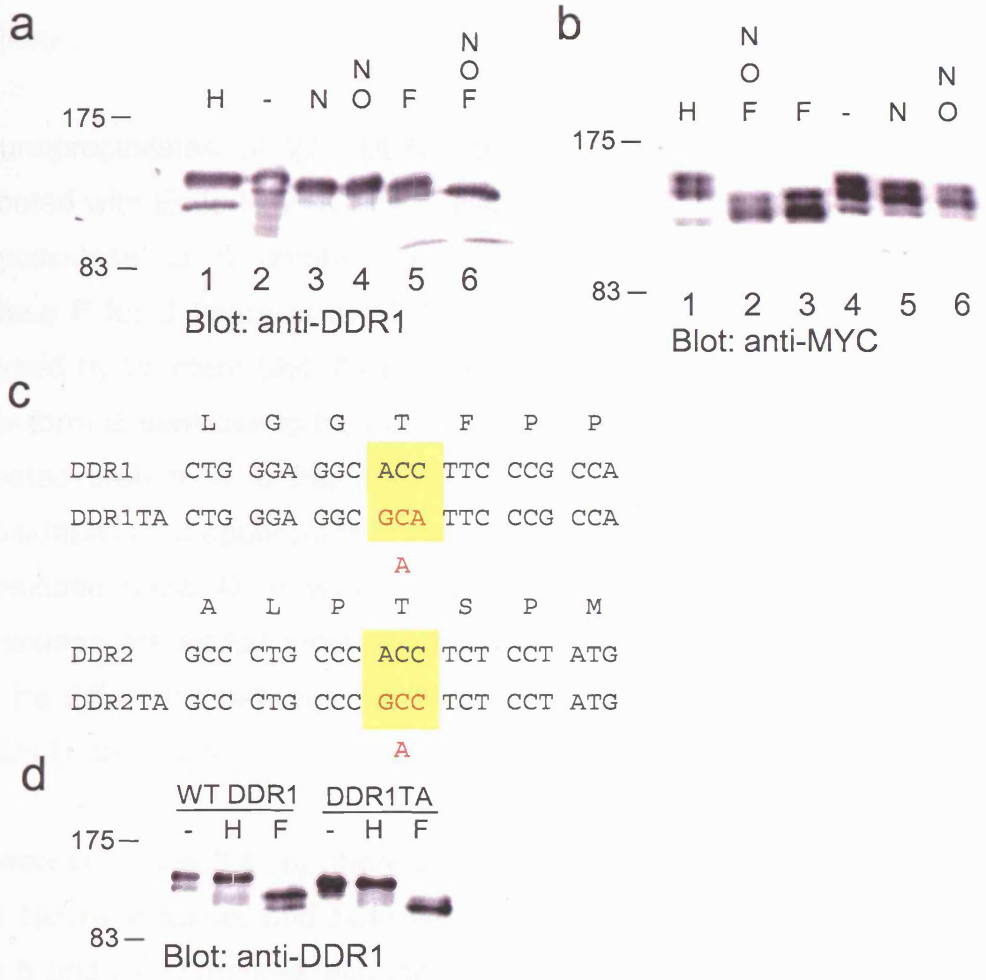

Figure 3.4: DDR1 and DDR2 are O-glycosylated. (a) and (b), O-glycosidase digestion of DDR1 WT and DDR2-MYC, respectively. (c) DNA sequence alignment of WT DDRs with DDRTA mutants. Bases coding for the conserved threonine residue (T361 in DDR1 and T358 in DDR2), predicted to be O-glycosylated, are in blue and the bases coding for the alanine residue in the corresponding mutant sequence are in red. The amino acids coding for WT DDR1 (358-364) and WT DDR2 (355-361) are shown. (d) Endo H and PNGase F digestion of WT DDR1 and DDR1TA mutant. Lysates of HEK293 cells transiently expressing WT DDR1 (a and d), DDR1TA (d) or DDR2-MYC (b) were immunoprecipitated with anti-DDR1 Ab (a and d) or anti-MYC Ab (b). The precipitated material was denatured and incubated with either Endo H (H), PNGase F (F), Neuraminidase (N), Neuraminidase, O-glycosidase (NO) or Neuraminidase, O-glycosidase and PNGase F (NOF) or no enzyme (-) for 3 hours at 37°C, then separated by SDS-PAGE, blotted onto nitrocellulose and probed with anti-DDR1 (a and d) or anti-MYC Ab (b). The position and sizes (in kDa) of MW markers are indicated.

Neuraminidase, an exoglycosidase which cleaves all non-reducing terminal branched and unbranched sialic acids, is required to enable O-glycosidase to function.

Immunoprecipitates of WT DDR1 and DDR2-MYC were denatured and incubated with Endo H, PNGase F, Neuraminidase, both Neuraminidase and O-glycosidase or a combination of Neuraminidase, O-glycosidase and PNGase F for 3 hours at 37°C. The digests were run on SDS-PAGE and analysed by Western blot. As seen in Figure 3.4 (a) lane 3 and 4, only the upper form is sensitive to Neuraminidase, shifting slightly compared with the untreated protein. A further potential shift produced in the presence of O-glycosidase is not apparent in the sample treated with Neuraminidase and O-glycosidase (lane 4). However, when PNGase F, Neuraminidase and O-glycosidase are added together, a single MW species is formed, indicating that the difference between the two DDR1 forms is due to N-glycosylation and O-glycosylation.

As seen in Figure 3.4 (b), there is a slight shift in the upper form of DDR2 upon Neuraminidase, and both Neuraminidase and O-glycosidase addition (lane 5 and 6), compared with the untreated sample (lane 4). Upon addition of PNGase F, Neuraminidase and O-glycosidase there is a slight shift in the upper form (lane 2) compared with sample treated with only PNGase F (lane 3), but all three MW forms are still present. This indicates that the uppermost form is O-glycosylated and that another post-translational modification, besides glycosylation, is responsible for the difference between the different forms of DDR2.

To confirm the above results, a point mutation was introduced in the DDR1 amino acid sequence, which resulted in the conversion of the conserved threonine which is predicted to be O-glycosylated (Thr 361), to an alanine, in order to prevent O-glycosylation. This mutant was digested with Endo H and PNGase F (in a similar manner as described for WT DDR) and analysed by SDS-PAGE and Western blot (Figure 3.4, d). Lanes 1 and 4 show untreated

controls and lanes 2 and 5 show Endo H treated samples, of WT DDR1 and mutant DDR1 (DDR1TA), respectively. Endo H treatment produces the expected shift in the lower MW form, however in this particular experiment the Endo H shift is observed as a fuzzy band. This might be due to the very low amounts of this species present in the samples.

Digestion with PNGase F produces the two forms of WT DDR1 that we normally observe (compare to Figure 3.4, a). However, digestion of DDR1TA with PNGase F produces a band which has the same MW as the fully deglycosylated receptor (~100 kDa, Figure 3.4, d; lane 3 versus lane 6). This result suggests that Thr 361 in DDR1 is a site for O-glycosylation. This result, taken together with the result obtained from deglycosylation using O-glycosidase, strongly indicates that the difference between the two DDR1 forms is due to N-linked and O-linked glycosylation. Experiments to confirm that DDR2 is O-glycosylated, using the DDR2 O-glycosylation mutant, are currently ongoing in the laboratory. However it is likely that for DDR2, there is another type of post-translational modification apart from glycosylation, which is responsible for the three different MW forms. The different types of potential modification are described in section 3.3.

3.2.2. Chemical cross-linking analysis of WT DDRs using BS^3

In order to investigate DDR oligomerisation in the context of the full-length receptor, chemical cross-linking of DDRs on the cell surface was carried out. A membrane impermeable, homobifunctional cross-linker, BS^3, was used to cross-link the cell surface receptors only. Full-length, WT DDRs were transiently over-expressed in HEK293 cells and 48 hours later varying concentrations of BS^3 were added to the cells and incubated at 37°C for 30 minutes. Whole cell lysates were run reduced on SDS-PAGE and blotted onto nitrocellulose. The blots were probed with anti-DDR1 or anti-DDR2 antibodies.

Figure 3.5 (a) shows that in the absence of cross-linker, the DDR1 protein migrates around 120 kDa (upper MW form); however, in the presence of BS^3, additional bands can be seen which migrate at higher MW. Lysates from cross-linker treated and untreated cells were run on 5% gels and MW analyses of DDR1 protein bands were carried out, as described in Methods. By this method, we calculated the size of the higher MW bands for DDR1 to be approximately 240 kDa, which correspond to DDR1 dimers. Cross-linking analysis was also performed at 4°C for 1 hour, as the low temperature would reduce potential receptor internalization. The experiment was carried out along with cross-linking at 37°C and the results were compared. There was no difference in the amount of cross-linked DDR1 between the two different temperatures (data not shown). The ability of DDR1 to oligomerise in the absence of ligand was seen in another cell line, MCF-7, a mammary carcinoma cell line containing endogenous DDR1 protein. In the presence of cross-linker a similar pattern of higher MW bands was visible (Figure 3.5, c). Similar results were also observed in a HEK293T cell line stably over-expressing DDR1 (data not shown) and in a Rat-1 cell line also stably over-expressing DDR1 (Figure 3.5, d).

DDR2 oligomerisation was studied in transiently transfected in HEK293 cells (Figure 3.5, b) and in HEK293T cells stably expressing DDR2 (data not shown). In the absence of BS^3 there was no cross-linked band, and the DDR2 protein migrated at approximately 130 kDa (upper MW form). However, on addition of increasing concentrations of cross-linker higher MW bands appeared of approximately 250 kDa, as obtained by MW analysis. This value corresponds to the MW of DDR2 dimers.

3.2.3. Co–immunoprecipitation studies of WT DDRs

Co-immunoprecipitation experiments were carried out to confirm that DDR1 and DDR2 dimerise in the absence of collagen. For these experiments, initially, N-terminal HA- and MYC-tagged cDNAs of DDR1 and DDR2 were made. However, these constructs showed defective expression patterns of

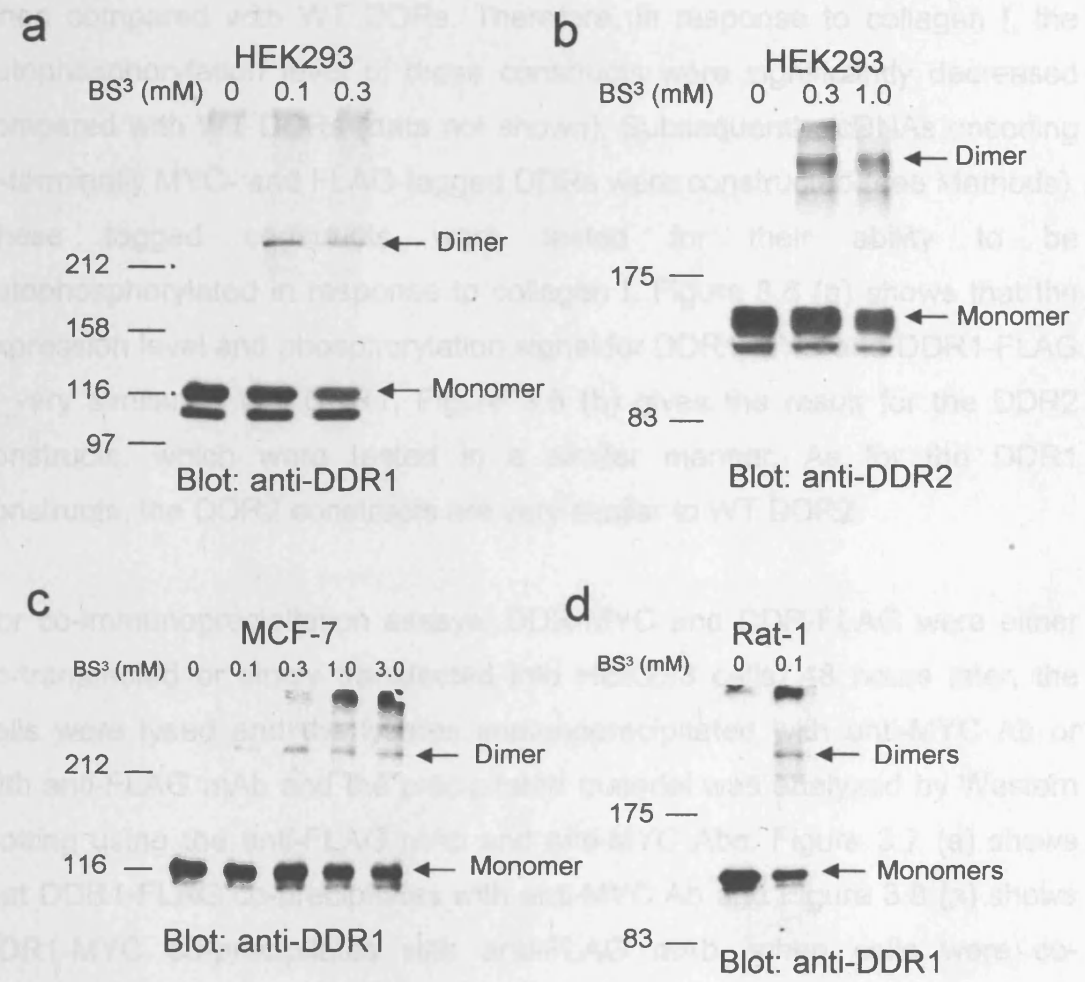

Figure 3.5: DDR1 and DDR2 form ligand-independent dimers on the cell surface. (a) and (b), chemical cross-linking analysis of WT DDR1 (a) and WT DDR2 (b) transiently over-expressed in HEK293 cells. (c) and (d), chemical cross-linking analysis of endogenous DDR1 in MCF-7 cells (c) and Rat-1 cells stably over-expressing WT DDR1 (d). The cells were washed once with cold PBS and incubated with BS^3 in PBS for 30 minutes at 37°C at the concentrations indicated. The reaction was quenched with 10 mM Tris pH 7.4, followed by cell lysis. Cell lysates were analysed by SDS-PAGE and Western blotting. The blots were probed with anti-DDR1 (a), (c) and (d) or anti-DDR2 (b) Abs. The position and sizes (in kDa) of MW markers are indicated.

DDR protein - the upper form being expressed to a significantly lower extent when compared with WT DDRs. Therefore, in response to collagen I, the autophosphorylation level of these constructs were significantly decreased compared with WT DDRs (data not shown). Subsequently, cDNAs encoding C-terminally MYC- and FLAG-tagged DDRs were constructed (see Methods). These tagged constructs were tested for their ability to be autophosphorylated in response to collagen I. Figure 3.6 (a) shows that the expression level and phosphorylation signal for DDR1-MYC and DDR1-FLAG is very similar to WT DDR1. Figure 3.6 (b) gives the result for the DDR2 constructs, which were tested in a similar manner. As for the DDR1 constructs, the DDR2 constructs are very similar to WT DDR2.

For co-immunoprecipitation assays, DDR-MYC and DDR-FLAG were either co-transfected or singly transfected into HEK293 cells. 48 hours later, the cells were lysed and the lysates immunoprecipitated with anti-MYC Ab or with anti-FLAG mAb and the precipitated material was analyzed by Western blotting using the anti-FLAG mAb and anti-MYC Abs. Figure 3.7 (a) shows that DDR1-FLAG co-precipitates with anti-MYC Ab and Figure 3.8 (a) shows DDR1-MYC co-precipitates with anti-FLAG mAb, when cells were co-transfected with both tagged constructs. To ensure that the anti-MYC Ab does not recognize the FLAG epitope and vice versa, controls were carried out where the lysate of cells singly transfected with one epitope-tagged receptor, e.g. DDR-FLAG, were immunopreciptated with anti-MYC Ab. When blotted with anti-FLAG mAb, no immunoprecipitated DDR-FLAG was seen (Figure 3.7, a and b, lower panels, lane 4) indicating that the anti-MYC antibody does not recognize the FLAG epitope. The anti-FLAG mAb was also tested and the results show that it does not react with the MYC epitope (Figure 3.8, a and b, lower panels, lane 1). *In vitro* mixing controls were carried out where lysates of cells singly transfected with DDR-MYC or DDR-Flag were mixed together and immunoprecipitated with one Ab and blotted with the other Ab (indicated by an asterisk in Figure 3.7 and 3.8). The mixing controls showed a negative result as no co-precipitation of two differently

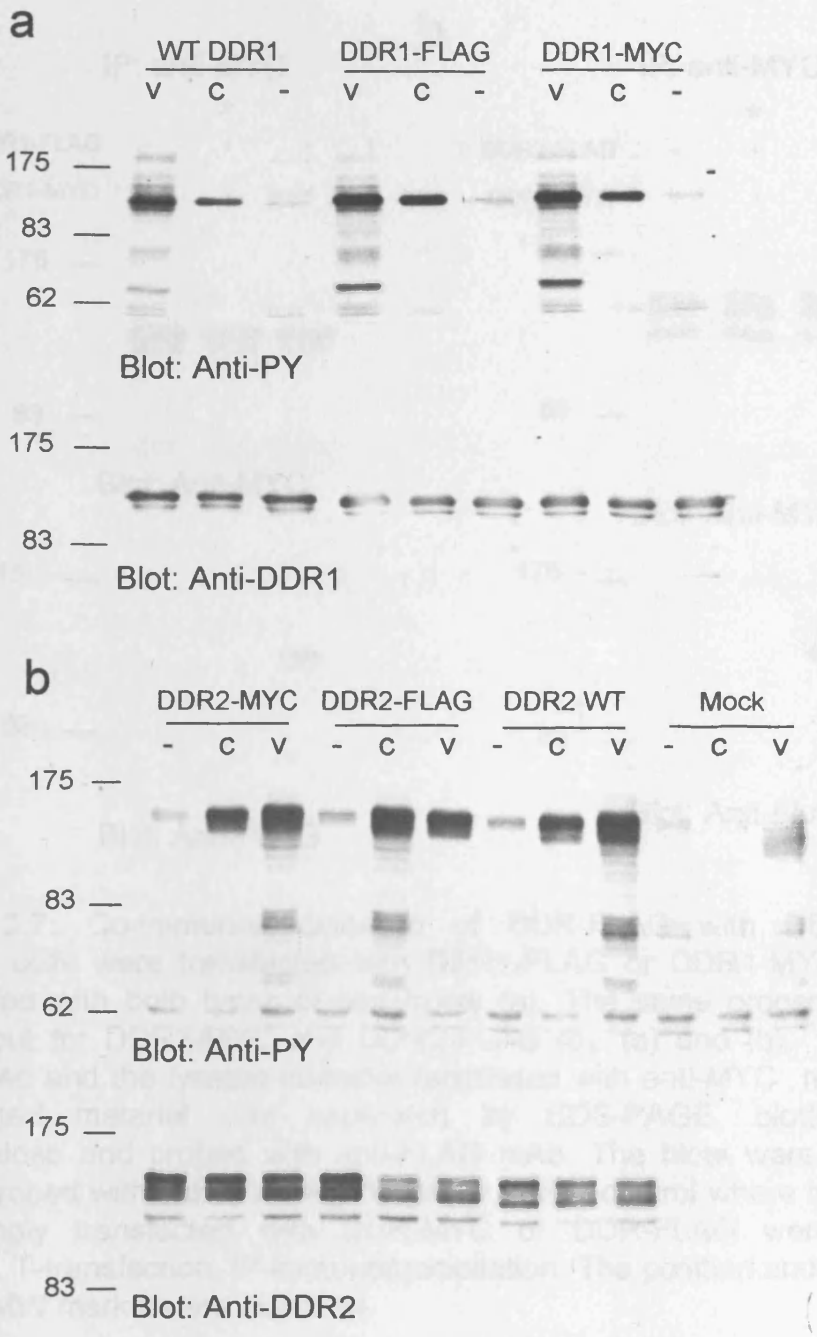

Figure 3.6: DDR-FLAG and DDR-MYC show normal autophosphorylation, similar to WT DDR. WT DDR1, DDR1-MYC or DDR1-FLAG (a), and WT DDR2, DDR2-MYC or DDR2-FLAG (b), were transiently over-expressed in HEK293 cells. After stimulation with 10 μg/ml collagen I (C) or 1 mM sodium orthovanadate (V) cell lysates were analysed by SDS-PAGE and Western blotting. The blots were probed with anti-phosphotyrosine mAb 4G10 (a and b, upper panels) or probed with anti-DDR1 Ab (a and b, lower panels). The position and sizes (in kDa) of MW markers are indicated.

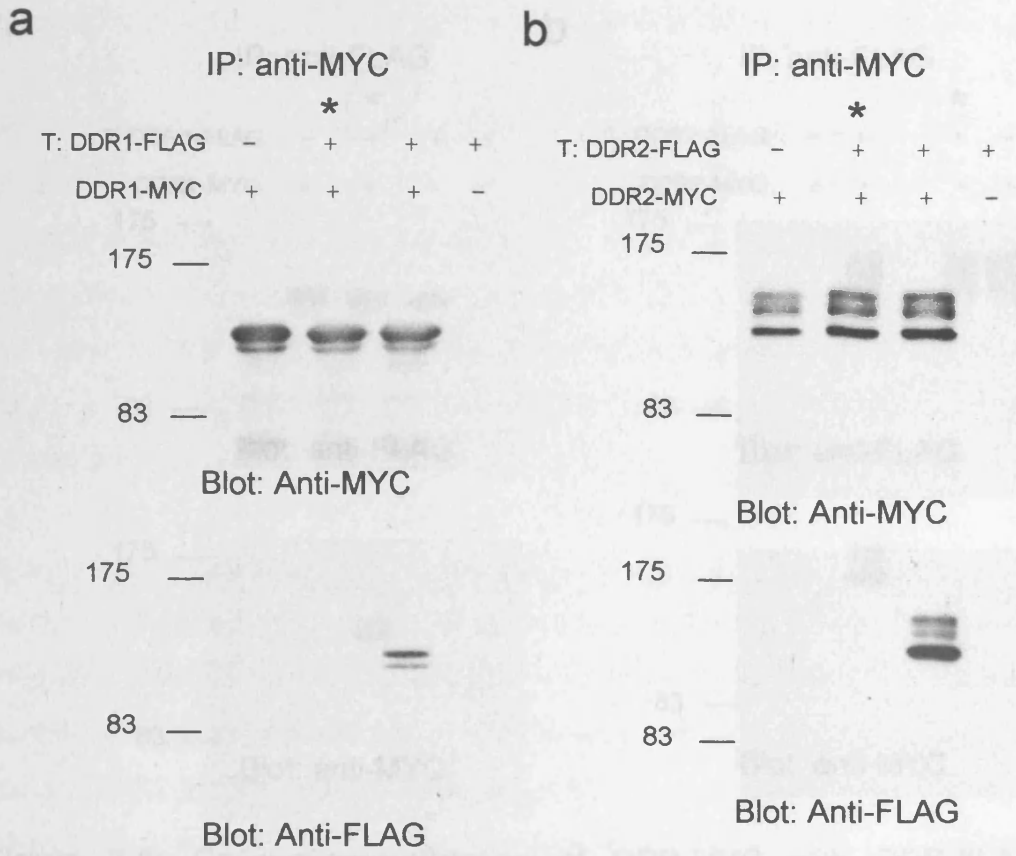

Figure 3.7: Co-immunoprecipitation of DDR-FLAG with DDR-MYC. HEK293 cells were transfected with DDR1-FLAG or DDR1-MYC or co-transfected with both types of constructs (a). The same procedure was carried out for DDR2-MYC and DDR2-FLAG (b). (a) and (b), The cells were lysed and the lysates immunoprecipitated with anti-MYC mAb. The precipitated material was separated by SDS-PAGE, blotted onto nitrocellulose and probed with anti-FLAG mAb. The blots were stripped and re-probed with anti-MYC Ab. *denotes mixing control where lysates of cells singly transfected with DDR-MYC or DDR-FLAG were mixed together. T-transfection, IP-immunoprecipitation. The position and sizes (in kDa) of MW markers are indicated.

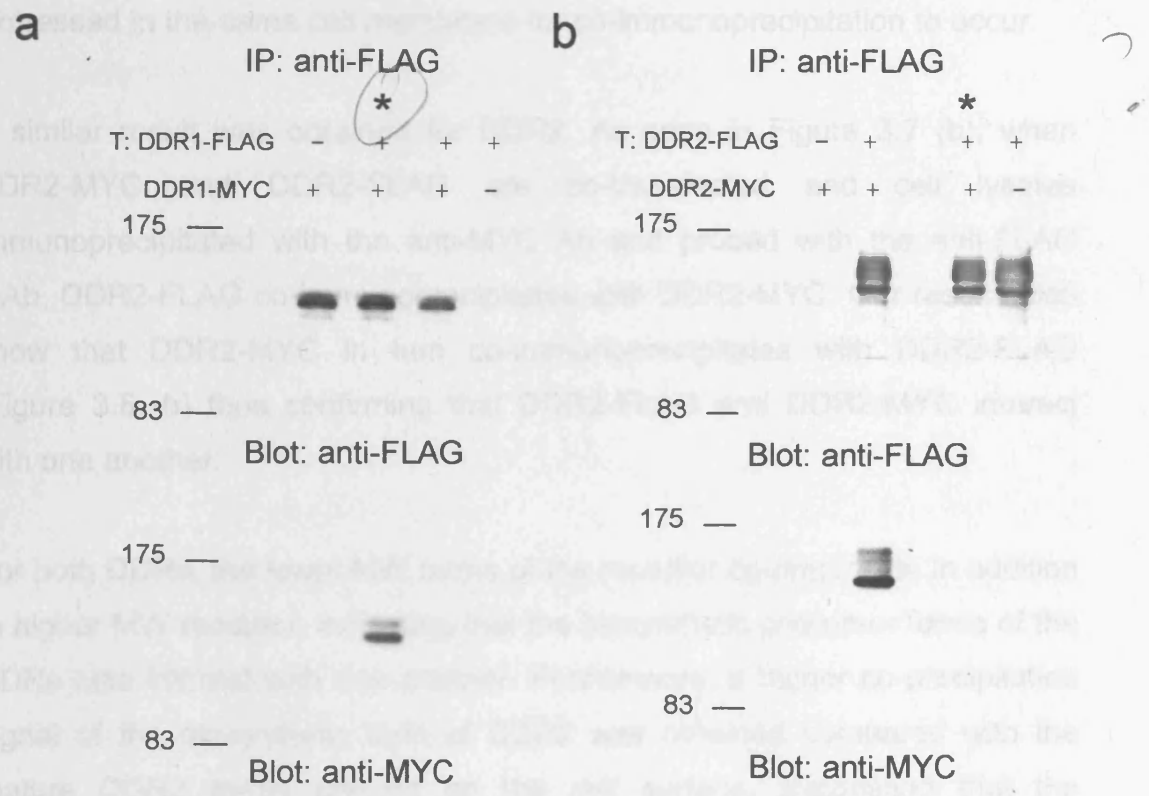

Figure 3.8: Co-immunoprecipitation of DDR-MYC with DDR-FLAG. HEK293 cells were transfected with DDR1-FLAG or DDR1-MYC or co-transfected with both types of constructs (a). The same procedure was carried out for DDR2-FLAG and DDR2-MYC constructs. (a) and (b), The cells were lysed and the lysates immunoprecipitated with anti-FLAG mAb. The precipitated material was separated by SDS-PAGE, blotted onto nitrocellulose and probed with anti-FLAG mAb. The blots were stripped and re-probed with anti-MYC Ab. *denotes mixing control where lysates of cells singly transfected with DDR-MYC or DDR-FLAG were mixed together. T-transfection, IP-immunoprecipitation. The position and sizes (in kDa) of MW markers are indicated.

tagged DDRs were seen, indicating that the tagged receptors need to be expressed in the same cell membrane for co-immunoprecipitation to occur.

A similar result was obtained for DDR2. As seen in Figure 3.7 (b), when DDR2-MYC and DDR2-FLAG are co-transfected and cell lysates immunoprecipitated with the anti-MYC Ab and probed with the anti-FLAG mAb, DDR2-FLAG co-immunoprecipitates with DDR2-MYC. Our results also show that DDR2-MYC in turn co-immunoprecipitates with DDR2-FLAG (Figure 3.8, b) thus confirming that DDR2-FLAG and DDR2-MYC interact with one another.

For both DDRs, the lower MW forms of the receptor co-precipitate in addition to higher MW receptor, indicating that the biosynthetic precursor forms of the DDRs also interact with one another. Furthermore, a higher co-precipitation signal of the biosynthetic form of DDR2 was obtained compared with the mature DDR2 forms present on the cell surface, suggesting that the biosynthetic form may oligomerise to a greater extent than the mature forms. As the DDRs are over-expressed in HEK293 cells, this may be due to the greater concentration of the precursor form present in the ER.

We next used the co-immunoprecipitation assay to investigate the effect of collagen on DDR oligomerisation. HEK293 cells, co-transfected with MYC- and FLAG-tagged DDRs, were treated for 90 minutes with collagen I and processed as described above. The lysates were immunprecipitated with the anti-MYC Ab (for DDR1) or anti-FLAG mAb (for DDR2) and the immunoprecipitates were subjected to SDS-PAGE and Western blotting. For both DDR1 and DDR2, the blots were first probed with anti-FLAG mAb. As seen in Figure 3.9 (a), the levels of DDR1-FLAG co-precipitated with the anti-MYC Ab after stimulation with collagen I is very similar to the levels in collagen untreated samples. The blot was stripped and re-probed with anti-MYC Ab to check the levels of DDR1-MYC, which was found to be similar in both stimulated and non-stimulated samples. For DDR2, a similar result was seen. The levels of DDR2-MYC co-precipitating with the anti-FLAG mAb was

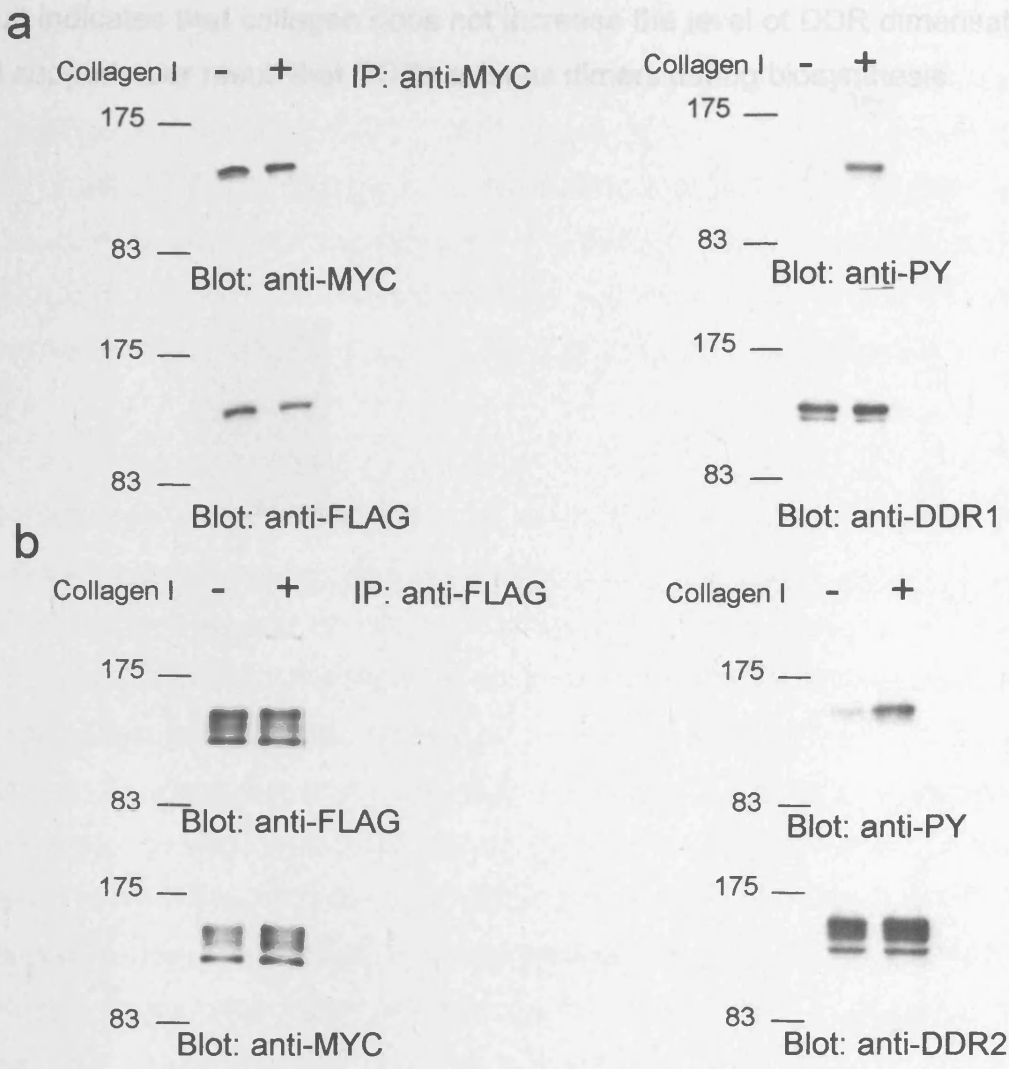

Figure 3.9: Collagen stimulation does not increase the levels of DDR oligomerisation. (a) Co-immunoprecipitation of DDR1-FLAG with DDR1-MYC in the presence of collagen I. (b) Co-immunoprecipitation of DDR2-MYC with DDR2-FLAG in the presence of collagen I. For both (a) and (b), HEK293 cells were co-transfected with plasmids encoding DDR-MYC and DDR-FLAG. Serum-starved cells were incubated with 10 μg/ml collagen I for 90 minutes. Cell lysates were immunoprecipitated with anti-MYC Ab (a) or anti-FLAG mAb (b), run on SDS-PAGE and blotting onto nitrocellulose. The blots were probed with anti-FLAG mAb, stripped and re-probed with anti-MYC Ab. The right panels show the corresponding activation levels of DDRs in co-immunoprecipitated samples. Aliquots of cell lysates were taken out prior to diluting the samples for immunoprecipitation, run on SDS-PAGE, blotted onto nitrocellulose and probed with anti-phosphotyrosine mAb, 4G10. The blots were stripped and re-probed with anti-DDR1 (a) or anti-DDR2 (b) Abs.

similar for collagen treated versus untreated samples (Figure 3.9, b). This result indicates that collagen does not increase the level of DDR dimerisation and supports our result that DDRs exist as dimers during biosynthesis.

3.3. Discussion

In the first part of this study, we have carried out basic biochemical characterisation of DDR1 and DDR2. We suspected that the lowest MW forms of the DDRs correspond to precursor forms of DDR1 and DDR2. Using cell surface biotinylation and digestion with Endo H, we have shown that the lowest MW weight forms of both DDRs are intracellularly localised, and represent an incompletely glycosylated, high mannose precursor form of the DDRs.

In addition, we wanted to know if the intermediate MW form of DDR2 was a precursor or a mature form of the receptor. Cell surface biotinylation showed that this form is present on the cell surface. In addition, this form is Endo H resistant and therefore corresponds to a mature, complex glycosylated form of DDR2 protein. Cell surface biotinylation after stimulating the receptors with collagen I revealed that whilst the highest MW form the DDRs show ligand-dependent activation, the intermediate MW form of DDR2 shows a highly reduced level of ligand-dependent autophosphorylation - suggesting that this form is in some way inhibited from autophosphorylation. To find out how the precursor forms differ from the mature forms, PNGase F digestion was carried out, which revealed that N-glycosylation is only partially responsible for the difference between the DDR MW forms. As the DDRs contain a putative O-glycosylation site in the ECD, we performed digestion analysis with neuraminidase and O-glycosidase, which suggested that the DDRs have an O-linked sugar modification. Furthermore, mutation of the potential O-glycosylation site in DDR1, followed by PNGase F digestion analysis confirmed that DDR1 is O-glycosylated.

Cell surface biotinylation in the presence of collagen I revealed that there is no change in total protein levels on the cell surface in the absence of collagen versus when collagen is present. This indicates that there is very little or no internalisation of DDRs upon collagen stimulation for 90 minutes. For most RTKs, the receptors are rapidly internalised after ligand stimulation

thus downregulating cellular responses (Mukherjee *et al.*, 1997). Most of the phosphorylated DDRs are found in the cell surface pool and there is no enhanced phosphorylation of DDRs located in the intracellular pool, after stimulation with collagen (Figure 3.2, a and b). This most likely means that the receptors are not endocytosed in an active form; and therefore are not signalling from within endosomes - a phenomenon that has been suggested for other RTKs such as EGFR and the insulin receptor (reviewed in Baass *et al.*, 1995). A plausible explanation for this result could be that, since the DDRs function as cell-matrix adhesion receptors, they therefore remain on the cell surface for a longer time than most other RTKs, transducing signals to the intracellular environment while maintaining adhesion with the ECM.

Although it is clear that in the case of DDR1, both N-linked and O-linked glycosylation is required to convert the precursor form to the mature receptor, for DDR2, the sugar modifications are not sufficient to convert the precursor to the intermediate MW form and subsequently to the highest MW form. The pattern of bands seen in HEK293 cells are also observed in primary hepatic stellate cells naturally expressing DDR2 (Olaso *et al.*, 2001). In addition, a constant ratio of upper versus intermediate form is obtained thus eliminating proteolytic degradation to cause this difference. Other potential post-translational modifications found on the DDR2 mature form could be, palmitoylation, ubiquitinylation or sumoylation. Palmitoylation is the covalent attachment of the lipid moiety, palmitic acid and is found on many proteins (reviewed in Bijlmakers and Marsh, 2003). For example, transmembrane proteins such as the T-cell receptor co-receptor CD8β (Kennedy and Limbird, 1994) and the GPCRs such as the α2A and β-2 adrenergic receptors (Belanger *et al.*, 2001) are modified by palmitoylation. Integral membrane proteins are palmitoylated on cysteines that are either close to the TM domain-cytosolic domain boundry, or located in the cytosolic domain itself, however a clear consensus sequence for palmitoylation of TM proteins has not been discovered (Kennedy and Limbird, 1994; Belanger *et al.*, 2001). In addition, not much is known about the function of palmitoylation in TM proteins, but there is emerging evidence that palmitoylation could be involved

in receptor trafficking, as shown by mutagenesis studies on the GPCR, CCR5 (Blanpain *et al.*, 2001) and localisation of TM proteins to lipid rafts (Webb *et al.*, 2000). However, it is unlikely that DDR2 is palmitoylated as there is no suitably localized cysteine residue within the TM domain or TM-cytosolic domain boundry.

Another type of post-translational modification is ubiquitination. Upon ligand binding, RTKs such as PDGFRβ (Mori *et al.*, 1995) and MET (Jeffers *et al.*, 1997) are modified by the covalent attachment of ubiquitin chains (polyubiquitination), which initiates targeting of these receptors to the proteasome or lysosome for degradation. In contrast, attachment of a single ubiquitin molecule (monoubiquitination) at multiple sites has been shown to play a role in receptor endocytosis and trafficking (reviewed in Hicke, 2001). Cell surface proteins which are polyubiquitinated or multi-monoubiquitinated, show a dense smearing at the higher MW region of the gel, in the presence of ligand, as demonstrated for PDGFβ and ErbB receptors (Mori *et al.*, 1992; Haglund *et al.*, 2003b). We have not observed such smearing in the Western blots of DDR immunoprecipitates, therefore it is unlikely that DDR2 is polyubiquitinylated or multi-monoubiquitinated. However it cannot be excluded that DDR2 is monoubiquitinated at a single site. Monoubiquitination at a single lysine residue has been found on other cell surface receptors which results in the addition of a single ubiquitin unit of approximately 8 kDa thus produces a shift in MW of the protein of interest (reviewed in Haglund *et al.*, 2003a). It is therefore possible that the addition of monoubiquitin could account for the difference between the intermediate and upper forms of DDR2.

However, as monoubiquitinylation is found to be induced upon ligand binding, it is likely that DDR2 contains a different type of post-translational modification, such as 'SUMO' modification. Post-translational modification of proteins by the small ubiquitin-like modifier (SUMO) was discovered relatively recently, and shown to regulate nuclear transport, stress response, signal transduction and cell cycle progression (Matunis *et al.*, 1996, Okura *et al.*,

1996). Like ubiquitin modification, covalent attachment of SUMO to protein targets occurs on lysine residues. Sequence analysis of DDR2 predicts a lysine residue in the cytosolic domain to be available for SUMO modification (www.abgent.com/doc/sumoplot). SUMO modification is reversible, and does not appear to target proteins for degradation. It rather alters the target protein function through changes in cellular localization, biochemical activation, or through protection from ubiquitin-dependent degradation (reviewed in Yeh *et al.*, 2000). Most of the known SUMO modified proteins are localized in the nucleus (such as p53, PML Ring Finger, RANGAP1) and the cytoplasm (IκBα). More recently the glucose transporters, GLUT1 which is localised on the cell membrane, and GLUT4, were shown to be substrates for sumoylation (Giorgino *et al.*, 2000). Future work would involve experimentally addressing the possibility of DDR2 to contain monoubiquitin or SUMO modification.

In the second part of this study, we investigated whether the DDRs exist as dimers on the cell surface, in the absence of ligand. Two different methods have been used to show that both DDR1 and DDR2 exist as preformed oligomers on the cell surface. Firstly, chemical cross-linking analysis of WT DDRs shows that at least a proportion of these receptors exist as ligand-independent dimers. This method enables the sizes of the DDR complexes to be obtained by MW analysis. In addition, we were able to use this method to observe endogenous DDR1 dimerisation in the MCF-7 cell line, and therefore a more natural environment for DDR1 than transient over-expression in HEK293 cells. Although the sizes of the higher MW bands produced by cross-linking correspond to dimers of DDR1 or DDR2, this does not necessarily point to the existence of oligomers since some other cellular protein of a similar size might be associated with the receptors. Therefore another method, co-immunoprecipitation, was used to demonstrate that DDRs form oligomers in the absence of ligand. Co-immunoprecipitation studies using two differently epitope-tagged DDRs confirmed the cross-linking results and demonstrated an association between DDR monomers.

As shown by experiments using ECD recombinant DDRs in vitro, the DDRs need to be dimerised in order to bind collagen - DDR1 only bound collagen with high affinity when fused to a dimerising Fc tag (Leitinger, 2003). The DDR2 ECD was shown to exist as dimers by chemical cross-linking, while DDR1 was a monomer, suggesting that cell surface DDR2 might be expected to form dimers in the absence of ligand. Another study using atomic force microscopy to investigate the DDR binding site on collagen reported that DDR2 needed to be dimerised via an Fc tag, and clustered, in order to bind collagen efficiently (Agarwal *et al.*, 2002).

The existence of preformed receptor oligomers in the absence of ligand have been reported for the RTKs, EGFR (Gadella and Jovin, 1995; Moriki *et al.*, 2001). The fibroblast growth factor receptor (FGFR) has also been implicated to exist as preformed dimers (Raffioni *et al.*, 1998). Upon studying a KD mutant of this receptor, the investigators found that the precursor form of the mutant receptor exhibits ligand-independent activation, which is not seen for the mature form of the receptor. Based on this, a model was proposed for the signalling of this receptor, which implies that normal FGFRs on the cell surface are likely to be dimerised in the absence of ligand. In addition, a number of cytokine receptors such as transforming growth factor-β (TGFβ) receptors I and II (Gilboa *et al.*, 1998), the Epo receptor (Constantinescu *et al.*, 2001) and the GH receptor (Gent *et al.*, 2002; Brown *et al.*, 2005) have been shown to exhibit ligand-independent dimerisation on the cell surface.

As shown by co-precipitation studies, the precursor receptor forms are able to interact, suggesting that the DDRs are already oligomerised during biosynthesis and remain associated during transport to the cell surface. It is likely that dimerisation is required for either DDR biosynthesis and/or transport of DDR protein to the cell surface. Oligomerisation of the GH receptor in the ER has been shown by co-immunoprecipitation (Gent *et al.*, 2002). Type I and II TGFβ receptors have been shown to form homodimers in the ER, as shown by sedimentation velocity of metabolically labelled receptors on sucrose gradients (Gilboa *et al.*, 1998).

Upon establishing that DDRs are predimerised in the absence of ligand, the next step was to investigate the effects of collagen on DDR dimerisation. Chemical cross-linking studies of DDRs upon stimulation with collagen I, did not produce a conclusive result, due to the problem of large MW of trimeric collagen-receptor complex (of approximately 500 KDa), which is stabilised upon cross-linking. These large complexes most likely do not enter SDS-PAGE gels efficiently (data not shown). We used co-immunoprecipitation to obtain a preliminary idea of the effect of collagen in DDR dimerisation. As shown in Figure 3.9, we did not see a difference in co-precipitation of epitope-tagged DDRs after stimulation with collagen I for 90 minutes, when compared with co-precipitation levels in unstimulated cells, indicating that collagen does not alter the abundance of preformed DDR dimers. This result is supported by our finding that the DDRs exist as dimers from the time of their synthesis in the ER.

It is therefore likely that collagen binding to DDR dimers results in a conformational change within dimeric receptors and not an increase in receptor dimers. However other types of experiments need to be carried to confirm this; such as fluorescence resonance energy transfer (FRET). FRET is a biophysical method which has been used to investigate the effect of ligand binding to other cell surface receptors such as the GH receptor (Brown *et al.*, 2005); and is a popular method for investigating oligomerisation of a number of receptors which belong to the GPCR family (Rocheville *et al.*, 2000; Cornea *et al.*, 2001; Floyd *et al.*, 2003; Overton *et al.*, 2003).

In summary, the results presented in this chapter suggest that the DDRs are dimerised in the ER during biosynthesis and are transported to the cell surface as dimers. This dimerised receptor complex is inactive by virtue of the cytoplasmic KDs being held in an inhibitory conformation. Collagen binding most likely induces a re-orientation of receptor monomers within the dimer, allowing the KDs to become activated.

Chapter 4

Analysis of receptor domains responsible for DDR oligomerisation and/or activation

4.1. Introduction

Both DDR1 and DDR2 are composed of an N-terminal discoidin domain (DS), followed by a region of no known homology (domain X), a TM domain, a juxtamembrane domain and a C-terminal catalytic tyrosine KD. DDR1 contains an additional region rich in proline and glycine situated between the domain X and the TM domain (see Introduction and Figure 1.9).

Studies with DDR1 and DDR2 deletion mutants (Leitinger, 2003) revealed a difference between DDR1 and DDR2 in the contribution of protein domains for collagen-induced DDR activation. DDR1 needed the whole ECD for collagen binding and receptor activation, whereas for DDR2 a large part of the ECD was not required. For DDR2 the DS domain seemed sufficient for both collagen binding and receptor activation. Therefore, DDR1 and DDR2 might show significant differences in the context of receptor domains involved in dimer formation. Chemical cross-linking of cell surface-expressed DDR1 and DDR2 deletion mutants were carried out in order to define which parts of the ECD was involved in dimerisation and to investigate the importance of the TM domain, cytoplasmic juxtamembrane domain and KD for DDR dimerisation. In addition, to confirm cross-linking results, co-immunoprecipitation studies of epitope-tagged DDR1 and DDR2 mutants were carried out.

4.2 Results

4.2.1. Chemical cross-linking analysis of DDR1 deletion mutants

Various DDR1 deletion mutants were tested for their ability to be cross-linked by BS^3. Figure 4.1 shows schematic drawings of full-length WT DDR1 and DDR1 deletion mutants. For these experiments the mutants were transiently over-expressed in HEK293 cells along with the WT DDR1. The cells were incubated with BS^3, followed by cell lysis, SDS-PAGE and Western blotting using the anti-DDR1 Ab.

So far, all studies have been carried out with the DDR1b isoform. An experiment was carried out to compare the cross-linking of two different isoforms of DDR1, DDR1a and DDR1b, with each other. The difference between the two isoforms is that DDR1b has a 37 amino acid insertion in the juxtamembrane region, and we wanted to investigate if the lack of this insertion in DDR1a would affect its ability to be cross-linked by BS^3. In the same manner, a DDR1 deletion mutant, MDN, which lacks the KD, was tested. For this experiment DDR1a, DDR1b and MDN cDNAs were expressed from a different vector, pRK5 (obtained from Sugen Inc, San Francisco, CA). The expression level from this vector is higher than that of DDR1 expressed from the pcDNA3.1 vector which was used to express all other DDR1 cDNAs. Both DDR1a and DDR1b isoforms show a very similar pattern of higher oligomer bands in the presence of BS^3 (Figure 4.2). The MDN mutant, which lacks the KD, showed oligomers which correspond to dimers. As this mutant is known to be dominant negative, it is expected to be able to dimerise, and the cross-linking result confirms this.

Subsequently a DDR1 mutant lacking the entire cytosolic region (DDR1 ECTM) was tested to investigate if the cytosolic juxtamembrane region was needed for DDR1 dimerisation (Figure 4.3, a and b). The blots were probed with anti-DDR1 Ab, 74A, which recognises an epitope at the N-terminus of DDR1. This Ab does not recognise WT DDR1 as strongly as the C-terminal anti-DDR1 Ab used in most other blots to detect DDR1 with intact

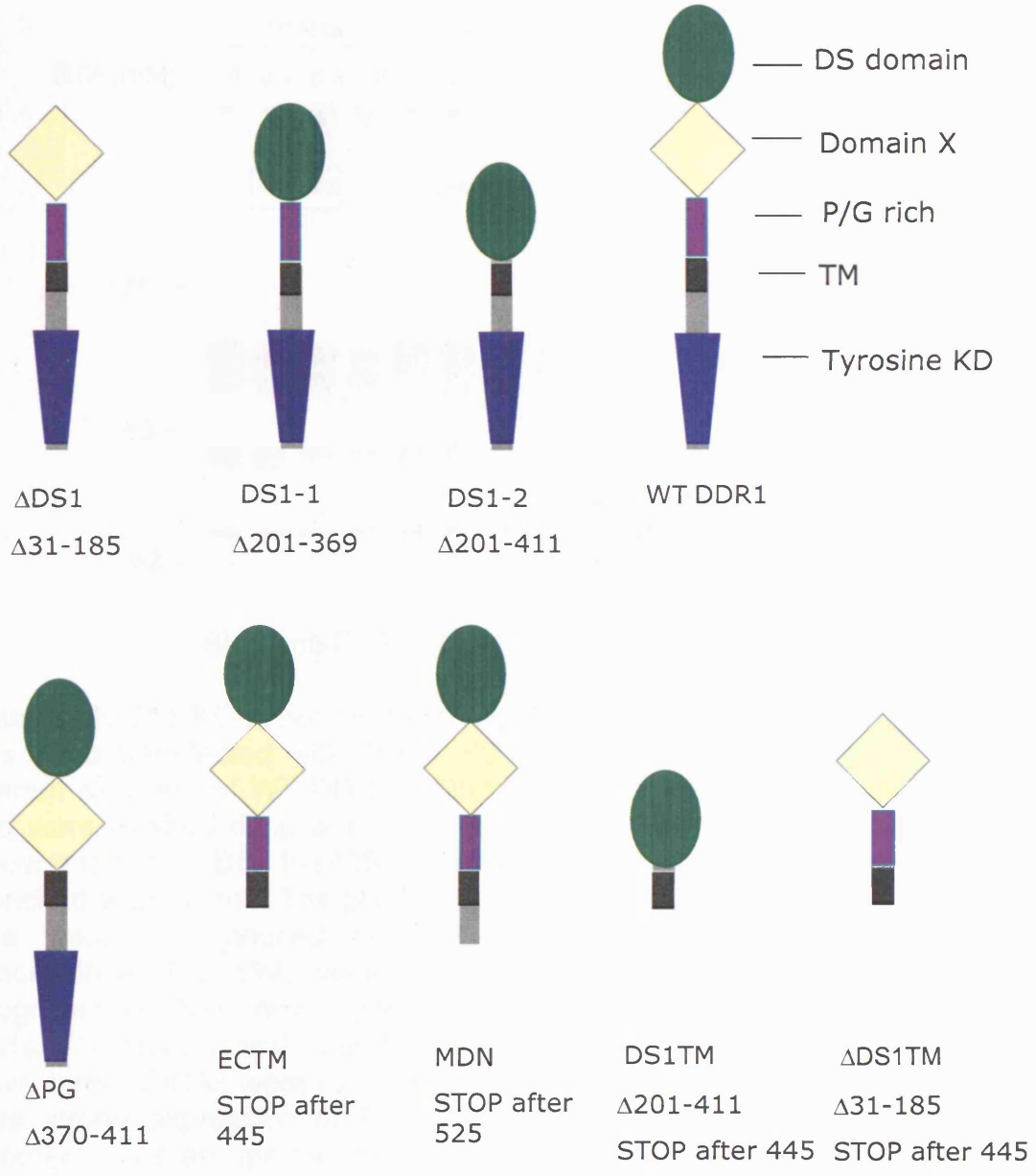

Figure 4.1: Schematic representation of WT DDR1 and DDR1 deletion mutants. The mutant ΔDS1 lacks the DS domain whilst DS1-1 lacks the region between the DS domain and P/G rich region (domain X), DS1-2 lacks most of the region between the DS domain and the TM domain (i.e. the domain X and P/G rich region). The ΔPG mutant has the P/G rich region deleted. The two cytoplasmic deletion mutants are ECTM (which lacks the entire cytoplasmic domain) and MDN (which lacks only the tyrosine KD). The double deletion mutant, DS1TM, contains deletion of the domain X, P/G rich region and the entire cytoplasmic domain, whilst the double mutant ΔDS1TM, has the DS domain and the entire cytoplasmic domain deleted. The numbers below each mutant refer to the deleted amino acids.

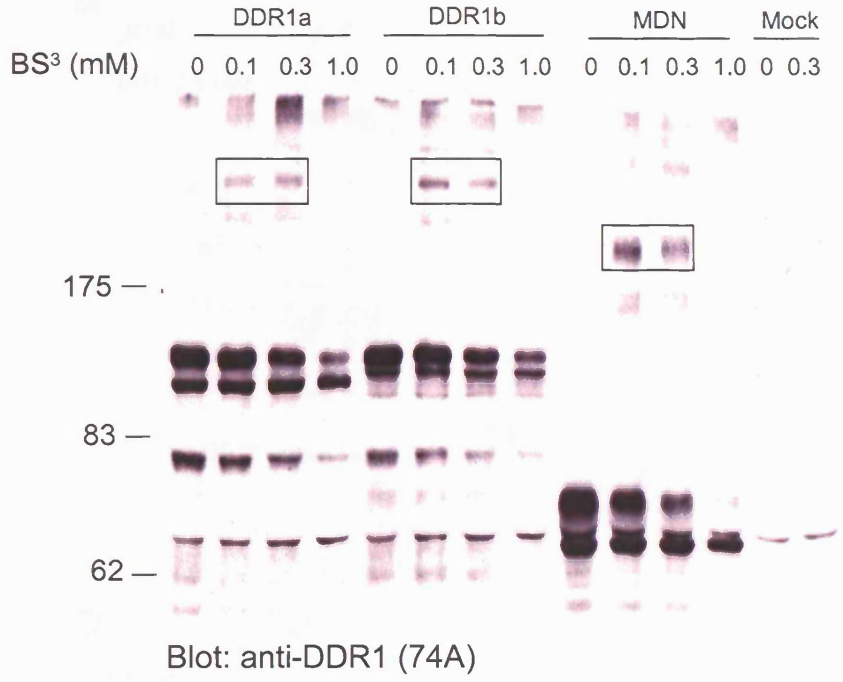

Figure 4.2: The KD is not necessary for DDR1 dimer formation. HEK293 cells were transfected with DDR1 KD deletion mutant, MDN, and two different isoforms of WT DDR1, DDR1a and DDR1b. 48 hours later, the cells were washed once with cold PBS and incubated with the indicated concentrations of BS^3 in PBS for 30 minutes at RT. The reaction was quenched with 10 mM Tris pH 7.4. The cells were lysed and cell lysates were were run reduced on 7.5% SDS-PAGE and blotted onto nitrocellulose. The blots were probed with anti-DDR1 (74A) Ab which recognises an N-terminal epitope of DDR1. Boxed areas show dimer bands. The position and sizes (in kDa) of MW markers are indicated. The above three cDNAs were expressed from a different vector, pRK5, which gives strong expression of DDRs, hence the signal for the WT DDR oligomer bands are greater than that obtained in Figure 4.3 (PTO), even though both blots were probed with the 74A Ab, which gives a weaker signal than the anti-DDR1 Ab against the C-terminus.

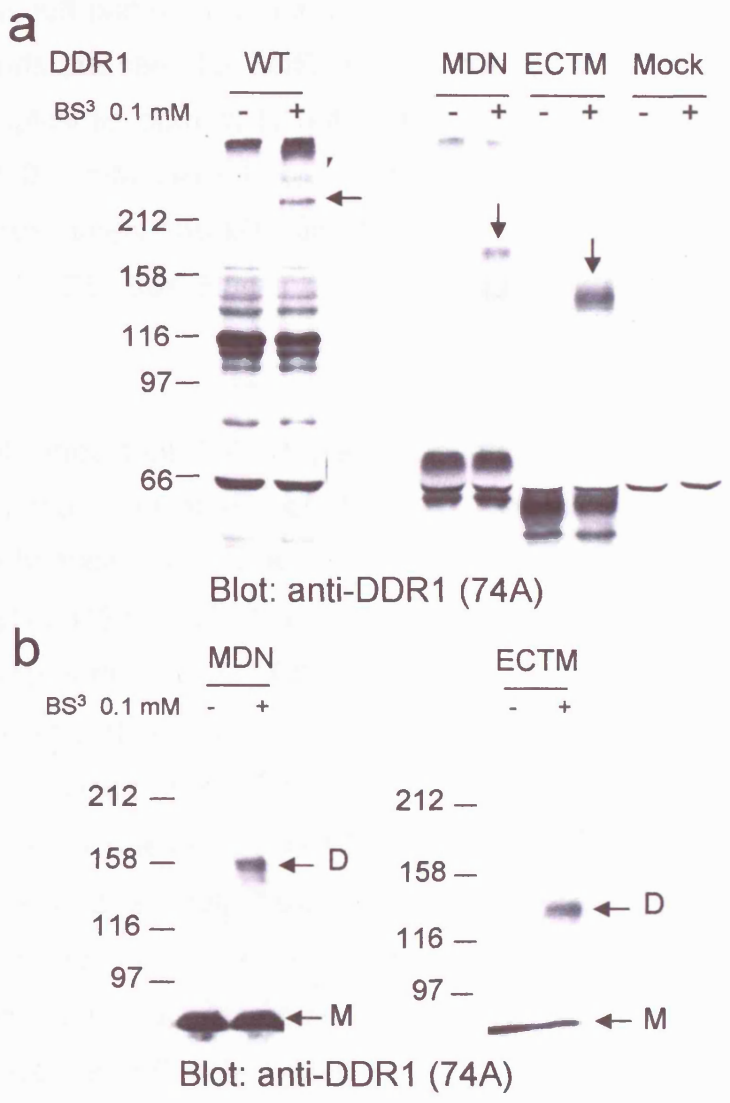

Figure 4.3: The cytoplasmic domain is not required for DDR1 dimerisation. (a) HEK293 cells were transiently transfected with the DDR1 deletion mutants MDN, ECTM or WT DDR1. 48 hours later, the cells were washed once with cold PBS and incubated with 0.3 mM BS^3 in PBS for 30 minutes, RT. The reaction was quenched with 10 mM Tris pH 7.4. The cells were lysed and cell lysates were were run reduced on 7.5% SDS-PAGE and blotted onto nitrocellulose. Black arrows point to the dimer bands. (b) Cell lysates of MDN and ECTM samples were loaded onto 5% SDS-PAGE and immunoblotted as described above. Black arrows point to the position of monomers (M) - which runs with the gel front - and dimers (D). The position and sizes (in kDa) of MW markers are shown.

cytoplasmic domains. Hence a longer exposure blot for WT DDR1 is shown separately (a, left panel), in order to clearly visualize the dimer band. Higher oligomer bands are seen for DDR1 ECTM mutant, and DDR1 MDN, proving that the cytoplasmic domain is not required for DDR1 dimerisation. In the presence of 0.1 mM cross-linker, dimers are clearly visible of molecular weights approximately 160 kDa and 140 kDa (as estimated by MW analysis on 5% SDS-PAGE, see Figure 4.3, b) for DDR1 MDN and DDR1 ECTM, respectively.

Having established that the cytoplasmic domain is not required for DDR1 dimerisation, the involvement of different subdomains of the ECDs was tested by chemical cross-linking analysis of four extracellular deletion mutants, DS1-1, DS1-2, ΔDS1 and ΔPG (schematically shown in Figure 4.1). Figure 4.4 shows the results of the chemical cross-linking analysis. As seen in Figure 4.4 (a), ΔDS1, which lacks the DS domain, shows a higher MW band in the presence of BS^3 (of approximately 200 kDa) which corresponds to ΔDS1 dimers. However, the DDR1 deletion mutant ΔPG, which lacks the P/G rich region, does not show a higher MW weight band which might correspond to dimers of ΔPG. Furthermore, as seen in Figure 4.4 (b), the DS1-1 mutant, which lacks the domain X, and DS1-2 mutant, which lacks the domain X plus the P/G rich region, do not show any corresponding dimer bands.

A reason for the lack of cross-linking of ΔPG, DS1-1 and DS1-2 could be that these proteins are not expressed on the cell surface, therefore the mutants were tested for cell surface expression.

4.2.2. Test for cell surface expression of DDR1 deletion mutants ΔPG, and DS1-1 and DS1-2

The DDR1 deletion mutants, DS1-1, DS1-2 and ΔDS1 were previously tested for collagen-dependent autophosphorylation (Leitinger, 2003), and found to be defective in this process. Subsequently, the ΔPG mutant was made and

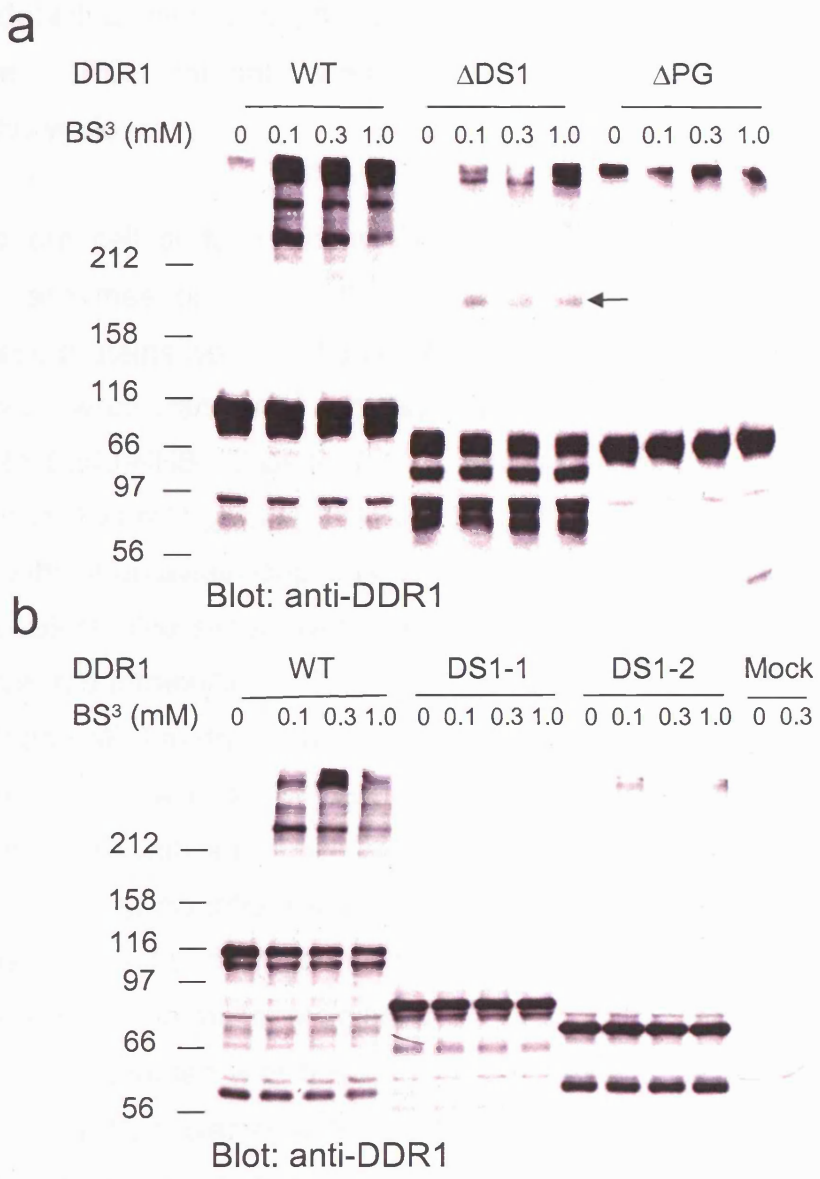

Figure 4.4: The ECD is not required for DDR1 dimerisation. HEK293 cells were transfected with each of the above DDR1 deletion mutants and WT DDR1. 48 hours later, the cells were washed once with cold PBS and incubated with 0.3 mM BS^3 in PBS for 30 minutes at RT. The reaction was quenched with 10 mM Tris pH 7.4. The cells were lysed and cell lysates were were run reduced on 7.5% SDS-PAGE and blotted onto nitrocellulose. The blots were probed with anti-DDR1 Ab. A black arrow points to ΔDS1 dimers. The position and sizes (in kDa) of MW markers are indicated.

tested for collagen-induced autophosphorylation. As seen in Figure 4.5, WT DDR1 produced a clear phosphorylation signal in response to collagen I whilst the ΔPG mutant was negative for collagen-dependent autophosphorylation.

We carried out cell surface biotinylation and digestion with Endo H and PNGase F enzymes on ΔPG, DS1-1 and DS1-2 mutants to investigate whether these proteins were on the cell surface. For cell surface biotinylation, these mutants were transiently expressed in HEK293 cells, and incubated with 3.5 mM Sulfo-NHS-LC-Biotin for 30 minutes on ice. The reaction was quenched with 100 mM glycine, followed by cell lysis. The cell lysates were incubated with streptavidin sepharose beads to pull-down biotinylated cell surface receptors. The supernatant was immunoprecipitated with anti-DDR1 Ab to recover the intracellular DDR1 receptor pool. Figure 4.6 (a) shows that both DS1-2 and ΔPG mutants are not present in the cell surface pool (lane S) and are instead intracellularly localised (lane I). Figure 4.6 (c) shows a control experiment with an intracellular protein Rho-GDI, carried out at the same time, showing no intracellular protein on the cell surface. To confirm the biotinylation results, digestion with Endo H and PNGase F were carried out (Figure 4.6, c). Immunoprecipitates of ΔPG, DS1-1 and DS1-2, were denatured and incubated with 5 units of Endo F or PNGase F enzyme for three hours at 37°C, subjected to SDS-PAGE and Western blotting. The ΔPG and DS1-1 proteins were both sensitive to Endo H, indicated by the shift to a lower MW form in the presence of this enzyme. Thus the ΔPG and DS1-1 proteins contain high mannose sugars and therefore all of the protein for these two mutants are most likely present as intracellular biosynthetic forms. For DS1-2, there is no shift upon Endo H or PNGase F digestion. The amino acid sequence of this mutant contains no potential N-linked glycosylation sites and therefore one cannot infer from Endo H digestion whether DS1-2 is present only as a biosynthetic precursor form.

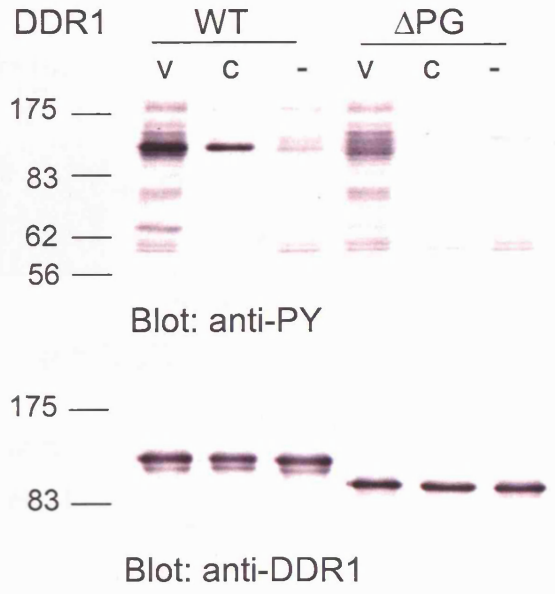

Figure 4.5: DDR1 ΔPG is defective in collagen-induced autophosphorylation. WT DDR1 or DDR1 ΔPG were transiently expressed in HEK293 cells. After stimulation with 10 μg/ml collagen 1 (C) or 1 mM sodium orthovanadate (V) cell lysates were analysed by SDS-PAGE and Western blotting. The blots were probed with anti-phosphotyrosine mAb 4G10 (upper panel) or probed with anti-DDR1 Ab (lower panel). The position and sizes (in kDa) of MW markers are indicated.

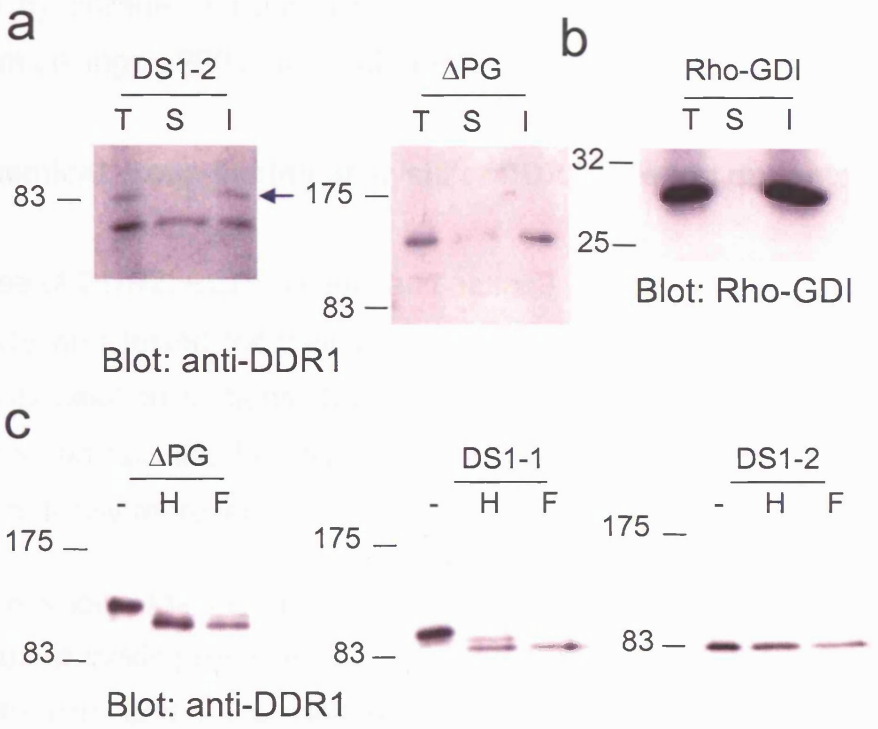

Figure 4.6: Cell surface expression of ΔPG, DS1-1 and DS1-2. (a) HEK293 cells transfected with cDNA of ΔPG or DS1-2 were incubated with 3.5 mM Sulfo-NHS-LC-Biotin in PBS for 30 minutes at 4°C. The reaction was terminated with 100 mM glycine. The cell lysates were incubated with streptavidin sepharose beads and bound and free protein was separated by centrifugation to pellet (containing cell surface receptors) and supernatant (containing intracellular receptors) fraction. The supernatant was immunoprecipitated with anti-DDR1 Ab (a) or Rho-GDI Ab (b). An equivalent lysate volume was incubated with anti-DDR1 Ab to analyze the total DDR protein in the sample. All samples were run reduced on 7.5% SDS-PAGE and blotted onto nitrocellulose and probed with anti-DDR1 Ab (a) or Rho-GDI (b). Blue arrow points to DS1-2 protein. T-total protein present in 0.5 ml lysate, S-cell surface receptors, I-intracellular receptors. (c) Enzymatic deglycosylation of ΔPG, DS1-1 and DS1-2. HEK293 cells were transfected with cDNAs of each of the constructs. 48 hours later the cells were lysed and the lysates immunoprecipitated with anti-DDR1 Ab. The precipitated material was denatured and incubated with either Endo H (H), PNGase F (F) or no enzyme (-) for 3 hours at 37°C, then separated by 7.5% SDS-PAGE, blotted onto nitrocellulose and probed with anti-DDR1 Ab. The position and sizes (in kDa) of MW markers are indicated.

Table 4.1 summarises the results of the various DDR1 mutants' ability to be activated by collagen I (results for DS1-1, DS1-2 and ΔDS2 mutants are taken from Leitinger, 2003) and their ability to be cross-linked by BS^3.

4.2.3. Chemical cross-linking analysis of DDR2 deletion mutants

In the case of DDR2, ECD mutants and mutants lacking the cytosolic domain were made and tested for their ability to be cross-linked by BS^3. The two DDR2 ECD deletion mutants DS2, which lacks most of the region between the DS domain and the TM region, and ΔDS2, which lacks the DS domain, are schematically represented in Figure 4.7.

Figure 4.8 shows the results of the chemical cross-linking analysis of the DDR2 mutant lacking the cytosolic domain (DDR2-ECTM-MYC). A MYC tag at the C-terminal end of the construct was introduced as there is no antibody which can recognise the ECD of DDR2. Dimers corresponding to a MW weight of 170 kDa were seen upon cross-linking with 0.3 mM BS^3 and 1.0 mM BS^3. Therefore the cytosolic domain is not necessary for DDR2 dimerisation.

To test whether a subdomain of the ECD was involved instead, we analysed cross-linking of the two DDR2 deletion mutants ΔDS2 and DS2 (Figure 4.9). For DS2, the monomeric protein has a MW of about 110 kDa and forms dimers which co-migrate with the marker of 212 kDa upon cross-linking. The dimer bands for ΔDS2, which appear around 220 kDa, are at low intensity due to the low expression of this mutant compared to WT DDR2 and ΔDS2 expression. Taken together, neither the DS domain nor the domain X are necessary for DDR2 dimerisation. Collagen-dependent activation assays of ΔDS2 and DS2 were carried out previously (Leitinger, 2003) and the results are summarised in Table 4.2, along with the cross-linking data.

	WT DDR1	DS1	DS1-2	ΔDS1	ΔPG	MDN	ECTM1	DS1TM
Collagen-dependent autophosphorylation	+	-	-	-	-	-	-	-
Ability to be cross-linked by BS^3	+	-	-	+	-	+	+	-

Table 4.1: Summary of the ability of DDR1 deletion mutants to activate in response to collagen I and to be cross-linked by BS^3

	WT DDR2	ΔDS2	DS2	ECTM2	DS2TM	ΔDS2TM
Collagen-dependent autophosphorylation	+	-	+	-	-	-
Ability to be cross-linked by BS^3	+	+	+	+	+	+

Table 4.2: Summary of the ability of DDR2 deletion mutants to activate in response to collagen I and to be cross-linked by BS^3.

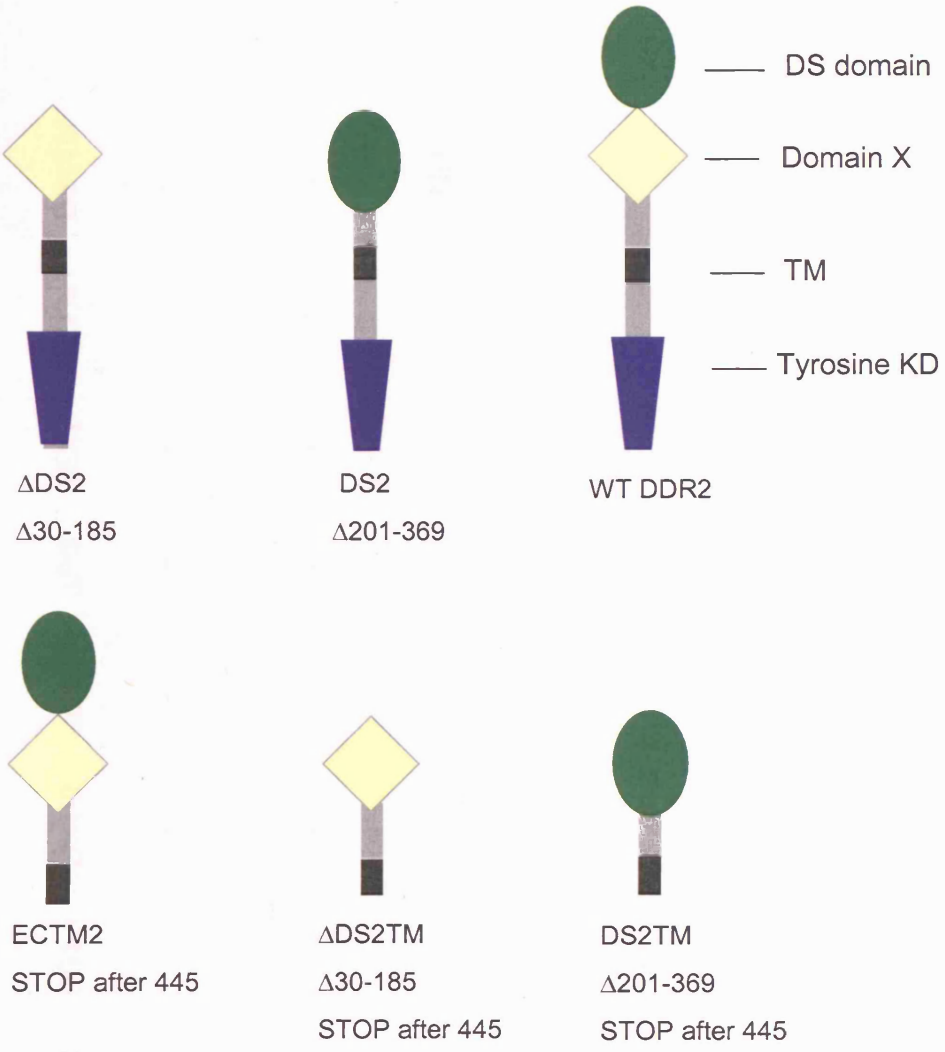

Figure 4.7: Schematic representation of WT DDR2 and DDR2 deletion mutants. The mutant ΔDS2 lacks the DS domain only and the mutant DS2 lacks most of the region between the DS domain and the TM domain. The ECTM2 mutant lacks the entire cytoslic region. The double mutants ΔDS2TM and DS2TM lack the DS domain and the cytosolic domain (ΔDS2TM) and the domain X and the cytoslic domain (DS2TM). The amino acids deleted are given below each mutant.

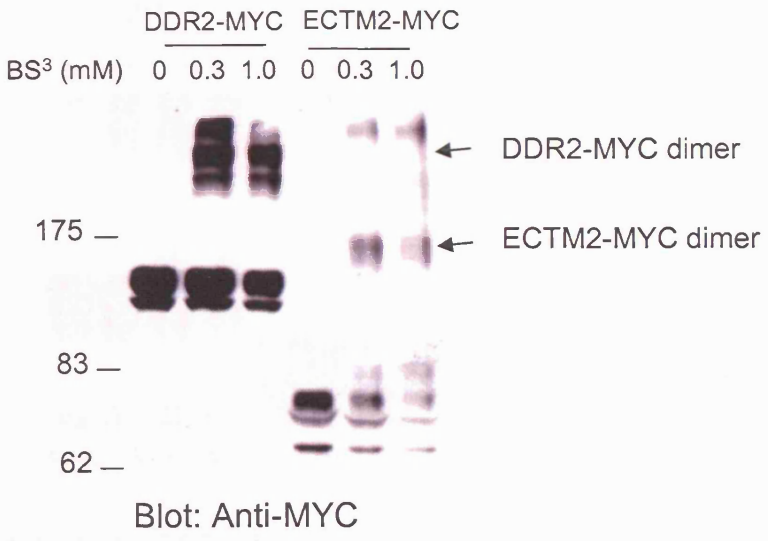

Figure 4.8: The cytosolic domain is not necessary for DDR2 dimerisation. HEK293 cells were transfected with DDR2 ECTM-MYC (ECTM2-MYC) or WT DDR2-MYC. 48 hours later, the cells were washed once with cold PBS and incubated with the indicated concentrations of BS^3 in PBS for 30 minutes at RT. The reaction was quenched with of 10 mM Tris pH 7.4. The cells were lysed and cell lysates were run reduced on 7.5% SDS-PAGE and blotted onto nitrocellulose. The blots were probed with anti-MYC Ab. The position and sizes (in kDa) of MW markers are indicated.

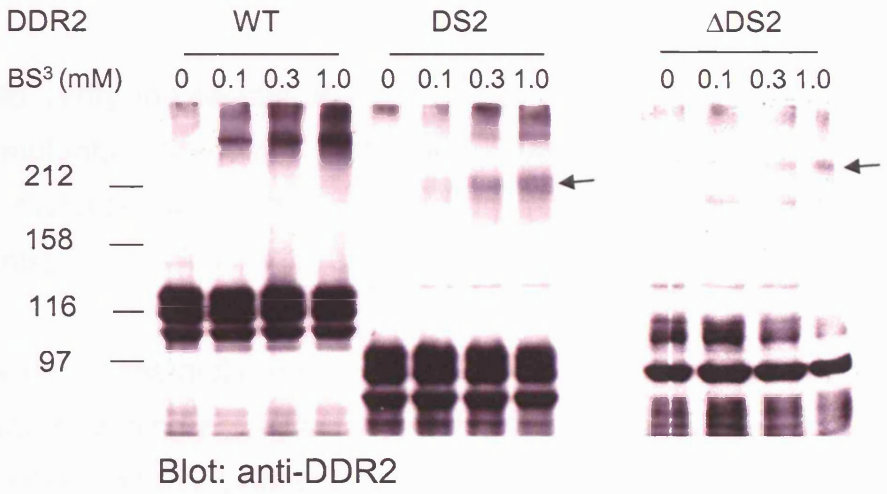

Figure 4.9: Most of the ECD of DDR2 is not necessary for DDR2 dimer formation. HEK293 cells were transfected with each of the above DDR2 deletion mutants, DS2, ΔDS2 or WT DDR2. 48 hours later, the cells were washed once with cold PBS and incubated with the indicated concentrations of BS^3 in PBS for 30 minutes at RT. The reaction was terminated by the addition of 10 mM Tris pH 7.4. The cells were lysed and cell lysates were were run reduced on 7.5% SDS-PAGE and blotted onto nitrocellulose. The blots were probed with anti-DDR2 mAb. The position and sizes (in kDa) of MW markers are indicated. Black arrows point to bands corresponding to dimers of DS2 and ΔDS2. The blot showing ΔDS2 had to be over-exposed as the expression level of this mutant is low.

4.2.4. Co-immunoprecipitation studies of epitope-tagged DDR1 deletion mutants

In order to verify the results of cross-linking analysis of DDR1 and DDR2 deletion mutants, C-terminal MYC- and FLAG-tagged DDR1 and DDR2 deletion mutants were made and used for co-immunoprecipitation experiments.

DDR1 deletion constructs, epitope-tagged with MYC or FLAG, were either co-transfected or singly transfected into HEK293 cells. The cells were lysed 48 hours later, and the lysates immunoprecipitated with anti-MYC Ab or with anti-FLAG mAb and the precipitated material was analyzed by Western blotting using the anti-FLAG mAb or anti-MYC Ab. As expected from the cross-linking results, the DDR1 cytoplasmic deletion mutant shows co-precipitation of FLAG-tagged protein with the anti-MYC Ab (Figure 4.10). The same experiment carried out with DDR1 ECD mutants gave a similar, positive result (Figure 4.11). As seen in Figure 4.11 (a), in cells co-transfected with ΔDS1-MYC and ΔDS1-FLAG, ΔDS1-FLAG co-precipitates with the anti-MYC Ab. The same experiment was carried out with the two ECD mutants, DS1-1 and DS1-2, which gave a negative result in the cross-linking assay and were shown to be most likely intracellulary localised. Both DS1-1-FLAG and DS1-2-FLAG co-precipitate with the respective MYC-tagged proteins, DS1-1-MYC and DS1-2-MYC (Figure 4.11, b and c). In addition, the intracellularly localised mutant, ΔPG, also shows co-precipitation of FLAG-tagged protein with the anti-MYC Ab. These results show that the above mentioned subdomains of the ECD of DDR1 are not required for DDR1 interaction. Furthermore, the intracellular DDR1 mutants can interact, which is similar to the result obtained for the lower forms of the WT DDRs.

To rule out that DDR1 dimerisation is due to multiple interactions along the entire ECD (in which case individual domain deletions within a homodimer might be tolerated), we co-expressed two different ECD deletion mutants that are not expected to be able to interact via their ECD. The DS1-2 construct retains the DDR1 DS domain, but places it in an unnatural position close to

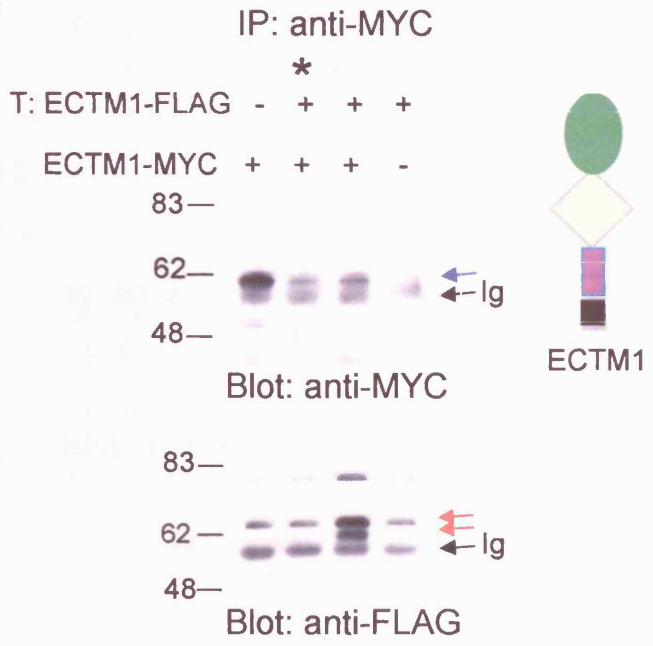

Figure 4.10: Co-immunoprecipitation of epitope-tagged DDR1 cytosolic domain deletion mutant. HEK293 cells were singly transfected with epitope-tagged cDNA of the deletion construct or co-transfected with both FLAG- and MYC-tagged cDNA. The cells were lysed and the lysates immunoprecipitated with anti-MYC Ab. The precipitated material was separated by 10% SDS-PAGE, blotted onto nitrocellulose and probed with anti-MYC or anti-FLAG mAb. *denotes mixing control where lysates of cells singly transfected with MYC- or FLAG-tagged mutants were mixed together. T-transfection; IP-immunoprecipitation. The blue arrow points to ECTM1-MYC, which is expressed only as a precursor form and runs just above Ig bands. Red arrows point to ECTM1-FLAG, of which both mature and precursor forms are expressed. The ECTM1 protein runs just above the Ig bands. The position and sizes (in kDa) of MW markers are indicated.

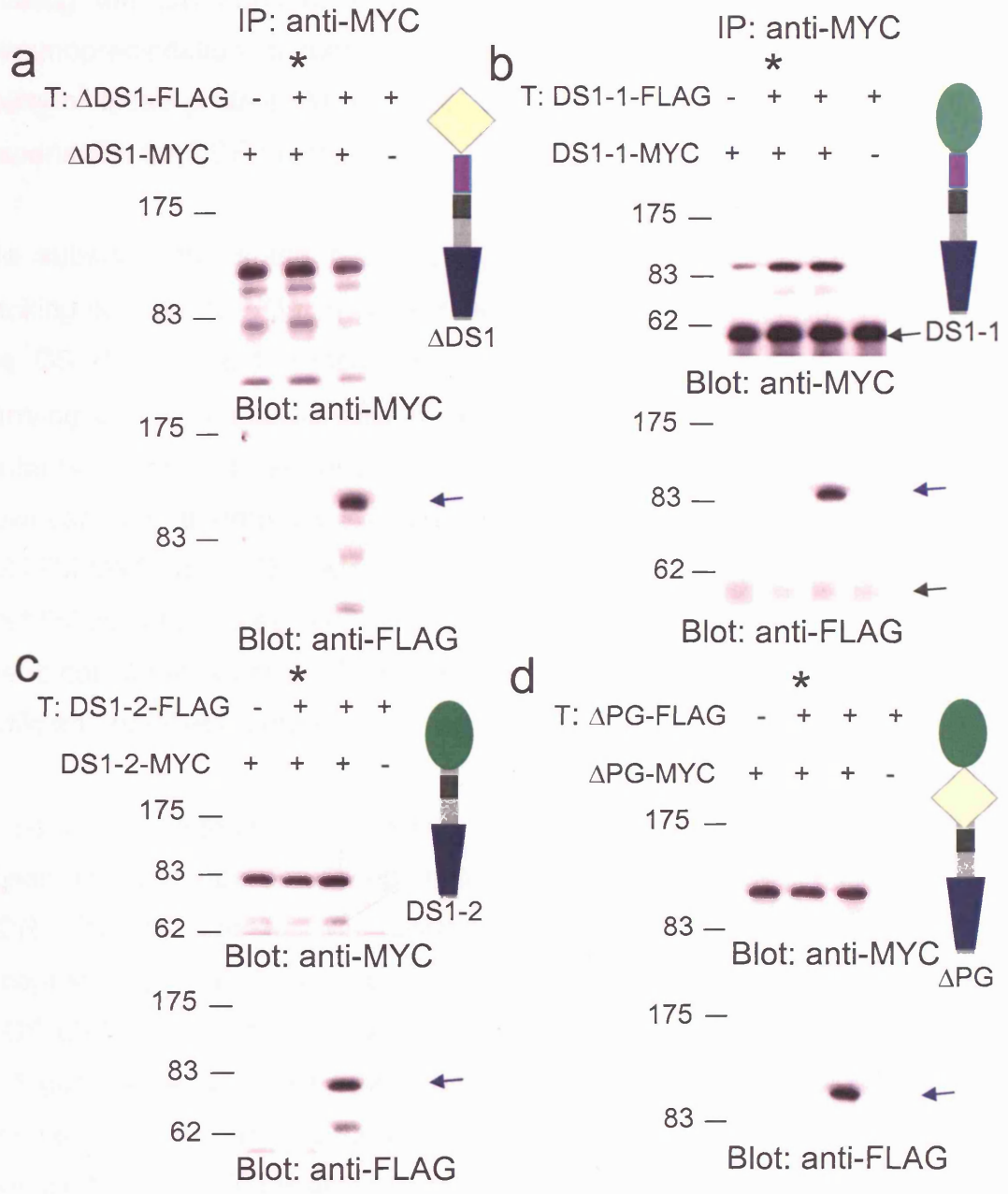

Figure 4.11: Co-immunoprecipitation of MYC- and FLAG-tagged DDR1 ECD deletion mutants. For each deletion mutant, HEK293 cells were singly transfected with epitope-tagged cDNA of the deletion construct or co-transfected with both FLAG- and MYC-tagged cDNA. The cells were lysed and the lysates immunoprecipitated with anti-MYC Ab. The precipitated material was separated by 7.5% SDS-PAGE, blotted onto nitrocellulose and probed with anti-MYC or anti-FLAG mAb. Blue arrows point to FLAG-tagged mutants. Black arrows point to Ig bands. *denotes mixing control where lysates of cells singly transfected with MYC- or FLAG-tagged mutants were mixed together. T-transfection; IP-immunoprecipitation. The position and sizes (in kDa) of MW markers are indicated.

the TM domain. The co-expressed ΔDS1 construct, on the other hand, is missing the DS domain, and retains the rest of the DDR1 ECD. Co-immunoprecipitation studies (Figure 4.12) indicated no impairment in the ability of these proteins to associate, showing that the entire DDR1 ECD is dispensable for DDR1 dimerisation.

We subsequently made two double deletion mutants of DDR1: DS1TM (lacking domain X, P/G rich and cytosolic regions) and ΔDS1TM (which lacks the DS domain and cytosolic region); both MYC- and FLAG-tagged for carrying out co-immunoprecipitation studies. The epitope-tagged ΔDS1TM mutants were not expressed by transiently transfected HEK293 cells however, and therefore we could only examine co-immunoprecipitation of DS1TM-MYC and DS1TM-FLAG. As seen in Figure 4.13, MYC-tagged DS1TM co-precipitates with DS1TM-FLAG, indicating that, in the absence of the cytoplasmic domain, both the DS domain and the TM domain are sufficient for DDR1 dimerisation.

A control experiment was carried out to establish that the interactions observed were not due to non-specific hydrophobic interactions between DDR1 mutant proteins. We used another RTK, fibroblast growth factor receptor 2 (FGFR2), tagged with six MYC epitopes at the C-terminus (FGFR2-6MYC), and co-transfected this receptor with DDR1-FLAG. As seen in Figure 4.14 (a), upon immunoprecipitation with the anti-MYC Ab and blotting with the anti-FLAG mAb, there is no DDR1-FLAG protein co-precipitating with FGFR-6MYC protein. The experiment was performed vice versa (Figure 4.14, b). Immunoprecipitating with the anti-FLAG mAb and blotting with anti-MYC Ab does not show FGFR-6MYC protein co-precipitating with DDR1-FLAG. A positive control for co-precipitation was carried out in the same experiment using DDR1-MYC and DDR1-FLAG, where DDR1-FLAG co-precipitates with the anti-MYC Ab.

Another control experiment was carried out where cells were lysed in RIPA buffer containing 0.1% SDS. RIPA buffer has been used in co-

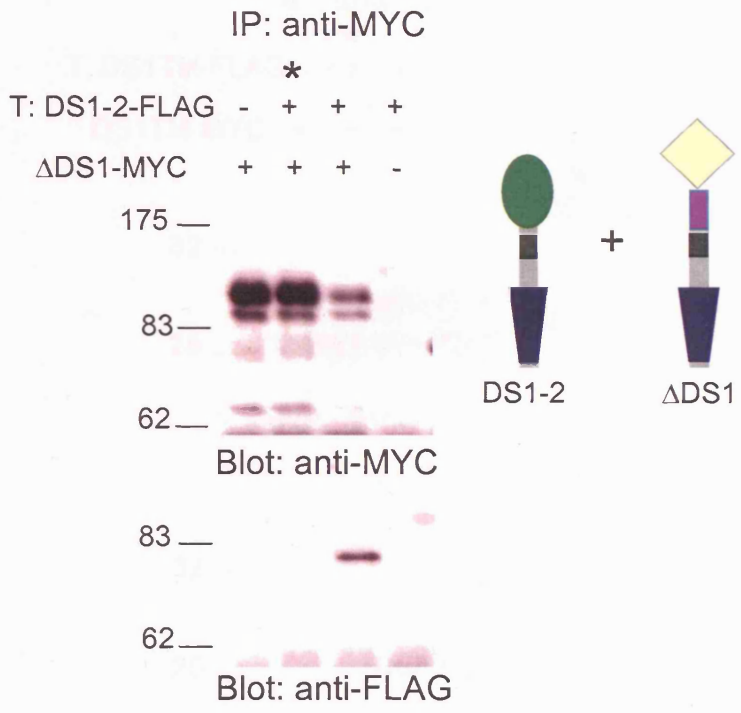

Figure 4.12: Co-immunoprecipitation of DDR1 ECD mutants, DS1-2-FLAG with ΔDS1-MYC. HEK293 cells were singly transfected with MYC- or FLAG-tagged cDNA of the deletion construct or co-transfected with both FLAG- and MYC-tagged constructs. The cells were lysed and the lysates immunoprecipitated with anti-FLAG mAb. The precipitated material was separated by 7.5% SDS-PAGE, blotted onto nitrocellulose and probed with the anti-MYC mAb. The blot was stripped and re-probed with the anti-FLAG mAb. *denotes mixing control where lysates of cells singly transfected with MYC- or FLAG-tagged mutants were mixed together. T-transfection; IP-immunoprecipitation. The position and sizes (in kDa) of MW markers are indicated.

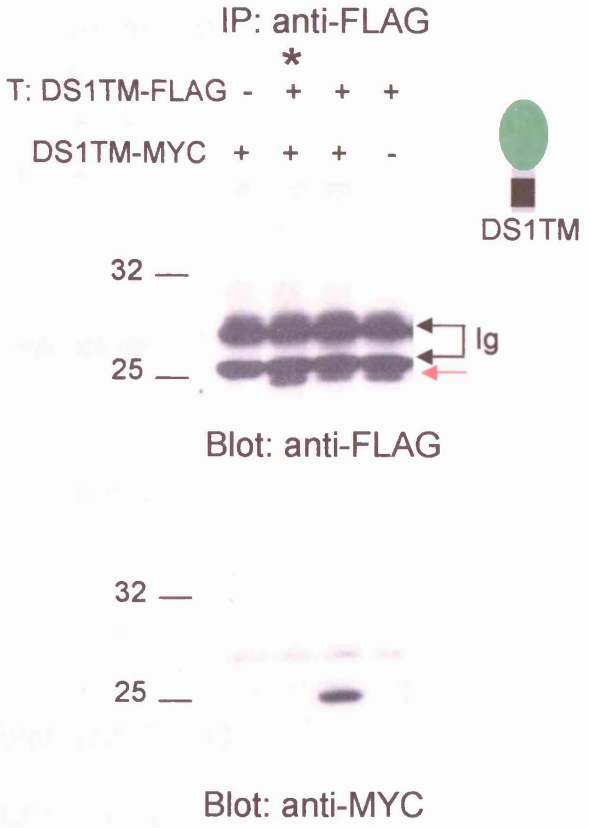

Figure 4.13: Co-immunoprecipitation of epitope-tagged DDR1 double deletion mutant, DS1TM-FLAG with DS1TM-MYC. HEK293 cells were singly transfected with MYC- or FLAG-tagged cDNA of the deletion construct or co-transfected with both FLAG- and MYC-tagged constructs. The cells were lysed and the lysates immunoprecipitated with anti-FLAG mAb. The precipitated material was separated by 10% SDS-PAGE, blotted onto nitrocellulose and probed with anti-FLAG mAb. The blot was stripped and re-probed with the anti-MYC Ab. *denotes mixing control where lysates of cells singly transfected with MYC- or FLAG-tagged mutants were mixed together. The red arrow points to DS1TM-FLAG protein which runs just below the Ig band. T-transfection; IP-immunoprecipitation. The position and sizes (in kDa) of MW markers are indicated.

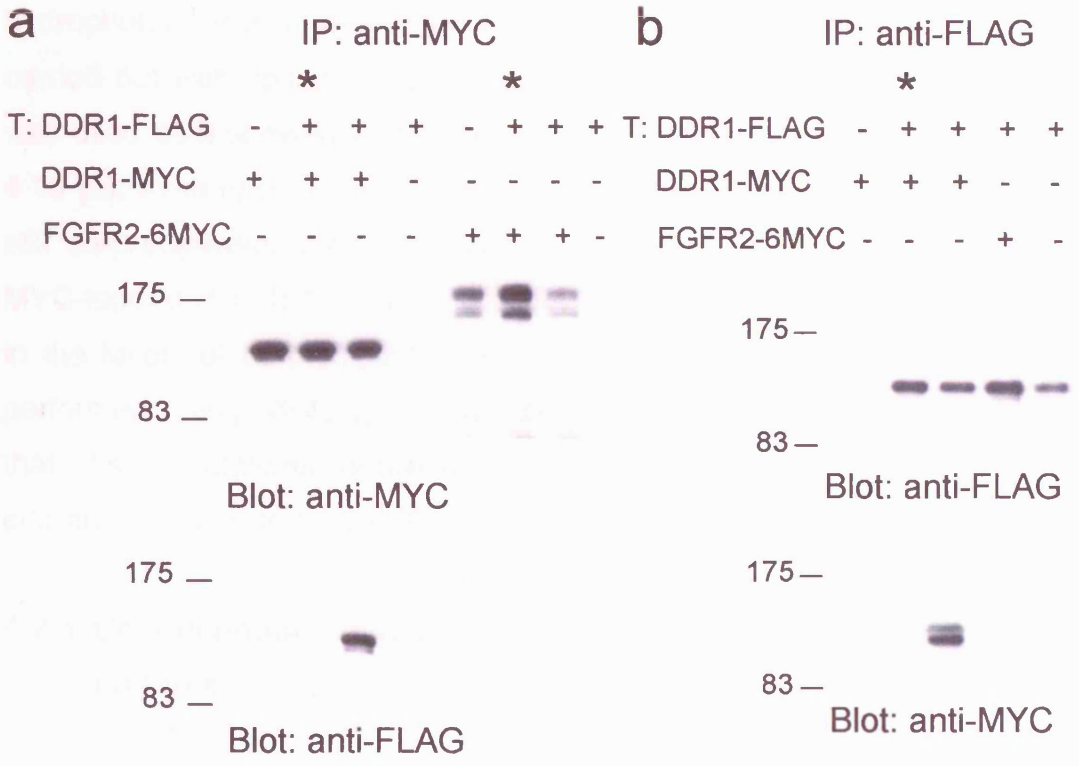

Figure 4.14: DDR1 does not interact with FGFR2 *in vivo*. (a) DDR1-FLAG does not co-precipitate with MYC-tagged FGFR2 (FGFR2-6MYC). (b) FGFR2-6MYC does not co-precipitate with WT DDR1-FLAG. For both (a) and (b), HEK293 cells were singly transfected with FGFR2-6MYC, DDR1-FLAG and DDR1-MYC cDNA or co-transfected with FGFR2-6MYC and DDR1-FLAG or DDR1-MYC or DDR1-FLAG cDNA. The cells were lysed and the lysates immunoprecipitated with anti-MYC Ab (a) or anti-FLAG mAb (b). The precipitated material was separated by 7.5% SDS-PAGE, blotted onto nitrocellulose and probed with anti-FLAG mAb. The blots were stripped and re-probed with anti-MYC Ab. *denotes mixing control where lysates of cells singly transfected with MYC- or FLAG-tagged constructs were mixed together. T-transfection; IP-immunoprecipitation. The position and sizes (in kDa) of MW markers are indicated.

immunoprecipitation studies of GPCRs, as the presence of SDS disrupts hydrophobic protein interactions (McVey *et al.*, 2000). The experiment was carried out with epitope-tagged DDR1 deletion mutant, DS1-1. This mutant was used as it showed a negative result for cross-linking. As seen in Figure 4.15 (a), even upon lysing in RIPA buffer, both DDR1-MYC and DS1-FLAG still co-precipitates with their respective FLAG-tagged (for WT DDR1) or MYC-tagged (for DS1-1 and WT DDR1) counterparts. There is no reduction in the levels of co-precipitation when compared with a parallel experiment performed using NP40 lysis buffer (Figure 4.15, b). These results indicate that the interactions between DDR1 are not non-specific hydrophobic interactions but due to specific domain contacts.

4.2.5. Co-immunoprecipitation studies of epitope-tagged DDR2 deletion mutants

In the case of DDR2, a very similar result was obtained for co-immunoprecipitation of domain deletion mutants. The cytosolic deletion mutant, DDR2 ECTM-FLAG, co-precipitates with DDR2-ECTM-MYC protein as seen Figure 4.16. In addition, when the epitope-tagged ECD mutants of DDR2 are co-transfected and cell lysates immunoprecipitated with the anti-MYC Ab and immunoblotted with the anti-FLAG mAb, DS2-FLAG co-immunoprecipitates with DS2-MYC (Figure 4.17, a) and ΔDS2-FLAG co-precipitates with ΔDS2-MYC (Figure 4.17, b), thus confirming that both the DS domain and the domain X, on their own, are not required for DDR2 to oligomerise.

Since neither of the single deletion mutants showed an inability to interact, double deletion mutants of DDR2 were made. The double mutant DS2TM has both the domain X and the cytosolic domain deleted while ΔDS2TM has both the discoidin domain and cytosolic domain deleted. The mutants contain C-terminal MYC/FLAG epitope tags in order to be used in co-immunoprecipitation experiments. Cross-linking studies have shown that these mutants are able to form oligomers, albeit at a low level (data not

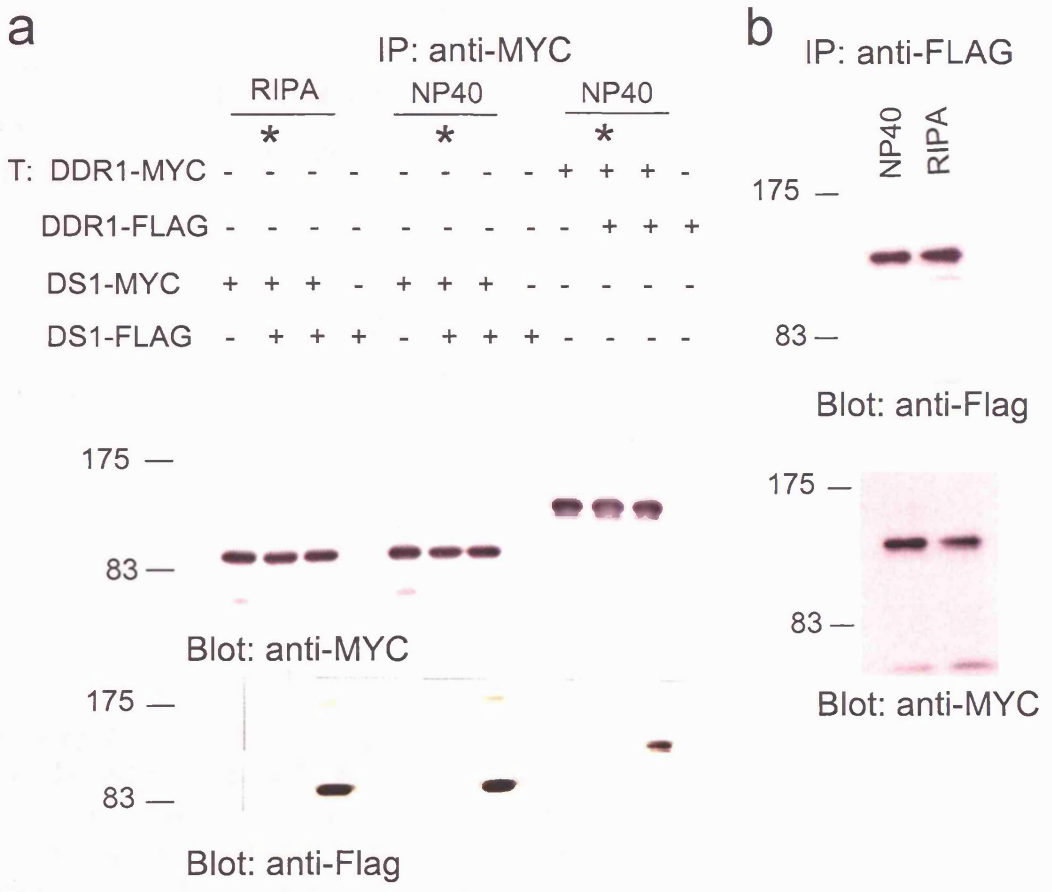

Figure 4.15: Co-immunoprecipitation of epitope-tagged DS1 mutant and WT DDR1 in RIPA lysis buffer versus NP40 lysis buffer. (a) Co-immunoprecipitation of DS1 mutant in RIPA versus NP40 lysis buffer. (b) Co-immunoprecipitation of WT DDR1 in RIPA versus NP40 lysis buffer. For both (a) and (b), HEK293 cells were singly transfected with epitope-tagged cDNA of the deletion construct or co-transfected with both FLAG- and MYC-tagged cDNA. The cells were lysed and the lysates immunoprecipitated with anti-MYC Ab (a) or anti-FLAG mAb (b). The precipitated material was separated by SDS-PAGE, blotted onto nitrocellulose and probed with anti-MYC Ab (a) or anti-FLAG mAb (b). The blots were stripped and re-probed with either anti-FLAG mAb (a) or anti-MYC Ab (b). *denotes mixing control where lysates of cells singly transfected with MYC or FLAG-tagged mutants were mixed together. T-transfection; IP-immunoprecipitation. The position and sizes (in kDa) of the MW markers are indicated.

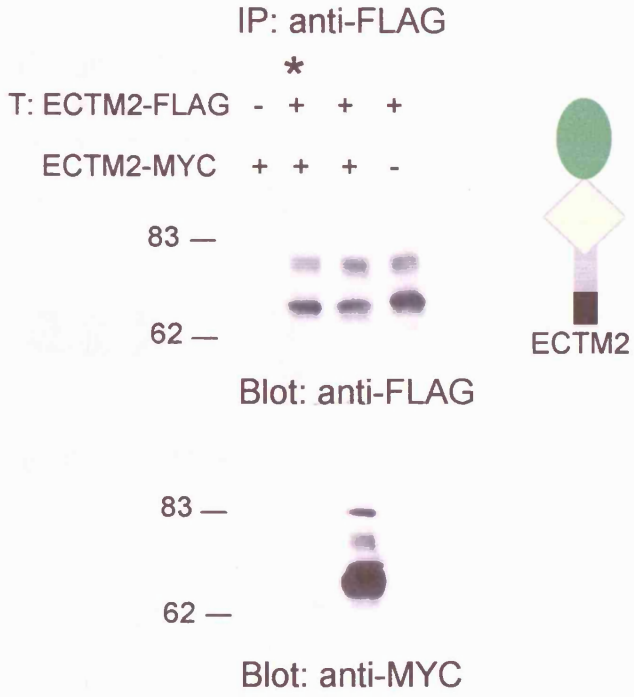

Figure 4.16: Co-immunoprecipitation of DDR2 cytosolic deletion mutant, ECTM2-MYC with ECTM2-FLAG. HEK293 cells were singly transfected with MYC- and FLAG-tagged cDNA of DDR2 ECTM (ECTM2) construct or co-transfected with both MYC- and FLAG-tagged cDNA. The cells were lysed and the lysates immunoprecipitated with anti-FLAG Ab. The precipitated material was separated by 7.5% SDS-PAGE, blotted onto nitrocellulose and probed with anti-MYC or anti-FLAG Ab. *denotes mixing control where lysates of cellssingly transfected with MYC- or FLAG-tagged mutants were mixed together. T-transfection; IP-immunoprecipitation. The position and sizes (in kDa) of MW markers are indicated.

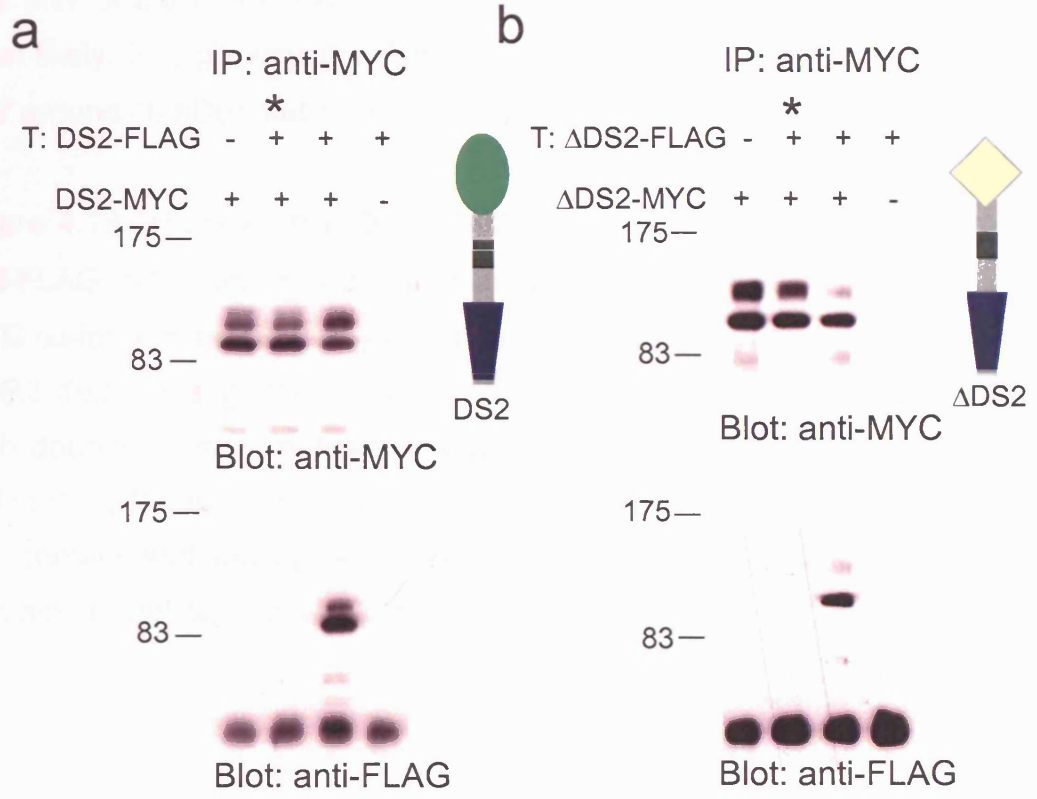

Figure 4.17: Co-immunoprecipitation of epitope-tagged DDR2 ECD deletion mutants. For each deletion mutant shown above, HEK293 cells were singly transfected with epitope-tagged cDNA of the deletion construct or co-transfected with both FLAG- and MYC-tagged cDNA. The cells were lysed and the lysates immunoprecipitated with anti-MYC Ab. The precipitated material was separated by SDS-PAGE, blotted onto nitrocellulose and probed with anti-MYC or anti-FLAG Ab. *denotes mixing control where lysates of cells singly transfected with MYC- or FLAG-tagged mutants were mixed together. T-transfection; IP-immunoprecipitation. The position and sizes (in kDa) of MW markers are indicated.

shown). Therefore, they are expressed on the cell surface to a certain extent. The MW of the cross-linked bands correspond to dimers of the upper, and most likely, fully glycosylated forms of both DS2TM, (which has an expected MW around 40 kDa) and ΔDS2TM (expected MW around 56 kDa).

Figure 4.18 (a) shows that DS2TM-MYC can co-immunoprecipitate with the anti-FLAG mAb, and in a similar manner, Figure 4.18 (b) shows ΔDS2TM-MYC co-immunoprecipitating with the anti-FLAG mAb. Again, as for the other DDR2 deletion mutants and WT DDR2, the lower MW, precursor forms of both double deletion mutants co-precipitate more strongly than the mature, cell surface forms. These results show that the combined deletion of both the DS domain and the cytosolic domain or the domain X and the cytosolic domain are not sufficient to disrupt DDR2 dimerisation.

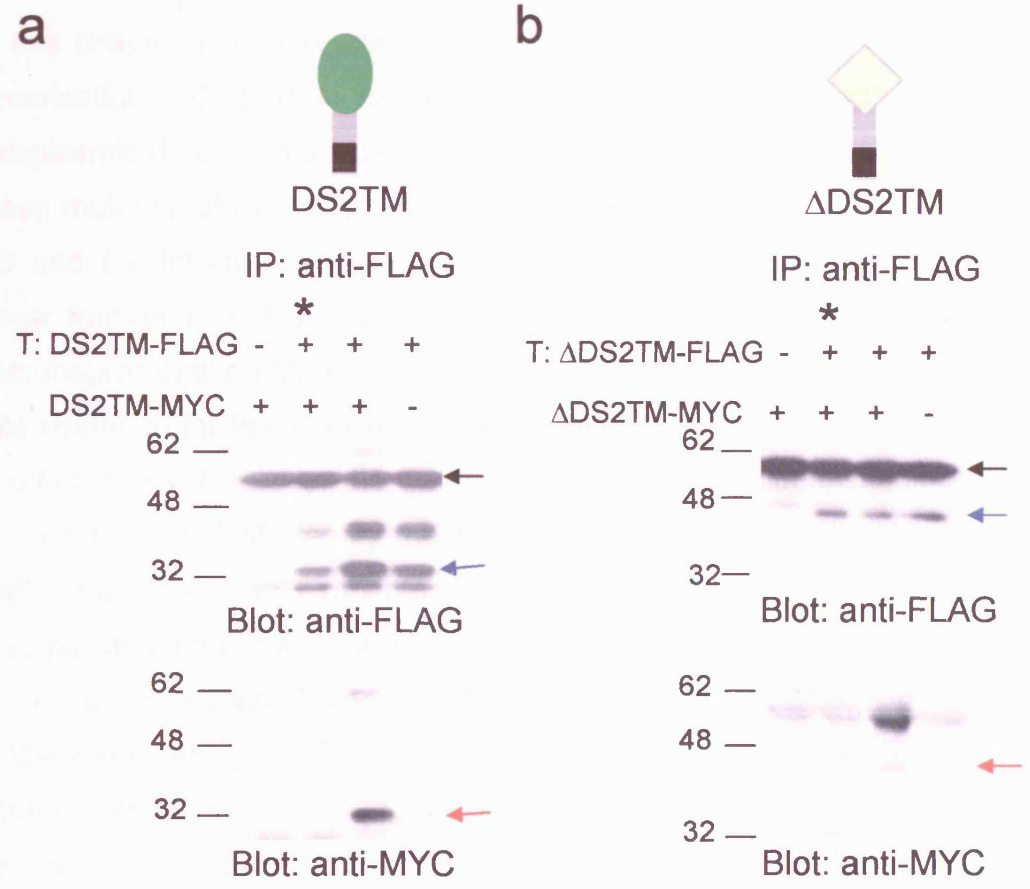

Figure 4.18: Co-immunoprecipitation of epitope-tagged DDR2 double deletion mutants, DS2TM and ΔDS2TM. For each double deletion mutant shown above, HEK293 cells were singly transfected with epitope-tagged cDNA of the construct or co-transfected with both FLAG- and MYC-tagged cDNA. The cells were lysed and the lysates immunoprecipitated with anti-FLAG mAb. The precipitated material was separated by SDS-PAGE, blotted onto nitrocellulose and probed with anti-MYC or anti-FLAG Ab. Panel (a) and (b) show the result for DS2TM and ΔDS2TM, respectively. *denotes mixing control where lysates of cells singly transfected with MYC or FLAG-tagged mutants were mixed together. Blue arrows point to FLAG-tagged mutants, and the red arrows point to the corresponding, co-precipitated MYC-tagged mutant. Black arrows point to Ig bands. T-transfection; IP-immunoprecipitation. The position and sizes (in kDa) of MW markers are indicated.

4.3. Discussion

In this chapter we have attempted to define the domain/s involved in DDR dimerisation. Chemical cross-linking studies carried out on DDR1 cytoplasmic deletion mutants, DDR1 MDN and DDR1 ECTM, showed clearly these mutants' ability to form ligand-independent dimers. Therefore both the KD and the intracellular juxtamembrane region are not required for DDR1 dimer formation in the absence of ligand. This result is confirmed by co-immunoprecipitation studies of epitope-tagged DDR1 ECTM. There has been little evidence for the involvement of the cytosolic domain in the dimerisation of other RTKs. A role for the cytosolic domain in RTK dimerisation has been implied for the ErbB family member, ErbB2 (Penuel *et al.*, 2002). ErbB2, unlike the other ErbB receptors, can be activated by ligand-independent mechanisms. One mechanism is by ErbB2 self-association, which is thought to be due to receptor over-expression (Di Fiore *et al.*, 1987). By chemical cross-linking analysis, Penuel *et al.*, have shown that a region within the intracellular domain consisting of three hydrophobic amino acids is necessary for homomeric association of ErbB2 monomers in the absence of ligand. Furthermore, a molecular modelling study (Bagossi *et al.*, 2005), based on the crystal structure of the KD of ErbB1 (Stamos *et al.*, 2002) predicts favourable dimerisation interactions for between the KDs of adjacent, membrane bound, ErbB2 monomers.

Having established that the entire cytosolic region of DDR1 is dispensable for receptor dimerisation, the effect of the ECD was next investigated. As mentioned before, the DDR1 ECD is composed of three subdomains - the DS domain at the N-terminus, followed by domain X and P/G rich region. DDR1 mutants with each of these domains deleted, in the context of the full-length receptor, and a double deletion mutant deleting the domain X and P/G rich region, were analysed by chemical cross-linking, to determine which of these domain/s were involved in dimer formation. Out of the four deletion mutants, only the DS domain deleted mutant, ΔDS1, showed ligand-independent dimers upon cross-linking. Co-precipitation of epitope-tagged ΔDS1, confirmed this result. However, the other three mutants, DS1-1, ΔPG

and DS1-2 did not produce higher oligomer bands upon cross-linking analysis, but co-immunoprecipitation studies showed that these mutants are able to oligomerise. Two likely explanations for the discrepancy between the two methods are that the reactive lysines on the protein that are required for covalent-bond formation with the cross-linker are not available or that these mutants are not present on the cell surface. Cell surface biotinylation and Endo H/F digestion showed that the major proportion of each of the three mutants are in fact intracellularly localised and represent a biosynthetic precursor species. Co-immunoprecipitation studies show that these mutants are present as preformed dimers. These mutants are most likely degraded before they are converted to a mature, fully glycosylated form. Therefore both the domain X and the P/G rich region are required for formation of the mature, fully glycosylated proteins, as well as targeting DDR1 to the cell surface. Furthermore, most of the ECD is dispensable for DDR1 dimerisation, as the deletion of either the DS domain, the domain X, the ΔPG region or the domain X in combination with the ΔPG region, does not disrupt dimer formation. Furthermore, the entire ECD is dispensable for DDR1 dimerisation, as shown by the ability of the deletion mutants, DS1-2 and ΔDS1, to associate.Therefore neither the ECD nor the cytoplasmic domain is required for DDR1 dimerisation.

As with the DDR1 cytosolic domain deletion mutant, the analogous DDR2 mutant showed clear dimer formation upon cross-linking. Therefore, DDR2 and DDR1 are similar in this aspect of not requiring the intracellular region for ligand-independent dimerisation. To investigate the ECD involvement in the case of DDR2 oligomerisation, two deletion mutants, one with the DS domain and the other with the domain X deleted, were investigated by both cross-linking and co-immunoprecipitation.

In contrast to the DDR1 deletion mutant DS1-1, the analogous DDR2 deletion mutant, DS2, which has most of the region between the DS domain and TM domains deleted, is able to dimerise in the absence of collagen, as shown by cross-linking and co-immunoprecipitation studies. In addition, previous studies have shown this mutant to be activated by collagen

(Leitinger, 2003). This result shows that the DS2 mutant is present on the cell surface and indicates that the domain X is not needed for DDR2 targeting to the cell surface, dimerisation, ligand binding or signalling. Furthermore, the deletion mutant ΔDS2 (which lacks the DS domain) is able to dimerise as shown by cross-linking analysis. Therefore this mutant is present on the cell surface and able to form ligand-independent dimers. However, the mature, cell surface targeted form of the receptor is expressed in very low amounts. Unlike the DS2 mutant, ΔDS2 does not show ligand-dependent autophosphorylation. This is due to the fact that the DS domain plays a pivotal role in collagen binding (Leitinger, 2003). Therefore the DS domain of DDR2 is not essential for receptor dimerisation, however, this domain could play a role in efficient targeting of DDR2 to the cell surface. As seen for the WT DDR2 mature, cell surface form, the mature (and therefore most likely cell surface) forms of the DDR2 mutants also co-precipitate to a much lower level, when compared with the respective precursor (and therefore intracellular) forms. This might suggest that oligomers of DDR2 are present at low levels on the cell surface when compared with DDR2 oligomers during biosynthesis. However, as these proteins are over-expressed, it is likely that due to the high density of proteins in the ER-Golgi biosynthetic pathway, there is a greater chance of forming homomeric receptor interaction.

It was shown in a previous study that a soluble ECD construct of DDR2, which contains the entire DDR2 ECD exists as a non-covalent dimer in solution (Leitinger, 2003), indicating that the DDR2 ECD contains sequences which mediate dimerisation. As the DS domain on its own formed monomers (Leitinger, 2003), and the DS domain plus domain X forms dimers (E. Hohenester, personal communications), this indicates that the domain X is responsible for dimerisation of DDR2 ECD in solution. However, dimerisation is not abolished for full-length DDR2 containing the domain X deletion. The discrepancy between the results with the DDR2 ECDs and full-length cell surface expressed DDR2 can be explained if one assumes that in the full-length receptor other sequences mediate dimerisation in addition to domain X. Interaction via these sequences would be sufficient for dimerisation and signalling in the absence of domain X. These sequences could be in the 28

amino acid sequence of the ECD not deleted in DS2 or in the cytoplasmic or TM domain of the full-length DDR2.

Having found that neither of the DDR2 single deletion mutants tested were disrupted in dimerisation, we then analysed if more than one domain was required for dimerisation. The two DDR2 double mutants, with the whole cytosolic region deleted plus the DS domain (ΔDS2TM) or the domain X and cytosolic region deleted (DS2TM), still retain the ability to dimerise, as shown by co-immunoprecipitation studies. Therefore as for DDR1, the DDR2 ECD and cytosolic domains are dispensable for ligand-independent dimerisation, although they may contribute to dimer stability (see Chapter 5). It is thus likely that the TM domain, which is present in all constructs tested so far, mediates DDR dimerisation. We have studied the contribution of the TM domain in DDR dimerisation, described in Chapter 5.

In contrast to the DDRs, for other RTKs such as MET and PDGFRβ, it was found that a specific domain in the ECD is required for ligand-independent receptor dimerisation (Kong-Beltran *et al.*, 2004; Omura *et al.*, 1997). Chemical cross-linking of MET deletion mutants in cells, revealed that the SEMA domain, contained in the extracellular region, was necessary for MET receptor dimerisation (Kong-Beltran *et al.*, 2004). However, the authors have not investigated if the deletion constructs used are expressed on the cell surface. Furthermore, chemical cross-linking analysis and co-immunoprecipitation studies of PDGFRβ deletion mutants and chimaeric receptor constructs, showed that ligand-independent PDGFβR dimerisation occurs via the extracellular immunoglobulin-like domain four (Omura *et al.*, 1997).

The ErbB family members (ErbB1, 2, 3 and 4) can homodimerise as well as heterodimerise, therefore defining the receptor domains responsible for oligomerisation is complex. Biochemical studies have shown that for ErbB2 heteromeric association with the ErbB1 receptor, the ECD is necessary and sufficient to mediate heterodimerisation (Qian *et al.*, 1999) and is thought to

be the main driving force for ErbB2 heterodimerisation in the presence of ligand (Fitzpatrick *et al.*, 1998). Crystal structures of the ECD of ErbB1, ErbB2 and ErbB3 shows a specific 'dimerisation loop' in the ECD which interacts to form homodimers (Cho and Leahy, 2002; Garrett *et al.*, 2002; Ogiso *et al.*, 2002; Cho *et al.*, 2003, Ferguson *et al.*, 2003; Garrett *et al.*, 2003). It should be noted that the above mentioned biochemical and structural studies describe ligand-dependent dimerisation. For ligand-independent oligomerisation of ErbB receptor family members, there is evidence for the requirement of the cytoplasmic domain in mediating homomeric receptor interactions. For ErbB1, co-immunoprecipitation studies have shown that the KD is required for homomeric interactions of this receptor in the absence of ligand (Chantry, 1995). As mentioned before, the ErbB2 receptor also contains a specific region in the cytosolic domain, of three hydrophobic amino acids, which is found to be important for ligand-independent homodimerisation (Penuel *et al.*, 2002).

Chapter 5

Investigating the role of the transmembrane domain in DDR receptor dimerisation and activation

5.1. Introduction

The TM domains of the DDRs contain two putative dimerisation sequences, either one of which could be involved in driving receptor dimerisation or contribute indirectly to receptor oligomerisation by being driven together by other receptor regions. The putative dimerisation motif GxxxG (Sternberg and Gullick, 1990; Russ and Engelman, 2000; Senes *et al.*, 2000) and the potential self-interacting leucine zipper motif (Langosch and Heringa 1998; Gurezka *et al.*, 1999; Gurezka and Langosch, 2001) are both found in the DDR1 and DDR2 TM sequences (Figure 5.1, a).

The leucine zipper heptad motif is found in the helical TM domain of a variety of single spanning membrane proteins and consists of hydrophobic aliphatic residues such as leucine and isoleucine, which form a repeated heptad pattern resulting in alignment of these residues on one face of an α-helix. This motif can therefore mediate oligomerisation of adjacent α-helices via hydrophobic side-chain packing interactions (Arkin *et al.*, 1994; Simmerman *et al.*, 1996; Pinto *et al.*, 1997; Langosch and Heringa 1998; Gurezka *et al.*, 1999). The leucine zipper motif was shown to be important for function and oligomeric assembly of a number of naturally occurring, single-span TM proteins (Gurezka *et al.*, 1999); for example, the Epo receptor (Kubatzky *et al.*, 2001; Ruan *et al.*, 2004) and E-cadherin (Huber *et al.*, 1999).

The five residue GxxxG sequence motif is found frequently in TM domains of RTKs and other TM proteins, and was shown to promote TM helix dimerisation (Russ and Engelman, 2000; Senes et al 2000; Sternberg and Gullick, 1990). The first position of the five residue sequence requires a small side-chain (Gly, Ala, Ser, Thr or Pro) and position five a very small side-chain such as Gly or Ala. The majority of research on the GxxxG motif has been carried out on the human erythrocyte sialoglycoprotein, glycophorin A (GpA), a cell surface receptor which was found to contain the GxxxG motif as part of a seven residue sequence in its TM domain (Adams *et al.*, 1996; Lemmon *et al.*, 1992; MacKenzie *et al.*, 1997). The presence of this motif was shown to be responsible for the strong dimerisation of GpA TM α-helices (Doura *et al.*,

a

Leucine zipper (red)

```
Heptad pattern  .ga..de.ga..de.ga..de.
DDR1            ILIGCLVAIILLLLLIIALMLW
DDR2            ILIGCLVAIIFILLAIIVIILW
```

GxxxG motif (underlined)

```
DDR1    ILIGCLVAIILLLLLIIALMLW
DDR2    ILIGCLVAIIFILLAIIVIILW
```

b

```
ILIGCLVAIILLLLLIIALMLW    WT DDR1
ILIGCLVAIILLGPLIIALMLW    DDR1 TM1
ILIGCLVAIILLLLLGPALMLW    DDR1 TM2
ILIGCLVVIILLLLLIIALMLW    DDR1 TM3

ILIGCLVAIIFILLAIIVIILW    WT DDR2
ILIGCLVAIIFIGPAIIVIILW    DDR2 TM1
ILIGCLVAIIFILLAGPVIILW    DDR2 TM2
ILIGCLVVIIFILLAIIVIILW    DDR2 TM3
```

Figure 5.1: The DDR TM mutants, TM1, TM2 and TM3. (a) The TM domain sequences of WT DDR1 (amino acids 418-439) and DDR2 (amino acids 415-436). The potential leucine zipper motif is shown in red and the GxxxG motif (GCLVA in the DDRs) is underlined. The WT sequence conforms to the requirements of a leucine zipper heptad repeat pattern of (iso)leucine residues, as indicated above the amino acid sequence. Positions a and d of a seven residue helical repeat consists of apolar residues, which mediate interactions between two parallel α helices. (b) Amino acid modifications of the DDR TM domain mutants TM1, TM2 and TM3. TM1 and TM2 contain mutations which interfere with the potential leucine zipper of the TM domains. The amino acids Leu^{430} and Leu^{431} (DDR1) and Leu^{427} and Leu^{428} (DDR2) are mutated to Gly and Pro in the TM1 mutants and Ile^{433} and Ile^{434} (DDR1) and Ile^{424}, Ile^{425} (DDR2) to Gly and Pro in the TM2 mutants. TM3 contains a point mutation in Ala^{425} (DDR1) and Ala^{422} (DDR2) to a Val, which interferes with the potential GxxxG motif.

2004). As revealed by solution NMR studies, GpA TM α-helices containing the GxxxG motif can interact with each other in a similar pattern to the right-handed crossing of two straight α-helices. Specifically, bulky side-chains (such as valine and leucine) on one monomer, can pack against a groove formed on the adjacent monomer helix, in a 'ridges into groove' manner (MacKenzie *et al.*, 1997).

Specific point mutations were introduced into DDR1 and DDR2 TM domain sequences which, according to previous studies on other cell surface receptors, were designed to disrupt the two dimerisation motifs of interest. For example, double point mutations (LL->GP) in the Epo receptor TM domain, disrupted self-assembly when analysed by the ToxR system, a system that measures dimerisation of isolated TM domains in bacterial membranes (Kubatzky *et al.*, 2001). Subsequently, asparagine scanning mutagenesis studies confirmed that the mutated amino acids correspond to a leucine zipper motif (Ruan *et al.*, 2004). The TM domains of the ErbB receptors contain the GxxxG motif. Mutagenesis of the fourth glycine of this motif to a valine residue, followed by analysis of these ErbB mutants using the TOXCAT system (which is similar to the ToxR system), showed that this specific mutation prevents homo-oligomerisation of isolated ErbB TM sequences (Mendrola *et al.*, 2002).

As shown in Figure 5.1 (c) and (d), DDR1 and DDR2 TM1 and TM2 mutants contain two point mutations which should disrupt the potential leucine zipper motif, by mutating two leucine or two isoleucine residues to glycine and proline residues. A proline residue was introduced, as proline usually introduces kinks into the α-helices (via restricted side-chain conformations), thereby reducing interactions between TM segments (Huber *et al.*, 1999).

A third DDR1 and DDR2 TM mutant, TM3, was made containing a potential disruption in the GxxxG motif (Figure 5.1 c and d). Mutation of the second glycine of this sequence to a bulky residue such as valine was shown to disrupt oligomerisation for members of the ErbB receptor family (Mendrola *et al.*, 2002). Therefore, an analogous mutation was introduced into the DDR

TM domain (Figure 5.1). We tested the DDR1 and DDR2 TM mutants for their protein expression, ability to dimerise and activate in response to collagen I.

5.2 Results

5.2.1. Chemical cross-linking analysis of DDR1 TM mutants

In order to investigate whether the DDR1 TM mutants were defective in their ability to dimerise, chemical cross-linking analysis was carried out. The three mutants or WT DDR1 were transiently over-expressed in HEK293 cells. The cells were washed and incubated with BS^3, for 30 minutes at RT, followed by cell lysis, SDS–PAGE and Western blotting using an anti-DDR1 Ab. As seen in Figure 5.2, all three mutants, as well as WT DDR1, show higher MW bands, in the presence of BS^3, which correspond to DDR1 oligomers. This indicates that none of the mutants are defective in dimerisation. A similar experiment was carried out, but with cross-linking at 4°C for 1 hour. The results were similiar to that seen in Figure 5.2 (data not shown).

5.2.2. Co-immunoprecipitation of DDR1 TM mutants

Co-immunoprecipitation of C-terminally MYC- and FLAG-tagged DDR1 TM mutants, TM1 and TM3, were carried out in order to verify the results of cross-linking analysis. As seen in Figure 5.3, both TM1 and TM3 FLAG-tagged receptors co-precipitate with the anti-MYC Ab, thus verifying the cross-linking results. Co-precipitation of WT DDR1-FLAG with the anti-MYC Ab, was carried out in parallel to estimate if there was a difference in the degree of co-precipitation between the TM mutants and WT DDR1. However, results from four different experiments indicate that there is no significant change in the levels of co-precipitation between WT DDR1 and TM mutants (data not shown). An additional protein is of MW approximately 62 kDa, is observed in co-precipitates of both TM1-MYC and TM3-MYC (Figure 5.3, lower panels, red arrows). This protein most likely corresponds to the membrane anchored β-subunit of DDR1, consisting of only the TM domain and cytosolic region, shown previously to be produced by proteolytic cleavage of the DDR1 ECD (Vogel, 2002). This result indicates that the entire DDR1 ECD is dispensable for dimerisation.

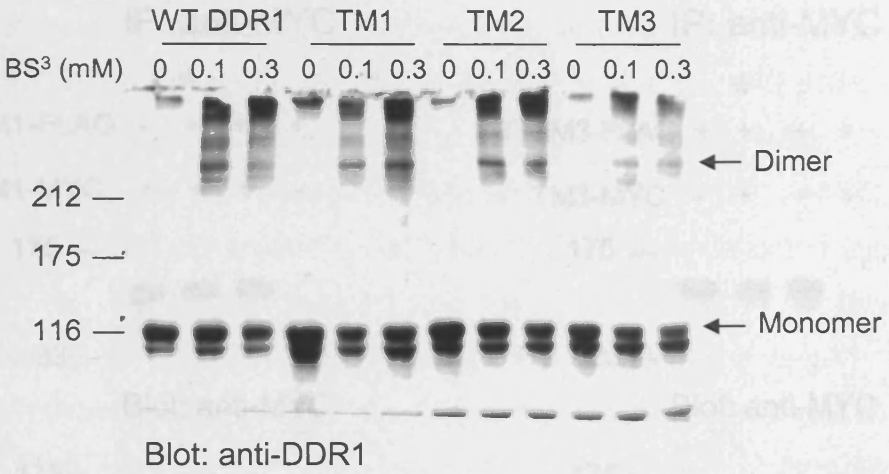

Figure 5.2: Ligand-independent oligomerisation of DDR1 TM mutants, TM1, TM2 and TM3. WT DDR1 and DDR1 TM mutants TM1, TM2 and TM3 were transiently expressed in HEK293 cells. After washing with cold PBS, BS^3 in PBS was added to the cells at the indicated concentrations, and incubated for 30 minutes, RT. The reaction was quenched with 10 mM Tris pH 7.4. Cell lysates were analysed by 7.5% SDS-PAGE and Western blotting. The blots were probed with anti-DDR1 Ab. The position and sizes (in kDa) of MW markers are indicated.

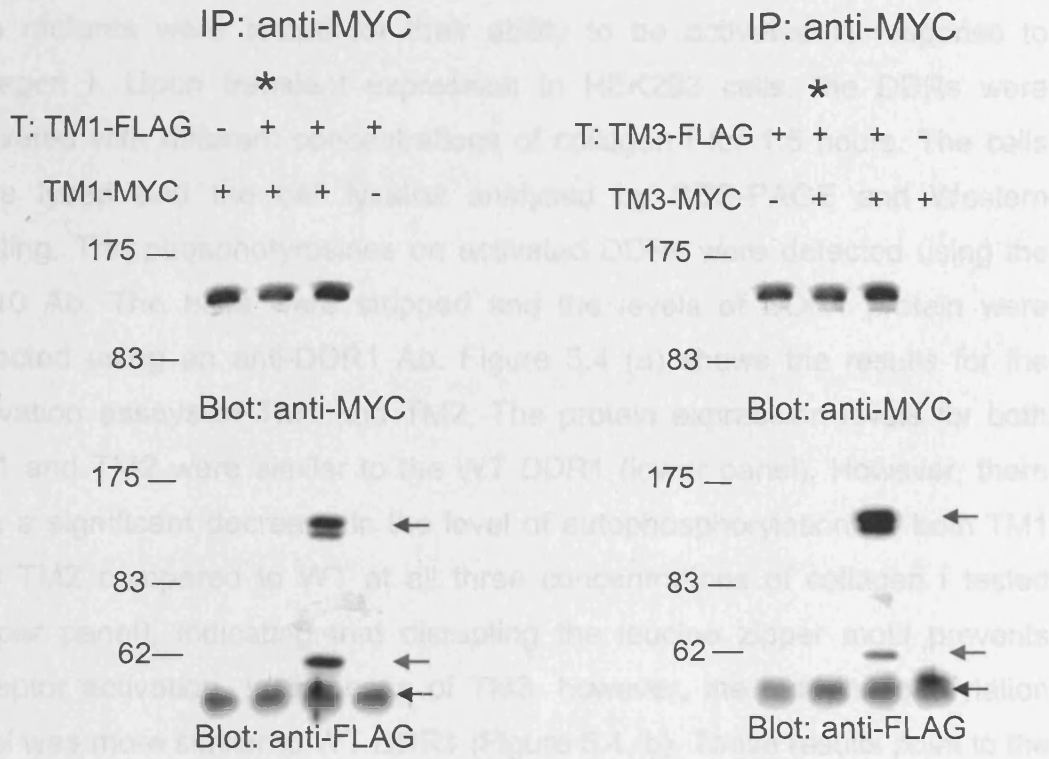

Figure 5.3: Co-immunoprecipitation of DDR1 TM1-FLAG and DDR1 TM3-FLAG with the anti-MYC Ab. HEK293 cells were singly transfected with MYC- or FLAG-tagged cDNA of DDR1 TM1 or DDR1 TM3 or co-transfected with both FLAG- and MYC-tagged constructs. The cells were lysed and the lysates immunoprecipitated with anti-MYC Ab. The precipitated material was separated by 7.5% SDS-PAGE, blotted onto nitrocellulose and probed with anti-MYC. The blots were stripped and re-probed with anti-FLAG mAb. *denotes mixing control where lysates of cells singly transfected with MYC- or FLAG-tagged mutants were mixed together. T-transfection; IP-immunoprecipitation. Blue arrows point to DDR1 TM1-FLAG and DDR1 TM3-FLAG. Red arrows point to the DDR1 β-subunit. Black arrows point to Ig bands. The position and sizes (in kDa) of MW markers are indicated.

5.2.3. Collagen-dependent activation assay of DDR1 TM mutants

The mutants were tested for their ability to be activated in response to collagen I. Upon transient expression in HEK293 cells, the DDRs were activated with different concentrations of collagen I for 1.5 hours. The cells were lysed and the cell lysates analysed by SDS-PAGE and Western blotting. The phosphotyrosines on activated DDRs were detected using the 4G10 Ab. The blots were stripped and the levels of DDR1 protein were detected using an anti-DDR1 Ab. Figure 5.4 (a) shows the results for the activation assays of TM1 and TM2. The protein expression levels for both TM1 and TM2 were similar to the WT DDR1 (lower panel). However, there was a significant decrease in the level of autophosphorylation for both TM1 and TM2 compared to WT at all three concentrations of collagen I tested (upper panel), indicating that disrupting the leucine zipper motif prevents receptor activation. In the case of TM3, however, the autophsophorylation level was more similar to WT DDR1 (Figure 5.4, b). These results point to the leucine zipper motif, and not the GxxxG motif, in mediating DDR1 assembly in the presence of collagen I.

5.2.4. Expression of DDR2 TM mutants and co-immunoprecipitation of DDR2 TM1 mutant

As seen in Figure 5.5 (a) the DDR2 TM mutants TM1 and TM2, did not express in a similar manner to WT DDR2, in that the expression level of the upper form of both TM1 and TM2 mutants was greatly decreased, compared to the two lower forms. However, the DDR2 TM3 mutant was expressed in a normal manner. Endo H and PNGase F digestion of analysis of the TM1 mutant showed that the higher MW form of TM1 is Endo H resistant and therefore represents a mature form, which is most likely expressed on the cell-surface (data not shown); this form most likely corresponds to the intermediate MW form seen in WT DDR2. Taken together, disrupting the leucine zipper motif prevents normal expression of the upper form of DDR2 whilst disruption of the GXXXG motif does not. We wanted to test if the defective DDR2 TM1 mutant was still able to oligomerise. Therefore, a C-

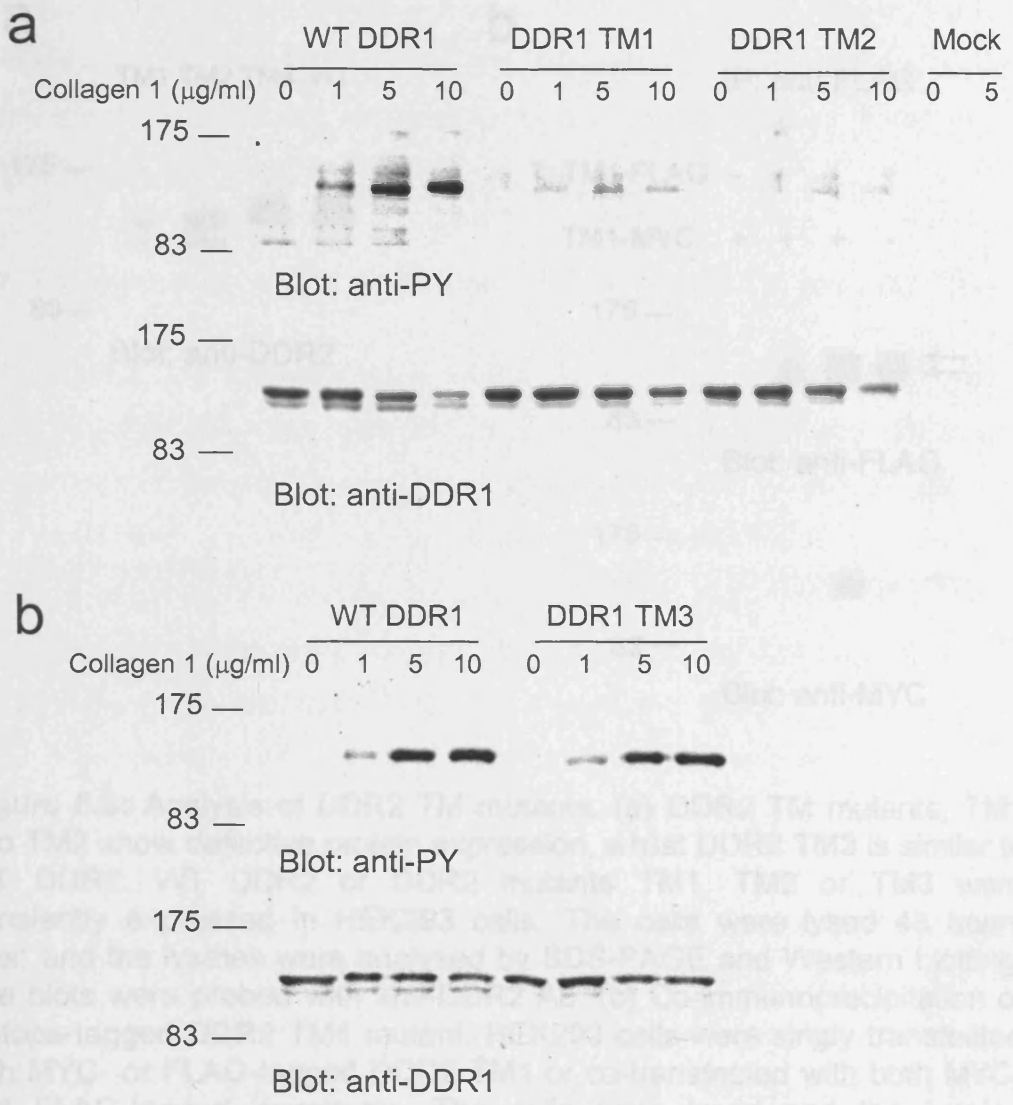

Figure 5.4: The DDR1 TM mutants, TM1 and TM2, but not TM3, are defective in collagen-induced autophosphorylation. WT DDR1 or DDR1 mutants TM1, TM2 or TM3 were transiently expressed in HEK293 cells. After stimulation with collagen I at the indicated concentrations, cell lysates were analysed by 7.5% SDS-PAGE and Western blotting. The blots were probed with anti-phosphotyrosine mAb 4G10 (upper panel) stripped and re-probed with anti-DDR1 Ab (lower panel). The position and sizes (in kDa) of MW markers are indicated.

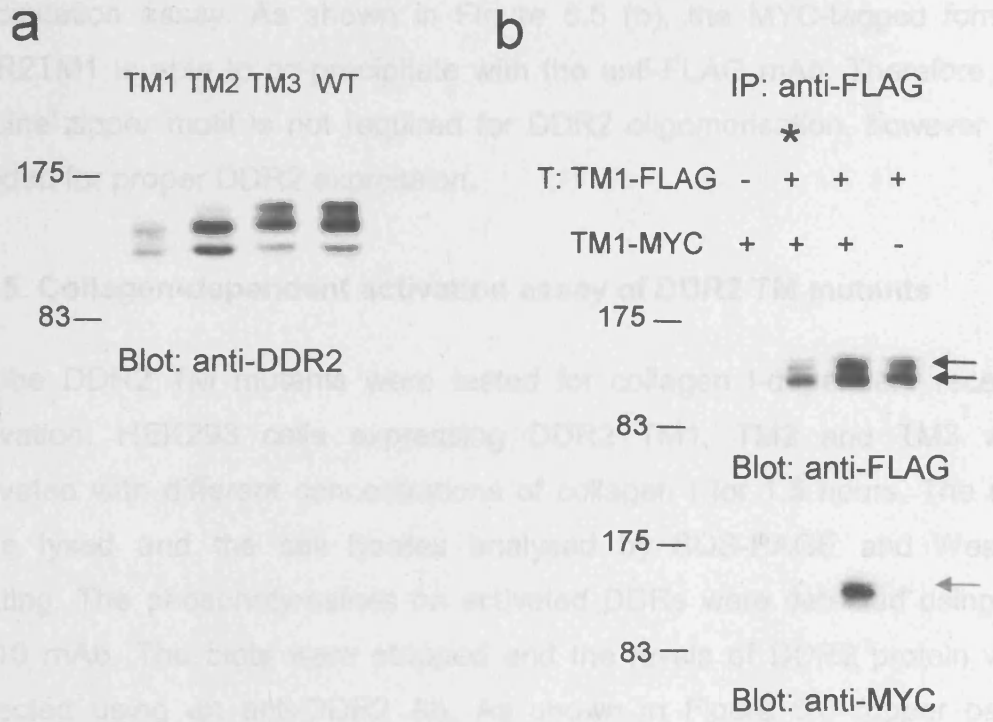

Figure 5.5: Analysis of DDR2 TM mutants. (a) DDR2 TM mutants, TM1 and TM2 show defective protein expression, whilst DDR2 TM3 is similar to WT DDR2. WT DDR2 or DDR2 mutants TM1, TM2 or TM3 were transiently expressed in HEK293 cells. The cells were lysed 48 hours later, and the lysates were analysed by SDS-PAGE and Western blotting. The blots were probed with anti-DDR2 Ab. (b) Co-immunoprecipitation of epitope-tagged DDR2 TM1 mutant. HEK293 cells were singly transfected with MYC- or FLAG-tagged DDR2 TM1 or co-transfected with both MYC- and FLAG-tagged constructs. The cells were lysed and the lysates immunoprecipitated with anti-FLAG mAb. The precipitated material was separated by 7.5% SDS-PAGE, blotted onto nitrocellulose and probed with anti-FLAG mAb. The blots were stripped and re-probed with anti-MYC Ab. Black arrow points to DDR2TM1-FLAG, middle and lower forms. Red arrow points to DDR2TM1-MYC. *denotes mixing control where lysates of cells singly transfected with MYC- or FLAG-tagged mutants were mixed together. T-transfection; IP-immunoprecipitation. The position and sizes (in kDa) of MW markers are indicated.

terminally MYC- and FLAG-tagged TM1 mutant was made and tested by co-precipitation assay. As shown in Figure 5.5 (b), the MYC-tagged form of DDR2TM1 is able to co-precipitate with the anti-FLAG mAb. Therefore, the leucine zipper motif is not required for DDR2 oligomerisation, however it is needed for proper DDR2 expression.

5.2.5. Collagen-dependent activation assay of DDR2 TM mutants

All the DDR2 TM mutants were tested for collagen I-dependent receptor activation. HEK293 cells expressing DDR2 TM1, TM2 and TM3 were activated with different concentrations of collagen I for 1.5 hours. The cells were lysed and the cell lysates analysed by SDS-PAGE and Western blotting. The phosphotyrosines on activated DDRs were detected using the 4G10 mAb. The blots were stripped and the levels of DDR2 protein were detected using an anti-DDR2 Ab. As shown in Figure 5.6 (upper panel) DDR2 TM3 mutant shows a phosphorylation signal similar to WT DDR2, indicating that the GxxxG motif is not required for DDR2 signalling.

There is a low level of phosphorylation seen for TM2 mutant, compared with TM3 and WT DDR2. This corresponds to there being a very small amount of the upper, mature form of TM2, which is the form that is phosphorylated upon stimulation with collagen I (Figure 5.6, lower panel). In the case of the TM1 mutant, the upper form is not visibly expressed, as seen by Western blot, (Figure 5.6, lower panel), and the expression of the middle and lower form is somewhat reduced compared with WT DDR2. Therefore, there is no visible phosphorylation signal for this mutant. Taken together with the fact that some phosphorylation of the upper form of TM2 was detected and the primary effect of the mutation is on the DDR2 upper form, these results indicate that the leucine zipper is required for normal expression of DDR2.

5.2.6. Co-precipitation of DDR1 double and triple mutants

Subsequently, to further test the role of the TM domain in DDR1 oligomerisation, double and triple DDR1 mutants were made, where more

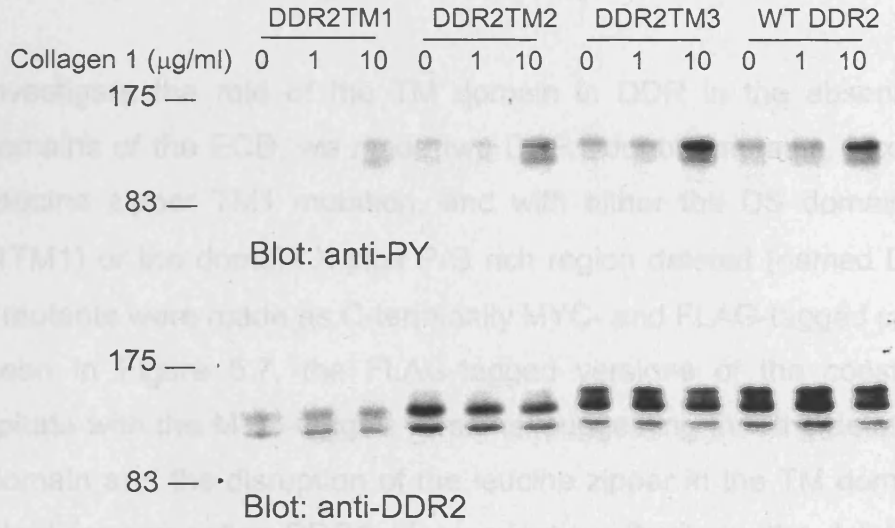

Figure 5.6: DDR2 TM domain mutants TM1 and TM2, but not TM3, are defective collagen I-dependent autophosphorylation. WT DDR2 or DDR2 mutants TM, TM2 or TM3, were transiently expressed in HEK293 cells. After stimulation with collagen I at the above concentrations, cell lysates were analysed by 7.5% SDS-PAGE and Western blotting. The blots were probed with anti-phosphotyrosine mAb 4G10 (upper panel) stripped and re-probed with anti-DDR2 Ab (lower panel). The position and sizes (in kDa) of MW markers are indicated.

than one DDR1 domain was deleted or disrupted. These mutants were tested for their ability to dimerise by co-immunoprecipitation.

To investigate the role of the TM domain in DDR in the absence of the subdomains of the ECD, we made two DDR1 double mutants, incorporating the leucine zipper TM1 mutation, and with either the DS domain (named ΔDS1TM1) or the domain X plus P/G rich region deleted (named DS1TM1). Both mutants were made as C-terminally MYC- and FLAG-tagged constructs. As seen in Figure 5.7, the FLAG-tagged versions of the constructs co-precipitate with the MYC-tagged versions, suggesting that the deletion of the DS domain and the disruption of the leucine zipper in the TM domain is not sufficient for preventing DDR1 oligomerisation. Similarly, the deletion of the domain X and P/G rich region together with the disruption of the leucine zipper motif, is not sufficient for preventing DDR1 oligomerisation.

In view of the above results, we wanted to know if an additional deletion of the DDR1 cytoplasmic domain would prevent receptor oligomerisation. To test this, two triple mutants of DDR1 were made. Both mutants had the whole cytoplasmic domain deleted as well as the TM1 mutation. One of the triple mutants contained deletion of the domain X and P/G rich region, named DS1TM1ΔCYTO, whilst the other mutant contained a deletion of the DS domain, named ΔDS1TM1ΔCYTO, in addition to the cytoplasmic domain deletion and TM mutation. Both mutants were MYC- and FLAG-tagged at the C-terminus. Upon checking for protein expression in HEK293 cells, it was observed that only the DS1TM1ΔCYTO mutant expressed whilst the ΔDS1TM1ΔCYTO mutant did not (data not shown). Co-immunoprecipitation was carried out to see whether the ΔDS1TM1ΔCYTO mutant was able to still oligomerise. As seen from Figure 5.8, the MYC-tagged mutant does co-precipitate with the anti-FLAG mAb. Therefore the DS domain in this mutant is most likely mediating the majority of the interactions between the two DDR monomers.

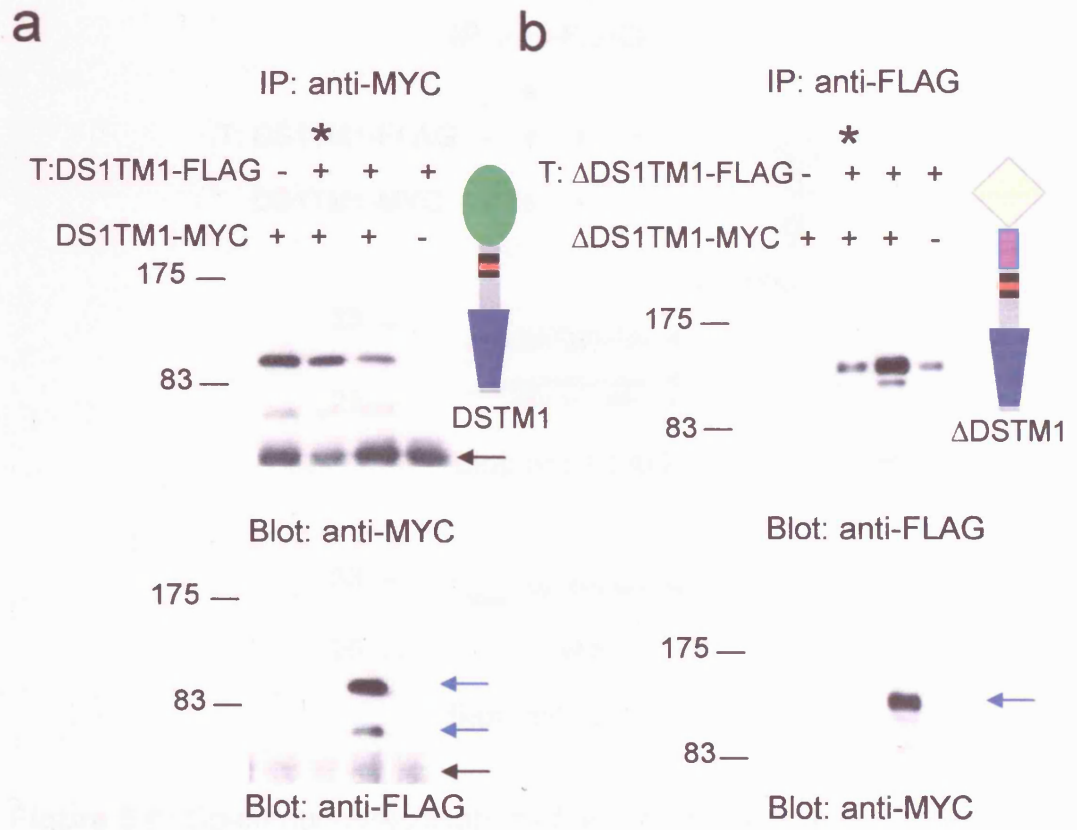

Figure 5.7: Co-immunoprecipitation of DDR1 double mutants, DS1TM1-FLAG and ΔDS1TM1-MYC with the anti-MYC Ab and anti-FLAG mAb, respectively. (a) and (b), HEK293 cells were singly transfected with MYC- or FLAG-tagged cDNA of DS1TM1 (a) or ΔDS1TM1 (b) or co-transfected with both MYC- and FLAG-tagged cDNA of the particular construct. The cells were lysed and the lysates immunoprecipitated with anti-MYC Ab (a) or anti-FLAG mAb (b). The precipitated material was separated by 7.5% SDS-PAGE, blotted onto nitrocellulose and probed with the anti-MYC Ab (a) or anti-FLAG mAb (b). The blots were stripped and re-probed with the anti-FLAG mAb (a) or anti-MYC Ab (b). Blue arrows point to DS1TM1-FLAG and ΔDS1TM1-FLAG. Black arrows point to Ig bands. *denotes mixing control where lysates of cells singly transfected with MYC- or FLAG-tagged mutants were mixed together. T-transfection; IP-immunoprecipitation. The position and sizes (in kDa) of MW markers are indicated.

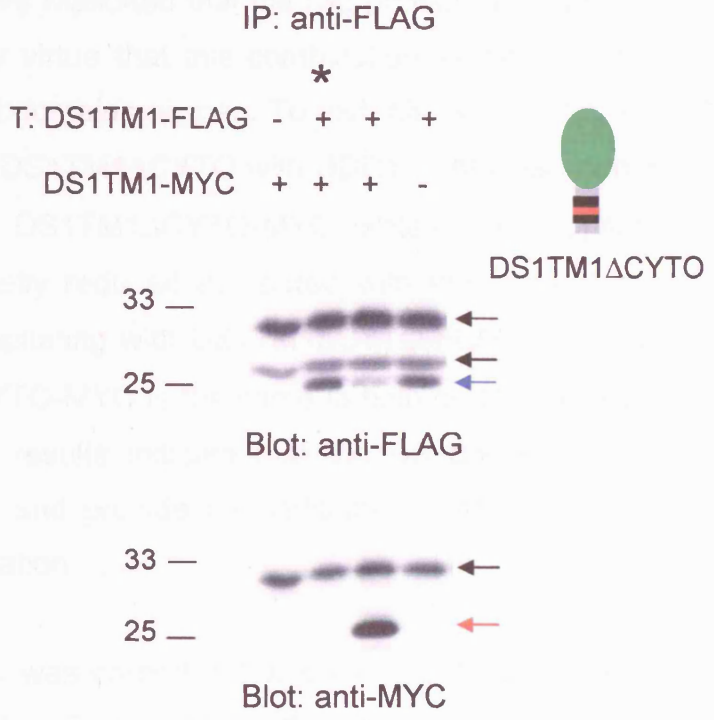

Figure 5.8: Co-immunoprecipitation of epitope-tagged DDR1 triple mutant DS1TM1ΔCYTO-MYC with the anti-FLAG mAb. HEK293 cells were singly transfected with MYC- or FLAG-tagged DS1TM1ΔCYTO or co-transfected with both MYC- and FLAG-tagged cDNA constructs. The cells were lysed and the lysates immunoprecipitated with anti-FLAG mAb. The precipitated material was separated by 10% SDS-PAGE, blotted onto nitrocellulose and probed with anti-FLAG mAb. The blot was stripped and re-probed with anti-MYC Ab. The red and blue arrows points to DS1TM1ΔCYTO-MYC and DS1TM1ΔCYTO-FLAG, respectively. Black arrows point to Ig bands. *denotes mixing control where lysates of cells singly transfected with MYC- or FLAG- tagged mutants were mixed together. T-transfection; IP-immunoprecipitation. The position and sizes (in kDa) of MW markers are indicated.

We further tested the DDR1 triple mutant for its ability to oligomerise with full-length DDR1. We reasoned that the two proteins would be unable to interact via the ECD by virtue that this combination would not have the respective extracellular subdomains aligned. To test this, we carried out co-precipitation experiments of DS1TM1ΔCYTO with DDR1-FLAG. As seen in Figure 5.9 (a), the amount of DS1TM1ΔCYTO-MYC protein co-precipitating with DDR1-FLAG was greatly reduced compared with the amount of the same triple mutant co-precipitating with DS1TM1ΔCYTO-FLAG. The level of expression of DS1TM1ΔCYTO-MYC is the same in both co-transfected samples (Figure 5.9, b). These results indicate that the DS domain is needed for DDR1 oligomerisation and provide an additional control for the specificity of co-immunoprecipitation.

A parallel study was carried out in a collaborating laboratory, to establish if the DDR1 TM domain mediates self-assembly. In this study, the effect of the three mutations, TM1, TM2 and TM3, on TM domain assembly was examined. The results from this study are described and discussed in section 5.3.

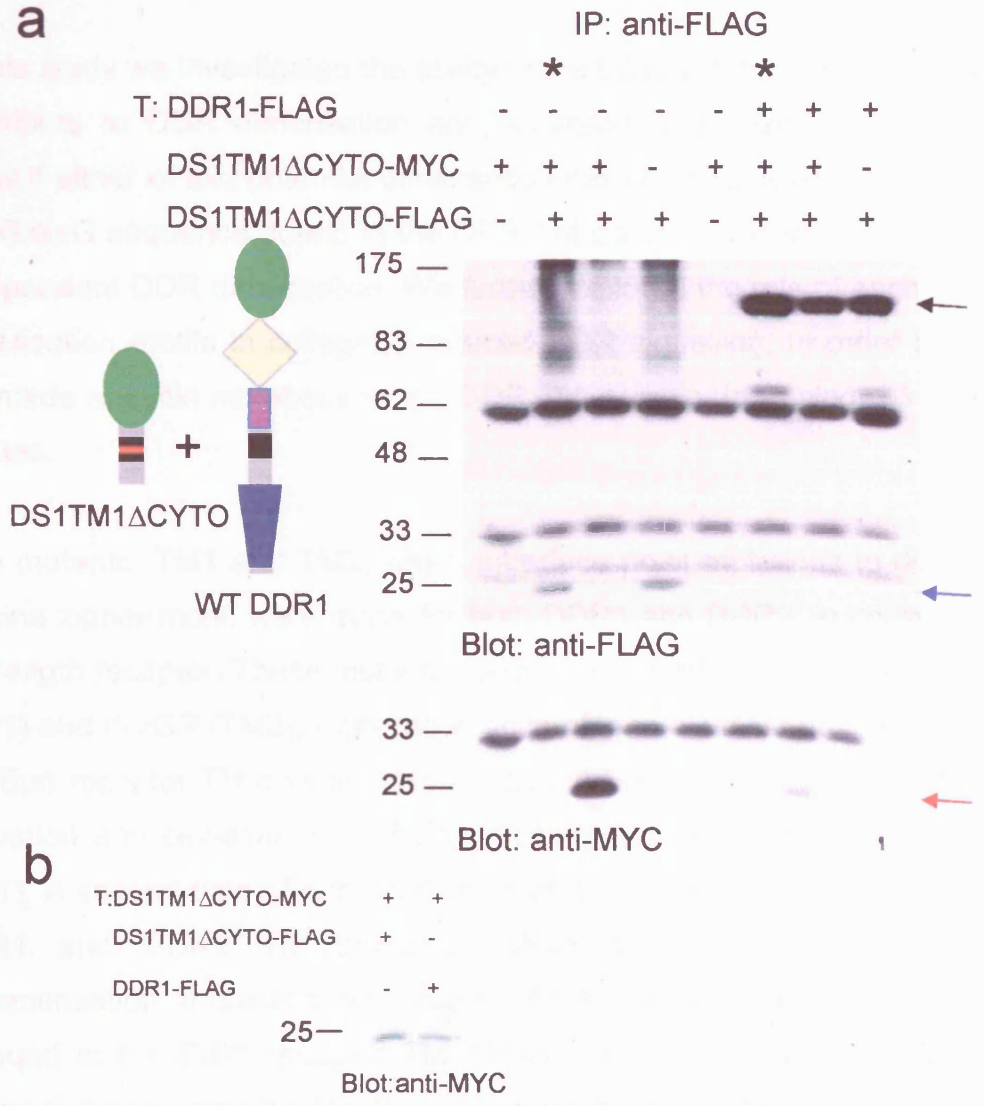

Figure 5.9: Co-immunoprecipitation of epitope-tagged DDR1 triple mutant, DS1TM1ΔCYTO, with epitope-tagged WT DDR1. (a) HEK293 cells were singly transfected with epitope-tagged cDNA of DS1TM1ΔCYTO or WT DDR1 or co-transfected with both DS1TM1ΔCYTO-MYC and WT DDR1-FLAG. As a comparison, cells were co-transfected with MYC- and FLAG-tagged cDNA of the triple mutant. The cells were lysed and the lysates immunoprecipitated with anti-MYC Ab. The precipitated material was separated by 10% SDS-PAGE, blotted onto nitrocellulose and probed with anti-MYC or anti-FLAG Ab. *denotes mixing control where lysates of cells singly transfected with MYC- or FLAG-tagged mutants were mixed together. (b) Aliquots of lysate from (a) was analysed by SDS-PAGE and Western blotting with anti-MYC Ab, to check the level of DS1TM1ΔCYTO-MYC expression. T-transfection; IP-immunoprecipitation. Black and blue arrows point to the position of WT DDR1-FLAG and DS1TM1ΔCYTO-FLAG, respectively. The red arrow points to DS1TM1ΔCYTO-MYC. The position and sizes (in kDa) of the MW markers are indicated.

5.3. Discussion

In this study we investigated the ability of the DDR TM domain to mediate, or contribute to DDR dimerisation and activation. We specifically wanted to know if either of two potential dimerisation motifs, the leucine zipper motif or the GxxxG sequence, found in the DDR TM domain, was involved in ligand-independent DDR dimerisation. We further explored the role of each of these dimerisation motifs in collagen I-induced DDR signalling. In order to do so, we made specific mutations in the DDR TM domain, in analogy to previous studies.

Two mutants, TM1 and TM2, which introduce point mutations to disrupt the leucine zipper motif, were made for both DDR1 and DDR2, in context of the full-length receptor. These mutants, which contain the double mutant LL->GP (TM1) and II->GP (TM2), were made according to a similar mutation made in the Epo receptor TM domain, which reduced Epo receptor ligand-dependent activation and self-assembly of Epo receptor TM domains (Kubatzky *et al.*, 2001). A second type of dimerisation motif, the GxxxG motif, is found in both DDR1 and DDR2 TM domains, which could be involved in DDR oligomerisation and activation, instead of the leucine zipper motif. This motif is found in the ErB1 receptor TM domain, and by mutation analysis, was shown to be required for TM domain self-association (Mendrola *et al.*, 2002). We thus made the TM3 mutant to disrupt the GxxxG motif.

As shown by chemical cross-linking analysis, none of the three DDR1 TM domain mutants was defective in dimerisation in the absence of ligand. These results were confirmed by co-immunoprecipitation of epitope-tagged DDR1 mutants. DDR1 TM1 and TM2 mutants show only a very low level of receptor activation in response to collagen I compared to WT DDR1, indicating that the propagation of conformational change is blocked. TM3, on the other hand was able to autophosphorylate to a similar level as WT DDR1 indicating that this motif is not involved in TM domain signalling. The above results can be interpreted as follows: the TM domain of DDR1 is not required for receptor dimerisation in the absence of ligand, however, when collagen is

present and bound to the ECD, the TM domains of adjacent DDR monomers can self-assemble via their leucine zipper motifs.

In the case of DDR2, both TM1 and TM2 mutations showed defective protein expression manifested in the loss of the upper form of DDR2. This results in decreased collagen dependent signaling for both TM1 and TM2. The DDR2 TM3 mutant was normal in terms of protein expression and collagen dependent signalling. However, the TM1 mutant can still dimerise as shown by co-immunoprecipitation study, indicating that the leucine zipper is not important for receptor dimerisation but likely plays a role in protein folding and targeting to the cell surface.

Further studies, on the ability of the DDR1 TM domain for self-assembly, were carried out by a collaborating group (Carafoli and Hohenester, Imperial College, London). The capacity for self-assembly of WT and mutant DDR1 TM domains was tested using the TOXCAT system (Russ and Engleman, 1999). This assay has been used previously for the ErbB receptors (Mendrola *et al.*, 2002), integrin αIIb (Li *et al.*, 2004), GpA (Russ and Engleman) and EpoR (Kubatzky *et al.*, 2001) TM domain interactions. The isolated WT DDR1 and mutant TM domain sequence was fused to N-terminal DNA binding domain of ToxR (a dimerisation dependent transcription activator), and a monomeric periplasmic anchor (the maltose binding protein). Association of the TM domains on the bacterial inner cell membrane would result in the ToxR mediated activation of a reporter gene encoding chloroamphenicol acetyltransferase (CAT). The level of CAT expression indicates the strength of the TM association. A construct containing the WT TM domain of GpA was used as a positive control for dimerisation, whilst a dimerisation defective GpA mutant TM domain containing construct was used as a negative control (Figure 5.10, A). According to the measured CAT activity, the WT DDR1 TM domain showed very strong dimerisation, more than the WT GpA TM domain (Figure 5.10, B). Both TM1 and TM2 show drastically reduced CAT activity compared to the WT DDR1, whilst TM3 CAT activity was very similar to WT DDR1 (Figure 5.10, C). These results suggest firstly that the DDR1 WT TM domain is able to self-associate *in vivo* and

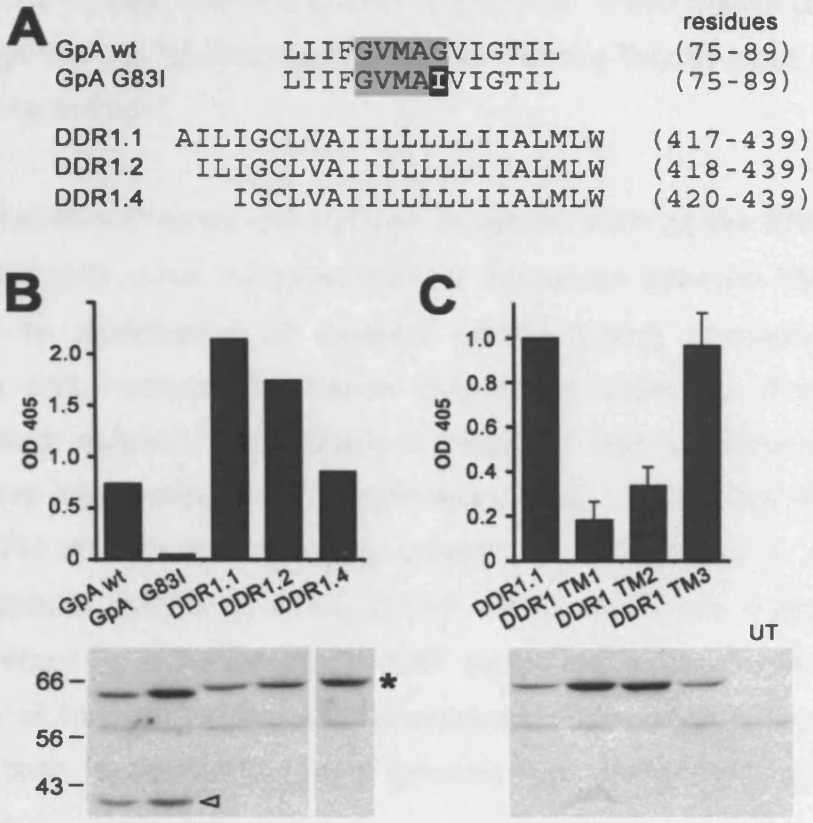

Figure 5.10: The DDR1 TM domain self-associates in bacterial membranes. (A) DDR1 TM sequences tested in the TOXCAT assay. The dimerising GpA sequence and the non-dimerising G83I GpA mutant were used as positive and negative controls, respectively. (B) Homodimerisation of ToxR[1] chimaeric constructs, as measured by CAT enzyme activity. Lysates from MM39 *E. coli* cells expressing chimaeras with the indicated TM sequences were used to measure CAT activity by ELISA. CAT activity is represented as absorbance at 405 nm. The experiment is representative of three independent experiments. The lower panel shows the relative expression levels of the chimaeric proteins. Lysates from MM39 cells expressing the chimaeric constructs were separated on 10% SDS-PAGE and immunoblotted with an Ab against the C-terminal MBP domain. The asterisk denotes full-length chimaeras; the arrowhead denotes proteolysed GpA chimaeras. (C) Homodimerisation of ToxR[1] chimaeric constructs containing wild-type and mutant DDR1 TM sequences, determined as in (B). The data are presented as mean ± standard deviation from three independent experiments, each performed in triplicate or quintuplicate and normalised to the values obtained with DDR1.1. The lower panel shows the relative expression levels, as in B; UT, untransformed cells.

secondly that the leucine zipper motif, but not the GxxxG motif is responsible for DDR1 TM domain self-association. Importantly, these results complement our findings that the leucine zipper motif, but not the GxxxG motif, is required for DDR1 signalling.

Several studies with other cell surface receptors, such as the ErbB receptor and Epo receptor, have indicated that the interaction between TM α-helices contribute to stabilization of receptor dimers. Using chimaeric receptor constructs and immunofluorescence co-patching technique, it was shown that the Epo receptor TM domain is essential and sufficient for ligand-independent oligomerisation (Constantinescu *et al.*, 2001). Similarly, the Epo receptor TM domain had a strong potential to self-interact in a bacterial reporter system (Kubatzky *et al.*, 2001). Furthermore, this interaction was shown to occur via a leucine zipper motif, as the introduction of simultaneous mutations of two conserved leucine residues in the TM domain, LL->GP, reduced both self-assembly and tyrosine phosphorylation upon ligand stimulation.

For the members of the ErbB receptor family, there are conflicting models for the involvement of the TM domain in dimer formation. Isolated ECDs of ErbB family members, ErbB1 and ErbB4, were shown to dimerise completely upon ligand binding, indicating that the ECD is solely responsible for receptor oligomerisation, whilst the TM and cytosolic domains are not involved (Ferguson *et al.*, 2000; Elleman *et al.*, 2001;). In contrast, another model argues that the ErbB1 TM domain is mainly responsible for ligand-induced dimerisation and provides the primary driving force for receptor dimerisation (Tanner and Kyte, 1999). The investigators showed this by comparing the dissociation/association kinetics of the ErbB1 ECD on its own to ErbB1 containing both ECD and TM domains. The latter construct showed a significantly lower degree of dissociation than the former construct, indicating that the TM domain helps ligand-induced dimerisation.

Recently, a study carried out by Bennasroune *et al.* revealed that specific hydrophobic peptides corresponding to the TM domain of ErbB1 and ErbB2

can act as inhibitors of receptor signalling by inhibiting ligand-dependent receptor dimerisation (Bennasroune *et al.*, 2004). This finding is supported by a study by Mendrola *et al.*, who showed, using the TOXCAT system, that the isolated TM domain of ErbB1, 2, 3 and 4 self-associate strongly in bacterial cell membranes, and through mutagenesis studies, pointed to the GxxxG motif of the TM domain which might be involved in dimer formation (Mendrola *et al.*, 2002).

The fact that two dimerisation motifs are found in the DDR TM domain could be significant, in the light of recent work done on ErbB1 and ErbB2 TM domain interactions (Gerber *et al.*, 2004). ErbB1 and ErbB2 contain two GxxxG like motifs, one on the N-terminal part and the other on the C-terminal part of the TM domain. The authors investigated the isolated WT and mutant TM domains for the ability to interact, using the ToxR system. The investigators showed that the N-terminal GxxxG motif was involved in ErbB1 heterodimerisation with ErbB2 TM domain, but not homodimerisation of ErbB1 receptors. Previous work showed that the C-terminal GxxxG motif was needed for ErbB receptors to homodimerisation (Mendrola *et al.*, 2002). Taken together, these results suggest that both GxxxG motifs play a role in ErbB1 TM domain interactions, with one motif involved in homodimerisation and the other GxxxG motif playing a role in heterodimerisation with ErbB2. It is conceivable that the GxxxG motif in the DDRs is involved in the interaction with another TM protein.

The GxxxG motif, though present in the DDR TM domain, does not seem to have a role in DDR TM assembly or signalling. The mere presence of this motif is not sufficient to suggest that it is responsible for TM domain interactions as residues surrounding the GxxxG framework have been shown to play an important role in determining if the GxxxG motif interactions are favourable for the particular protein in question (Lemmon *et al.*, 1992; Russ and Engelman, 1999; Melnyk *et al.*, 2003). Mutagenesis studies have suggested that other amino acids in the TM domain, besides the two glycine residues of the GxxxG motif, are involved in mediating GpA homodimerisation (Langosch *et al.*, 1996). Another more recent study on the

GpA TM domain, where specific TM helix interfacial residues were introduced into the TM domain of another protein, the M13 major coat protein (MCP), found that interfacial residues 12 residues apart are able to modulate TM helix-helix interactions (Melnyk *et al.*, 2004).

As both TM1 and TM2 mutants were able to oligomerise in the absence of ligand, we made and tested two DDR1 double mutants, containing the TM1 mutation with either the DS domain or the domain X plus the P/G rich region deleted. Both these mutants were able to co-precipitate and therefore homo-oligomerise, indicating that the KD or the region of the ECD, which is still present, is mediating receptor dimerisation. We then made and tested by co-immunoprecipitation, a DDR1 triple mutant containing the TM1 mutation plus the domain X plus the P/G rich region deleted. This mutant was able to oligomerise, indicating that the DS domain, which is still intact in this mutant, is mediating receptor dimerisation. This result taken together with DDR domain deletion analysis described in Chapter 4, suggests that the DDRs are able to interact with each other via both the ECD and cytosolic regions. The importance of each region in driving and/or stabilising receptor dimers in the presence of ligand would be the next step for investigation as it is expected that a conformation change would occur within the receptor dimers upon ligand binding. Receptor conformation changes upon ligand binding have been shown for EGFR (Moriki *et al.*, 2001), and Neu (or ErbB2) receptor (Bell *et al.*, 2000). The investigators carried out Cys-scanning mutagenesis of the receptor juxtamembrane region and proposed a model by which ligand binding to the ECD of preformed, inactive receptor dimers induced rotation of the extracellular juxtamembrane region and hence the TM domain, leading to dissociation of the dimeric, inactive form of the cytosolic region. It could be that a mechanism of activation of DDRs involves a similar 'rotation model', and experiments similar to that performed for EGFR and ErbB2 need to be carried out to determine this.

In conclusion, a mechanism of DDR1 activation is proposed as follows. Inactive receptors exist as preformed dimers on the cell surface via interactions between the ECD and TM domain and possibly the cytoplasmic

domain, with the cytoplasmic KDs most likely in an inhibitory conformation. Collagen binding to the DS domain leads to a conformational change in the ECD, and self-assembly of the two TM α-helices allows the tyrosine KD to come closer together. We speculate that this causes a release of the KD inhibitory conformation and activation of the tyrosine kinase, enabling autophosphorylation of conserved tyrosine residues in the cytoplasmic region. A schematic diagram of DDR1 activation based this model is shown in Figure 5.11.

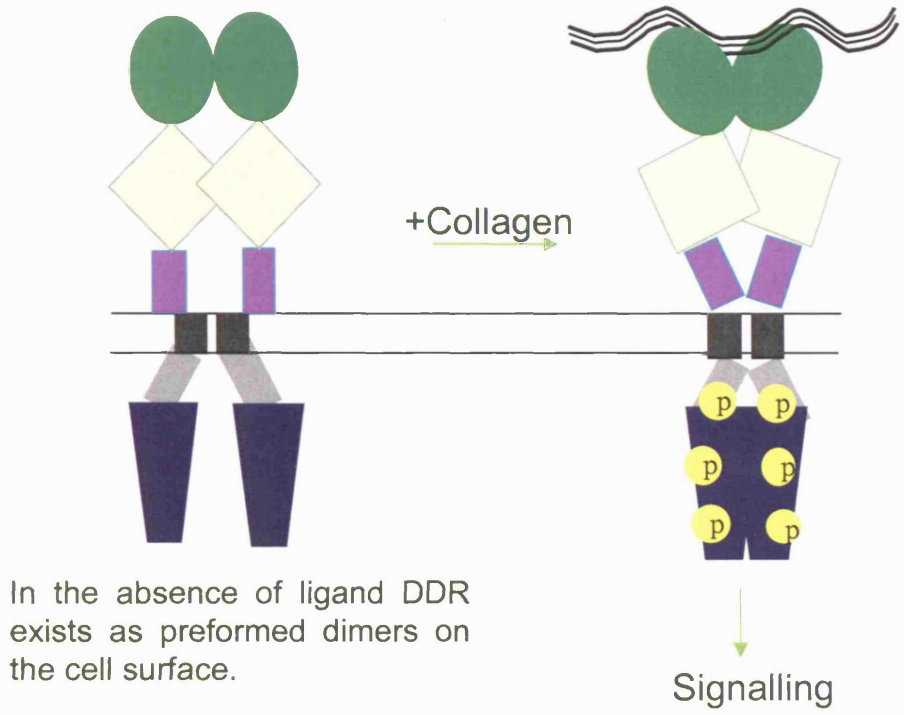

In the absence of ligand DDR exists as preformed dimers on the cell surface.

Signalling

Conformational change and self-assembly of the TM helices via the leucine zipper motif enables autophosphorylation.

Figure 5.11: A model for DDR1 activation. In the absence of ligand, DDR1 exist as preformed dimers on the cell surface. The two DDR1 monomers interact with each other via the ECD and TM domain to give an inactive conformation where the KDs are too far apart to interact. Upon collagen binding to the DS domain, there is a conformational change in the extracellular region and self-assembly of TM α-helices, via the leucine zipper motif, which draws the two receptor monomers closer together enabling the KDs to phosphorylate each other on conserved tyrosine residues.

Chapter 6

General Discussion

6.1. Introduction

In this thesis I have shown firstly, that full-length WT DDR1 and DDR2 exist as preformed dimers on the cell surface. The precursor forms of both DDRs exist as preformed dimers during biosynthesis. Once dimerised, the receptors are most likely associated during transport to the cell surface, suggesting that the DDRs are most likely constitutive dimers. Secondly, the DDR domains essential for receptor dimerisation were investigated, and it was found that neither the ECDs nor the cytosolic domains were required for dimerisation. In the third part of this thesis, the role of the TM domain in DDR dimerisation and activation was explored. Two potential dimerisation motifs are found in the DDR TM domain – a leucine zipper and a GxxxG motif. Mutations to disrupt both these motifs did not effect receptor dimerisation in the absence of ligand. However, in the presence of ligand, it was found that the leucine zipper motif, but not the GxxxG motif, was required for DDR1 signal transduction. A parallel study which looked at the potential for self-association of the isolated DDR1 TM domain in bacterial inner membranes, revealed that the WT DDR1 TM domain interacts strongly. A DDR1 mutant TM domain containing disrupting mutations in the GxxxG motif did not affect self-assembly, whereas mutations in the leucine zipper motif drastically reduced self-association. Thus, the DDR1 TM domain self-associates in biological membranes via the leucine zipper motif.

The observations made in this study in relation to the literature on similar investigations carried out for other cell surface receptors, and the wider implications of the findings presented in this thesis will be discussed below.

Future directions of the research based on the constructs and information from the research presented in this thesis are also discussed.

6.2. Preformed dImerisation of DDRs and other cell surface receptors

The results of this study have shown that the DDRs exist as dimers on the cell surface and during receptor biosynthesis. This is a novel finding, and ligand-independent dimerisation has only been found for a few other RTKs. Our finding is consistent with the earlier report that used soluble ECD constructs of DDRs to investigate DDR collagen binding *in vitro*, which showed that the DDRs needed to be dimerised in order to bind collagen (Leitinger, 2003).

There have been a number of studies investigating the dimerisation state of the ErbB receptors in the absence and presence of ligand. Analysis of recently solved crystal structures of the ECDs of these receptors in the absence and presence of ligand put forward a mechanism by which ligand binding induces dimerisation of the ECD (Cho and Leahy, 2002; Garrett *et al.*, 2002; Ogiso *et al.*, 2002; Cho *et al.*, 2003; Ferguson *et al.*, 2003; Garrett *et al.*, 2003). However, challenges to the dogma of ligand-mediated receptor dimerisation have been put forward by several independent groups, whose research support the hypothesis that the ErbB receptors exists as preformed dimers (Chu *et al.*, 1997; Gadella and Jovin, 1995; Moriki *et al.*, 2001, Sako *et al.*, 2000; Yu *et al.*, 2002). The latter studies suggest that activation involves ligand-induced conformational changes within a dimeric receptor.

We have found that for DDRs, the dogma that RTKs are dimerised upon ligand binding may not be relevant. Our data show dimerisation of biosynthetic precursor receptors and therefore provide evidence of constitutive DDR dimers. For other cell surface receptors, the main evidence for ligand-induced dimerisation is based on the crystal structures of receptor ECD, and therefore proteins in solution. These receptors include the ErbB receptor family, described above, and the cytokine receptors such as the Epo receptor (Livinah *et al.*,1996) and the GH receptor (Fuh *et al.*, 1992; de Vos *et al.*, 1992). In full-length receptors, the TM or cytosolic domains likely influence receptor dimerisation. According to initial crystallographic evidence, the Epo receptor was thought dimerise upon ligand binding, but a

subsequent structural study showed that receptor dimerisation is not suficient for activation (Livinah *et al.*, 1998). Furthermore, recent biochemical studies strongly indicate these receptors to be present as ligand-independent dimers on the cell-surface (Constantinescu *et al.*, 2000). This is also true for the GH receptor; recent evidence using biophysical studies with BRET and FRET in addition to co-immunoprecipitation studies have provided strong evidence for ligand-independent receptor dimers (Brown *et al.*, 2005). Evidence that these receptors form dimers in the ER underscore the result that these receptors are constitutively dimerised (Gent *et al.*, 2002)

For ErbB1 (EGFR), it has been suggested that without predimers, dimerisation would take longer as receptor monomers would need to diffuse in the PM looking for partner receptors and the existence of preformed dimers would enable accelerated EGFR activation and signal transduction (Yu *et al.*, 2002). However, as DDRs normally take longer than other RTKs to be activated by their ligand, the above hypothesis is difficult to apply for these receptors, and other slower processes, such as receptor clustering may be involved in DDR activation.

6.3. The role of the ECD and cytoplasmic domain in ligand-independent oligomerisation of DDRs and other RTKs

The study described in Chapter 4 shows that both the ECD and cytosolic region are not essential for DDR dimerisation in the absence of ligand. However this does not imply that these regions are not involved in receptor monomer contacts within the preformed dimers. It is possible that there are interactions, as found for the ErbB receptors, in both the ECD and cytoplasmic domains, but these interactions are dispensable due to strong interactions via the DDR TM domains. The findings that the DDRs are still dimerised when the leucine zipper motif is disrupted, demonstrates that other domains contribute to receptor stability.

In RTKs such as FGFR2 and RET, disulphide bonds between cysteine residues in the ECD have been implicated in ligand-dependent receptor

dimerisation (Robertson *et al.*, 2000). In the DDR ECD, there is one unpaired cysteine which was hypothesized to be involved in receptor dimerisation. However mutation analysis of this cysteine to disrupt a potential inter-receptor disulphide bridge did not affect receptor signalling or dimerisation (Leitinger and Bhattia, personal communication).

Biochemical studies with a chimaeric receptor comprising of ECD and TM of EGFR and cytosolic domain of Epo receptor showed that this protein did not dimerise in the absence of ligand, as shown by chemical cross-linking analysis, whilst the full-length WT EGFR did predimerise (Yu *et al.*, 2002). These results indicate that the cytoplasmic domain is required for ligand-independent EGFR homodimerisation. Another study by Penuel *et al.*, further identified specific hydrophobic amino acids in the C-terminal tail of ErbB2 that are required for ligand-independent receptor homodimerisation (Penual *et al.*, 2002). When ligand is present and bound, it seems that the ECD of EGFR plays a major role in dimerisation, as suggested from the crystal structures. However, the role of the TM domain and cytosolic domain contacts in the presence of bound ligand have not yet been investigated. It has been suggested that these receptors could exist in a monomer/dimer equilibrium which is stabilized upon ligand binding (Garett *et al.*, 2002).

The therapeutic implications for finding a specific domain required for receptor dimerisation is shown by the discovery of the mAb pertuzumab (Omnitarg), which blocks ErbB2 heterodimerisation with EGFR, ErbB3 and ErbB4. The crystal structure of pertuzumab in complex with ErbB2 ECD reveals the mechanism of action of this mAb. Pertuzumab binds to a binding pocket in domain II of ErbB2 thus preventing the dimerisation 'hairpin' or 'arm' of partner EGFR/ErbB3/ErbB4 receptor from fitting into the binding pocket (Franklin *et al.*, 2004).

The MET RTK has also been suggested to predimerise and by deletion analysis it was shown that the SEMA domain in the ECD is essential for MET signalling (Kong-Beltran *et al.*, 2004). The investigators showed that deletion of this domain prevents receptor activation both in the presence and absence

of ligand. The study suggests that in the absence of ligand recombinant SEMA domain (rSEMA) most likely blocks receptor dimerisation whereas in the presence of ligand rSEMA binds ligand and therefore prevents MET activation. The study further suggests that rSEMA could be used as a 'biotherapeutic' - as the treatment of MET overexpressing tumour cells with recombinant SEMA in the presence or absence of ligand resulted in decreased MET signal transduction, cell motility and migration.

6.4. The role of the TM domain in receptor oligomerisation and activation of DDRs and other cell surface receptors

In the third part of our study we investigated the role of the TM domain in DDR dimerisation and signalling. Results from a parallel study using the TOXCAT assay provide strong evidence for the DDR1 TM domain to self-interact. Therefore the TM domain must play a major role in ligand-independent receptor–receptor interactions. Our study shows that the TM domain is important for DDR1 signal transduction, revealing a critical role for the leucine zipper motif in DDR1 activation.

As described in Chapter 1, the DDRs are found up-regulated in a number of human disease and pathological conditions such liver fibrosis, idiopathic pulmonary fibrosis and inflammation, atherosclerosis, lymphangioleiomyomatosis, osteoarthritis, rheumatoid arthritis, primary biliary cirrhosis and malignant tumours. Based on these findings that the specific motif in the DDR1 TM domain is essential for transmitting the conformational change induced upon ligand binding, future work would be to look towards finding an effective method to block DDR signalling. For example, short hydrophobic TM peptides corresponding to the WT DDR TM domain could be designed and tested for the ability to block receptor dimerisation and signalling. Such a study was carried out for the EGFR and ErbB2 receptors where hydrophobic TM peptides inhibited specifically the autophosphorylation and down stream signalling of EGFR and ErbB2 (Bennasroune *et al.*, 2004). In addition mutant DDR TM peptides could be made with mutations similar to TM1 and TM2, and used for confirmation of the mechanism of action of the WT TM peptides.

In conclusion, the findings presented in this thesis strongly argue in favour of the important role of the TM domain in DDR function. It cannot be excluded that the TM interactions could act in concert with the ECD, as studies by Leitinger, 2003 showed that deletion of subdomains of the ECD inhibits DDR1 signalling (Leitinger, 2003). In the presence of ligand, the co-ordinated association of the TM domains could favour productive interaction of the intracellular KDs leading to autophosphorylation and signalling. Even though the cytoplasmic juxtamembrane region is not essential for DDR dimerisation as shown in this study, further deletion analysis needs to be carried out to explore the role of the cytosolic juxtamembrane region in DDR signalling, as this region could be important in preventing DDR activation in the absence of ligand.

DDR activation is a result of ligand binding to the ECD, as shown for all other RTKs. The data presented in this thesis suggests that in the absence of collagen, the DDRs exist as inactive dimers with the KDs held in an inactive conformation. We propose that collagen binding induces a conformational change that is transmitted to the cytoplasmic domain, allowing the KDs to become activated. We show that the leucine zipper in the DDR1 TM domain is critical for transmitting the conformational change imposed on the receptor dimer by collagen binding. Thus, self-assembly of the DDR1 TM domain, although not essential for dimerisation, promotes a ligand-induced conformational switch required for the activation of signalling. Although we do not know the nature of the conformational rearrangement, a possible mechanism would be that TM domain interactions involve relative rotation of receptor protomers within the dimer, as have been suggested for EGFR (Moriki *et al.*, 2001), the Epo receptor (Seubert *et al.*, 2003), or the GH receptor (Brown *et al.*, 2005).

6.5. Future work

6.5.1. Determining the nature of a possible post-translational modification in DDR2

As detailed in Chaper 3, we were unable to fully determine the type of post-translational modification that might be responsible for the presence of the different MW forms of DDR2. In section 3.3, we suggested that either monoubiquitination or SUMO modification might be responsible for the difference. The presence of monoubiquitin can be detected by SDS-PAGE and immunoblotting using a commercially available anti-ubiquitin Ab, which is able to distinguish between monoubiquitin and polyubiquitin structures. A similar approach can be used for detecting SUMO modifications.

6.5.2. Investigate the effect of collagen on DDR dimerisation in live cells

One or more of the following methods can be used to look at the effect of collagen on DDR dimerisation in live cells - BRET, FRET or Fluorescence Lifetime Imaging Microscopy (FLIM) analysis. FRET analysis is a useful method for measuring conformational changes and spatial proximity of a membrane protein of interest. These non-invasive biophysical methods do not require detergent solubilization (as used in co-immunoprecipitation studies) and therefore allow one to look at the receptor in its natural environment. Another advantage of FRET over BRET or co-immunoprecipitation studies is that it allows one to measure conformation changes and/or interactions of the mature, cell surface population of the membrane protein. For FRET analysis, the membrane protein can be N-terminally or C-terminally tagged with cyan fluorescent protein (CFP) and yellow fluorescent protein (YFP). We have made DDR constructs C-terminally tagged with a monomeric version of C/YFP. Four constructs DDR1-CFP, DDR1-YFP, DDR2-CFP and DDR2-YFP were made and checked for receptor expression and functionality. The presence of the C/YFP tag does not affect expression and collagen-dependent autophosphorylation when compared with WT DDRs (Leitinger and McCaine, personal communications). Thus these constructs will be used for FRET

analysis to explore the oligomeric state of DDRs *in situ* and determine the effect of collagen on DDR oligomerisation in live cells.

References

Abdulhussein, R., McFadden, C., Fuentes-Prior, P., and Vogel, W. F. (2004). Exploring the collagen-binding site of the DDR1 tyrosine kinase receptor. J Biol Chem *279*, 31462-70.

Adams, P. D., Engelman, D. M., and Brunger, A. T. (1996). Improved prediction for the structure of the dimeric transmembrane domain of glycophorin A obtained through global searching. Proteins *26*, 257-261.

Agarwal, G., Kovac, L., Radziejewski, C., and Samuelsson, S. J. (2002). Binding of discoidin domain receptor 2 to collagen I: an atomic force microscopy investigation. Biochemistry *41*, 11091-11098.

Alberts, B., Johnson, A., Lewis, J., Raff, M., Roberts, K., and Walter, P. (2001) in Molecular Biology of the Cell, 4th ed. Garland Science, New York, N.Y.

Alves, F., Saupe, S., Ledwon, M., Schaub, F., Hiddemann, W., and Vogel, W. F. (2001). Identification of two novel, kinase-deficient variants of discoidin domain receptor 1: differential expression in human colon cancer cell lines. Faseb J *15*, 1321-1323.

Alves, F., Vogel, W., Mossie, K., Millauer, B., Hofler, H., and Ullrich, A. (1995). Distinct structural characteristics of discoidin I subfamily receptor tyrosine kinases and complementary expression in human cancer. Oncogene *10*, 609-618.

Arkin, I. T., Adams, P. D., MacKenzie, K. R., Lemmon, M. A., Brunger, A. T., and Engelman, D. M. (1994). Structural organization of the pentameric transmembrane alpha-helices of phospholamban, a cardiac ion channel. Embo J *13*, 4757-4764.

Assoian, R. K., and Schwartz, M. A. (2001). Coordinate signaling by integrins and receptor tyrosine kinases in the regulation of G1 phase cell-cycle progression. Curr Opin Genet Dev *11*, 48-53.

Baass, P. C., Di Guglielmo, G. M., Authier, F., Posner, B. I., and Bergeron, J. J. (1995). Compartmentalized signal transduction by receptor tyrosine kinases. Trends Cell Biol *5*, 465-470.

Bagossi, P., Horvath, G., Vereb, G., Szollosi, J., and Tozser, J. (2005). Molecular modeling of nearly full-length ErbB2 receptor. Biophys J *88*, 1354-1363.

Banyai, L., Tordai, H., and Patthy, L. (1994). The gelatin-binding site of human 72 kDa type IV collagenase (gelatinase A). Biochem J *298*, 403-407.

Barker, K. T., Martindale, J. E., Mitchell, P. J., Kamalati, T., Page, M. J., Phippard, D. J., Dale, T. C., Gusterson, B. A., Crompton, M. R. (1995). Expression patterns of the novel receptor-like tyrosine kinase, DDR, in human breast tumours. Oncogene *10*, 569-75.

Baumgartner, S., Hofmann, K., Chiquet-Ehrismann, R., and Bucher, P. (1998). The discoidin domain family revisited: new members from prokaryotes and a homology-based fold prediction. Protein Sci *7*, 1626-1631.

Behrendt, N., Jensen, O. N., Engelholm, L. H., Mortz, E., Mann, M., and Dano, K. (2000). A urokinase receptor-associated protein with specific collagen binding properties. J Biol Chem *275*, 1993-2002.

Belanger, C., Ansanay, H., Qanbar, R., and Bouvier, M. (2001). Primary sequence requirements for S-acylation of beta(2)-adrenergic receptor peptides. FEBS Lett *499*, 59-64.

Bell, C. A., Tynan, J. A., Hart, K. C., Meyer, A. N., Robertson, S. C., and Donoghue, D. J. (2000). Rotational coupling of the transmembrane and kinase domains of the Neu receptor tyrosine kinase. Mol Biol Cell *11*, 3589-3599.

Bella, J., Eaton, M., Brodsky, B., and Berman, H. M. (1994). Crystal and molecular structure of a collagen-like peptide at 1.9 A resolution. Science *266*, 75-81.

Bennasroune, A., Fickova, M., Gardin, A., Dirrig-Grosch, S., Aunis, D., Cremel, G., and Hubert, P. (2004). Transmembrane peptides as inhibitors of ErbB receptor signaling. Mol Biol Cell *15*, 3464-3474.

Bhatt, R. S., Tomoda, T., Fang, Y., and Hatten, M. E. (2000). Discoidin domain receptor 1 functions in axon extension of cerebellar granule neurons. Genes Dev *14*, 2216-2228.

Bijlmakers, M. J., and Marsh, M. (2003). The on-off story of protein palmitoylation. Trends Cell Biol *13*, 32-42.

Blanpain, C., Wittamer, V., Vanderwinden, J. M., Boom, A., Renneboog, B., Lee, B., Le Poul, E., El Asmar, L., Govaerts, C., Vassart, G., *et al.* (2001). Palmitoylation of CCR5 is critical for receptor trafficking and efficient activation of intracellular signaling pathways. J Biol Chem *276*, 23795-23804.

Blume-Jensen, P., and Hunter, T. (2001). Oncogenic kinase signalling. Nature *411*, 355-365.

Boot-Handford, R. P., and Tuckwell, D. S. (2003). Fibrillar collagen: the key to vertebrate evolution? A tale of molecular incest. Bioessays *25*, 142-151.

Boskovic, J., Arnold, J. N., Stilion, R., Gordon, S., Sim, R. B., Rivera-Calzada, A., Wienke, D., Isacke, C. M., Martinez-Pomares, L., and Llorca, O. (2006). Structural model for the mannose receptor family uncovered by electron microscopy of Endo180 and the mannose receptor. J Biol Chem *281*, 8780-8787.

Briddon, S. J., and Watson, S. P. (1999). Evidence for the involvement of p59fyn and p53/56lyn in collagen receptor signalling in human platelets. Biochem J *338 (Pt 1)*, 203-209.

Brodsky, B., and Ramshaw, J. A. (1997). The collagen triple-helix structure. Matrix Biol *15*, 545-554.

Brown, R. J., Adams, J. J., Pelekanos, R. A., Wan, Y., McKinstry, W. J., Palethorpe, K., Seeber, R. M., Monks, T. A., Eidne, K. A., Parker, M. W., and Waters, M. J. (2005). Model for growth hormone receptor activation based on subunit rotation within a receptor dimer. Nat Struct Mol Biol *12*, 814-821.

Burgess, A. W., Cho, H. S., Eigenbrot, C., Ferguson, K. M., Garrett, T. P., Leahy, D. J., Lemmon, M. A., Sliwkowski, M. X., Ward, C. W., and Yokoyama, S. (2003). An open-and-shut case? Recent insights into the activation of EGF/ErbB receptors. Mol Cell *12*, 541-552.

Calderwood, D. A., Shattil, S. J., and Ginsberg, M. H. (2000). Integrins and actin filaments: reciprocal regulation of cell adhesion and signaling. J Biol Chem *275*, 22607-22610.

Carpenter, G., and Cohen, S. (1990). Epidermal growth factor. J Biol Chem *265*, 7709-7712.

Carpenter, G., King, L., Jr., and Cohen, S. (1978). Epidermal growth factor stimulates phosphorylation in membrane preparations in vitro. Nature *276*, 409-410.

Chantry, A. (1995). The kinase domain and membrane localization determine intracellular interactions between epidermal growth factor receptors. J Biol Chem *270*, 3068-3073.

Cho, H. S., and Leahy, D. J. (2002). Structure of the extracellular region of HER3 reveals an interdomain tether. Science *297*, 1330-1333.

Cho, H. S., Mason, K., Ramyar, K. X., Stanley, A. M., Gabelli, S. B., Denney, D. W., Jr., and Leahy, D. J. (2003). Structure of the extracellular region of HER2 alone and in complex with the Herceptin Fab. Nature *421*, 756-760.

Chu, C. T., Everiss, K. D., Wikstrand, C. J., Batra, S. K., Kung, H. J., and Bigner, D. D. (1997). Receptor dimerization is not a factor in the signalling activity of a transforming variant epidermal growth factor receptor (EGFRvIII). Biochem J *324 (Pt 3)*, 855-861.

Clemetson, J. M., Polgar, J., Magnenat, E., Wells, T. N., and Clemetson, K. J. (1999). The platelet collagen receptor glycoprotein VI is a member of the immunoglobulin superfamily closely related to FcalphaR and the natural killer receptors. J Biol Chem *274*, 29019-29024.

Constantinescu, S. N., Keren, T., Socolovsky, M., Nam, H., Henis, Y. I., and Lodish, H. F. (2001). Ligand-independent oligomerization of cell-surface erythropoietin receptor is mediated by the transmembrane domain. Proc Natl Acad Sci U S A *98*, 4379-4384.

Cornea, A., Janovick, J. A., Maya-Nunez, G., and Conn, P. M. (2001). Gonadotropin-releasing hormone receptor microaggregation. Rate monitored by fluorescence resonance energy transfer. J Biol Chem *276*, 2153-2158.

Curat, C. A., Eck, M., Dervillez, X., and Vogel, W. F. (2001). Mapping of epitopes in discoidin domain receptor 1 critical for collagen binding. J Biol Chem *276*, 45952-45958.

Curat, C. A., and Vogel, W. F. (2002). Discoidin domain receptor 1 controls growth and adhesion of mesangial cells. J Am Soc Nephrol *13*, 2648-2656.

Curino, A. C., Engelholm, L. H., Yamada, S. S., Holmbeck, K., Lund, L. R., Molinolo, A. A., Behrendt, N., Nielsen, B. S., and Bugge, T. H. (2005). Intracellular collagen degradation mediated by uPARAP/Endo180 is a major pathway of extracellular matrix turnover during malignancy. J Cell Biol *169*, 977-985.

Dejmek, J., Dib, K., Jonsson, M., and Andersson, T. (2003). Wnt-5a and G-protein signaling are required for collagen-induced DDR1 receptor activation and normal mammary cell adhesion. Int J Cancer *103*, 344-351.

Dejmek, J., Leandersson, K., Manjer, J., Bjartell, A., Emdin, S. O., Vogel, W. F., Landberg, G., and Andersson, T. (2005). Expression and signaling activity of Wnt-5a/discoidin domain receptor-1 and Syk plays distinct but decisive roles in breast cancer patient survival. Clin Cancer Res *11*, 520-528.

de Vos, A. M., Ultsch, M., and Kossiakoff, A. A. (1992). Human growth hormone and extracellular domain of its receptor: crystal structure of the complex. Science *255*, 306-312.

Dickeson, S. K., Walsh, J. J., and Santoro, S. A. (1997). Contributions of the I and EF hand domains to the divalent cation-dependent collagen binding activity of the alpha2beta1 integrin. J Biol Chem *272*, 7661-7668.

Di Marco, E., Cutuli, N., Guerra, L., Cancedda, R., and De Luca, M. (1993). Molecular cloning of trkE, a novel trk-related putative tyrosine kinase receptor isolated from normal human keratinocytes and widely expressed by normal human tissues. J Biol Chem *268*, 24290-24295.

Doura, A. K., and Fleming, K. G. (2004). Complex interactions at the helix-helix interface stabilize the glycophorin A transmembrane dimer. J Mol Biol *343*, 1487-1497.

East, L., McCarthy, A., Wienke, D., Sturge, J., Ashworth, A., and Isacke, C. M. (2003). A targeted deletion in the endocytic receptor gene Endo180 results in a defect in collagen uptake. EMBO Rep *4*, 710-716.

East, L., Rushton, S., Taylor, M. E., and Isacke, C. M. (2002). Characterization of sugar binding by the mannose receptor family member, Endo180. J Biol Chem *277*, 50469-50475.

Elleman, T. C., Domagala, T., McKern, N. M., Nerrie, M., Lonnqvist, B., Adams, T. E., Lewis, J., Lovrecz, G. O., Hoyne, P. A., Richards, K. M., *et al.* (2001). Identification of a determinant of epidermal growth factor receptor ligand-binding specificity using a truncated, high-affinity form of the ectodomain. Biochemistry *40*, 8930-8939.

Emsley, J., King, S. L., Bergelson, J. M., and Liddington, R. C. (1997). Crystal structure of the I domain from integrin alpha2beta1. J Biol Chem *272*, 28512-28517.

Emsley, J., Knight, C. G., Farndale, R. W., Barnes, M. J., and Liddington, R. C. (2000). Structural basis of collagen recognition by integrin alpha2beta1. Cell *101*, 47-56.

Emsley, J., Knight, C. G., Farndale, R. W., and Barnes, M. J. (2004). Structure of the integrin alpha2beta1-binding collagen peptide. J Mol Biol *335*, 1019-1028.

Engelholm, L. H., List, K., Netzel-Arnett, S., Cukierman, E., Mitola, D. J., Aaronson, H., Kjoller, L., Larsen, J. K., Yamada, K. M., Strickland, D. K., *et al.* (2003). uPARAP/Endo180 is essential for cellular uptake of collagen and promotes fibroblast collagen adhesion. J Cell Biol *160*, 1009-1015.

Erb, E. M., Tangemann, K., Bohrmann, B., Muller, B., and Engel, J. (1997). Integrin alphaIIb beta3 reconstituted into lipid bilayers is nonclustered in its activated state but clusters after fibrinogen binding. Biochemistry *36*, 7395-7402.

Ezumi, Y., Kodama, K., Uchiyama, T., and Takayama, H. (2002). Constitutive and functional association of the platelet collagen receptor glycoprotein VI-Fc receptor gamma-chain complex with membrane rafts. Blood *99*, 3250-3255.

Faraci-Orf, E., McFadden, C., Vogel, W. F. (2006). DDR1 signaling is essential to sustain Stat5 function during lactogenesis. J Cell Biochem *97*,109-21.

Farndale, R. W., Siljander, P. R., Onley, D. J., Sundaresan, P., Knight, C. G., and Barnes, M. J. (2003). Collagen-platelet interactions: recognition and signalling. Biochem Soc Symp, 81-94.

Farndale, R. W., Sixma, J. J., Barnes, M. J., and de Groot, P. G. (2004). The role of collagen in thrombosis and hemostasis. J Thromb Haemost *2*, 561-573.

Ferguson, K. M., Darling, P. J., Mohan, M. J., Macatee, T. L., and Lemmon, M. A. (2000). Extracellular domains drive homo- but not hetero-dimerization of erbB receptors. EMBO J *19*, 4632-4643.

Ferguson, K. M., Berger, M. B., Mendrola, J. M., Cho, H. S., Leahy, D. J., and Lemmon, M. A. (2003). EGF activates its receptor by removing interactions that autoinhibit ectodomain dimerization. Mol Cell *11*, 507-517.

Ferri, N., Carragher, N. O., Raines, E. W. (2004). Role of discoidin domain receptors 1 and 2 in human smooth muscle cell-mediated collagen remodeling: potential implications in atherosclerosis and lymphangioleiomyomatosis. Am J Pathol 164, 1575-85.

Floyd, D. H., Geva, A., Bruinsma, S. P., Overton, M. C., Blumer, K. J., and Baranski, T. J. (2003). C5a receptor oligomerization. II. Fluorescence resonance energy transfer studies of a human G protein-coupled receptor expressed in yeast. J Biol Chem *278*, 35354-35361.

Fitzpatrick, V. D., Pisacane, P. I., Vandlen, R. L., and Sliwkowski, M. X. (1998). Formation of a high affinity heregulin binding site using the soluble extracellular domains of ErbB2 with ErbB3 or ErbB4. FEBS Lett *431*, 102-106.

Foehr, E. D., Tatavos, A., Tanabe, E., Raffioni, S., Goetz, S., Dimarco, E., De Luca, M., and Bradshaw, R. A. (2000). Discoidin domain receptor 1 (DDR1) signaling in PC12 cells: activation of juxtamembrane domains in PDGFR/DDR/TrkA chimeric receptors. Faseb J *14*, 973-981.

Fuentes-Prior, P., Fujikawa, K., Pratt, K. P. (2002). New insights into binding interfaces of coagulation factors V and VIII and their homologous lessons from high resolution crystal structures. Curr Protein Pept Sci *3*, 313-339

Fuh, G., Cunningham, B. C., Fukunaga, R., Nagata, S., Goeddel, D. V., and Wells, J. A. (1992). Rational design of potent antagonists to the human growth hormone receptor. Science *256*, 1677-1680.

Kjoller, L., Engelholm, L. H., Hoyer-Hansen, M., Dano, K., Bugge, T. H., and Behrendt, N. (2004). uPARAP/endo180 directs lysosomal delivery and degradation of collagen IV. Exp Cell Res *293*, 106-116.

Gadella, T. W., Jr., and Jovin, T. M. (1995). Oligomerization of epidermal growth factor receptors on A431 cells studied by time-resolved fluorescence imaging microscopy. A stereochemical model for tyrosine kinase receptor activation. J Cell Biol *129*, 1543-1558.

Gardner, H., Broberg, A., Pozzi, A., Laato, M., and Heino, J. (1999). Absence of integrin alpha1beta1 in the mouse causes loss of feedback regulation of collagen synthesis in normal and wounded dermis. J Cell Sci *112 (Pt 3)*, 263-272.

Gardner, H., Kreidberg, J., Koteliansky, V., and Jaenisch, R. (1996). Deletion of integrin alpha 1 by homologous recombination permits normal murine development but gives rise to a specific deficit in cell adhesion. Dev Biol *175*, 301-313.

Garrett, T. P., McKern, N. M., Lou, M., Elleman, T. C., Adams, T. E., Lovrecz, G. O., Zhu, H. J., Walker, F., Frenkel, M. J., Hoyne, P. A., *et al.* (2002). Crystal structure of a truncated epidermal growth factor receptor extracellular domain bound to transforming growth factor alpha. Cell *110*, 763-773.

Garrett, T. P., McKern, N. M., Lou, M., Elleman, T. C., Adams, T. E., Lovrecz, G. O., Kofler, M., Jorissen, R. N., Nice, E. C., Burgess, A. W., and Ward, C. W.

(2003). The crystal structure of a truncated ErbB2 ectodomain reveals an active conformation, poised to interact with other ErbB receptors. Mol Cell *11*, 495-505.

Gent, J., van Kerkhof, P., Roza, M., Bu, G., and Strous, G. J. (2002). Ligand-independent growth hormone receptor dimerization occurs in the endoplasmic reticulum and is required for ubiquitin system-dependent endocytosis. Proc Natl Acad Sci U S A *99*, 9858-9863.

Gerber, D., Sal-Man, N., and Shai, Y. (2004). Two motifs within a transmembrane domain, one for homodimerization and the other for heterodimerization. J Biol Chem *279*, 21177-21182.

Giancotti, F. G., and Ruoslahti, E. (1999). Integrin signaling. Science *285*, 1028-1032.

Gibbins, J., Asselin, J., Farndale, R., Barnes, M., Law, C. L., and Watson, S. P. (1996). Tyrosine phosphorylation of the Fc receptor gamma-chain in collagen-stimulated platelets. J Biol Chem *271*, 18095-18099.

Gilboa, L., Wells, R. G., Lodish, H. F., and Henis, Y. I. (1998). Oligomeric structure of type I and type II transforming growth factor beta receptors: homodimers form in the ER and persist at the plasma membrane. J Cell Biol *140*, 767-777.

Giorgino, F., de Robertis, O., Laviola, L., Montrone, C., Perrini, S., McCowen, K. C., and Smith, R. J. (2000). The sentrin-conjugating enzyme mUbc9 interacts with GLUT4 and GLUT1 glucose transporters and regulates transporter levels in skeletal muscle cells. Proc Natl Acad Sci U S A *97*, 1125-1130.

Gumbiner, B. M. (1996). Cell adhesion: the molecular basis of tissue architecture and morphogenesis. Cell *84*, 345-357.

Gurezka, R., Laage, R., Brosig, B., and Langosch, D. (1999). A heptad motif of leucine residues found in membrane proteins can drive self-assembly of artificial transmembrane segments. J Biol Chem *274*, 9265-9270.

Gurezka, R., and Langosch, D. (2001). In vitro selection of membrane-spanning leucine zipper protein-protein interaction motifs using POSSYCCAT. J Biol Chem *276*, 45580-45587.

Haglund, K., Di Fiore, P. P., and Dikic, I. (2003a). Distinct monoubiquitin signals in receptor endocytosis. Trends Biochem Sci *28*, 598-603.

Haglund, K., Sigismund, S., Polo, S., Szymkiewicz, I., Di Fiore, P. P., and Dikic, I. (2003b). Multiple monoubiquitination of RTKs is sufficient for their endocytosis and degradation. Nat Cell Biol *5*, 461-466.

Haigler, H. T., McKanna, J. A., and Cohen, S. (1979). Direct visualization of the binding and internalization of a ferritin conjugate of epidermal growth factor in human carcinoma cells A-431. J Cell Biol *81*, 382-395.

Harris, E. S., McIntyre, T. M., Prescott, S. M., and Zimmerman, G. A. (2000). The leukocyte integrins. J Biol Chem *275*, 23409-23412.

Heino, J. (2000). The collagen receptor integrins have distinct ligand recognition and signaling functions. Matrix Biol *19*, 319-323.

Heinzelmann-Schwarz, V. A., Gardiner-Garden, M., Henshall, S. M., Scurry, J., Scolyer, R. A., Davies, M. J., Heinzelmann, M., Kalish, L. H., Bali, A., Kench, J. G., *et al.* (2004). Overexpression of the cell adhesion molecules DDR1, Claudin 3, and Ep-CAM in metaplastic ovarian epithelium and ovarian cancer. Clin Cancer Res *10*, 4427-4436.

Heldin, C. H. (1996). Protein tyrosine kinase receptors. Cancer Surv *27*, 7-24.

Hemler, M.E. (1999) in Integrins. in Guidebook to the extracellular matrix, anchor and adhesion proteins (Kreis, T., Vale, R., eds) pp 196-212, Oxford University Press, New York, N.Y.

Hicke, L. (2001). Protein regulation by monoubiquitin. Nat Rev Mol Cell Biol *2*, 195-201.

Horton, R. M., Ho, S. N., Pullen, J. K., Hunt, H. D., Cai, Z., and Pease, L. R. (1993). Gene splicing by overlap extension. Methods Enzymol *217*, 270-279.

Hou, G., Vogel, W., and Bendeck, M. P. (2001). The discoidin domain receptor tyrosine kinase DDR1 in arterial wound repair. J Clin Invest *107*, 727-735.

Hou, G., Vogel, W. F., and Bendeck, M. P. (2002). Tyrosine kinase activity of discoidin domain receptor 1 is necessary for smooth muscle cell migration and matrix metalloproteinase expression. Circ Res *90*, 1147-1149.

Howard, M. J., Chambers, M. G., Mason, R. M., and Isacke, C. M. (2004). Distribution of Endo180 receptor and ligand in developing articular cartilage. Osteoarthritis Cartilage *12*, 74-82.

Hubbard, S. R., Mohammadi, M., and Schlessinger, J. (1998). Autoregulatory mechanisms in protein-tyrosine kinases. J Biol Chem *273*, 11987-11990.

Huber, O., Kemler, R., and Langosch, D. (1999). Mutations affecting transmembrane segment interactions impair adhesiveness of E-cadherin. J Cell Sci *112*, 4415-4423.

Humphries, M. J. (2000). Integrin structure. Biochem Soc Trans *28*, 311-339.

Hunter, T. (1998). The Croonian Lecture 1997. The phosphorylation of proteins on tyrosine: its role in cell growth and disease. Philos Trans R Soc Lond B Biol Sci *353*, 583-605.

Hunter, T. (2000). Signaling--2000 and beyond. Cell *100*, 113-127.

Hynes, R. O. (1992). Integrins: versatility, modulation, and signaling in cell adhesion. Cell *69*, 11-25.

Ikeda, K., Wang, L. H., Torres, R., Zhao, H., Olaso, E., Eng, F. J., Labrador, P., Klein, R., Lovett, D., Yancopoulos, G. D., *et al.* (2002). Discoidin domain receptor 2 interacts with Src and Shc following its activation by type I collagen. J Biol Chem *277*, 19206-19212.

Jeffers, M., Taylor, G. A., Weidner, K. M., Omura, S., and Vande Woude, G. F. (1997). Degradation of the Met tyrosine kinase receptor by the ubiquitin-proteasome pathway. Mol Cell Biol *17*, 799-808.

Johnson, J. D., Edman, J. C., and Rutter, W. J. (1993). A receptor tyrosine kinase found in breast carcinoma cells has an extracellular discoidin I-like domain. Proc Natl Acad Sci U S A *90*, 5677-5681.

Jonsson, M., and Andersson, T. (2001). Repression of Wnt-5a impairs DDR1 phosphorylation and modifies adhesion and migration of mammary cells. J Cell Sci *114*, 2043-2053.

Julenius, K., Molgaard, A., Gupta, R., and Brunak, S. (2005). Prediction, conservation analysis, and structural characterization of mammalian mucin-type O-glycosylation sites. Glycobiology *15*, 153-164.

Kadler, K. E., Holmes, D. F., Trotter, J. A., and Chapman, J. A. (1996). Collagen fibril formation. Biochem J *316 (Pt 1)*, 1-11.

Kamata, T., Liddington, R. C., and Takada, Y. (1999). Interaction between collagen and the alpha(2) I-domain of integrin alpha(2)beta(1). Critical role of conserved residues in the metal ion-dependent adhesion site (MIDAS) region. J Biol Chem *274*, 32108-32111.

Kamata, T., and Takada, Y. (1994). Direct binding of collagen to the I domain of integrin alpha 2 beta 1 (VLA-2, CD49b/CD29) in a divalent cation-independent manner. J Biol Chem *269*, 26006-26010.

Kamohara, H., Yamashiro, S., Galligan, C., and Yoshimura, T. (2001). Discoidin domain receptor 1 isoform-a (DDR1alpha) promotes migration of leukocytes in three-dimensional collagen lattices. Faseb J *15*, 2724-2726.

Karn, T., Holtrich, U., Brauninger, A., Bohme, B., Wolf, G., Rubsamen-Waigmann, H., and Strebhardt, K. (1993). Structure, expression and chromosomal mapping of TKT from man and mouse: a new subclass of receptor tyrosine kinases with a factor VIII-like domain. Oncogene *8*, 3433-3440.

Katz, E. P., and David, C. W. (1990). Energetics of intrachain salt-linkage formation in collagen. Biopolymers *29*, 791-798.

Katz, E. P., and David, C. W. (1992). Unique side-chain conformation encoding for chirality and azimuthal orientation in the molecular packing of skin collagen. J Mol Biol *228*, 963-969.

Katz, B. Z., Zamir, E., Bershadsky, A., Kam, Z., Yamada, K. M., and Geiger, B. (2000). Physical state of the extracellular matrix regulates the structure and molecular composition of cell-matrix adhesions. Mol Biol Cell *11*, 1047-1060.

Kehrel, B., Wierwille, S., Clemetson, K. J., Anders, O., Steiner, M., Knight, C. G., Farndale, R. W., Okuma, M., and Barnes, M. J. (1998). Glycoprotein VI is a major collagen receptor for platelet activation: it recognizes the platelet-activating quaternary structure of collagen, whereas CD36, glycoprotein IIb/IIIa, and von Willebrand factor do not. Blood *91*, 491-499.

Kennedy, M. E., and Limbird, L. E. (1994). Palmitoylation of the alpha 2A-adrenergic receptor. Analysis of the sequence requirements for and the dynamic properties of alpha 2A-adrenergic receptor palmitoylation. J Biol Chem *269*, 31915-31922.

Kern, A., Briesewitz, R., Bank, I., and Marcantonio, E. E. (1994). The role of the I domain in ligand binding of the human integrin alpha 1 beta 1. J Biol Chem *269*, 22811-22816.

Kim, M., Carman, C. V., and Springer, T. A. (2003). Bidirectional transmembrane signaling by cytoplasmic domain separation in integrins. Science *301*, 1720-1725.

Kjoller L., Engelholm L. H., Hoyer-Hansen M., Dano K., Bugge T. H., Behrendt N. (2004). uPARAP/endo180 directs lysosomal delivery and degradation of collagen IV. Exp Cell Res *293*, 106-16.

Knight, C. G., Morton, L. F., Onley, D. J., Peachey, A. R., Ichinohe, T., Okuma, M., Farndale, R. W., and Barnes, M. J. (1999). Collagen-platelet interaction: Gly-Pro-Hyp is uniquely specific for platelet Gp VI and mediates platelet activation by collagen. Cardiovasc Res *41*, 450-457.

Knight, C. G., Morton, L. F., Onley, D. J., Peachey, A. R., Messent, A. J., Smethurst, P. A., Tuckwell, D. S., Farndale, R. W., and Barnes, M. J. (1998).

Identification in collagen type I of an integrin alpha2 beta1-binding site containing an essential GER sequence. J Biol Chem *273*, 33287-33294.

Knight, C. G., Morton, L. F., Peachey, A. R., Tuckwell, D. S., Farndale, R. W., and Barnes, M. J. (2000). The collagen-binding A-domains of integrins alpha(1)beta(1) and alpha(2)beta(1) recognize the same specific amino acid sequence, GFOGER, in native (triple-helical) collagens. J Biol Chem *275*, 35-40.

Kong-Beltran, M., Stamos, J., and Wickramasinghe, D. (2004). The Sema domain of Met is necessary for receptor dimerization and activation. Cancer Cell *6*, 75-84.

Kramer, R. Z., Vitagliano, L., Bella, J., Berisio, R., Mazzarella, L., Brodsky, B., Zagari, A., and Berman, H. M. (1998). X-ray crystallographic determination of a collagen-like peptide with the repeating sequence (Pro-Pro-Gly). J Mol Biol *280*, 623-638.

Kramer, R. Z., Bella, J., Mayville, P., Brodsky, B., and Berman, H. M. (1999). Sequence dependent conformational variations of collagen triple-helical structure. Nat Struct Biol *6*, 454-457.

Kubatzky, K. F., Ruan, W., Gurezka, R., Cohen, J., Ketteler, R., Watowich, S. S., Neumann, D., Langosch, D., and Klingmuller, U. (2001). Self assembly of the transmembrane domain promotes signal transduction through the erythropoietin receptor. Curr Biol *11*, 110-115.

Kucharz, E. J. (1992). The Collagens: Biochemistry and Pathophysiology. Springer-Verlag, New York.

Labrador, J. P., Azcoitia, V., Tuckermann, J., Lin, C., Olaso, E., Manes, S., Bruckner, K., Goergen, J. L., Lemke, G., Yancopoulos, G., *et al.* (2001). The

collagen receptor DDR2 regulates proliferation and its elimination leads to dwarfism. EMBO Rep *2*, 446-452.

Lai, C., and Lemke, G. (1994). Structure and expression of the Tyro 10 receptor tyrosine kinase. Oncogene *9*, 877-883.

Langholz, O., Rockel, D., Mauch, C., Kozlowska, E., Bank, I., Krieg, T., and Eckes, B. (1995). Collagen and collagenase gene expression in three-dimensional collagen lattices are differentially regulated by alpha 1 beta 1 and alpha 2 beta 1 integrins. J Cell Biol *131*, 1903-1915.

Langosch, D., and Heringa, J. (1998). Interaction of transmembrane helices by a knobs-into-holes packing characteristic of soluble coiled coils. Proteins *31*, 150-159.

Langosch, D., Brosig, B., Kolmar, H., and Fritz, H. J. (1996). Dimerisation of the glycophorin A transmembrane segment in membranes probed with the ToxR transcription activator. J Mol Biol *263*, 525-530.

Laval, S., Butler, R., Shelling, A. N., Hanby, A. M., Poulsom, R., and Ganesan, T. S. (1994). Isolation and characterization of an epithelial-specific receptor tyrosine kinase from an ovarian cancer cell line. Cell Growth Differ *5*, 1173-1183.

Lee, J. O., Bankston, L. A., Arnaout, M. A., and Liddington, R. C. (1995). Two conformations of the integrin A-domain (I-domain): a pathway for activation? Structure *3*, 1333-1340.

Lee, C. C., Kreusch, A., McMullan, D., Ng, K., Spraggon, G. (2003). Crystal structure of the human neuropilin-1 b1 domain. Structure *11*, 99-108

Leitinger, B. (2003). Molecular analysis of collagen binding by the human discoidin domain receptors, DDR1 and DDR2. Identification of collagen binding sites in DDR2. J Biol Chem *278*, 16761-16769.

Leitinger, B., Steplewski, A., and Fertala, A. (2004). The D2 period of collagen II contains a specific binding site for the human discoidin domain receptor, DDR2. J Mol Biol *344*, 993-1003.

Lemmon, M. A., Bu, Z., Ladbury, J. E., Zhou, M., Pinchasi, D., Lax, I., Engelman, D. M., and Schlessinger, J. (1997). Two EGF molecules contribute additively to stabilization of the EGFR dimer. EMBO J *16*, 281-294.

Lemmon, M. A., Flanagan, J. M., Hunt, J. F., Adair, B. D., Bormann, B. J., Dempsey, C. E., and Engelman, D. M. (1992). Glycophorin A dimerization is driven by specific interactions between transmembrane alpha-helices. J Biol Chem *267*, 7683-7689.

L'Hote C, G., Thomas, P. H., and Ganesan, T. S. (2002). Functional analysis of discoidin domain receptor 1: effect of adhesion on DDR1 phosphorylation. Faseb J *16*, 234-236.

Li, R., Gorelik, R., Nanda, V., Law, P. B., Lear, J. D., DeGrado, W. F., and Bennett, J. S. (2004). Dimerization of the transmembrane domain of Integrin alphaIIb subunit in cell membranes. J Biol Chem *279*, 26666-26673.

Livnah, O., Johnson, D. L., Stura, E. A., Farrell, F. X., Barbone, F. P., You, Y., Liu, K. D., Goldsmith, M. A., He, W., Krause, C. D., *et al.* (1998). An antagonist peptide-EPO receptor complex suggests that receptor dimerization is not sufficient for activation. Nat Struct Biol *5*, 993-1004.

Livnah, O., Stura, E. A., Johnson, D. L., Middleton, S. A., Mulcahy, L. S., Wrighton, N. C., Dower, W. J., Jolliffe, L. K., and Wilson, I. A. (1996). Functional mimicry of a protein hormone by a peptide agonist: the EPO receptor complex at 2.8 A. Science *273*, 464-471.

Martin-Fernandez, M., Clarke, D. T., Tobin, M. J., Jones, S. V., and Jones, G. R. (2002). Preformed oligomeric epidermal growth factor receptors undergo an ectodomain structure change during signaling. Biophys J *82*, 2415-2427.

Matsuyama, W., Faure, M., and Yoshimura, T. (2003a). Activation of discoidin domain receptor 1 facilitates the maturation of human monocyte-derived dendritic cells through the TNF receptor associated factor 6/TGF-beta-activated protein kinase 1 binding protein 1 beta/p38 alpha mitogen-activated protein kinase signaling cascade. J Immunol *171*, 3520-3532.

Matsuyama, W., Kamohara, H., Galligan, C., Faure, M., and Yoshimura, T. (2003b). Interaction of discoidin domain receptor 1 isoform b (DDR1b) with collagen activates p38 mitogen-activated protein kinase and promotes differentiation of macrophages. Faseb J *17*, 1286-1288.

Matsuyama, W., Mitsuyama, H., Watanabe, M., Shirahama, Y., Higashimoto, I., Osame, M., and Arimura, K. (2005). Involvement of discoidin domain receptor 1 in the deterioration of pulmonary sarcoidosis. Am J Respir Cell Mol Biol *33*, 565-573.

Matsuyama, W., Wang, L., Farrar, W. L., Faure, M., and Yoshimura, T. (2004). Activation of discoidin domain receptor 1 isoform b with collagen up-regulates chemokine production in human macrophages: role of p38 mitogen-activated protein kinase and NF-kappa B. J Immunol *172*, 2332-2340.

Matsuyama, W., Watanabe, M., Shirahama, Y., Hirano, R., Mitsuyama, H., Higashimoto, I., Osame, M., and Arimura, K. (2006a). Suppression of discoidin domain receptor 1 by RNA interference attenuates lung inflammation. J Immunol *176*, 1928-1936.

Matsuyama, W., Watanabe, M., Shirahama, Y., Mitsuyama, H., Higashimoto, I., Osame, M., and Arimura, K. (2006b). Discoidin domain receptor 1 contributes to the survival of lung fibroblast in idiopathic pulmonary fibrosis. Am J Pathol *168*, 866-877.

MacKenzie, K. R., Prestegard, J. H., and Engelman, D. M. (1997). A transmembrane helix dimer: structure and implications. Science *276*, 131-133.

Matunis, M. J., Coutavas, E., and Blobel, G. (1996). A novel ubiquitin-like modification modulates the partitioning of the Ran-GTPase-activating protein RanGAP1 between the cytosol and the nuclear pore complex. J Cell Biol *135*, 1457-1470.

McVey, M., Ramsay, D., Kellett, E., Rees, S., Wilson, S., Pope, A. J., and Milligan, G. (2001). Monitoring receptor oligomerization using time-resolved fluorescence resonance energy transfer and bioluminescence resonance energy transfer. The human delta -opioid receptor displays constitutive oligomerization at the cell surface, which is not regulated by receptor occupancy. J Biol Chem *276*, 14092-14099.

Melnyk, R. A., Kim, S., Curran, A. R., Engelman, D. M., Bowie, J. U., and Deber, C. M. (2004). The affinity of GXXXG motifs in transmembrane helix-helix interactions is modulated by long-range communication. J Biol Chem *279*, 16591-16597.

Melnyk, R. A., Partridge, A. W., Yip, J., Wu, Y., Goto, N. K., and Deber, C. M. (2003). Polar residue tagging of transmembrane peptides. Biopolymers *71*, 675-685.

Mendrola, J. M., Berger, M. B., King, M. C., and Lemmon, M. A. (2002). The single transmembrane domains of ErbB receptors self-associate in cell membranes. J Biol Chem *277*, 4704-4712.

Miranti, C. K., and Brugge, J. S. (2002). Sensing the environment: a historical perspective on integrin signal transduction. Nat Cell Biol *4*, E83-90.

Miura, Y., Ohnuma, M., Jung, S. M., and Moroi, M. (2000). Cloning and expression of the platelet-specific collagen receptor glycoprotein VI. Thromb Res *98*, 301-309.

Miura, Y., Takahashi, T., Jung, S. M., and Moroi, M. (2002). Analysis of the interaction of platelet collagen receptor glycoprotein VI (GPVI) with collagen. A dimeric form of GPVI, but not the monomeric form, shows affinity to fibrous collagen. J Biol Chem *277*, 46197-46204.

Morales, M. O., Price, R. L., and Goldsmith, E. C. (2005). Expression of Discoidin Domain Receptor 2 (DDR2) in the developing heart. Microsc Microanal *11*, 260-267.

Mori, S., Claesson-Welsh, L., Okuyama, Y., and Saito, Y. (1995). Ligand-induced polyubiquitination of receptor tyrosine kinases. Biochem Biophys Res Commun *213*, 32-39.

Mori, S., Heldin, C. H., and Claesson-Welsh, L. (1992). Ligand-induced polyubiquitination of the platelet-derived growth factor beta-receptor. J Biol Chem *267*, 6429-6434.

Moriki, T., Maruyama, H., and Maruyama, I. N. (2001). Activation of preformed EGF receptor dimers by ligand-induced rotation of the transmembrane domain. J Mol Biol *311*, 1011-1026.

Moroi, M., Jung, S. M., Shinmyozu, K., Tomiyama, Y., Ordinas, A., and Diaz-Ricart, M. (1996). Analysis of platelet adhesion to a collagen-coated surface under flow conditions: the involvement of glycoprotein VI in the platelet adhesion. Blood *88*, 2081-2092.

Morton, L. F., Peachey, A. R., Zijenah, L. S., Goodall, A. H., Humphries, M. J., and Barnes, M. J. (1994). Conformation-dependent platelet adhesion to collagen involving integrin alpha 2 beta 1-mediated and other mechanisms: multiple alpha 2 beta 1-recognition sites in collagen type I. Biochem J *299*, 791-797.

Mousavi, S. A., Sato, M., Sporstol, M., Smedsrod, B., Berg, T., Kojima, N., and Senoo, H. (2005). Uptake of denatured collagen into hepatic stellate cells: evidence for the involvement of urokinase plasminogen activator receptor-associated protein/Endo180. Biochem J *387*, 39-46.

Mukherjee, S., Ghosh, R. N., and Maxfield, F. R. (1997). Endocytosis. Physiol Rev *77*, 759-803.

Myllyharju, J., and Kivirikko, K. I. (2001). Collagens and collagen-related diseases. Ann Med *33*, 7-21.

Nemoto, T., Ohashi, K., Akashi, T., Johnson, J. D., and Hirokawa, K. (1997). Overexpression of protein tyrosine kinases in human esophageal cancer. Pathobiology *65*, 195-203.

Nieswandt, B., Bergmeier, W., Schulte, V., Rackebrandt, K., Gessner, J. E., and Zirngibl, H. (2000). Expression and function of the mouse collagen receptor

glycoprotein VI is strictly dependent on its association with the FcRgamma chain. J Biol Chem *275*, 23998-24002.

Nieswandt, B., and Watson, S. P. (2003). Platelet-collagen interaction: is GPVI the central receptor? Blood *102*, 449-461.

Ogiso, H., Ishitani, R., Nureki, O., Fukai, S., Yamanaka, M., Kim, J. H., Saito, K., Sakamoto, A., Inoue, M., Shirouzu, M., and Yokoyama, S. (2002). Crystal structure of the complex of human epidermal growth factor and receptor extracellular domains. Cell *110*, 775-787.

Okura, T., Gong, L., Kamitani, T., Wada, T., Okura, I., Wei, C. F., Chang, H. M., and Yeh, E. T. (1996). Protection against Fas/APO-1- and tumor necrosis factor-mediated cell death by a novel protein, sentrin. J Immunol *157*, 4277-4281.

Olaso, E., Ikeda, K., Eng, F. J., Xu, L., Wang, L. H., Lin, H. C., and Friedman, S. L. (2001). DDR2 receptor promotes MMP-2-mediated proliferation and invasion by hepatic stellate cells. J Clin Invest *108*, 1369-1378.

Olaso, E., Labrador, J. P., Wang, L., Ikeda, K., Eng, F. J., Klein, R., Lovett, D. H., Lin, H. C., and Friedman, S. L. (2002). Discoidin domain receptor 2 regulates fibroblast proliferation and migration through the extracellular matrix in association with transcriptional activation of matrix metalloproteinase-2. J Biol Chem *277*, 3606-3613.

Olayioye, M. A., Neve, R. M., Lane, H. A., and Hynes, N. E. (2000). The ErbB signaling network: receptor heterodimerization in development and cancer. EMBO J *19*, 3159-3167.

Omura, T., Heldin, C. H., and Ostman, A. (1997). Immunoglobulin-like domain 4-mediated receptor-receptor interactions contribute to platelet-derived growth factor-induced receptor dimerization. J Biol Chem *272*, 12676-12682.

Ongusaha, P. P., Kim, J. I., Fang, L., Wong, T. W., Yancopoulos, G. D., Aaronson, S. A., and Lee, S. W. (2003). p53 induction and activation of DDR1 kinase counteract p53-mediated apoptosis and influence p53 regulation through a positive feedback loop. EMBO J *22*, 1289-1301.

Overton, M. C., Chinault, S. L., and Blumer, K. J. (2003). Oligomerization, biogenesis, and signaling is promoted by a glycophorin A-like dimerization motif in transmembrane domain 1 of a yeast G protein-coupled receptor. J Biol Chem *278*, 49369-49377.

Parsons, J. T., Martin, K. H., Slack, J. K., Taylor, J. M., and Weed, S. A. (2000). Focal adhesion kinase: a regulator of focal adhesion dynamics and cell movement. Oncogene *19*, 5606-5613.

Pawson, T. (1995). Protein modules and signalling networks. Nature *373*, 573-580.

Penuel, E., Akita, R. W., and Sliwkowski, M. X. (2002). Identification of a region within the ErbB2/HER2 intracellular domain that is necessary for ligand-independent association. J Biol Chem *277*, 28468-28473.

Perez, J. L., Jing, S. Q., and Wong, T. W. (1996). Identification of two isoforms of the Cak receptor kinase that are coexpressed in breast tumor cell lines. Oncogene *12*, 1469-1477.

Perret, S., Eble, J. A., Siljander, P. R., Merle, C., Farndale, R. W., Theisen, M., and Ruggiero, F. (2003). Prolyl hydroxylation of collagen type I is required for

efficient binding to integrin alpha 1 beta 1 and platelet glycoprotein VI but not to alpha 2 beta 1. J Biol Chem *278*, 29873-29879.

Pickford, A. R., Smith, S. P., Staunton, D., Boyd, J., and Campbell, I. D. (2001). The hairpin structure of the (6)F1(1)F2(2)F2 fragment from human fibronectin enhances gelatin binding. EMBO J *20*, 1519-1529.

Pinto, L. H., Dieckmann, G. R., Gandhi, C. S., Papworth, C. G., Braman, J., Shaughnessy, M. A., Lear, J. D., Lamb, R. A., and DeGrado, W. F. (1997). A functionally defined model for the M2 proton channel of influenza A virus suggests a mechanism for its ion selectivity. Proc Natl Acad Sci U S A *94*, 11301-11306.

Playford, M. P., Butler, R. J., Wang, X. C., Katso, R. M., Cooke, I. E., and Ganesan, T. S. (1996). The genomic structure of discoidin receptor tyrosine kinase. Genome Res *6*, 620-627.

Plow, E. F., Haas, T. A., Zhang, L., Loftus, J., and Smith, J. W. (2000). Ligand binding to integrins. J Biol Chem *275*, 21785-21788.

Poole, A., Gibbins, J. M., Turner, M., van Vugt, M. J., van de Winkel, J. G., Saito, T., Tybulewicz, V. L., and Watson, S. P. (1997). The Fc receptor gamma-chain and the tyrosine kinase Syk are essential for activation of mouse platelets by collagen. Embo J *16*, 2333-2341.

Pozzi, A., Wary, K. K., Giancotti, F. G., and Gardner, H. A. (1998). Integrin alpha1beta1 mediates a unique collagen-dependent proliferation pathway in vivo. J Cell Biol *142*, 587-594.

Prockop, D. J., and Kivirikko, K. I. (1995). Collagens: molecular biology, diseases, and potentials for therapy. Annu Rev Biochem *64*, 403-434.

Qian, X., O'Rourke, D. M., Fei, Z., Zhang, H. T., Kao, C. C., and Greene, M. I. (1999). Domain-specific interactions between the p185(neu) and epidermal growth factor receptor kinases determine differential signaling outcomes. J Biol Chem *274*, 574-583.

Qu, A., and Leahy, D. J. (1995). Crystal structure of the I-domain from the CD11a/CD18 (LFA-1, alpha L beta 2) integrin. Proc Natl Acad Sci U S A *92*, 10277-10281.

Raffioni, S., Zhu, Y. Z., Bradshaw, R. A., and Thompson, L. M. (1998). Effect of transmembrane and kinase domain mutations on fibroblast growth factor receptor 3 chimera signaling in PC12 cells. A model for the control of receptor tyrosine kinase activation. J Biol Chem *273*, 35250-35259.

Ram, R., Lorente, G., Nikolich, K., Urfer, R., Foehr, E., and Nagavarapu, U. (2005). Discoidin Domain Receptor-1a (DDR1a) Promotes Glioma Cell Invasion and Adhesion in Association with Matrix Metalloproteinase-2. J Neurooncol.

Raynal, N., Hamaia, S. W., Siljander, P. R., Maddox, B., Peachey, A. R., Fernandez, R., Foley, L. J., Slatter, D. A., Jarvis, G. E., and Farndale, R. W. (2006). Use of synthetic peptides to locate novel integrin alpha2beta1-binding motifs in human collagen III. J Biol Chem *281*, 3821-3831.

Ravanti, L., Heino, J., Lopez-Otin, C., and Kahari, V. M. (1999). Induction of collagenase-3 (MMP-13) expression in human skin fibroblasts by three-dimensional collagen is mediated by p38 mitogen-activated protein kinase. J Biol Chem *274*, 2446-2455.

Renne, C., Willenbrock, K., Kuppers, R., Hansmann, M. L., and Brauninger, A. (2005). Autocrine- and paracrine-activated receptor tyrosine kinases in classic Hodgkin lymphoma. Blood *105*, 4051-4059.

Rivera-Calzada, A., Robertson, D., MacFadyen, J. R., Boskovic, J., Isacke, C. M., and Llorca, O. (2003). Three-dimensional interplay among the ligand-binding domains of the urokinase-plasminogen-activator-receptor-associated protein, Endo180. EMBO Rep *4*, 807-812.

Robertson, S. C., Tynan, J., and Donoghue, D. J. (2000). RTK mutations and human syndromes: when good receptors turn bad. Trends Genet *16*, 368.

Rocheville, M., Lange, D. C., Kumar, U., Sasi, R., Patel, R. C., and Patel, Y. C. (2000). Subtypes of the somatostatin receptor assemble as functional homo- and heterodimers. J Biol Chem *275*, 7862-7869.

Ruan, W., Becker, V., Klingmuller, U., and Langosch, D. (2004). The interface between self-assembling erythropoietin receptor transmembrane segments corresponds to a membrane-spanning leucine zipper. J Biol Chem *279*, 3273-3279.

Sako, Y., Minoghchi, S., and Yanagida, T. (2000). Single-molecule imaging of EGFR signalling on the surface of living cells. Nat Cell Biol *2*, 168-172.

Sakuma, S., Saya, H., Tada, M., Nakao, M., Fujiwara, T., Roth, J. A., Sawamura, Y., Shinohe, Y., and Abe, H. (1996). Receptor protein tyrosine kinase DDR is up-regulated by p53 protein. FEBS Lett *398*, 165-169.

San Antonio, J. D., Karnovsky, M. J., Gay, S., Sanderson, R. D., and Lander, A. D. (1994). Interactions of syndecan-1 and heparin with human collagens. Glycobiology *4*, 327-332.

Sanchez, M. P., Tapley, P., Saini, S. S., He, B., Pulido, D., and Barbacid, M. (1994). Multiple tyrosine protein kinases in rat hippocampal neurons: isolation of

Ptk-3, a receptor expressed in proliferative zones of the developing brain. Proc Natl Acad Sci U S A *91*, 1819-1823.

Schlessinger, J. (2000). Cell signaling by receptor tyrosine kinases. Cell *103*, 211-225.

Schlessinger, J. (2002). Ligand-induced, receptor-mediated dimerization and activation of EGF receptor. Cell *110*, 669-672.

Schnack Nielsen, B., Rank, F., Engelholm, L. H., Holm, A., Dano, K., and Behrendt, N. (2002). Urokinase receptor-associated protein (uPARAP) is expressed in connection with malignant as well as benign lesions of the human breast and occurs in specific populations of stromal cells. Int J Cancer *98*, 656-664.

Schwartz, M. A. (2001). Integrin signaling revisited. Trends Cell Biol *11*, 466-470.

Schwartz, M. A., and Ginsberg, M. H. (2002). Networks and crosstalk: integrin signalling spreads. Nat Cell Biol *4*, E65-68.

Senes, A., Gerstein, M., and Engelman, D. M. (2000). Statistical analysis of amino acid patterns in transmembrane helices: the GxxxG motif occurs frequently and in association with beta-branched residues at neighboring positions. J Mol Biol *296*, 921-936.

Seubert, N., Royer, Y., Staerk, J., Kubatzky, K. F., Moucadel, V., Krishnakumar, S., Smith, S. O., and Constantinescu, S. N. (2003). Active and inactive orientations of the transmembrane and cytosolic domains of the erythropoietin receptor dimer. Mol Cell *12*, 1239-1250.

Sheikh, H., Yarwood, H., Ashworth, A., and Isacke, C. M. (2000). Endo180, an endocytic recycling glycoprotein related to the macrophage mannose receptor is expressed on fibroblasts, endothelial cells and macrophages and functions as a lectin receptor. J Cell Sci *113 (Pt 6)*, 1021-1032.

Shelling, A. N., Butler, R., Jones, T., Laval, S., Boyle, J. M., and Ganesan, T. S. (1995). Localization of an epithelial-specific receptor kinase (EDDR1) to chromosome 6q16. Genomics *25*, 584-587.

Shrivastava, A., Radziejewski, C., Campbell, E., Kovac, L., McGlynn, M., Ryan, T. E., Davis, S., Goldfarb, M. P., Glass, D. J., Lemke, G., and Yancopoulos, G. D. (1997). An orphan receptor tyrosine kinase family whose members serve as nonintegrin collagen receptors. Mol Cell *1*, 25-34.

Shyu, K. G., Chao, Y. M., Wang, B. W., and Kuan, P. (2005). Regulation of discoidin domain receptor 2 by cyclic mechanical stretch in cultured rat vascular smooth muscle cells. Hypertension *46*, 614-621.

Siljander, P.R-M and Farndale, R.W. (2002) in Platelets in Thrombotic and Nonthrombotic Disorders: Pathophysiology, Pharmacology, and Therapeutics (Gresele, P., Page, C. P., Fuster, V., and Vermylen, J., eds) pp. 158-178, Cambridge University Press, Cambridge, UK.

Siljander, P. R., Hamaia, S., Peachey, A. R., Slatter, D. A., Smethurst, P. A., Ouwehand, W. H., Knight, C. G., and Farndale, R. W. (2004). Integrin activation state determines selectivity for novel recognition sites in fibrillar collagens. J Biol Chem *279*, 47763-47772.

Simmerman, H. K., Kobayashi, Y. M., Autry, J. M., and Jones, L. R. (1996). A leucine zipper stabilizes the pentameric membrane domain of phospholamban and forms a coiled-coil pore structure. J Biol Chem *271*, 5941-5946.

Slack, B. E., Siniaia, M. S., and Blusztajn, J. K. (2006). Collagen type I selectively activates ectodomain shedding of the discoidin domain receptor 1: Involvement of Src tyrosine kinase. J Cell Biochem *98*, 672-684

Smethurst, P. A., Joutsi-Korhonen, L., O'Connor, M. N., Wilson, E., Jennings, N. S., Garner, S. F., Zhang, Y., Knight, C. G., Dafforn, T. R., Buckle, A., *et al.* (2004). Identification of the primary collagen-binding surface on human glycoprotein VI by site-directed mutagenesis and by a blocking phage antibody. Blood *103*, 903-911.

Springer, W. R., Cooper, D. N., Barondes, S. H. (1984). Discoidin I is implicated in cell-substratum attachment and ordered cell migration of Dictyostelium discoideum and resembles fibronectin. Cell *39*, 557-564.

Stamos, J., Sliwkowski, M. X., and Eigenbrot, C. (2002). Structure of the epidermal growth factor receptor kinase domain alone and in complex with a 4-anilinoquinazoline inhibitor. J Biol Chem *277*, 46265-46272.

St Croix, B., Rago, C., Velculescu, V., Traverso, G., Romans, K. E., Montgomery, E., Lal, A., Riggins, G. J., Lengauer, C., Vogelstein, B., and Kinzler, K. W. (2000). Genes expressed in human tumour endothelium. Science *289*, 1197-1202.

Sternberg, M. J., and Gullick, W. J. (1990). A sequence motif in the transmembrane region of growth factor receptors with tyrosine kinase activity mediates dimerization. Protein Eng *3*, 245-248.

Tanner, K. G., and Kyte, J. (1999). Dimerization of the extracellular domain of the receptor for epidermal growth factor containing the membrane-spanning segment in response to treatment with epidermal growth factor. J Biol Chem *274*, 35985-35990.

Thomas, E. K., Nakamura, M., Wienke, D., Isacke, C. M., Pozzi, A., and Liang, P. (2005). Endo180 binds to the C-terminal region of type I collagen. J Biol Chem *280*, 22596-22605.

Tsuji, M., Ezumi, Y., Arai, M., and Takayama, H. (1997). A novel association of Fc receptor gamma-chain with glycoprotein VI and their co-expression as a collagen receptor in human platelets. J Biol Chem *272*, 23528-23531.

Tuckwell, D., Calderwood, D. A., Green, L. J., and Humphries, M. J. (1995). Integrin alpha 2 I-domain is a binding site for collagens. J Cell Sci *108*, 1629-1637.

Valent, A., Meddeb, M., Danglot, G., Duverger, A., Nguyen, V. C., and Bernheim, A. (1996). Assignment of the NTRK4 (trkE) gene to chromosome 6p21. Hum Genet *98*, 12-15.

van der Rest, M., and Garrone, R. (1991). Collagen family of proteins. Faseb J *5*, 2814-2823.

Vogel, W. (1999). Discoidin domain receptors: structural relations and functional implications. Faseb J *13 Suppl*, S77-82.

Vogel, W., Brakebusch, C., Fassler, R., Alves, F., Ruggiero, F., and Pawson, T. (2000). Discoidin domain receptor 1 is activated independently of beta(1) integrin. J Biol Chem *275*, 5779-5784.

Vogel, W., Gish, G. D., Alves, F., and Pawson, T. (1997). The discoidin domain receptor tyrosine kinases are activated by collagen. Mol Cell *1*, 13-23.

Vogel, W. F., Aszodi, A., Alves, F., and Pawson, T. (2001). Discoidin domain receptor 1 tyrosine kinase has an essential role in mammary gland development. Mol Cell Biol *21*, 2906-2917.

Wall S. J., Werner E., Werb, Z., and DeClerck, Y. A. (2005). Discoidin domain receptor 2 mediates tumour cell cycle arrest induced by fibrillar collagen. J Biol Chem *280*, 40187-40194.

Wang, C. Z., Hsu, Y. M., and Tang, M. J. (2005). Function of discoidin domain receptor I in HGF-induced branching tubulogenesis of MDCK cells in collagen gel. J Cell Physiol *203*, 295-304.

Webb, Y., Hermida-Matsumoto, L., and Resh, M. D. (2000). Inhibition of protein palmitoylation, raft localization, and T cell signaling by 2-bromopalmitate and polyunsaturated fatty acids. J Biol Chem *275*, 261-270.

Weiner, H. L., Huang, H., Zagzag, D., Boyce, H., Lichtenbaum, R., and Ziff, E. B. (2000). Consistent and selective expression of the discoidin domain receptor-1 tyrosine kinase in human brain tumours. Neurosurgery *47*, 1400-1409.

Weiner, H. L., Rothman, M., Miller, D. C., and Ziff, E. B. (1996). Pediatric brain tumors express multiple receptor tyrosine kinases including novel cell adhesion kinases. Pediatr Neurosurg *25*, 64-71; discussion 71-62.

Weiss, A., and Schlessinger, J. (1998). Switching signals on or off by receptor dimerization. Cell *94*, 277-280.

Wienke, D., MacFadyen, J. R., and Isacke, C. M. (2003). Identification and characterization of the endocytic transmembrane glycoprotein Endo180 as a novel collagen receptor. Mol Biol Cell *14*, 3592-3604.

Wiley, H. S., Herbst, J. J., Walsh, B. J., Lauffenburger, D. A., Rosenfeld, M. G., and Gill, G. N. (1991). The role of tyrosine kinase activity in endocytosis, compartmentation, and down-regulation of the epidermal growth factor receptor. J Biol Chem *266*, 11083-11094.

Xiong, J. P., Stehle, T., Diefenbach, B., Zhang, R., Dunker, R., Scott, D. L., Joachimiak, A., Goodman, S. L., and Arnaout, M. A. (2001). Crystal structure of the extracellular segment of integrin alpha Vbeta3. Science *294*, 339-345.

Xiong, J. P., Stehle, T., Zhang, R., Joachimiak, A., Frech, M., Goodman, S. L., and Arnaout, M. A. (2002). Crystal structure of the extracellular segment of integrin alpha Vbeta3 in complex with an Arg-Gly-Asp ligand. Science *296*, 151-155.

Xu, L., Peng, H., Wu, D., Hu, K., Goldring, M. B., Olsen, B. R., and Li, Y. (2005). Activation of the discoidin domain receptor 2 induces expression of matrix metalloproteinase 13 associated with osteoarthritis in mice. J Biol Chem *280*, 548-555.

Xu, Y., Gurusiddappa, S., Rich, R. L., Owens, R. T., Keene, D. R., Mayne, R., Hook, A., and Hook, M. (2000). Multiple binding sites in collagen type I for the integrins alpha1beta1 and alpha2beta1. J Biol Chem *275*, 38981-38989.

Yang, K., Kim, J. H., Kim, H. J., Park, I. S., Kim, I. Y., and Yang, B. S. (2005). Tyrosine 740 phosphorylation of discoidin domain receptor 2 by Src stimulates intramolecular autophosphorylation and Shc signaling complex formation. J Biol Chem *280*, 39058-39066.

Yayon, A., Klagsbrun, M., Esko, J. D., Leder, P., and Ornitz, D. M. (1991). Cell surface, heparin-like molecules are required for binding of basic fibroblast growth factor to its high affinity receptor. Cell *64*, 841-848.

Yeh, E. T., Gong, L., and Kamitani, T. (2000). Ubiquitin-like proteins: new wines in new bottles. Gene *248*, 1-14.

Yoshimura, T., Matsuyama, W., and Kamohara, H. (2005). Discoidin domain receptor 1: a new class of receptor regulating leukocyte-collagen interaction. Immunol Res *31*, 219-230.

Yu, J., Ustach, C., and Kim, H. R. (2003). Platelet-derived growth factor signaling and human cancer. J Biochem Mol Biol *36*, 49-59.

Yu, X., Sharma, K. D., Takahashi, T., Iwamoto, R., and Mekada, E. (2002). Ligand-independent dimer formation of epidermal growth factor receptor (EGFR) is a step separable from ligand-induced EGFR signaling. Mol Biol Cell *13*, 2547-2557.

Zamir, E., and Geiger, B. (2001). Components of cell-matrix adhesions. J Cell Sci *114*, 3577-3579.

Zerlin, M., Julius, M. A., and Goldfarb, M. (1993). NEP: a novel receptor-like tyrosine kinase expressed in proliferating neuroepithelia. Oncogene *8*, 2731-2739.

Presentations and submitted manuscript

Presentations at international meetings

September, 2005
Noordeen, A.N. and Leitinger, B. 'Analysis of the structural domains involved in the activation of the Discoidin Domain Receptors, DDR1 & DDR2' European Life Science Organization (ELSO 2005), Dresden, Germany. (poster presentation).

May, 2004
Noordeen, A.N. and Leitinger, B. 'Analysis of the structural domains involved in the activation of the Discoidin Domain Receptors, DDR1 & DDR2' FEBS Lecture Course on Cellular Signalling & 4th Dubrovnik Signalling Conference, Cavtat, Croatia. (poster presentation)

Submitted manuscript

Noordeen, A.N., Carafoli, F., Hohenester, E., Horton, M.A., and Leitinger, B. 'A transmembrane leucine zipper is required for activation of the dimeric receptor tyrosine kinase, DDR1'.